



UNIVERSITAT_{DE}
BARCELONA

Limnology of Tropical Mountain Lakes: Analysis of the hydromorphological, physical and biogeochemical variability of the Cajas Massif lake district

Pablo Mosquera Vintimilla



Aquesta tesi doctoral està subjecta a la llicència **Reconeixement 4.0. Espanya de Creative Commons.**

Esta tesis doctoral está sujeta a la licencia **Reconocimiento 4.0. España de Creative Commons.**

This doctoral thesis is licensed under the **Creative Commons Attribution 4.0. Spain License.**

Limnology of Tropical Mountain Lakes: Analysis of the hydromorphological, physical and biogeochemical variability of the Cajas Massif lake district

Pablo Mosquera Vintimilla



UNIVERSITAT DE
BARCELONA

Pablo Mosquera Vintimilla. Limnology of Tropical Mountain Lakes: Analysis of the hydromorphological, physical and biogeochemical variability of the Cajas Massif lake district.

PhD thesis. Universitat de Barcelona, Barcelona.

Cover design: DUAL dmw

Cover photographs: Pablo Mosquera Vintimilla

Chapters' covers: DUAL dmw

TESI DOCTORAL



UNIVERSITAT DE
BARCELONA

*Universitat de Barcelona
Departament de Biologia Evolutiva, Ecologia i Ciències Ambientals
Programa de Doctorat en Ecologia, Ciències Ambientals i Fisiologia Vegetal*

**Limnology of Tropical Mountain Lakes: Analysis of the
hydromorphological, physical and biogeochemical variability
of the Cajas Massif lake district**

*Limnologia dels llacs tropicals de Muntanya: Anàlisi de la variabilitat
hidromorfològica, física i biogeoquímica del districte lacustre del Massís del
Cajas.*

*Memòria presentada per Pablo Mosquera Vintimilla per optar al títol de Doctor
per la Universitat de Barcelona*

Pablo Mosquera Vintimilla
Barcelona, desembre de 2022

Vist-i-plau del director i tutora de la tesi:



Dr. Jordi Catalan Aguilà
*Professor de recerca
CSIC*

Dra. Marisol Felip Benach
*Professora agregada
Universitat de Barcelona*

A la luz de mi vida
Amelia

“Un lago es la característica más bella y expresiva del paisaje. Es el ojo de la tierra, en el que el espectador mide la profundidad de su propia naturaleza”.

Henry David Thoreau

AGRADECIMIENTOS

Ha sido un largo camino de muchos años poder llegar a este punto, en donde me siento completamente agradecido con todas las personas que han formado parte de este proyecto de tesis, primeramente gracias porque han depositado su confianza en mi persona y segundo porque han sido parte del día a día de la construcción de este proyecto con mucho esfuerzo y sacrificio, trabajar en los lagos de las montañas siempre es un reto, simplemente quiero decirles gracias a todos porque al final lo hemos construido.

Quiero empezar por la Dra. Henrietta Hampel de la Universidad de Cuenca, siempre su apoyo hacia mi persona ha sido incondicional desde el año 2012 en que la conocí, le agradezco por permitirme formar parte de su equipo de investigación y propiciar este trabajo pionero del estudio de la limnología de los Andes del sur de Ecuador.

Muchas gracias a mi director el Dr. Jordi Catalán, creo que tuve la gran suerte de la vida en tener un maestro como lo es Jordi, aún recuerdo el día que fui a su despacho por primera vez y le hablé de los lagos de Cajas y me dijo *“hace muchos años vino una chica y me mostró un mapa de unos lagos de los Andes llamados Cajas, que son muy interesantes de monitorearlos y mírate hoy vienes tú y ya los has estudiado”*. Gracias Jordi por tu infinita paciencia, tu disciplina y tu don de ser humano.

A mi tutora la Dra. Marisol Felip por su apoyo en todo este proceso y su apoyo incondicional constante, muchas gracias Marisol. De igual manera al Dr. Raúl Vázquez de la Universidad de Cuenca que también ha formado parte activa de este proyecto aportado con sus conocimientos y sus ideas y a Meritxell Batalla del CREA por todo su soporte incondicional.

A Mario Domínguez, Jhonatan Aguirre, Don Simón Quiroz y a todos los compañeros guardaparques del Parque Nacional Cajas por su

gran entrega y apoyo brindado en las duras jornadas de monitoreo, sin ustedes no lo hubiésemos conseguido, han sido un gran equipo siempre.

Al Dr. Rolando Céleri y al Departamento de Recursos Hídricos y Ciencias Ambientales (iDRHICA) de la Universidad de Cuenca, por facilitarme la información meteorológica de la estaciones ubicadas en el Macizo del Cajas.

Gracias a la Empresa Pública Municipal de Telecomunicaciones, Agua Potable, Alcantarillado y Saneamiento Ambiental de Cuenca - ETAPA EP y a la Dirección de Investigación de la Universidad de Cuenca-DIUC por financiar el proyecto “Caracterización limnológica de los lagos y lagunas del Parque Nacional Cajas”.

Gracias a mis padres y a mis hermanos Juana y Xavier por todo el cariño y apoyo que me han brindado no solamente este año sino toda la vida. Los llevo siempre en mi corazón.

A mi gran amigo el Dr. Juan Alfredo Martínez por confiar en mí persona, por siempre impulsarme a nuevos retos y darme esta hermosa oportunidad de colaborar en la noble labor de investigar y proteger los recursos del Macizo del Cajas.

Barcelona, diciembre de 2022

ADVISOR'S REPORT

Dr. Jordi Catalan, advisor of the Doctoral Thesis submitted by the candidate Pablo Mosquera Vintimilla, which is entitled “Limnology of Tropical Mountain Lakes: Analysis of the hydromorphological, physical and biogeochemical variability of the Cajas Massif lake district,”

INFORM

That the research work carried out by Pablo Mosquera Vintimilla as part of his pre-doctoral training and included in his Doctoral Thesis thesis has resulted in three chapters, two of which have already been published, and the third is in the final process of being sent to an international journal. Below the articles are listed, including some indicators of the impact of the journals according to the ISI Web of Science.

1. **Mosquera, P. V.**, Hampel, H., Vázquez, R. F., Alonso, M. & Catalan, J. (2017) Abundance and morphometry changes across the high-mountain lake-size gradient in the tropical Andes of Southern Ecuador. *Water Resources Research*, 53, 7269-7280. Doi: 10.1002/2017WR020902. **Impact factor 2021: 6.159**. JCR category: Limnology Q1 (2/21), Water resources Q1 (13/100), Environmental sciences Q1 (rank 68/278).
2. **Mosquera, P. V.**, Hampel, H., Vázquez, R. F. & Catalan, J. (2022) Water chemistry variation in tropical high-mountain lakes on old volcanic bedrocks. *Limnology and Oceanography*, 67, 1522–1536. Doi: 10.1002/lno.12099. **Impact factor 2021: 5.438**. JCR category: Limnology Q1 (3/21), Oceanography Q1 (4/66).
3. **Mosquera, P.V.**, Batalla, M., Hampel, H., Vázquez, R.F., Catalan, J. Mixing regimes in tropical high-mountain lakes. Preparing to submit to *Limnology and Oceanography*.

CERTIFY


That Pablo Mosquera Vintimilla has actively participated in developing the research work associated with each of the articles and in the preparation of the publications. Specifically, participation in each of the articles was as follows:

- Setting the objectives and design of the fieldwork
- Realization of the fieldwork associated with each of the articles
- Participation in laboratory analysis and data processing
- Writing the articles and monitoring the revision process thereof

That none of the co-authors of the articles included in this report, and which are part of the Doctoral Thesis of Pablo Mosquera Vintimilla will explicitly or implicitly use these works to prepare a doctoral thesis.

Barcelona, December 2022

JORDI
CATALAN
AGUILÀ - DNI
77093062Y



Firmado digitalmente por JORDI
CATALAN AGUILÀ - DNI 77093062Y
Nombre de reconocimiento (DN):
c=ES, sn=CATALAN AGUILÀ,
givenName=JORDI,
serialNumber=IDCES-77093062Y,
cn=JORDI CATALAN AGUILÀ - DNI
77093062Y
Fecha: 2022.12.12 21:39:05 +01'00'

Director de tesi
Dr. Jordi Catalan Aguilà
Professor de recerca del CSIC
CREAF

CONTENTS

Abstract	1
Resumen	3
Chapter 1 - General Introduction	5
1.1 High-mountain tropical limnology.....	7
1.2 Lake density and morphometry.....	9
1.3 Water chemistry.....	11
1.4 Mixing regimes.....	13
1.5 The Cajas massif lake district.....	14
Objectives	17
Chapter 2 - Abundance and morphometry changes across the high mountain lake-size gradient in the tropical Andes of Southern Ecuador	18
2.1 Introduction.....	20
2.2 Materials and methods.....	23
2.3 Results.....	29
2.4 Discussion.....	35
2.5 Conclusions.....	40
2.6 Acknowledgments.....	42
Chapter 3 - Water chemistry variation in tropical high-mountain lakes on old volcanic bedrocks	43
3.1 Introduction.....	46
3.2 Material and methods.....	48
3.3 Results.....	56
3.4 Discussion.....	66
3.5 Acknowledgments.....	75
Chapter 4 - Mixing regimes in tropical high-mountain lakes	76
4.1 Introduction.....	79

4.2 Material and methods	83
4.3 Results	88
4.4 Discussion.....	107
General discussion and conclusions	112
5.1 Altitude	116
5.2 Lake size	118
5.3 Bedrock.....	118
5.4 Wetlands	119
5.5 Anoxic layers	119
6. Conclusions	121
References	125
Supporting information.....	139
Appendix A.....	139
Appendix B.....	169

ABSTRACT

High-mountain tropical lakes in the South American continent are located in the upper part of the Andes range in the equatorial zone (Venezuela, Colombia, Ecuador, Peru, and Bolivia), altitudinally, usually above the forest line (3000-5000 m a.s.l.). They are generally in remote areas, which makes them comparable with other mountainous lake areas of the planet. They play an essential role in the hydrology of the tropical Andean zones, regulating the flow and water availability, being a vital source of drinking water, irrigation, and hydroelectricity, and supplying water to significant effluents of the Amazon River and rivers of the Pacific Ocean coast. The development of tropical limnology has been slow; priority has been given to studying large rivers such as the Amazon and its peripheral lagoons, partly due to their exceptional biotic richness. Long-term studies are not common in tropical regions despite the number of existing lakes that constitute a significant proportion of the world's freshwater resources. The limnology of high-mountain tropical lakes has been relegated even though most of these systems are located in natural reserve areas. The relatively few studies show that the limnology of tropical lakes differs from those of temperate zones.

The main objective of this thesis is to broaden the knowledge of tropical limnology of the high-mountain lakes of the southern Andes of Ecuador through the study of their morphometric characteristics, the chemical variation of the water, and the mixing processes.

The thesis results show that the lake abundance distribution of the Cajas Massif is similar to that found in other high mountain districts of glacial origin, differing at both ends of a power law relationship. The deviations for large lakes could be attributed to the space restriction that the altitude imposes in mountain ranges, and, for small lakes, it can be due to many of them already being filled in over time. One of the consequences of this skewed distribution is that most of the lentic water surface is found in medium-sized lakes

and not in shallow lakes and pools. The lake water chemistry is remarkably variable in the area studied, including ionic composition, dissolved organic matter, and metals. The high variation is primarily due to complex overlapping of different volcanic lithologies in the catchments. The chemical diversity is comparable to that of European mountains with complex lithology. The variety of aquatic chemical niches in small territories could foster species richness. The lakes of the Cajas Massif show primarily warm monomictic mixing regimes and not annual polymixis, as traditionally suggested for these lakes. Polymixis occurs only during a limited period of the year (2-3 months) and more permanently in the highest lakes (~4,000 m a.s.l.). The results obtained in this thesis can likely represent other lake districts of the Andean range.

RESUMEN

Los Lagos tropicales de alta montaña en el continente Sudamericano están ubicados en las partes altas de la cordillera de los Andes en la zona ecuatorial (Venezuela, Colombia, Ecuador, Perú y Bolivia), altitudinalmente se encuentran sobre la línea de bosque (3000-5000 m s.n.m.). Generalmente son ecosistemas remotos lo que los hace muy comparables con otras zonas lacustres montañosas del planeta. Cumplen un rol importante en la hidrología de las zonas andinas tropicales, regulando el flujo y la disponibilidad del agua, además son fuente vital de agua potable, regadío e hidroelectricidad y suministran agua a grandes afluentes del río Amazonas y costas del Océano Pacífico.

El desarrollo de la limnología tropical ha sido lento, se ha dado énfasis al estudio de los grandes ríos como el Amazonas y sus lagunas periféricas debido en parte a su riqueza biótica excepcional, pero estudios a largo plazo no son comunes en las regiones tropicales a pesar del número de lagos existentes y que constituyen una importante proporción de los recursos mundiales de agua dulce. Paradójicamente la limnología de los lagos tropicales de alta montaña ha sido relegada a un segundo plano a pesar de que la mayoría de estos sistemas se ubican en zonas de reserva natural, los escasos estudios disponibles muestran que la limnología de los lagos tropicales varía significativamente a lagos de zonas templadas, es por eso que la limnología tropical no sería de extraordinaria importancia si los ambientes acuáticos tropicales pudieran entenderse fácilmente a partir de los principios que se aplican a los sistemas templados.

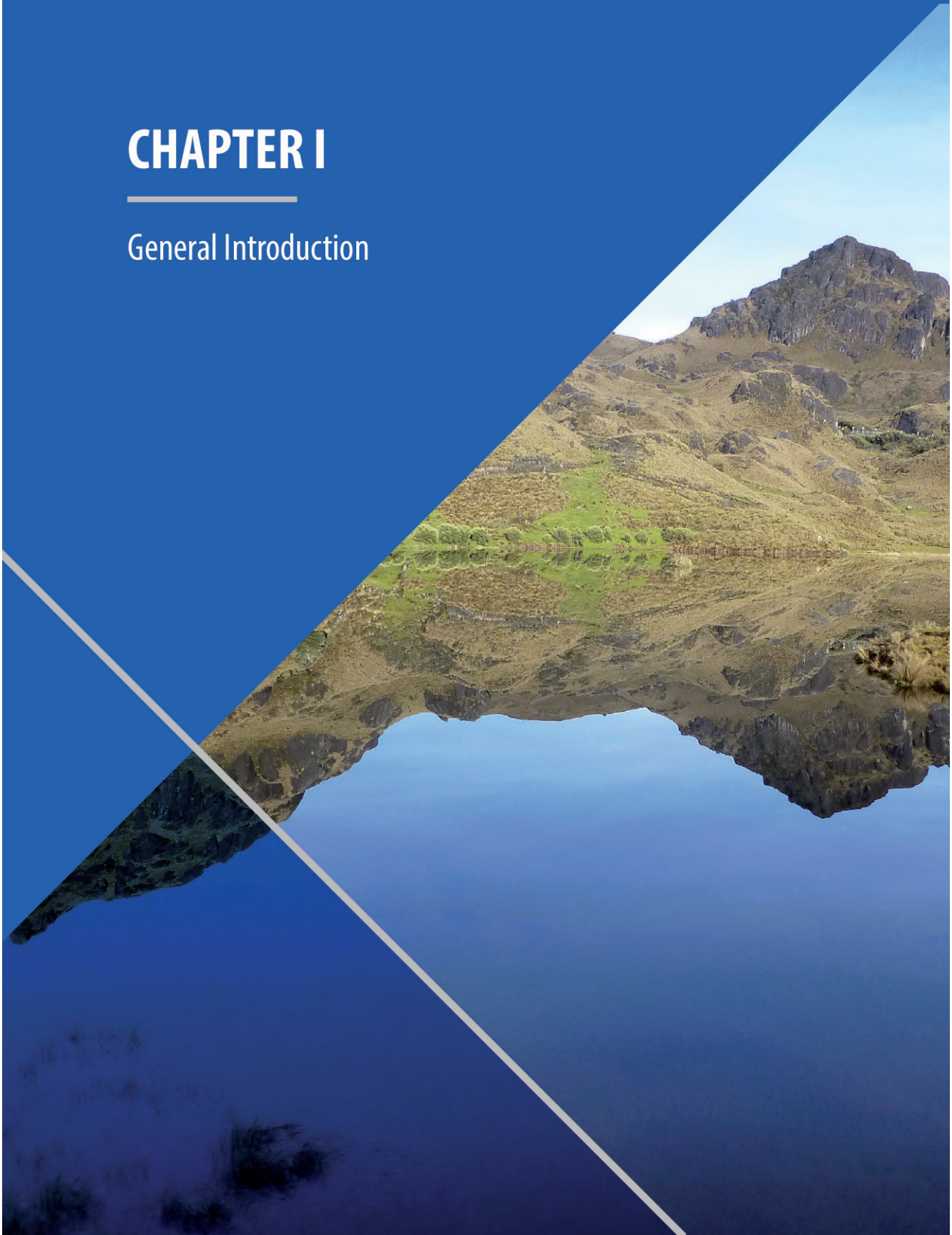
El principal objetivo de la presente tesis es ampliar el conocimiento de limnología tropical de los lagos de alta montaña de los Andes sur de Ecuador a través del estudio de las características hidromorfométricas de los vasos lacustres, la variación química del agua y de los procesos de mezcla. Nuestros resultados muestran que

el patrón de distribución de la abundancia del área lacustre del Macizo del Cajas es similar al encontrado en otros distritos de alta montaña de origen glaciar, difiriendo en ambos extremos de una relación de ley de potencias. Esta desviación para lagos grandes puede ser atribuida a la restricción de espacio que la altitud impone en las cadenas montañosas y para lagos pequeños puede deberse a que muchos de ellos ya han sido rellenados en el tiempo. Una de las consecuencias de esta distribución sesgada es que la mayor parte de la superficie del agua léntica se encuentra en lagos de tamaño mediano y no en lagos someros y charcas, lo que tiene relevancia en los procesos hidrológicos y biogeoquímicos. La química de las aguas lacustres es extremadamente variable en los Andes (composición de iones, materia orgánica disuelta y metales) la misma que se asocia a complejas sobreposiciones de litologías volcánicas en las cuencas, produciendo una diversidad química que es comparable al rango de todas las cadenas montañosas europeas, lo que genera una variedad de nichos químicos acuáticos en territorios relativamente pequeños que podrían fomentar la riqueza de especies que son sensibles a una composición química del agua específica. En cuanto al régimen de mezcla en los lagos del Macizo del Cajas se observa que un régimen cálido monomíctico es el patrón más extendido y no la polimixis anual, como se ha sugerido tradicionalmente para estos lagos. La polimixis ocurre solo durante un período limitado del año (2-3 meses). Un régimen polimíctico se limita a los lagos más altos (~4.000 m s.n.m.).

Esta tesis contribuye a aumentar el conocimiento de la limnología tropical de alta montaña, los resultados obtenidos probablemente podrían ser extrapolables hacia otros distritos lacustres de las cadenas montañosas Andinas.

CHAPTER I

General Introduction



1.1 High-mountain tropical limnology

Across the planet's high mountains, lakes are primary landscape components and probably one of the most comparable ecosystems globally. The main mountain systems (the Alps, the Pyrenees, Sierra Nevada, Scandinavian mountains, the Tatras, the Caucasus, the Pamirs, the Hindu Kush, Karakorum, Himalayas, Rocky Mountains, the Andes, Kenya, Rwenzori, Kilimanjaro, the Carsteusz Mountains, Ruapehu, among others) have associated lake districts (Catalan et al., 2006). Many of them are the product of the Last Glaciation, therefore, being relatively young ecosystems.

High-mountain lakes are often remote, so their ecological dynamics are not primarily driven by human action in their catchments. They are in environments characterized by cold temperatures, high incident solar radiation, with an even higher ultraviolet fraction (UVR), experiencing prolonged ice and snow cover in temperate regions, and diluted waters in a usually oligotrophic state (Moser et al., 2019). These characteristics, in turn, affect the biota composition and ecosystem functioning of mountain lakes, differentiating them from other lakes across the planet (Wolfe et al., 2003; Catalan et al., 2006; Hobbs et al., 2010).

Despite their latitudinal variation and local conditions, due to their remoteness and wide distribution, high-mountain lakes are excellent sentinel ecosystems to assess present and past environmental changes at regional and global scales (Catalan, & Rondón, 2016). Many are part of areas of high natural value, also becoming flagships of natural heritage conservation.

The high-mountain tropical lakes are located between the Tropic of Cancer in the northern hemisphere at approximately 23°26' N and the Tropic of Capricorn in the southern hemisphere at 23°26' S. In South America, they are present in the upper parts of the Andes range, in Venezuela, Colombia, Ecuador, Peru, and Bolivia.

Altitudinally, they are above the continuous forest line in the Páramo biome (Gunkel, 2000; Vásconez, et al. 2011; Sarmiento, 2012).

High-mountain lakes in the Andes are typically referred to as Andean lakes. This terminology groups lakes in the tropical zone and those in the Andean temperate zone (Chile and Argentina). Therefore, although there is no classification of Andean lakes, the most appropriate terminology to refer to the lakes considered in this thesis would be “Tropical Andean lakes.” Their glacial origin mainly characterizes them, although there are also lakes of volcanic origin, which in terms of morphometry, water chemistry, and biology, could be considered a different group within the high Andean panorama (Steinitz- Kannan et al., 1983; Gunkel & Beulker, 2009).

The lower limit of high-mountain lake districts tends to be at a higher altitude in tropical zones (>3000 m a.s.l.) than in temperate regions due to the predominance of glacial origin. The upper limit depends on the orogenic features. Lakes can be found close to 5000 m a.s.l. in some parts of the Andes (Cordillera Blanca – Peru). In general, high-mountain tropical lake districts tend to show lower lake density and greater isolation between lake groups than the large mountain ranges of the temperate zone (Lewis, 1996).

High-mountain lakes play an essential role in the hydrology of the tropical Andean zones, regulating the flow and availability of water and being a vital source of drinking water, irrigation and hydroelectricity for more than 10 million people living in or near the Andes. (Luteyn, 1992; Bradley et al., 2006). They also supply water to the large tributaries of the Amazon River and rivers that flow to the Pacific Ocean. Despite this high relevance for the populations located in the upper part of the basins (Balslev & Luteyn, 1992; Bradley et al., 2006), little is known about the lake characteristics and limnological functioning. Few studies are available; most were developed in the 1980s in an isolated way in the Andean context.

The limnology of tropical zones has suffered a disconnection of almost three decades in the tropical Andean region.

At present, the interest of the scientific community in these tropical lake districts has increased, fostered by the impacts of global change in mountain systems. However, the lack of limnological studies at large spatial and long temporal scales has limited the interpretation of the newly gathered data. Therefore, it is necessary to be able to clearly define the fundamental aspects of Andean high-mountain tropical lakes, such as the range and variation patterns of lake morphology, the chemistry and biogeochemistry of water, the stratification regimes, and the interaction between them (Catalan & Donato Rondón, 2016).

1.2 Lake density and morphometry

The number, size, and shape of lakes are critical determinants of the ecological functionality of a lake district, many key ecological processes in lakes scale with size (Fee, 1992; Post et al., 2000). Therefore, the size distribution of lakes is a crucial constraint on their ecological and biogeochemical patterns. In particular, an accurate characterization of the size distribution of Earth's lakes is critical for estimating global rates of productivity and greenhouse gas emissions (Lewis, 2011).

The estimate of the number of lakes on the planet indicates that they could be distributed according to the power law throughout the size gradient (Downing et al., 2006). Consideration of a broader size range has shown that small lakes (Lakes < 1 km²) deviate from the power law distribution and are less abundant than expected (Seekell et al., 2013; Cael et al., 2022). Investigations of the deviation of small lakes from a power law distribution are of great practical importance since estimates of global lake productivity and greenhouse gas emissions are generally based in part on calibrating a power law distribution based on large area lakes and then using

this distribution to extrapolate the size and abundance of small lakes. If the lakes were to fit a power law distribution over the entire range of lake sizes, there would be an order of magnitude error, i.e., more lakes with sizes from 0.01 to 1 km² than exist on the surface of the Earth (Cael and Seekell, 2016).

To increase the reliability and comparability of the observations, it is essential to develop comprehensive regional inventories of high montane lakes and to characterize the distribution along the lake size gradient, mainly in tropical areas where there are not yet complete inventories of the high mountain lake districts. The structuring mechanism of the geomorphology of the majority of Andean lakes (Colinvaux et al., 1997) was the glacial processes that persisted until the late Pleistocene (~126,000-11,800 cal. BP), possibly generating a morphological uniformity of these systems in the different lake districts of the Andean region or at least in those of the tropical zones of the Andes.

On the other hand, the lakes' average aspect ratio (length versus depth) resulting from the glacier's erosive action depends on the landscape's unevenness. Subarctic lakes are larger than alpine lakes of similar depths. Few studies have shown that tropical lakes of glacial origin are morphologically closer to sub-Arctic lakes than temperate-zone alpine lakes, perhaps because they occur at higher altitudes in more open landscapes (Catalan & Donato Rondón, 2016). Studies have focused on relatively large lakes, and some regions have mostly ignored the multitude of small lakes. Less biased studies probably provide a distribution with more features similar to temperate high montane lakes. Furthermore, lakes with other origins are more common in tropical areas than temperate ones. Lakes of volcanic origin may predominate over large tropical areas on different continents (Catalan & Donato Rondón, 2016).

The aspect ratio is relevant because depth provides stability, while length facilitates the action of the wind (Imberger, 1985). Therefore, in low-aspect-ratio lakes, lower density gradients can maintain upwind stratification. In general, high-mountain lakes tend to have a low aspect ratio. However, based on the few existing data, high-mountain lakes in the tropics could be morphologically closer to subarctic lakes than temperate alpine lakes.

1.3 Water chemistry

Within the tropical limnology literature, one of the topics with the most publications available after phytoplankton studies is the chemistry of lakes. However, many studies only refer to a particular lake, either of glacial or volcanic origin. Few studies address groups of lakes, and, in particular, there are no complete studies of lake districts relating the chemistry of water bodies to the characteristics of the catchment (e.g., geology, soils, and vegetation cover). The interpretation of the water chemistry of high-mountain tropical lakes is still very biased by the existing few studies.

These studies describe these systems as oligotrophic with cold waters all year round (temperature < 20 °C); well oxygenated, although the deep layers may present a well-marked oxycline during the year; low ionic strength (conductivity < 100 $\mu\text{S cm}^{-1}$) due to low solubility of the rock of its basins; high values of allochthonous dissolved organic matter; and absence of the ice cover that is common in temperate zones (Steinitz-Kannan et al., 1983).

Because most mountain lake districts in the tropics are located in areas influenced by volcanism (Donato-Rondón, 2010), the most significant differences in chemistry compared to temperate zones may be related to the major ions, organic matter, and metals. Calcium is usually the dominant cation; however, in areas with strong volcanic influence, other cations may become dominant (e.g., Mg, Na) (Degefu et al., 2014).

In temperate zones, organic carbon loads from the watershed, vegetation, and soils are generally low, and lake water shows low dissolved organic carbon content (DOC generally $<1 \mu\text{g C L}^{-1}$). In general, DOC is correlated with the development of soils in the basins (Camarero et al., 2009b). In some tropical areas, the development of coarse organic soils is common (e.g., páramo vegetation); therefore, higher allochthonous carbon loads may be expected (Buytaert et al., 2006). Unfortunately, available measurements of DOC in these regions are still scarce (Eggermont et al., 2007); despite that, colored waters have been reported from the Andes in Ecuador, Colombia, and Bolivia.

High DOC contents have several limnological implications for high mountain lakes, including a screening effect against high UV radiation (Aguilera et al., 2013) and an increase in oxygen demand unrelated to the production within the lake. In stratified waters, oxygen related to DOC decomposition can give rise to thick hypoxic and anoxic layers despite being oligotrophic systems. These deep anoxic layers could have relevant implications for the biogeochemical pathways within these lakes and the biota inhabiting them.

Little information is available on nitrogen deposition in tropical high mountain areas and the effects it may cause (Matson et al., 1999). In general, the atmospheric load in a particular site depends on the geographical position of the lake with respect to the emission areas and the circulation of the air masses (Camarero and Catalán, 1996). Continuous fire episodes in tropical lowland areas can drive the high-altitude deposition of some elements (Peters et al., 2013), as can continuous burning in the same tropical mountains.

1.4 Mixing regimes

The concept that tropical high-mountain lakes are weakly stratified, showing a polymictic regime, is widespread (Hutchinson, & Löffler, 1956; Löffler, 1964; Steinitz-Kannan et al., 1983). However, other authors classified these lakes as warm monomictic with stratification periods more extended than temperate lakes (Lewis, 2000). Currently, some authors speak of changes in the stratification regime of these lakes in recent decades, suggesting a change from a polymictic regime to one of continuous stratification for most of the year. These changes would result from the effects of the increase in regional temperature and decrease in wind speed in the Andean region (Michelutti et al., 2016). Indeed, the lack of studies in lakes of the high Andean tropics and the discontinuity in time have not allowed for defining their morphological characteristics, thermal mixing regimes, and much less the processes that direct them.

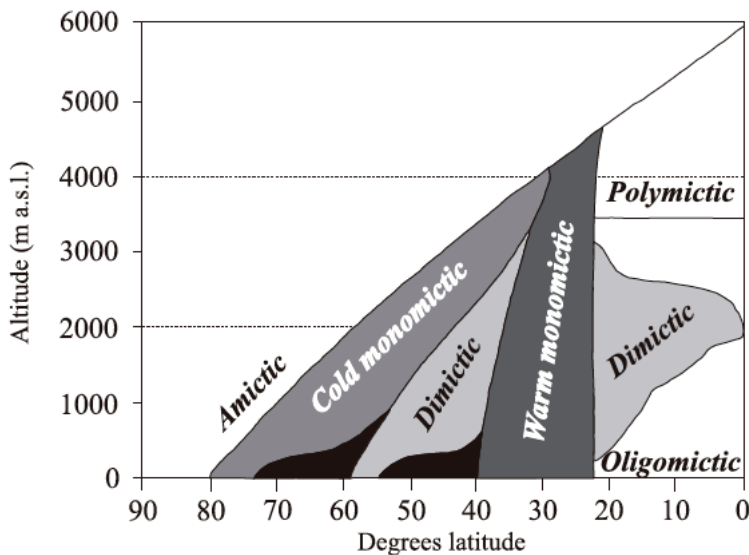


Figure 1. The global distribution of lake mixing regimes concerning latitude and altitude (after Wetzel 2001, from Skowron, 2009).

The importance of defining the mixing regime of a lake lies in the fact that the stratification and mixing processes are the predominant regulators of almost all the physicochemical cycles and, therefore, the metabolism of the lake and its productivity (Wetzel, 2001). On the other hand, the lake's morphology and drainage basin directly influence the water's physical and chemical properties, such as turbulence levels, circulation currents, gas exchanges, and thermal stratification (Hutchinson, 1957; Ambrosetti & Barbanti, 2002).

Lewis (2000) describes the importance of tropical lakes in the world context and highlights the confusion that still exists in the typological classification proposed by Hutchinson and Löffler (1956). Lewis, in turn, defines that the correct typology for lowland tropical lakes is monomictic but with variations of polymixis in lakes whose relative depth is less and meromixis in lakes with greater relative depths. Since the high-mountain tropical lakes deviate from the tropical context of the lowlands, with totally different geomorphological and climatic conditions, it is relevant to assess in greater detail its morphological characteristics, stratification and mixing processes, and the variations in temperature and oxygen associated with these processes, as well as the influence of altitude, regional and local climate, and the interactions between morphological elements and thermal conditions of these lakes (Catalan, & Rondón, 2016).

1.5 The Cajas Massif lake district

In Ecuador, most high-mountain lakes are protected, and most of them are located in territories that are part of the National System of Protected Areas (SNAP) established in 1981. Of the 51 defined areas, 17 are wholly or partially protected. páramo areas of the Andean mountains (Steinitz-Kannan, 1997; MAE, 2007). The Cajas National Park (PNC) within the Cajas Massif, as an Andean ecosystem, constitutes a lake district of high national importance since it supplies more than 60% of the water required for

consumption in the city of Cuenca, the third largest in Ecuador. The lake district is the source of the two main rivers that cross the city: the Tomebamba and the Yanuncay. It is located in the southern center of the Republic of Ecuador, 20 km west of Cuenca. Geographically, the lake district occupies the territories of the Western Cordillera of the South of the Ecuadorian Andes between $2^{\circ} 44' 29''$ - $2^{\circ} 56' 23''$ S and $79^{\circ} 8' 21''$ - $79^{\circ} 23' 3''$ W, with an altitudinal range from 3,150 to 4,460 m a.s.l., and an area of 285 km² (Fig. 2).



Figure 2. Location of the Cajas National Park in Ecuador.

The Cajas Massif contains the complete record of the geological-geomorphological processes of the last glacial period that gave rise to the formation of pronounced “U”-shaped valleys, numerous rosary-type or “paternoster” lakes, lateral and terminal moraines, and other glacial elements (Hutchinson, 1957; Hansen et al., 2003). It constitutes a unique physiographic formation within the Andean mountain system, with approximately 13 water bodies per square

kilometer. The lake district holds more than 5000 water bodies, many protected within the Cajas National Park (Fig.2). The diversity in the morphology of the ponds and lakes is high, and there is a wide range of lithologies of volcanic origin. These properties facilitate studies with general implications for tropical high-mountain limnology.

OBJECTIVES

This doctoral thesis aims to analyze the limnological variability of tropical high-mountain lakes through the study of the lacustrine masses of the Cajas Massif (Ecuador). The thesis is divided into three chapters addressing fundamental aspects, such as morphometry, water chemistry, and lake mixing regimes.

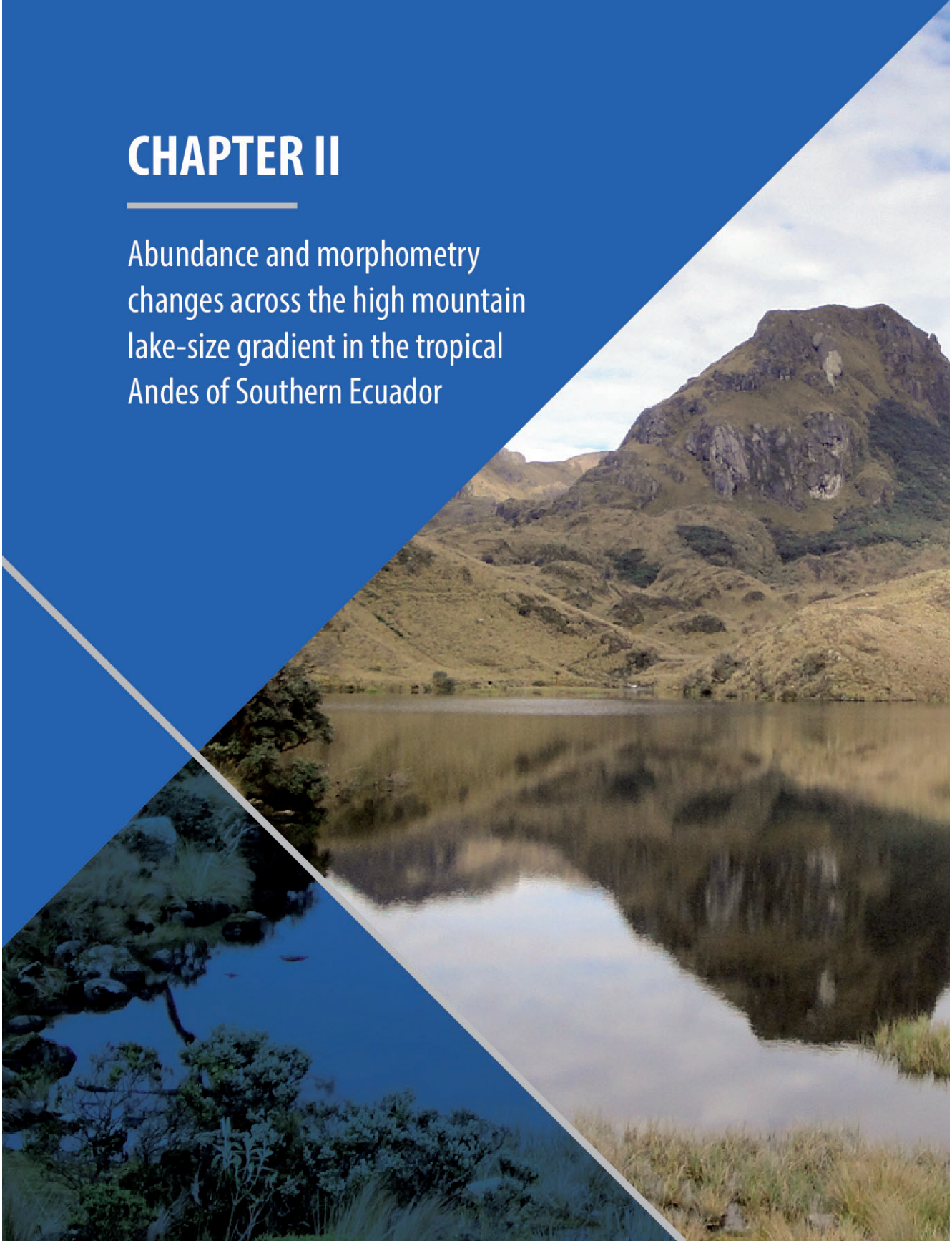
Chapter 2 aims to determine the lakes' morphometric characteristics (2D and 3D) across the size gradient and discuss its relationship with their origin and ontogenic processes.

Chapter 3 aims to characterize the water chemical variation and analyze how it correlates with the catchments' lithology, soil characteristics, and vegetation.

Chapter 4 aims to characterize the mixing regimes based on temperature high-resolution time series at characteristic depths across the year and in a set of lakes distributed across the altitudinal gradient. For one of the lakes, the processes are further characterized by calculating the heat and momentum fluxes.

CHAPTER II

Abundance and morphometry
changes across the high mountain
lake-size gradient in the tropical
Andes of Southern Ecuador



The number, size, and shape of lakes are key determinants of the ecological functionality of a lake district. The lake area scaling relationships with lake number and volume enable upscaling biogeochemical processes and spatially considering organisms' metapopulation dynamics. These relationships vary regionally depending on the geomorphological context, particularly in the range of lake area $<1 \text{ km}^2$ and mountainous regions. The Cajas Massif (Southern Ecuador) holds a tropical mountain lake district with 5955 water bodies. The number of lakes deviates from a power-law relationship with the lake area at both ends of the size range; similarly to the distributions found in temperate mountain ranges. The deviation of each distribution tail does not respond to the same cause. The marked relief limits the size of the largest lakes at high altitudes, whereas ponds are prompt to a complete infilling. A bathymetry survey of 202 lakes, selected across the full-size range, revealed a volume-area scaling coefficient larger than those found for other lake areas of glacial origin but softer relief. Water renewal time is not consistently proportional to the lake area due to the volume-area variation in mid-size lakes. The 85% of the water surface is in lakes $>10^4 \text{ m}^2$, and 50% of the water resources are held in a few ones (ca. 10) deeper than 18 m. Therefore, mid and large lakes are by far more biogeochemically relevant than ponds and shallow lakes in this tropical mountain lake district.

2.1 Introduction

Many ecological processes in lakes scale with size (Fee 1992; Post et al. 2000). Lake-size distributions play a pivotal role from biogeochemistry to community ecology; e.g., for upscaling metabolism or emission processes to regional and global contexts or investigating species distribution and metacommunity dynamics. Based on this interest, the estimation of the number of Earth's lakes indicated that they could be power-law distributed across the full size-gradient (Downing et al. 2006). In the initial data sets used, nonetheless, there was a cut-off for small lakes or were operatively underrepresented. Consideration of a broader size range has shown that small lakes deviate from the power-law distribution and are less abundant than previously expected, although they still dominate inventories (Cael and Seekell 2016). Consequently, there is a current need to investigate the regional patterns of small water bodies (sub-kilometer scales) and unveil the geomorphological processes that may drive and constrain them.

Remote lakes, defined as those in which human activities in the catchment are not the primary drivers of their dynamics, are of interest for tracking the footprint of global change at regional and planetary scales (Hobbs et al. 2010; Catalan et al. 2013). Many of these lakes are of glacial origin and located in high mountains all over the planet and Arctic and subarctic regions. They are typically relatively small (Catalan et al. 2009b) and thus their abundance may likely deviate from the general Earth's scaling (Cael and Seekell 2016). In the case of mountain lakes, the relieve imposes additional topographical limitations that cause deviations from lake size distributions in flatter regions (Seekell et al. 2013). There is an increasing relevance of high mountain lakes in the assessment of global change, including climatic (Smol 2012; O'Reilly et al. 2015), pollution aspects (Grimalt et al. 2001; Yang et al. 2010) and the interaction among both (Psenner and Schmidt 1992).

To increase the reliability and comparability of the observations, it becomes fundamental to develop comprehensive regional mountain lake inventories and characterize the abundance-area distribution across the lake-size gradient. Recent changes in the thermal seasonal patterns in remote lakes are calling attention in the current warming situation (Sorvari et al. 2002; Smol 2012). Inevitably, observations are performed on a few sites. The degree by which the observations can be extended to a large number of lakes requires some regional knowledge of the lake basin morphometric scaling.

Under a similar external forcing, the physical behavior of lakes depends on to the lake aspect ratio (area vs. volume) (Imberger 2012). The available data on lake volume distributions are more limited than the lake area ones as the former cannot be easily inferred from remote sensing and GIS modeling as the latter. In practice, it is commonly assumed that the lake volume-area scaling does not change for lakes of similar origin. However, this assumption may not always apply, or dispersion around a general pattern may be high (Cael et al. 2017). Some lakes may be on watersheds with relief, bedrocks or soils that erode more quickly than others. On the other hand, high mountain lake districts provide excellent frameworks for the understanding of species distribution in habitats that occur discretely (that is as “islands”) in a matrix of unsuitable leaving space for organisms (de Mendoza et al. 2017). The metapopulation and metacommunity dynamics of the species highly depend on the abundance, density and size structure of the habitats (Logue et al. 2011). One can expect that research on this topic will increasingly take advantage of the high mountain natural experimental setting.

There is an increasing interest in tropical high-mountain lake systems and climate change (Michelutti et al. 2015a). The information about these ecosystems is sparser than for mountain lakes in temperate zones (Catalan and Donato-Rondón 2016). Particularly, there is still only a partial knowledge of the seasonal and interannual variability in the lake mixing and stratification

patterns. If there is any current paradigm, this is based on a few sites of unknown representability for the whole set of lakes. A large group of tropical high mountain lakes is situated along the Andean range in the equatorial zone (i.e., at Venezuela, Colombia, Ecuador, Peru and Bolivia), above the tree line, between 3500 and 4500 m a.s.l. in the Paramo ecosystem (Gunkel 2000; Donato-R 2010). These lakes play a significant role in the hydrology of the region by regulating the availability and supply of water. Eventually, they feed both the great tributaries of the Amazon and rivers draining to the Pacific Ocean. Part of the water is used for human consumption, industry, irrigation, and electricity generation for millions of people who live in or nearby the Andean range (Luteyn 1992; Buytaert et al. 2006). Climate change may result in severe threats for water supply (Bradley et al. 2006). Despite their relevance as ecosystems and water resources, there is little information available on the limnology of the Andean tropical lakes (Catalan and Donato-Rondón 2016; Van Colen et al. 2017). Some of the studies were carried out in the 1980s, and 1990s (Steinitz-Kannan et al. 1983; Donato-R 2010) but knowledge on the hydrogeomorphology of these lakes is extremely scarce (Rivera Rondon et al. 2010).

In Ecuador, most of the high mountain tropical lakes are situated within national protected areas, out of which, 17 areas are found entirely or partially in the Paramo mountain belt (Steinitz-Kannan 1997). Herein, the Cajas National Park (Cajas NP), located in the austral region of Ecuador, contains a large number of lentic systems, which provide drinking water to nearly the 60% of the population of Cuenca, the third largest city in Ecuador. In fact, the National Park is embedded in a large UNESCO Biosphere reserve comprising the entire Cajas Massif. In this area, geomorphological processes occurring at the last glacial period resulted in an exceptionally high density of lakes above 3400 m a.s.l. (i.e., 13 lake km⁻²). In this study, we aim at characterizing the lake's morphometry across the full-size gradient and providing scaling relationships for the region and similar tropical high-mountain lake districts in the Andes.

We performed an inventory of all the high-mountain lakes of glacial origin in the Cajas Massif and determined their area using GIS information. For a representative lake subset in the Cajas NP, we carried out a bathymetry survey to complete the morphometric characterization. We compare the relationships found with those in other alpine and lowland locations and discuss the results according to current geomorphological theories. The lake abundance and morphometric relationships derived constitute a comparative framework for current and future ecological, biogeochemical and physical research in these lakes and the basis for a more robust geographic upscaling of the processes investigated and informed management of the protected areas.

2.2 Materials and Methods

The region and study sites

The studied lakes are situated in the Cajas Massif by the south of Ecuador, between 3° 11' 26" and 2° 40' 21" South; and 79° 9' 09" and 79° 17' 57" West. An inventory of all the lakes and ponds of glacial origin (5955) was intended for the region, and a representative subset of them (202) was selected within the Cajas NP for a bathymetry survey (Figure 1). For the sake of brevity, we will use “lake” as the general name for water bodies of any size throughout most of the text. The 45 % of the area drains to the Pacific Ocean, and the remaining 55% to the Atlantic. The primary bedrock is volcanic (Tarqui formation), including rhyolite, andesite, tuff, pyroclastic and ignimbrites (Hungerbühler et al. 2002).

The regional geomorphology was shaped by glacier activities until the late Pleistocene when the ice retreated around 17,000 – 15,000 years ago (Colinvaux et al. 1997; Hansen et al. 2003; Rodbell et al. 2009). Part of the glacier footprint is a large density of relatively small lakes above 3400 m above the sea level (a.s.l.), except Lake Llaviucu located at a lower altitude (3146 m a.s.l.) at the backside of a terminal frontal moraine of a large glacial tongue. The main soil

types at the region are non-allophanic Andosols and Histosols from volcanic origin (Borja and Cisneros 2009; Crespo et al. 2011). Both types present dark colored epipedons characterized by high organic matter content, high porosity, low apparent density (400 kg m^{-3}) and a high water retention capacity (in average, 6 g g^{-1} at a pressure of 1500 kPa), with higher values in the H horizon (Buytaert et al. 2005).

Most of the rainfall is retained in soils and released gradually to the water courses, regulating the hydrology of these ecosystems (Poulenard et al. 2003; Buytaert et al. 2005). The vegetation in 91% of the total extent of the Cajas NP and about 50% of the massif is herbaceous with a dominating presence of the genera *Stipa* and *Calamagrostis* (Ramsay and Oxley 1997). Concerning woody vegetation, only *Polylepis* spp. is present above the 3400 m a.s.l. Lower altitudes -below the alpine lake inferior limit- are covered by the high mountain forest (“bosque montano”). At present, the main impacts of land use and human activities on vegetation are tourism, fishery, grazing and localized burning of the vegetation. Annual precipitation is between $900 - 1600 \text{ L m}^{-2} \text{ y}^{-1}$ with contrasting seasons and high variation from year to year (Vuille et al. 2000; Celleri et al. 2007; Padrón et al. 2015). High rainfall causes enhanced soil erosion with deposition of light-colored clastic laminae in the sediments of some lakes (Rodbell et al. 1999).

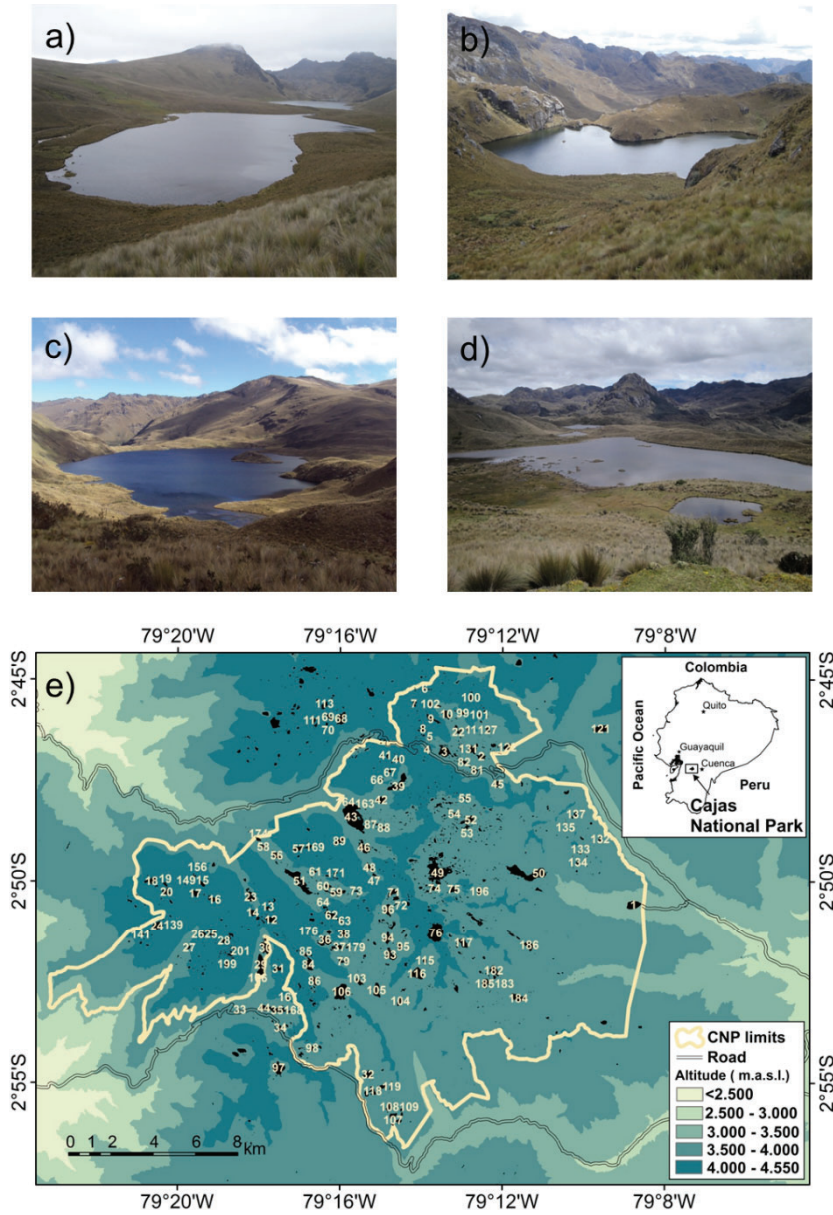


Figure 1. Some representative lake images from the Cajas National Park (CNP) (Cascarilla 3-086 (a), Fondococha-007 (b), Luspa-043 (c), and Apicocha 1-081 (d)) and a map (e) with an indication of the lakes included in the bathymetry survey. The numbers refer to identification codes that have been used in the scope of the current study (see **Table S1**).

Lake inventory and area, and perimeter estimation

The boundaries of each lake were generated by heads-up digitalization of the aerial photographs of the project SIG-Tierras (2010-2014, www.sigtierras.gob.ec/) for the zone of the Cajas Massif. The images were orthorectified and georeferenced and had a spatial resolution of 30 x 30 cm². Only one digitizer performed the manual task, for consistency, and several people repeatedly checked for omissions and mistakes. ArcGIS 10.0 (ESRI Inc., Redlands, CA, USA) was used with a screen zoom of the photographs always below a scale of 1:200. The scale of cartographic digitalization was 1:5000. The area and perimeter of each lake were calculated from the digitized contour shapefile using the ArcGIS 10.0 calculator and the altitude from the raster of the SIG-Tierras digital elevation model that has a spatial resolution of 3 x 3 m².

Bathymetry survey and lake basin modeling

A selection of 202 lakes and ponds, covering the full size-gradient, was made to perform a bathymetry survey (Figure S1) within the Cajas NP (Figure 1). The survey was carried out with the aid of an inflatable rubber boat (Navigator II, RTS, China), approximately 3.5 m long, equipped with a propeller (2 HP, Yamaha, Japan) and an echo sounder Humminbird® model 1198c SI (Eufaula, AL, USA). The previously digitized lake boundary was used as zero depth reference and for the planning of the number of gridded profiling transects and the spacing between them according to the lake size: for lakes with area > 0.2 km², the transect spacing was around 100 m; for lakes between 0.1 and 0.2 km², around 50 m; and for lakes < 0.1 km², around 25 m. The distance between the bathymetry points not exceeded 5 m. In the shallow lakes and ponds, where the use of the boat was not possible, measurements were taken at several points of the water body using a topographic measuring rod.

The digital bathymetry procedure is described in detail in the supporting information (Text S1). The main steps included: (i) integration of the depth data collected in the field with the data derived from the digitalisation of the orthophotos (i.e. boundaries of

the lakes associated with zero-depth); (ii) data preparation according to the demands of the following processing steps; (iii) selection and application of an appropriate interpolation algorithm for each lake; and (iv) production of the digital bathymetric models and geomorphological parameters. Given the number of lakes considered in the bathymetry survey, the interpolation and quality control analyses were carried out automatically, using the programming framework that Surfer® 13.0 enables in conjunction with PERL (Practical Extraction and Report Language) subroutines.

From the digitalized lake basins several morphometric variables and indicative ratios were determined (Table 1). Fetch, defined as the maximum distance that the wind can travel on the surface of the water before it is intersected, was estimated according to Hakanson (1981).

Table 1. Morphometric descriptors of the 202 lakes and ponds included in the bathymetry survey of the Cajas National Park (Ecuador).

Variable	Acronym	Unit	Mean	Median	Minimum	Maximum
Area	A	m ²	58860	25708	6	774775
Perimeter	S	m	1146	895	10	8795
Fetch	Fetch	m	324	271	4	1563
Maximum length	L _{max}	m	341	274	4	2142
Maximum width	B _{max}	m	175	153	2	956
Mean width	B _{mean}	m	105	92	1	531
Volume	V	m ³	692717	38046	0.6	22369167
Maximum depth	Z _{max}	m	11.0	6.0	0.2	75.5
Mean depth	Z _{mean}	m	4.2	1.9	0.1	30.6
Shoreline development	D _L	--	1.6	1.5	1.0	3.1
Volume development	D _v	--	1.0	1.0	0.4	1.8
Z _{mean} /Z _{max} ratio	Z _{mean} /Z _{max}	--	0.3	0.3	0.1	0.6
L _{max} /B _{mean} ratio	L _{max} /B _{mean}	--	3.3	2.9	1.4	9.9
Relative depth	Z _r	%	4.6	4.2	0.1	15.5
Watershed area	A _w	km ²	2	1	0.000015	48
A _w /V ratio	A _w /V	--	173	12	0.1	10113
Water renewal time	tw _R	day	167	48	< 1	4261

2.3 Results

Lake abundance and size

In the Cajas Massif, all the lakes of glacial origin are $< 1 \text{ km}^2$ in area. Lake abundance (N) increases with declining area (A). Although the fitting of a scaling factor (b) is significant, the distribution deviates from a true power-law at both ends (Figure 2a).

$$N \sim A^b \quad (1)$$

The deviation in the low-size range is not related to a methodological bias as the distribution starts to diverge at values without orthophoto image resolution problems for digitalization (Seekell and Pace 2011). The distribution is also truncated at the large-size range. This kind of truncation has been attributed to the particular situation of mountain lake districts, where there is a decline of the available surface at higher elevations and, therefore, the probability to find large lakes drops above certain altitude (Seekell et al. 2013). The maximum density of lakes in the Cajas Massif occurs about 3936 m a.s.l., and declines symmetrically towards both ends, although without following a normal distribution (Figure S2).

The highest lake is located at 4424 m a.s.l., and the lowest at 3146 m., although the latter is an exception corresponding to a terminal moraine and, in fact, the rest of the lakes are located at elevations > 3400 m a.s.l. If one considers only the lakes around the mean altitude of the lakes (Figure 2b), the distribution becomes less bent at the large-size extreme, whereas, at the small-size end, the shape of the distribution scarcely changes respect to the whole lake set. This feature indicates that the deviation of a power-law at each extreme does not respond to the same cause. The large lake-size tail of the distribution is much affected by altitude than the small lake-size end. Nevertheless, some restriction to the appearance of large lakes remains as the log-log representation of the tail is still not linear (Figure 2b). The truncation may also happen if the study extent is small, which could be the case with the altitudinal restriction.

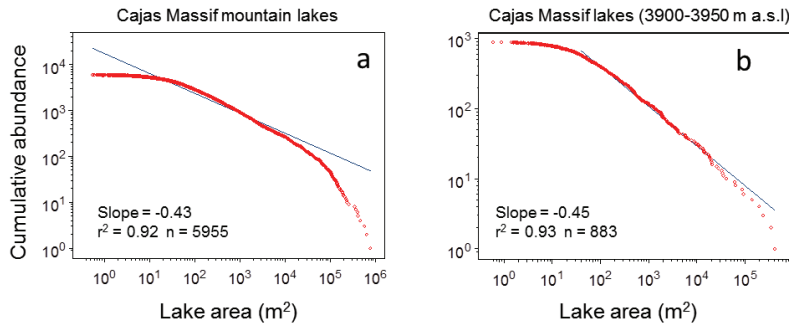


Figure 2. Lake-area distribution in the Cajas Massif (southern Ecuador). a) All high-mountain lakes and ponds from the Cajas Massif. b) Sub-set of lakes around the average altitude of the lake distribution. The straight line indicates a power-law fitting (Equation 1). In (b) only the right linear range was fitted.

Lake shape

The complexity of the shoreline geometry is captured by the relationship between the lake area and the perimeter (Figure 3a). The fractal dimension (D), defined as

$$S \sim \sqrt{A}^D \quad (2),$$

is close to one ($D = 1.079$) for the whole lake set of the Cajas Massif, indicating as such that the lake shape, in general, corresponds to polygons scarcely ramified. Through the size range, there is no significant deviation from this general pattern (Figure 3a).

The shoreline development (D_L) evaluates the departure of the shape from a circle ($D_L = 1$). Most of the lakes show D_L values close to one (Table 1, Figure 3b). This feature, however, relaxes when the size of the lakes increases as larger lakes tend to be more convoluted than the smaller ones (Figure 3b, Figure S3). A few large lakes show elongated sub-rectangular or subcircular forms with sinuous shorelines such as Osohuayco ($D_L = 3.1$) and Toreadora ($D_L = 2.6$), both being within the Cajas NP.

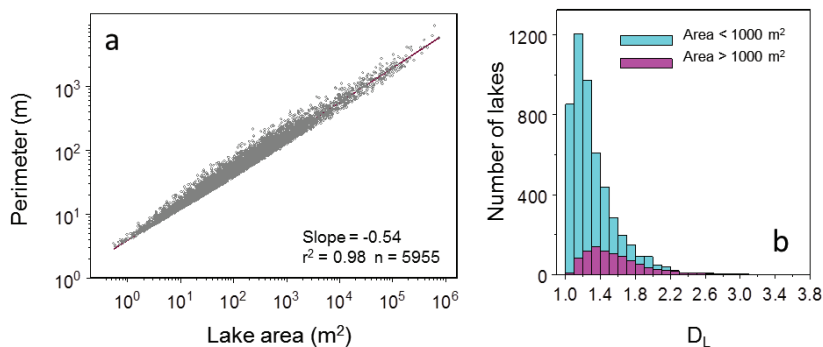


Figure 3. a) Allometric relationship between the area and the perimeter of the Cajas Massif lakes. b) Distribution of the shoreline development (D_L) for lakes with size above and below 1000 m², respectively.

Lake 3-D shape

The bathymetry survey in the Cajas NP provided the basis for extending the lake shape analysis to a third dimension. There is a general significant allometric relationship between lake area (A , m²) and volume (V , m³) that describes the invariance in shape as size changes:

$$V = 0.0107 A^{1.52} \quad r^2 = 0.93 \quad n = 202 \quad (3)$$

The distribution of the deviations from the general relationship (Figure 4) does not appear to be homogeneous across the entire lake-size gradient. Particularly, between 10⁴ to 10⁵ m² the range of lake volumes that correspond to the same lake area may cover two orders of magnitude. In this range, one could suspect the coexistence of two lake morphologies (Figure S4). However, the examination of available geological, geomorphological and edaphological information did not provide any conclusive and robust evidence for such a distinction.

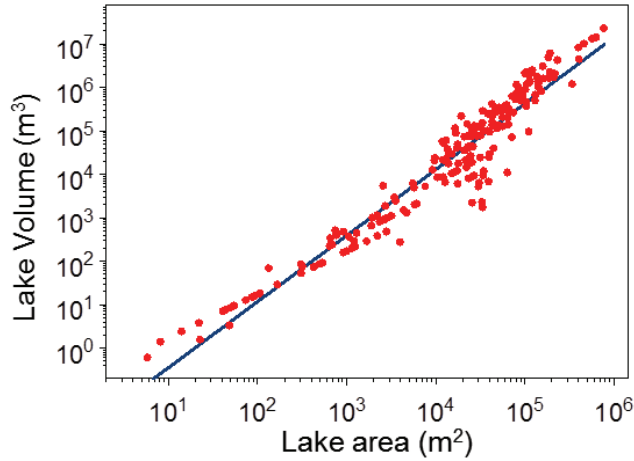


Figure 4. The relationship between area and volume for the lakes of the Cajas Massif based on a survey of 202 lakes and ponds in the Cajas National Park.

Mean and relative lake depth

The majority of lakes are very shallow ($Z_{\max} < 5$ m) (Table 1) as could be expected from the dominance of the small lake areas (Figure S5). Lakes from 10 to 20 m depth (Z_{\max}) are relatively common, and there are only a few deep lakes ($40 < Z_{\max} < 80$ m). The bias towards shallow forms accentuates when considering the mean depth of the lakes (Figure S5) as Z_{mean} is nearly isomorphically proportional to about one-third of the maximum depth.

$$Z_{\text{mean}} = 0.33 Z_{\text{max}}^{1.0268} \quad r^2 = 0.98 \quad n = 202 \quad (4)$$

A vast majority of the water bodies, therefore, show $Z_{\text{mean}} < 5$ m, only a few exhibits $Z_{\text{mean}} > 10$ m and none $Z_{\text{mean}} > 35$ m. The close relationship between Z_{\max} and Z_{mean} facilitates a quick estimation of the lake volume of the Cajas Massif water bodies from a single bathymetric transect and the lake area.

Mean depth is a stabilizing factor against wind mixing action. The amount of momentum that the wind can transfer to the water column depends on the lake fetch. In general, it could be expected a large influence of the wind on the physical structure of most of the lakes. However, there can be contrasting situations among the Cajas NP lakes as there is more variation in fetch than in mean depth (Figure 5a).

The relative depth (Z_r) indicates the ratio between the lake's maximum depth and its mean diameter. It has been used as an indicator of the degree of the basin excavation by the glacier and posterior filling. The Cajas NP lakes show low Z_r values (Figure 5b). Only a few lakes show $Z_r > 10\%$; a value considered the threshold for high over-excavation. It can be thought that either the basins were not so much excavated as in other high mountain ranges, the infilling process has advanced more or a combination of both considerations. In fact, about 20% of the water bodies show $Z_r < 2\%$, which is considered an indication of being closer to an eventual complete filling. The Z_r patterns do not show any correspondence with the watershed orientation and main river basins distribution. Only at the level of relatively small sub-basins, they display a geographical pattern (Figure 5b). Some of these sub-basins show a high proportion of water bodies close to filling up (i.e. Canoas, Culebrillas, Jerez), whereas the highly over-excavated lake basins are scattered over many sub-basins, only Atugyacu is particularly rich in these latter lakes.

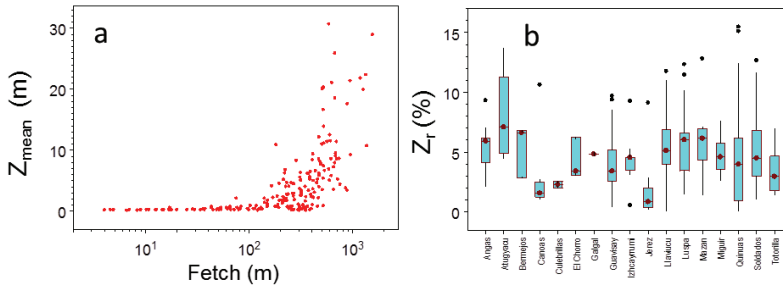


Figure 5. a) Fetch versus Z_{mean} for the lakes of the Cajas National Park (Cajas NP). b) Relative depth (Z_r) distribution (box-plots) for the main lakes in the Cajas NP.

Lake watershed

As could be expected from glacier erosive processes, the larger the watershed, the larger the lake (Figure 6a). However, the tendency is allometric so that the lake's area increases at a lower rate than the respective watershed.

$$A = 1.95 A_w^{0.71} \quad r^2 = 0.86 \quad n = 202 \quad (7)$$

There is not a marked geographical pattern in the lake size distribution across the main sub-basins (Figure 6a). The watershed area and lake volume are the primary determinants of the average water renewal time (t_{WR}) in the lakes of the Cajas NP, provided the relatively homogeneous climate and geological landscape of the area. Under a similar amount of average precipitation, the runoff entering the lakes is proportional to the watershed area, whereas the retention capacity is proportional to the lake volume. Consequently, the morphological dissimilarities among lakes of a similar size result in marked differences in the t_{WR} (Figure 6b). Overall, t_{WR} of a few weeks to a few months largely predominate, and only a few lakes may show average t_{WR} above one or several years.

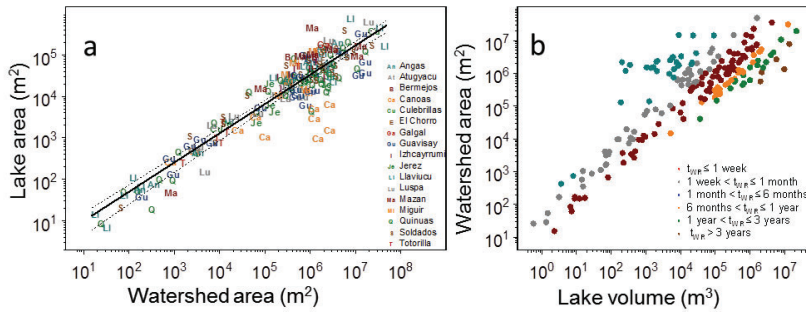


Figure 6. a) Relationship between the watershed area and lake area. The legend lists the sub-basins in the Cajas National Park. b) The relationship between lake volume and watershed area as proxies for water retention capacity by the lake and watershed runoff, respectively. Colors indicate water renewal time (t_{WR}) estimated assuming $1000 \text{ L m}^{-2} \text{ y}^{-1}$ and 35% average precipitation and evapotranspiration, respectively (Crespo et al. 2011).

2.4 Discussion

Lake size distribution

The shape of the distribution of the lake-area abundance from the Cajas Massif (Figure 2a) is similar to those found in other high mountain lake districts of glacial origin (Hanson et al. 2007; Seekell and Pace 2011). The general features are deviations at both ends from a power-law relationship and a slope around -0.5 of a log-log linear fitting (-0.66, -0.43, -0.43 in the Adirondack Mountains, the Northern Highland Lake District and our study, respectively) (Seekell and Pace 2011). It appears as a general feature that the mountain lake distribution differs from a power-law, and the scaling slope is well below one; thus not following the two features that characterize the self-similar distribution of lakes $>1 \text{ km}^2$ in the planet (Lehner and Doll 2004; Downing et al. 2006; Cael and Seekell 2016).

The deviation in the large-size lake extreme has been attributed to the restriction imposed by the departure from a flat surface so that the available area declines with altitude and thus the probability for large lakes diminishes (Seekell et al. 2013). Considering a belt of lakes around the elevation of the highest lake density mitigates this restriction; however, even only fitting the large-size long tail, the slope remains around 0.5, and the distribution does not significantly fit a power-law in the Cajas Massif. It seems, therefore, that there is an additional factor, beyond elevation, modifying the lake size distribution in high-mountain lake districts. Periglacial processes, steep slopes, thin soils and torrential stream flows may have enhanced the lake filling, perhaps at an early phase during deglaciation, when retreating glaciers move high amounts of detrital material and stream flows are rich in glacier flour. The large lakes in the central valleys may have been particularly affected by these processes so that their presence in the landscape has been substituted by flat lands of meandering streams or peatlands.

One of the consequences of the biased distribution is that within the Cajas Massif - and probably in similar mountain lake districts- most of the lentic water surface is in mid-size lakes and not in ponds (Figure 7a). About 50% and more than 85% of the water surface area is on lakes $>10^5$ and $>10^4$ m², respectively. Biogeochemical processes in these systems are thus particularly relevant in the context of gas emissions and watershed and fluvial network dynamics. On the other hand, the still enormous numbers of ponds may be of interest for the metacommunity dynamics of some aquatic organisms restricted or with a preference for these systems (e.g., amphibians).

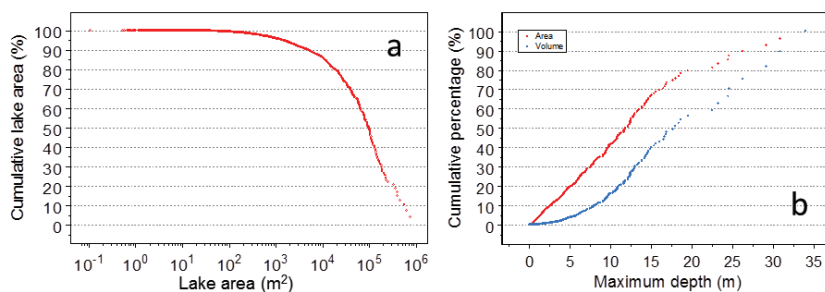


Figure 7. a) Percentage of cumulative lake area from the largest lake to the smallest pond in the Cajas Massif. b) Percentage of cumulative lake volume (blue) and lake area (red) with increasing maximum depth in the Cajas Massif as estimated with equations 3 and 7, respectively.

Lake basin morphology

Earth's lakes $>4.7 \text{ km}^2$ show shorelines with a fractal dimension $D = 1.34$, close to expected predictions ($D = 4/3$) of the percolation theory (Cael and Seekell 2016); whereas lakes $<4.7 \text{ km}^2$ depart from this pattern and show $D = 1.00$. The Cajas Massif lakes are close to the last model ($D = 1.08$), in this case in agreement with the general pattern in relatively flat landscapes. There is no clear departure from this scaling along the lake-size range (Figure. 3a) as may occur if a subset of lakes or ponds become particularly convoluted (Hohenegger et al. 2012). Nevertheless, the shoreline development ratio (D_L) indicates that the larger the lake there is an increasing probability to become sub-rectangular and present sinuous shorelines in some cases (Figure 3b), yet the high scattering prevents from a significant departure from the general pattern. The lakes with higher D_L (e.g., >2) may correspond to cases of flooding of several sub-basins (Figure S3). In any case, for most of the lakes, the differences are relatively small. One can conclude that in these lakes the interaction with terrestrial systems and littoral environments scale similarly throughout the lake-size range.

Large scattering in some parts of the lake-size gradient (e.g., 10^4 - 10^5 m^2) indicate some variation in the geomorphological process

configuring the current lake basins. Several particularities point to a differential lake filling as the cause of the high depth (volume) variation at this mid lake size range. (1) The markedly less noisy relationship between area and perimeter than between area and volume indicates that there has been a transformation of the lake bottoms processes posterior to the lake formation; otherwise, the shape heterogeneity in surface usually also correspond with the 3-D variation (Hakanson 1981). A comparison of the sediment records and detailed watershed bedrock and soil characteristics could provide the necessary evidence on this issue. Up to now, only the sediments of one of the “relatively-shallow” lakes have been cored up to the bedrock (i.e. Pallcacoha, (Rodbell et al. 1999)).

The sedimentary record shows a relatively fast accumulation of light-colored inorganic sediment during Late Glacial and a transition to dark organic-rich gyttja at the onset of the Holocene, with lower accumulation rates. The average rates increase again and accelerate up to present by Mid-Holocene. Part of this acceleration may be due to the observed increasing frequency of ENSO events throughout the Holocene. This situation implies torrential rains that produce clastic laminae in the sediment profile. The volcanic bedrock of the watershed erodes easily, and debris flows and talus are abundant and located not far from the lake. However, the accumulation rate of the dark facies also increases. This feature may be due to natural processes, such as aquatic and subaquatic vegetation growth, with higher retention of fine sediment, or to human land perturbation (e.g. fire) as early cultures in the Andes have affected vegetation and soil stability since ancient times (Coblentz and Keating 2008).

(2) The relative depth of many lakes ($Z_r \ll 10\%$) depart from values typical of over-excavation by glaciers. Assuming that there is no reason for a differential excavation of glaciers in tropical areas, the explanation should rely on an enhanced infilling compared to the temperate zone, which could be related to the soil erodibility and littoral vegetation development both enhanced in tropical volcanic

humid regions. (3) The lakes deviating more from the general relationship between lake and watershed area (Figure 6a) also are lakes that are relatively shallow compared to their areas; for example, those in the Canoas sub-basin. That is, the filling process may have also contributed to reducing the shoreline, although not as much as it has affected mean depth. (4) Lakes relatively deep and relative shallow for intermediate lake areas can be found in the same sub-basins, which indicates that they do not respond to a geographical differentiation of the glacier erosion but rather to strictly nearby site geomorphological particularities.

Despite of the likely profound transformation of some of the Cajas Massif lakes after the excavation of the basin, the general pattern of lake basin formation, illustrated by the patterns between lake area and maximum depth (Figure 8), still agrees with that from alpine lakes in European ranges and differ from those in subarctic areas. In the latter region, lakes are much larger compared to depth than in high mountains (Catalan et al. 2009b). Glacier excavation in the ice accumulation zones depends on the steepness of the slope of the basin. In this aspect, the Cajas' lakes follow the pattern of some of the high-mountain lakes in the Colombian Andes and differ from others there that are closer to subarctic forms (Catalan and Donato-Rondón 2016). Accurate bathymetry surveys comprising a relatively large numbers of high-mountain lakes are not broadly available. It would be interesting to investigate whether the pattern of differential lake filling found in the Cajas NP lakes repeats elsewhere or, alternatively, they are more likely in particular climatic regions (e.g. tropical) and bedrock substrates (e.g. volcanic). Development of littoral and subaquatic vegetation may also play a role, and this could be particularly relevant in tropical high-mountain lakes.

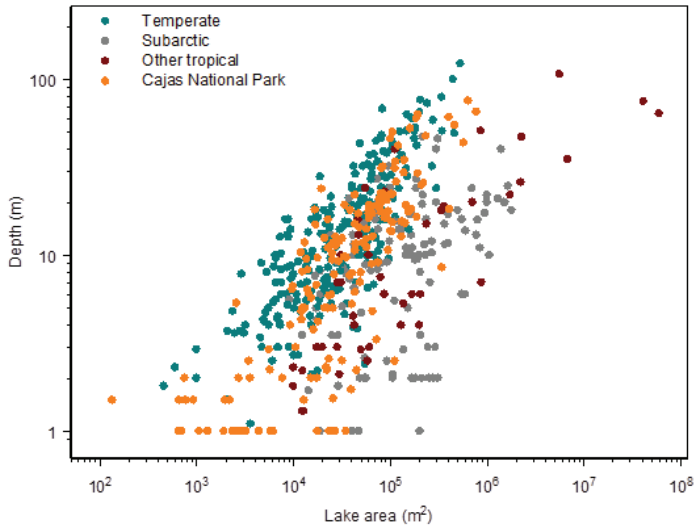


Figure 8. The relationship between lake area and maximum depths for remote lakes. Cajas National Park lakes are compared with a set of European temperate high-mountain lakes, subarctic lakes and tropical high-mountain from other parts of the world, mostly Colombian lakes.

2.5 Conclusions

Inventories of lake and pond areas are increasingly available at higher spatial resolution and become useful for multiple purposes. Lake-size distributions are the basis for upscaling biogeochemical processes to landscape scales, design research projects that depend on the selection of a few sites, and applying management criteria in protected or land used areas. The three activities require either some categorization of the water bodies or the characterization of the continuum variation. The use of lake surface area, which is broadly available, is not sufficient for an accurate functional classification of the water bodies in the Cajas Massif. At long-term, the goal should be to increase the number of maximum depth measurements, at least for those lakes between 7000 and 40,000 m², the range of higher volume-area variation. Then, the use of the corresponding allometric

equations can provide acceptable mean depth and lake volume estimations.

Concerning biogeochemical processes, the results presented herein show that lakes rather than ponds cover much more landscape surface and hold an even larger percentage of water volume (Figure 7). About 50% of the water is contained in a few lakes (ca. 10) >18 m depth (Figure 7b). Water bodies <5 m depth, only account for about 5% of the total water stored. Research regarding the water column physical structure, biogeochemical process and responses to global change merits concentrating in lakes >12 m depth as they hold about 80% of the volume and 50% of the pond and lake surface. However, lake morphology is not the only criteria to take into account. The size of the lake watershed cannot be ignored as they led to renewal times that differ markedly (Figure 6b). The issue becomes particularly critical for lakes with volume >10⁵ m³ as the water renewal times may vary from a few weeks to a few years depending on the watershed size and lake connectivity to the drainage network.

Beyond the identified allometric relationships that allow large-scale estimations and provide criteria for site selection, the detailed bathymetry survey within the Cajas NP constitutes a precise piece of information for research studies and management in the context of climate and other environmental changes. Studies on the thermal structure related to climate change may be preferentially accomplished in the relatively deep lakes, whereas those focusing on watershed transport may select relative-shallow lakes. In any case, all the lakes cannot be accommodated under a similar interpretative umbrella. For instance, in the Cajas NP, paleolimnological studies have been performed in several lakes, some of them referring to climatic and environmental changes during the Holocene and Late Glacial, others addressing current climatic change. The relatively shallow lake Pallcacocha provided a record of El Niño-Southern Oscillation (ENSO) throughout the last 15,000 years by the light-

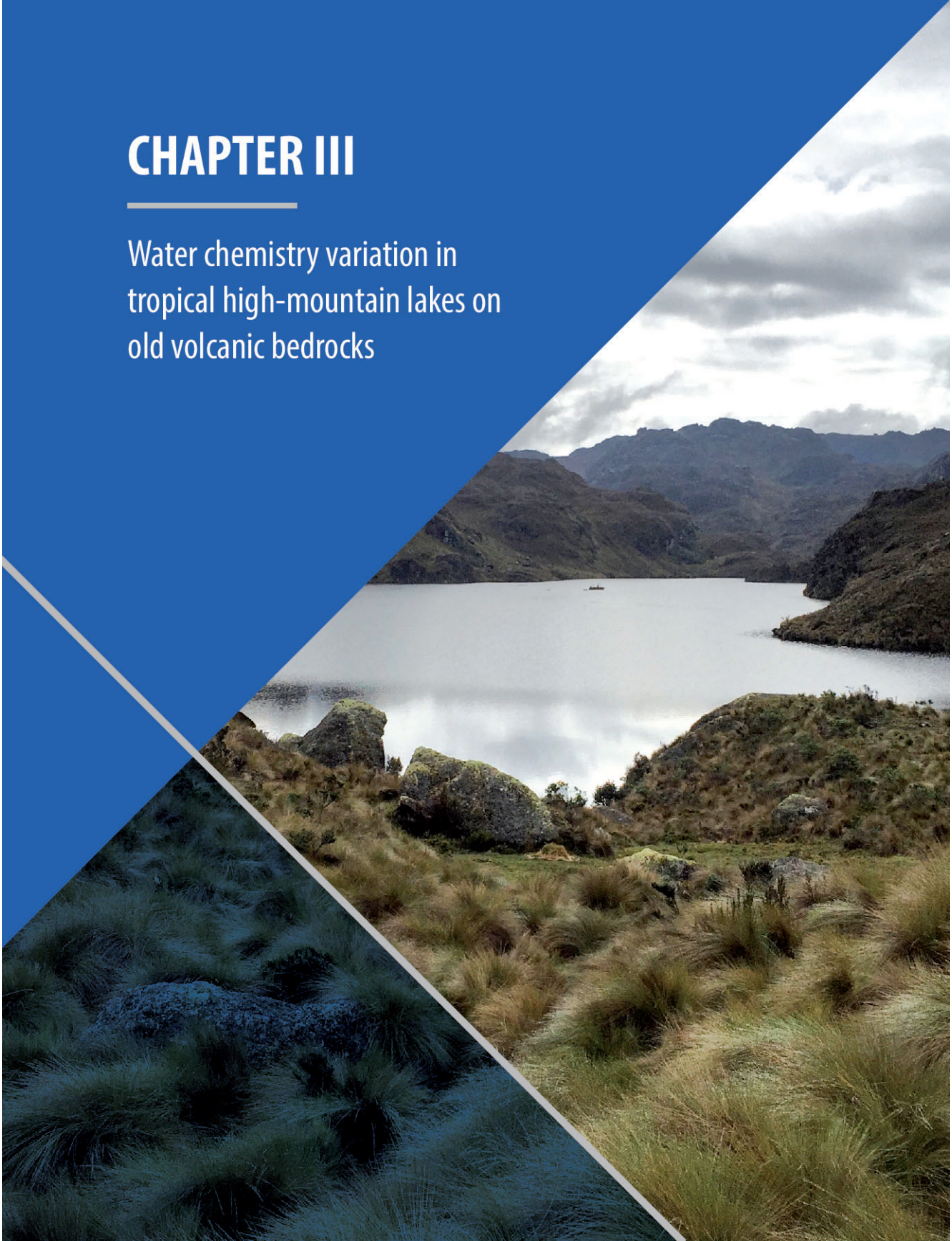
colored clastic laminae produced by storm-induced events (Rodbell et al. 1999). The dynamics of these relatively-shallow lakes, with high water renewal, are mainly dominated by what happens in the watershed and associated stream transport; therefore, they are excellent for reconstruction of extreme rainfall events, vegetation (Hansen et al. 2003) and land use changes. The relatively deep lakes, with water renewal longer than one year, are more appropriate for addressing issues related with proxies generated within the lake (e.g. diatom records) that respond to the physical and chemical characteristics of the water column and their changes throughout the year. These changes may also depend on extreme events, but also on more gentle climatic fluctuations and, particularly, interannual tendencies (Michelutti et al. 2015b). The allometric patterns found in the tropical high-mountain lakes of Southern Ecuador are worth to be investigated in other ranges with the aim of building up a full understanding of the morphometric structure of high-mountain lakes and their implications for biogeochemical and ecological dynamics.

2.6 Acknowledgments

The authors would like to express their gratitude to the “Empresa Publica Municipal de Telecomunicaciones, Agua Potable, Alcantarillado y Saneamiento de Cuenca-Ecuador” (ETAPA EP) and the “Universidad de Cuenca” (UC, Ecuador) for funding this study through the project “Caracterización limnológica de los lagos y lagunas del Parque Nacional Cajas”, which was carried out in the Aquatic Ecology Laboratory (LEA) of the UC and directed by HH and RFV. Additionally, MA and HH were funded by the PROMETEO Project of the Ecuadorian Secretary for Higher Education, Science, Technology and Innovation (SENESCYT). Special thanks go to the assistant Mario Dominguez who worked in the LEA and contributed to the development of the different field sampling campaigns. JC was supported by LACUS project funded by the Spanish Government research grant CGL2013-45348-P, Ministerio de Economía y Competitividad.

CHAPTER III

Water chemistry variation in
tropical high-mountain lakes on
old volcanic bedrocks



Water chemistry and its ecological implications have been extensively investigated in temperate high-mountain lakes because of their role as sentinels of global change. However, few studies have considered the drivers of water chemistry in tropical mountain lakes underlain by volcanic bedrock. A survey of 165 páramo lakes in the Cajas Massif of the Southern Ecuador Andes identified four independent chemical variation gradients, primarily characterized by divalent cations (hardness), organic carbon, silica, and iron levels. Hardness and silica factors showed contrasting relationships with parent rock type and age, vegetation, aquatic ecosystems in the watershed, and lake and watershed size. Geochemical considerations suggest that divalent cations (and alkalinity, conductivity, and pH) mainly respond to the cumulative partial dissolution of primary aluminosilicates distributed throughout the subsurface of watersheds, and silica and monovalent cations are associated with the congruent dissolution of large amounts of secondary aluminosilicates localized in former hydrothermal or tectonic spots. Dissolved organic carbon was much higher than in temperate high-mountain lakes, causing extra acidity in water. The smaller the lakes and their watersheds, the higher the likelihood of elevated organic carbon and metals and low hardness. The wetland area in the watershed favored metals in lakes but not organic carbon. Phosphorus, positively, and nitrate, negatively, weakly correlated with the metal gradient, indicating common influence by in-lake processes. Overall, the study revealed that relatively small tropical lake districts on volcanic basins can show chemical variation equivalent to that in large mountain ranges with a combination of plutonic, metamorphic, and carbonate rock areas.

3.1 Introduction

Orogenesis provides crystalline bedrock with low permeability and, consequently, past glacial excavation promoted lake districts on many high mountains around the world (Jacobsen and Dangles 2017). The water chemical composition of these lakes is driven by atmospheric deposition, geological background, watershed and in-lake biological activity, and human influence (Psenner and Catalan 1994). Crystalline rocks usually lack readily soluble minerals; therefore, lakes and headwaters in mountains show low salt content and low acid-neutralizing capacity, making them sensitive to acidic deposition. As a consequence of the "Great acceleration" (Steffen et al. 2015), emissions of sulfur and nitrogen oxides to the atmosphere caused the acidification of ecosystems in remote areas, including mountains in North America (Beamish and Harvey 1972) and Europe (Massabuau et al. 1987).

High-mountain lakes became indicators of the acidification process and its ecological impact (Kopáček et al. 1998; Rogora et al. 2001). Interest in the biogeochemistry and biota of mountain lakes has increased, and as a result, information and knowledge have been accumulating over the last decades (Catalan et al. 2009b). Currently, high-mountain lakes across the globe are considered sentinels of the systemic change of the planet (Moser et al. 2019).

In this context, there is a growing interest in tropical high-mountain lakes (Michelutti et al. 2015b; Van Colen et al. 2017; Benito et al. 2019; Steinitz-Kannan et al. 2020; Zapata et al. 2021), which have historically received less attention (Eggermont et al. 2007). Although high-mountain lakes are amongst the most comparable ecosystems globally, and a common conceptual framework might be used to analyze them (Catalan and Donato-Rondón 2016), tropical high-mountain lake regions have unique environmental characteristics that require special attention. Seasonal weather changes are low, and mean air temperature and rainfall are higher

than in temperate high-mountain lake districts (Jacobsen and Dangles 2017).

The chemical composition of water in temperate high-mountain lake districts is primarily related to the bedrock (Psenner 1989; Nauwerck 1994; Marchetto et al. 1995; Kamenik et al. 2001). Although the ionic strength is consistently lower than that of low-land waters, temperate mountain lakes on metamorphic, plutonic, or carbonate rocks may markedly vary in acidity and dominant ions under similar sea salt- and human-influenced atmospheric deposition (Catalan et al. 1993). Mountain lake districts that show considerable chemical variation usually have a high diversity of bedrock composition, common in large massifs and ranges resulting from old collisional orogeny (Camarero et al. 2009). Uplifted and bent sedimentary rock landscapes may include highly metamorphosed materials, which eventually surround intrusive igneous rocks. Slates rich in sulfides may provide highly acidic waters, granitic batholiths have very low ionic levels, whereas carbonate bedrock holds alkaline waters (Marchetto et al. 1995). This broad range of chemical conditions provides niche gradients for species segregation (Catalan et al. 2009a).

Many tropical lake districts are located on volcanic bedrock in young accretionary orogenic belts. Therefore, the chemical diversity that results from weathering could be expected to be lower than in the ranges of high lithologic diversity. Furthermore, alpine areas in temperate zones continuously expose fresh rock to chemical weathering, fostered by cryofracturing of bare rock and unstable slopes. In tropical zones, warmer conditions and high vegetation cover likely diminish the availability of exposed surfaces, with rock weathering relegated to deep subsoils. Soils in tropical high-mountain lake districts have a postglacial origin. Despite their relatively young origin, they are depleted in exchangeable cations because of the high rainfall and relatively warm temperature (Molina et al. 2019).

Therefore, we might expect less chemical diversity and lower acid-neutralizing capacity in mountain lakes on tropical volcanic bedrock than in temperate mountain lake districts. However, the limited data available suggests that significant variation may occur (Armienta et al. 2008; Catalan and Donato-Rondón 2016), perhaps related to the higher weatherability of basaltic lithologies compared to granite (Dupre et al. 2003), which may result in higher temporal and spatial heterogeneity of the process over the same substrate.

Consequently, this study aimed to comprehensively analyze the primary drivers of water chemistry variation in a tropical lake district on volcanic bedrock. We performed an extensive survey of the lakes and ponds (n=165) in the Cajas Massif in the Andes of Southern Ecuador and measured the main chemical components of surface waters. The chemical variation was related to lake and watershed morphological characteristics, volcanic geological formations, and land cover. We evaluated the possible mechanisms behind the observed patterns concerning rock weathering in the spatially complex lithology provided by volcanism and a water-saturated cold tropical landscape that fosters organic matter accumulation. Finally, we briefly discuss the potential ecological implications of the chemical variation for constraints and ecological thresholds in species distributions and metacommunity dynamics.

3.2 Material and methods

Study sites and sampling

The Cajas Massif in the Southern Ecuador Andes contains approximately 6000 lakes and ponds of glacial origin (Mosquera et al. 2017a). The present study included data from 165 water bodies (Fig. 1), mainly within the Cajas National Park (CNP). Lakes (> 0.5 ha) were selected proportionally to their density in the two main hydrological basins of the CNP (western, eastern) and fifteen subbasins (Fig. S1). Two other watersheds outside the park were also included to consider the lakes at the highest altitudes. In each

subbasin, we sampled the largest lakes and a proportion of the rest (>50%) based on altitude and size distribution (Table 1). When visiting the lakes, ponds were opportunistically sampled by heuristically selecting those of varying characteristics (e.g., transparency, macrophyte cover). Lake bathymetries are available from all water bodies (Mosquera et al. 2017a). Although the area studied was relatively small (~334 km²), it represented the entire Cajas Massif variation in lithology, vegetation, and aquatic ecosystems.

The landscape corresponds to páramo ecosystems with surplus water (Carrillo-Rojas et al. 2016). Seasonal and interannual rainfall modes correspond to the equatorial Andes (5° S-1° N), characterized by a bimodal regime with wet periods from February to April and October to November associated with a westward humidity transport from the equatorial Amazon (Segura et al. 2019) with occasional extreme fluctuations conditioned by the equatorial Pacific (Oñate-Valdivieso et al. 2018; Schneider et al. 2018). Although the Amazonian air masses tend to lose humidity over the eastern flanks of the cordillera, rainfall occurs throughout the year (only ~12% dry days) at the lake district elevation, primarily as drizzle (~80% duration), with mean annual precipitation in the Cajas Massif from ca. 900 to 1400 mm, with the maximum around 3400 m a.s.l. (Padrón et al. 2015). Cloud condensation is common, and fog interception can increase conventional rainfall by > 25% (Rollenbeck et al. 2011).

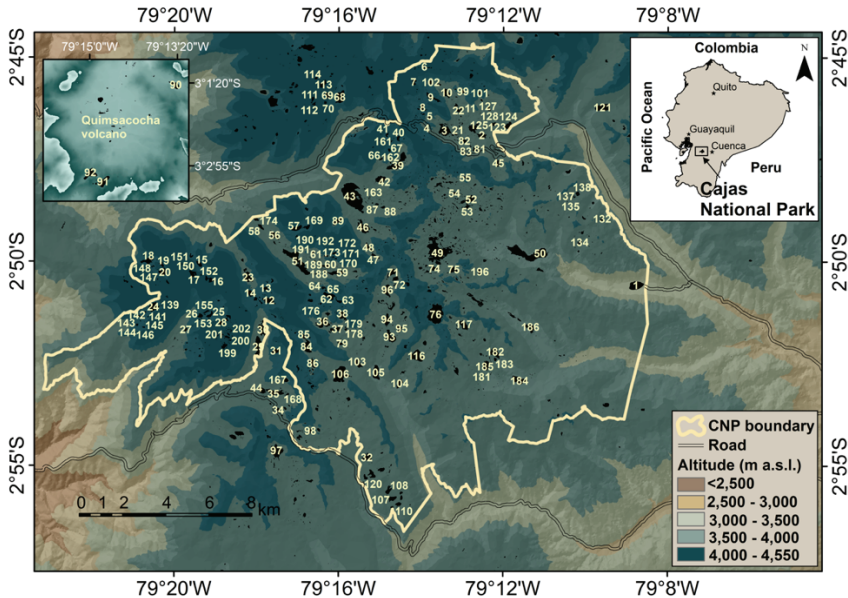


Figure 1. Location of the study area and lakes. The large majority are located in the Cajas National Park (162), and some are in the Quimsacocha volcano area (3) and Sangay National Park (Culebrillas lake, #157, not shown). Identifiers correspond to codes from Mosquera et al. (2017b).

A lake survey for chemical analysis was carried out during 2014–2015. Lakes with >1-m depth (76%) were sampled at the deepest point from a dinghy; shallower lakes and ponds were sampled from the shoreline. The upper mixed layer was determined by performing temperature profiles, and water samples were collected using Van Dorn bottles (3 L) every two meters and integrated. Water samples were immediately screened (64- μ m mesh) to remove zooplankton and debris before being cold stored and transported to ETAPA EP labs in the nearby city of Cuenca (Ecuador) for analysis. For nitrate, soluble reactive phosphorus (SRP) and dissolved organic carbon (DOC) samples were filtered using precombusted (450 °C, 4 h) GF/F Whatman® (Maidstone, UK) 47-mm \varnothing glass fiber filters and Swinnex® (Merck Millipore, USA) syringes.

Table 1. Summary of the physical features of 165 lakes and ponds sampled for this study.

Variable	Unit	Minimum	1st Quartile	Median	Mean	3rd Quartile	Maximum
Latitude, N	degrees	-3.05	-2.86	-2.84	-2.83	-2.80	-2.42
Longitude, E	degrees	-79.35	-79.29	-79.26	-79.26	-79.23	-78.86
Altitude	m a.s.l.	3152	3856	3958	3945	4043	4294
Maximum depth	m	0.15	1.50	8.25	13	18	76
Mean depth	m	0.05	0.50	2.5	4.8	6.6	30.6
Area	m ²	22	12,177	32,012	68,698	81,331	774,775
Volume	m ³	3.2	6214	72,124	841,645	521,336	22,369,167
Watershed area	km ²	0.00002	0.28	0.98	2.74	2.19	47.70

Chemical analysis

Standard methods for water chemical analyses were followed (APHA-AWWA-WEF 2012). Sodium, potassium, silica, aluminum (only for 2019-2020 samples), iron, and manganese were determined by inductively coupled plasma spectrometry (SM 3120 B; ICP-OES, Optima 7000 DV, PerkinElmer, USA); calcium and magnesium by EDTA titrimetric methods (SM 3500-Ca B and 3500-Mg B); alkalinity by potentiometric titration (SM 2320Bb); sulfate by a turbidimetric method (SM 4500 SO₄²⁻ E); chloride by mercuric nitrate titration (SM 4500-Cl⁻ C); SRP and total phosphorus (TP) following the method of Murphy and Riley (1962), the latter after potassium persulfate digestion; nitrate was reduced to nitrite and determined by colorimetry (SM 4500-NO₃⁻ E); ammonium by the salicylate method (10012, HACH, USA), total organic carbon (TOC), and DOC by acidic digestion (Method 10129, HACH).

Conductivity at 20 °C was measured using a YSI-EXO-1 sensor (Yellow Springs, Ohio) and pH with a WTW 3320 pH meter (Xylem Analytics, Weilheim, Germany) equipped with a sensor for low-ionic-strength samples (SenTix® HW). Apparent color was determined spectrophotometrically using platinum-cobalt standards (SM 2120 C). Ultrapure water type 1 was used in blanks and reagents. Precision varied across compounds, and the wide range of concentrations analyzed: 3-20% relative standard deviations. Accuracy was better than 5% in all analyses. Analytical quality assessment was performed using ion balance, ion-calculated vs. measured conductivity, and ion-estimated vs. measured alkalinity (Moiseenko et al. 2013). Samples with marked deviations corresponded to low ionic strength, which showed overestimated calcium (1) or magnesium (4) levels, which were substituted by zero values in the numerical analyses. Chloride was not considered in the factorial analysis because of the high number of values below the quantification limit. For other variables, limits of quantification were used in the numerical analyses (Table 2). During the 2014-2015 laboratory analysis, no aluminum measures were performed.

However, for a subset of ten lakes of the original survey, aluminum data were available from monthly sampling during 2019-2020, which were only used to confirm some mineral equilibrium assumptions.

Geomorphology, lithology, and land cover

Three main drivers important for water chemistry variation were considered: the parent rock, the ultimate primary source of solutes; land cover, which may condition water-rock interactions; and watershed and waterbody morphology that may determine the interaction duration. Climate is relatively similar across the survey area (Padrón et al. 2015); therefore, altitude was the only variable considered as a surrogate of potential climatic effects.

Lake and watershed geomorphological descriptors (1:5000) were available from Mosquera et al. (2017b), whose site coding was maintained. Geological information was extracted from a 1:100,000 geological map (Dunkley and Gaibor 2009), which was used to calculate the area of the main lithostratigraphic classes for each lake watershed. The Cajas bedrock corresponds to a complex imbricate layering of volcanic formations (i.e., eight in the surveyed lakes) of varying age (7-37 Ma), from the late Eocene to Miocene, and some minor areas of intrusive rocks (Table S1, Fig. S1). The geological formations vary in dominant parent rock (rhyolite, andesite, dacite, and diorite) and material (tuffs, breccia, lava, lapilli, and sandstone), but all of them show a large secondary variability within the formation.

Although the páramo landscape appears relatively homogeneous at first glance, lake watersheds may markedly differ in vegetation cover and development (Fig. 2). The identified land cover classes included páramo grassland vegetation (e.g., *Calamagrostis*), *Loricaria* and *Gynoxis* shrubs, *Polylepis* open forest, montane evergreen forest, rocky páramo, bare rock, eroded land, wetlands, rivers, and water bodies (Fig. S2). The land covered by the respective classes was

uneven (Table S2), and the montane forest was exclusively present in the Lake Llaviucu watershed. The land cover map was produced by heads-up digitalization of the aerial photographs of the project SIG-Tierras (2010–2014, www.sigtierras.gob.ec). The images ($30 \times 30 \text{ cm}^2$ resolution) were orthorectified and georeferenced. Only one digitizer performed the manual task for consistency, and several people repeatedly checked for omissions and mistakes. ArcGIS 10.0 (ESRI Inc., Redlands, CA, USA) was used with a screen zoom of the photographs consistently below a 1:200 scale. The scale of cartographic digitalization was 1:5000. The area of each land cover class within the lake watershed was calculated from the digitized land cover contour shapefile, and the lake watershed shapefile ($3 \times 3 \text{ m}^2$ resolution) using the ArcGIS 10.0 analysis tools and summarize function.

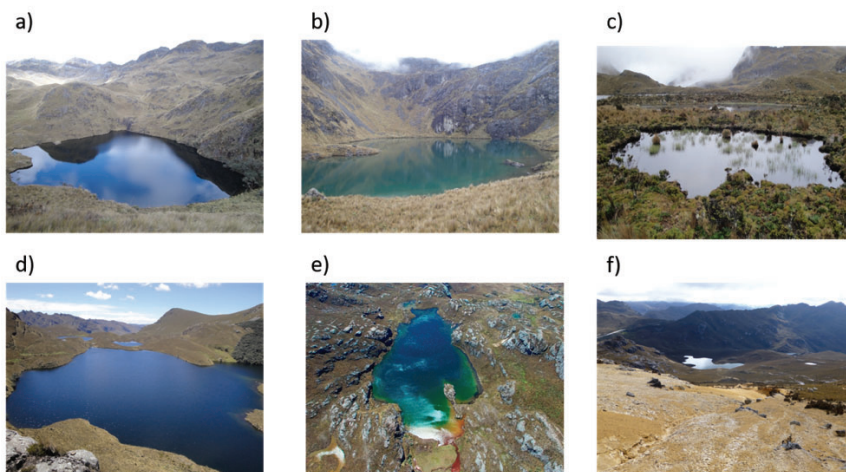


Figure 2. Some illustrative lakes and landscapes from Cajas Massif in Southern Ecuadorian Andes: (a) Laguna de la Cascada, #99; (b) Cardenillo, #100; (c) Cocha totorilla 1, #149; (d) Ingacasa, #36; (e) Estrellascocha de Quitahuayco; and (f) example of the land cover class "eroded land".

Numerical analyses

Descriptive statistics, analyses of variance, Tukey's honest significant differences, and other statistical analyses detailed below were performed using R (v. 4.0.4). Except for pH and silica, most water chemistry components had a skewed distribution; hence they were log-transformed in numerical studies. Maximum likelihood factor analysis (*factanal* R-function) was used to investigate the correlation structure among the water chemistry variables. Varimax rotation was applied to facilitate axis interpretation, and the optimal number of factors was determined using the *nFactors* R-package. The influence of potential drivers on the main water chemistry variation was investigated using multivariate linear regression (*lm* R-function) based on altitude, geomorphological, lithological, and landcover descriptors. Fifteen explanatory variables were considered; lake mean depth, watershed/lake area ratio, main rock proportions (rhyolite, dacite, and diorite), geological formation age, land cover proportions (páramo, rocky páramo, *Polylepis* forest, shrubs, bare rock, eroded land, water bodies, and wetlands), and altitude. Andesite, the most common substrate across lake basins, determines the typical conditions from which other substrates can cause deviations. Therefore, only the percentages of the other three substrates were included as potential deviations from the andesite norm.

Drivers with skewed distributions were log-transformed (i.e., mean depth, watershed/lake ratio), and all of them were standardized (z-scores) to obtain coefficients that directly indicate the degree of influence in the regression. We ranked all possible models (2^{15}) using the corrected Akaike's information criterion (AIC_c), which is more appropriate for relatively small datasets, and the *dredge* function from the MuMIn R package (v.1.43.17). Regression coefficients were standardized to allow comparisons of their relative magnitudes between the models. The coefficients of all models with an $AIC_c < 4$ higher than the lowest AIC_c were averaged (*model.avg* function): the coefficient absolute mean deviation from zero

indicates the variable explanatory capacity and the coefficient range shows the uncertainty associated with that deviation (Dormann et al. 2018). Speciation and solubility diagrams were determined using Geochemist's Workbench® (Aqueous Solutions LLC, Champaign, IL, USA), version GWB 2021, SpecE8, and Act2 programs, respectively (Bethke 2008).

3.3 Results

Water chemical variation

The Cajás lakes typically showed low ionic content, circumneutral pH, low nutrient, and slightly brownish conditions (Table 2). Although the ionic content was relatively low (conductivity always $<200 \mu\text{S}_{20} \text{ cm}^{-1}$), most water bodies were not sensitive to acidification (alkalinity $> 200 \mu\text{eq L}^{-1}$). Acidic water bodies (i.e., $\text{pH} \ll 6.5$) were uncommon and limited to small ponds. Calcium was commonly the dominant cation, although magnesium also showed high values and was dominant in a subset of lakes (Fig. 3). The potassium concentration was extremely low compared to other cations, including sodium. Bicarbonate and sulfate could be dominant among the anions (Fig. 3), yet the latter was not associated with acidic conditions. Chloride levels were generally below quantification limits (Table 2), which indicated an atmospheric origin consistent with the low chloride content ($<10 \mu\text{eq L}^{-1}$) in the deposition of Southern Andes (Beiderwieden et al. 2005). High values ($\sim 30 \mu\text{eq L}^{-1}$) were only found in the Quinuas river basin, close to the only mountain road crossing the study area, which connects Cuenca and Guayaquil cities (e.g., lakes 81-83, Fig. 1). Nitrogen components had extremely low concentrations; ammonium was always below the quantification limit, while nitrate concentration seldom exceeded $>1 \mu\text{eq L}^{-1}$. Phosphorus values were also usually low; therefore, water bodies were oligotrophic, with few exceptions. The lake color ranged from crystal clear to reddish and brown tones. Accordingly, organic matter (TOC and DOC) and iron content revealed a wide variation (Table 2).

Table 2. Summary of the water chemistry variation in the study lakes of the Cajas Massif, Southern Ecuadorian Andes.

Variable	Units	Minimum	Quartile-1	Median	Mean	Quartile-3	Maximum
Conductivity	$\mu\text{S}_{20} \text{ cm}^{-1}$	4.3	28	48	52	69	191
pH		4.6	6.6	7.0	7.0	7.5	8.5
Calcium	$\mu\text{eq L}^{-1}$	$\sim 0^{\dagger}$	200	400	457	640	1922
Magnesium	$\mu\text{eq L}^{-1}$	$\sim 0^{\dagger}$	71	116	138	194	697
Sodium	$\mu\text{eq L}^{-1}$	5	29	44	47	61	117
Potassium	$\mu\text{eq L}^{-1}$	$<3^{\ddagger}$	$<3^{\ddagger}$	3	4	6	37
Alkalinity	$\mu\text{eq L}^{-1}$	47	260	440	525	720	2208
Sulfate	$\mu\text{eq L}^{-1}$	10	55	76	88	104	343
Chloride	$\mu\text{eq L}^{-1}$	$<10^{\ddagger}$	$<10^{\ddagger}$	$<10^{\ddagger}$	-	$<10^{\ddagger}$	30
Silica	$\mu\text{mol L}^{-1}$	13	67	90	90	108	196
Nitrate	$\mu\text{eq L}^{-1}$	0.01	0.02	0.15	0.26	0.34	2.8
TP	$\mu\text{mol L}^{-1}$	0.02	0.12	0.22	0.26	0.31	1.40
SRP	$\mu\text{mol L}^{-1}$	$<0.02^{\ddagger}$	$<0.02^{\ddagger}$	$<0.02^{\ddagger}$	0.05	0.05	0.61
TOC	mg L^{-1}	0.15	3.6	5.0	5.9	6.6	$>21^{\ddagger}$
DOC	mg L^{-1}	0.15	2.1	3.0	4.1	5.3	$>21^{\ddagger}$
Apparent color	CU	7	20	28	37	39	187
Iron	$\mu\text{mol L}^{-1}$	0.18	0.64	1.07	1.71	1.92	15.25
Manganese	$\mu\text{mol L}^{-1}$	0.05	0.11	0.25	0.43	0.48	5.04
Aluminum*	$\mu\text{mol L}^{-1}$	1.30	1.83	1.97	2.11	2.15	3.20

TP, total phosphorus. SRP, soluble reactive phosphorus. TOC, total organic carbon. DOC, dissolved organic carbon. \dagger , estimated by cation-anion balance because below quantification limits ($20 \mu\text{eq L}^{-1}$ for calcium and magnesium, and $15 \mu\text{eq L}^{-1}$ for chloride). \ddagger , beyond quantification limit values. *, data only for 10 lakes. Ammonium was below the quantification limit ($1 \mu\text{eq L}^{-1}$) in all lakes.

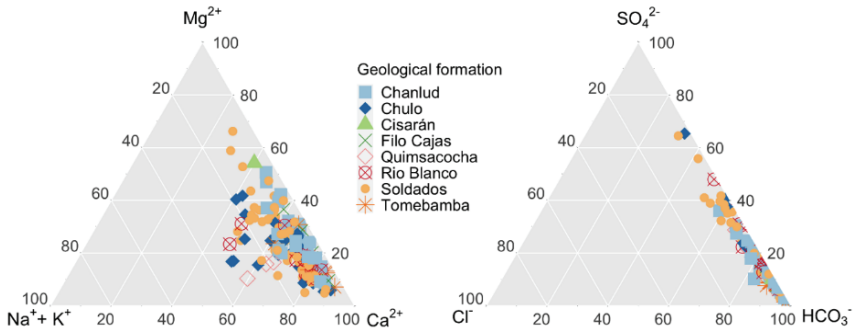


Figure 3. Ternary diagrams of the relative ionic water composition of the study lakes. Symbols indicate the predominant geological formation in the lake watershed.

The chemical variables showed clear correlation patterns (Fig. S3). The factor analysis indicated that these relationships could be summarized by four main latent factors, which explained 53% of the total variance (Table 3). F1 could be interpreted as a total ionic strength factor, provided mainly by calcium and magnesium cations (water hardness) that primarily determined alkalinity and conductivity values, with a secondary sodium contribution (Table 3). The higher the F1 score, the lower the apparent color and TP. Therefore, the higher the alkalinity, the more transparent and less productive the environment becomes. F2 denoted the organic matter content, which appeared largely independent of the inorganic chemical characteristics, and was only weakly associated with the apparent color.

Table 3. Variable loadings on four significant main axes (F1-F4) of a water chemistry factorial analysis.

Variable	F1	F2	F3	F4
log (Alkalinity)	0.98		0.17	
log (Conductivity)	0.91		0.29	
log (Calcium)	0.90			
pH	0.70		0.17	
log (Magnesium)	0.50			
log (TOC)		0.98		0.16
log (DOC)		0.77		
log (Sodium)	0.41		0.83	
Silica		-0.20	0.74	
log (Potassium)			0.43	0.34
log (Sulfate)			0.26	
log (SRP)			-0.22	0.14
log (Iron)	-0.18			0.93
log (Manganese)				0.56
log (Apparent color)	-0.34	0.33	-0.22	0.50
log (TP)	-0.31			0.23
log(Nitrate)				-0.17

*Only loadings $>|0.14|$ are shown. Factors explained 22, 11, 10, and 10 percent of the total variation, respectively.

F3 was primarily related to silica and monovalent cations, indicating a more congruent dissolution of aluminum-silicate minerals than F1. The association of sulfate with this factor, although weak, might point to a particular bedrock type. Finally, F4 was characterized by metals, particularly iron. Interestingly, the iron present was not strongly bonded to organic content. Indeed, the apparent color showed a higher loading on F4 than F2, likely related to the reddish color when the iron level was very high. TP (positively) and nitrate (negatively) were associated with F4, indicating that water bodies richer in metals tend to be slightly more productive.

Drivers of water hardness variation

Chemical rock weathering should be connected to both the F1 and F3 axes of the factor analysis. They should, however, be linked to different underlying processes because they emerge in the factor analysis as orthogonal components, indicating independence. Alkalinity and conductivity high loadings on F1 link the factor to a dominant rock weathering process. High calcium and magnesium (hardness) contributions to F1, but not silica, point to a non-congruent mineral dissolution of aluminum-silicates bearing divalent cations and consequently forming secondary minerals that retain silica. Given the wide alkalinity and conductivity range, this primary process should be highly variable across space (Table 2). Indeed, the geological formations showed significant differences in water hardness (Fig. 4a). The high variability within formations was initially unexpected because the lithological composition in most formations comprised andesite and dacite in varying proportions and mixed volcanic materials (Table S1). Rhyolite, which in principle is less weatherable, only predominated in the Chulo unit, which indeed showed lower than average ionic strength.

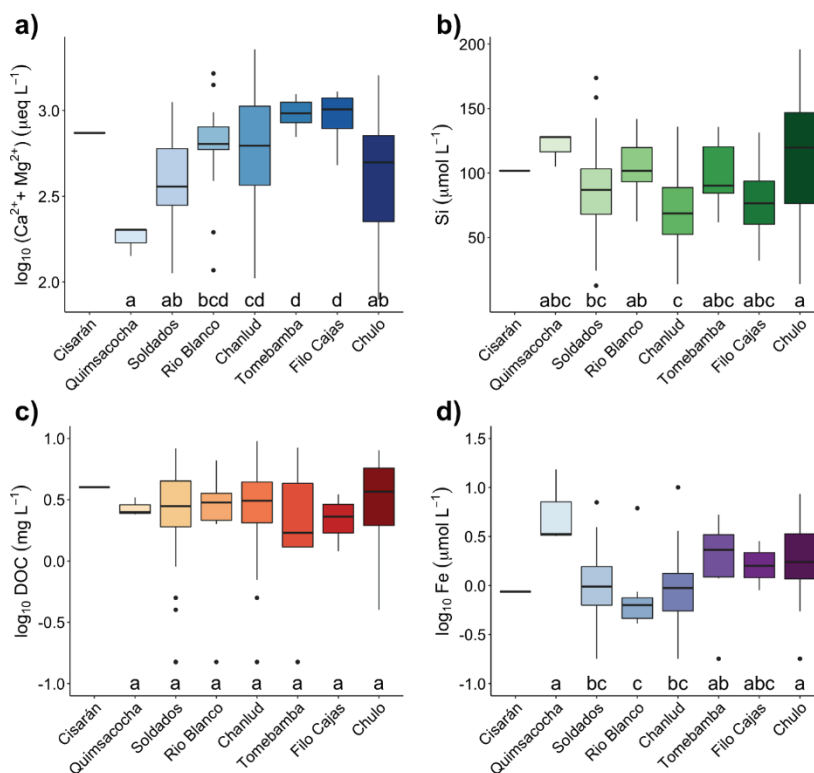


Figure. 4. Chemical variation distribution within the geological formations: (a) water hardness (calcium + magnesium), (b) silica, (c) dissolved organic carbon, and (d) iron. The four chemical components were selected to represent the four axes of the factorial analysis (Table 3). Each lake was assigned to the geological formation with the highest percentage in the watershed. Sharing a lower case letter on the x-axis indicates a non-significant mean difference between a pair of geological formations (p -value, >0.05). The number of lakes, characteristics, and geographical distribution of the geological formations are shown in Table S1 and Fig. S1, respectively.

Interestingly, the differences in divalent cation levels (and thus ionic strength, alkalinity, and weathering rates) between the geological formations corresponded to their age within the andesite-dacite dominion. The older the volcanic formations, the higher the cation levels (Fig. 4a). Formations of comparable age (i.e., Tomebamba-Filo Cajas, Río Blanco-Chanlud) showed similar hardness

distributions. In contrast, Chulo formation (rhyolite) showed significantly lower hardness levels than the closest andesite-dacite formation by age.

Despite the general rock type and age patterns, F1-related variables showed broad variability within some formations (i.e., Soldados, Chanlud, Chulo). Part of this variation could be because some lakes included more than one formation in their watersheds, although this is not a common feature (Table S2). Therefore, most of the variability should be due to other weathering drivers that may increase the contact between water, carbon dioxide, and minerals. The multivariate regression analysis confirmed, with low uncertainty, that water hardness was favored by rock age and limited by rhyolite (Fig. 5a).

The most significant hardness drivers were geomorphological variables (i.e., mean depth and watershed/lake area ratio). Increasing the hardness with watershed and waterbody size indicated an accumulation process in the drainage basin. In contrast, the influence of land cover features was less conclusive in the models; the coefficients showed considerable variability (Fig. 5a). Wetland, bare rock, and *Polylepis* forest showed positive coefficients in the models. They might enhance the divalent cation content by providing more substrate or moisture and CO₂ at the interface where weathering occurs. Páramo and rocky páramo influence were highly uncertain; despite some models showing the highest coefficients, they were inconsistently positive or negative, depending on the combination with other variables. To understand the effect of vegetation in weathering, finer resolution in vegetation, soil, and topography details is required. Overall, these models explained approximately 36% of the total hardness variation.

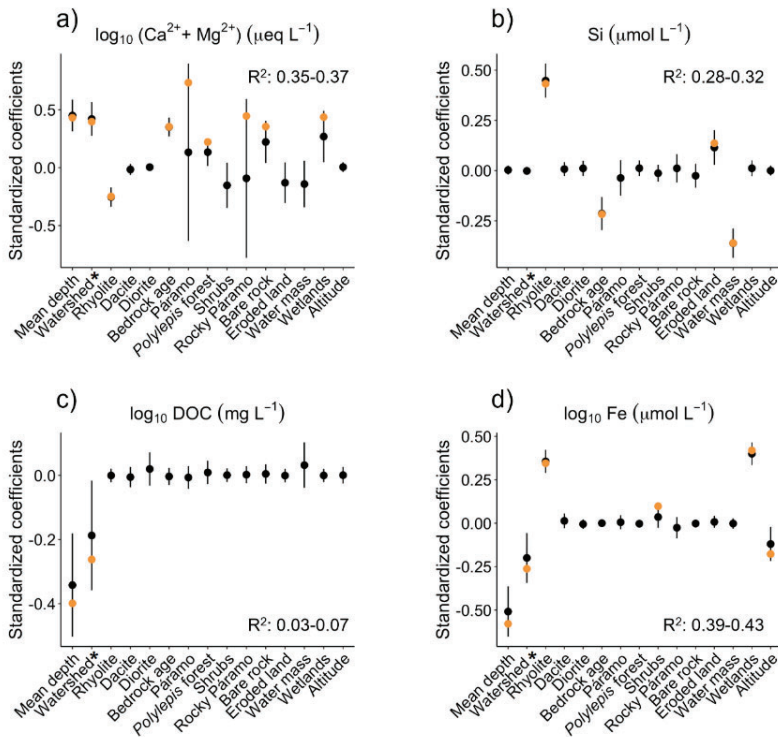


Figure 5. Driver significance for selected water chemistry components: (a) hardness (calcium + magnesium); (b) silica; (c) dissolved organic carbon; and (d) iron. The plots indicate the mean and range of the standardized regression coefficients of multivariate models with a < 4 AIC_c difference from the best model (indicated by an orange dot). All possible models (2^{15}) were assessed and ranked by the lowest AIC_c . The larger the mean departure from zero and the smaller the range of coefficients, the greater the probability of relevance of the driver. The range of variance explained (R^2) by the selected models is included in the plots. (*) Watershed/lake area ratio.

Drivers of silica variation

The contribution of silica to the F3 axis in the factorial analysis and the poor loading of divalent cations suggested a secondary weathering process. There were marked average differences between the geological formations (Fig. 4b). However, the differentiating patterns changed from those shown by hardness, which is a clear

indication that the causal drivers for F1- and F3-related variables were relatively independent. Indeed, the multivariate regression models showed that geomorphological features were not significant for silica levels (Fig. 5b), in contrast to the water hardness case.

Despite the high variation in calcium levels, the relatively constrained silica concentration indicated oversaturation or equilibrium of secondary silicates, such as kaolinite ($\text{Al}_2\text{Si}_2\text{O}_5(\text{OH})_4$) clay (Fig. 6a). Only a few cases were more likely related to aluminum hydroxide minerals (i.e., gibbsite, $\text{Al}(\text{OH})_3$); those with the lowest silica levels.

Rhyolite bedrock contributed positively to silica levels, while rock age contributed negatively, just opposite effects of drivers than on hardness. The presence of eroded land in the watershed had a positive effect. This landscape feature occupies only a small part of the overall territory (Fig. 2e); it may have a marked influence when it is present. The proportion of water mass in the watershed resulted in a pronounced negative effect on silica levels, likely related to biological consumption (e.g., diatoms).

Overall, the regression models explained approximately 30% of silica variation. The patterns found, particularly the decline with rock age and association with eroded land, suggested some relationship with secondary volcanism processes with less extension and more random spatial distribution, which may be exhausted over time. The lack of any relationship with watershed or lake geomorphological features indicates that source areas are relatively small and do not show accumulative effects at the watershed scale.

Drivers of organic matter variation

The organic matter content in lake water (F2 in the factor analysis) did not differ between geological formations (Fig. 4c). Indeed, the regression models only showed some relevance of the geomorphological variables (Fig. 5c). The smaller the lake and its watershed, the higher the DOC levels that could be expected. While

these parameters were significant, their explanation was limited (~5% of the overall variation), indicating high DOC scattering regardless of lake depth (Fig. S4) or watershed size.

Drivers of metal variation

There were significant differences in the metal levels among the geological formations (Fig. 4d). The concentrations were higher on average in Chulo, Filo Cajas, Tomebamba, and, particularly, Quimsacocha, although only three lakes were sampled in the latter case. The variation was substantial in the other formations, and the higher values overlapped with those in the metal-rich formations.

High iron levels were more likely in small water bodies with smaller watersheds (Fig. 5d), as occurs for DOC, indicating that point sources were not evenly distributed in the landscape. These point sources were markedly more when the rhyolite bedrock was dominant. In addition, the higher the proportion of wetlands in the watershed, the higher the iron levels. These significant drivers accounted for approximately 41% of the variation. Altitude (negatively) and shrubs (positively) contributed appreciably to some models, but the general uncertainty may indicate a spurious contribution.

Water bodies with higher iron concentrations were oversaturated (Fig. 6b). In some lakes, iron precipitation was particularly evident and colorful, associated with inlets connected to wetlands (Fig. 2f). As the metal levels declined and the pH increased, soluble iron hydroxide forms were more likely to occur. Nevertheless, some measured iron could be associated with colloidal and small particles in lakes where hematite (Fe_2O_3) oversaturation is indicated.

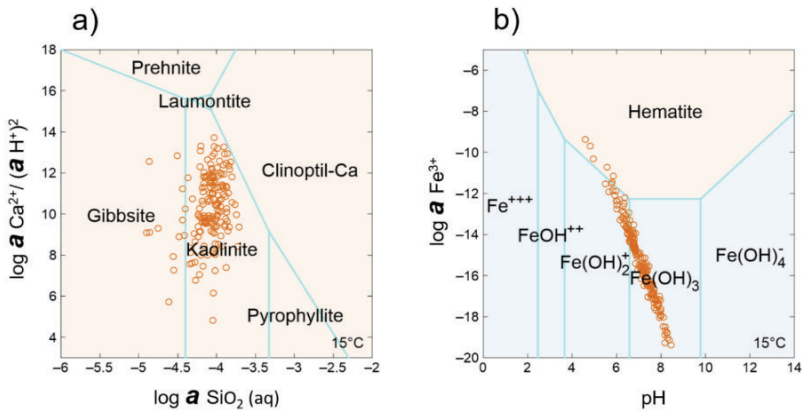


Figure 6. Water chemistry position of the lakes in theoretical stability diagrams. (a) Mineral stability in a system with varied activities of calcium and silica, and activity = 1 of aluminum (in mineral form) and water. (b) Iron solubility assuming a 0.0002512 oxygen fugacity; an average oxygen value in the surface lake water samples. Temperature was fixed at 15 °C in both cases. Reddish background indicates a solid phase, while bluish background represents an aqueous form. Calculations were performed using GWB 2021.

3.4 Discussion

Water chemical variation and rock weathering

Our results show that high mountain lakes in volcanic basins can present extremely variable water chemistry in relatively small areas. The variation found in Cajas NP was comparable to that in large mountain ranges (Fig. 7 and Fig. S5 for pH), where the substrate includes plutonic, metamorphic, and carbonate bedrock changing over large areas (Camarero et al. 2009). Active volcanism produces lava flows that overlap unevenly and heterogeneously distributed tuff, lapilli, and ash. Even more locally, hydrothermal processes reaching the surface create patches of substrate that differ from the dominant rock. Cajas Massif lakes show that this heterogeneity still influences water composition variation in volcanic bedrock dating millions of years. Indeed, the spatial heterogeneity and eventual

water chemical variation may be increased by the presence in the watersheds of layers corresponding to several volcanic phases that differ in dominant rock, age, and associated secondary processes.

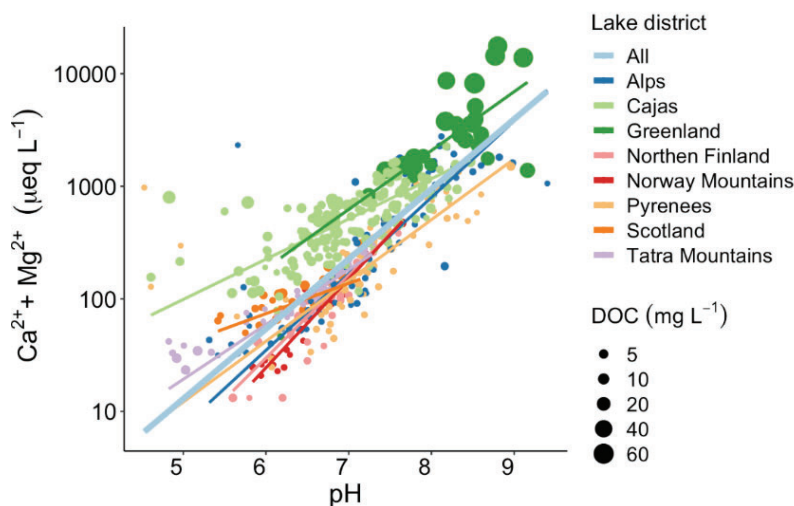


Figure 7. Relationship between pH and divalent cations in several lake districts in temperate mountain ranges and boreal areas (data from Catalan et al. (2009b)) for comparison with Cajas NP (this study data). Theil-Sen linear robust regression (*mblm* R package) was applied to downscale the influence of the outliers, mostly from waters affected by sulfide oxidation. High DOC waters show a higher intercept due to the effect of organic acids on pH.

Lakes on watersheds where rhyolite bedrock dominated had softer water than lake basins where andesite, dacite, or diorite predominated. The latter rock types are richer in plagioclase and pyroxene, which are minerals that are more easily weathered than quartz and orthoclase (White and Brantley 1995). Calcium and silica levels indicate that the weathering of these primary minerals is not complete; secondary silicates, most likely kaolinite, are formed. This incongruent dissolution has been found in other volcanic rock areas (Di Figlia et al. 2007). The high correlation of calcium with alkalinity and conductivity indicates that this partial aluminosilicate dissolution is the primary source of cations. Recent studies of Cajas'

andesitic soils indicate that they are depleted in mono- and divalent cations with an accumulation of Al-humus complexes in the soil matrix (Molina et al. 2019) even though these soils are postglacial and therefore relatively young. Consequently, water alkalinity generation primarily occurs in the subsoil saprolite, which explains why water hardness increases with watershed and lake size. The cation excess increases the longer the water travels through the subsurface before reaching the lake or pond.

In addition to rock type, the surface area available for the reaction influences weathering rates (White and Brantley 2003). Older volcanic bedrock presents higher porosity and surface area for hydration and reaction. Our results indicate that the age of the geological formation is a significant driver for divalent cation levels and alkalinity. This finding is consistent with 5-year field investigations that indicate that older rhyolite rocks with similar initial compositions have faster chemical weathering rates than younger ones (Matsukura et al. 2001). The significance of the bare rock proportion in the watershed also points to the same mechanism, as these outcrops are usually heavily fractured, providing more and fresher surfaces for reaction (Kopáček et al. 2017). Vegetation has been identified as a factor promoting weathering (Burgelea et al. 2015) because it increases the availability of carbon dioxide and protons; however, our results were inconclusive. Páramo and rocky páramo both show positive and negative effects depending on the regression model. Conversely, the role of wetlands appeared robust; it always indicated weathering enhancement when included in the regression models. Nevertheless, there is still a considerable proportion of the hardness variation to be explained. Molina et al. (2019) showed a significant difference in soil chemical weathering related to topographic gradients and vegetation change at spatial scales that cannot be documented in our macroscale landscape study. The uncertainty associated with vegetation variables in the multiple regressions could be related to the lack of resolution at fine spatial scales.

Our factorial analysis suggested a complementary weathering process beyond the predominant cation source. Silica levels, which indicate complete aluminosilicate dissolution, were associated with monovalent cations and sulfate as part of a third main orthogonal factor. The silica drivers identified in the multivariate regression analysis supported the interpretation of an independent complementary weathering process. It was not related to the size of the watershed or the lake; hence, it did not have an extended occurrence that could sustain an accumulative process like that of divalent cations. This process likely occurs in hot spots sparsely distributed in watersheds. The association with eroded land was also noted in this local character. Furthermore, contrary to the hardness factors, silica levels were favored in the rhyolite bedrock and declined with rock age. This evidence points to a bedrock affected by former hydrothermal processes, which occur during periods of active volcanism (Pozzo et al. 2002). High water temperatures modify the original aluminosilicates, making secondary ones deficient in cations (Ohba and Kitade 2005) and other processes such as albitization (Engvik et al. 2008). The latter may eventually result in chemical weathering, providing sodium (Cruz et al. 1999). The hydrothermal activity may or may not be associated with sulfur. Both types have been described in the Quimsacocha formation during exhaustive mining prospecting (Morán-Reascos 2017). There is no reason to think that they are not present in other formations, particularly in the Chulo unit, where rhyolite predominates, and thus the likely contingent association with this bedrock in the driver analysis. The decline with the formation age indicates that this original mineral material was not replaced by rock fragmentation, which makes sense if these are spots in the landscape where the initial rock already consists of secondary aluminosilicates, which offer more reaction surfaces (e.g., clays), and thus can provide locally higher silicate values. Sodium-rich volcanic rocks can also be related to tectonic processes (Sun et al. 2020), and faults could be another location for this particular weathering.

Weathering occurring in two distinct environments has been described in other tropical watersheds (White et al. 1998). Plagioclase and hornblende reacted at the heavily fractured bedrock – the saprock interface, as likely occurred in our case. Secondly, biotite and quartz reacted preferentially in the overlying thick saprolitic regolith, providing more K, Mg, and Si to water chemistry. This latter mechanism shows Si delivery in common with our case but differs in the main cations (i.e., Mg). Overall, independent weathering mechanisms seem to be more likely in tropical volcanic watersheds than in temperate watersheds with less intense weathering. Investigating the water systems (streams, subsurface, ponds, and lakes) associated with the eroded land identified in the land cover classification and areas with tectonic faults should shed light on our conjectures.

Silica levels were negatively affected by the water mass proportion in the watershed. This relationship points to aquatic biological consumption without evidence of terrestrial biological pumping effects, as found in other volcanic areas (Benedetti et al. 2002). In contrast, the observed low potassium levels could reflect uptake by terrestrial plants.

No specific atmospheric chemical deposition studies have been conducted in the Cajas NP area. Occasionally, dust deposition arriving at the equatorial Andes as far as the Sahara desert may provide divalent cations (Boy and Wilcke 2008), and biomass burning in the Amazon basin may provide acidifying sulfur and nitrogen compounds, as found in other areas of Southern Ecuador (Fabian et al. 2005). However, it is not possible to evaluate the deposition incidence on the average chemical composition of lakes and its variation without specific studies. ANC in the Cajas waterbodies is usually high ($>200 \mu\text{eq L}^{-1}$), but some sensitive sites could be influenced by atmospheric deposition. Low chloride levels indicate that most of the deposition is from westward air masses.

However, significant rainfall episodes from the Pacific have been described for nearby areas during the wet season, bringing high salt deposition (Makowski Giannoni et al. 2016). Therefore, atmospheric deposition can provide seasonal and interannual variability in Cajas Massif waterbodies. Higher chloride values associated with the only road across the park indicate the system sensitivity.

Brown waters

Average and extreme DOC levels are higher in Cajas Massif lakes than in temperate mountain lake districts (Fig. 7) and similar to some boreal areas (Camarero et al. 2009). In contrast to cations related to rock weathering, DOC is higher in ponds and small lakes with relatively small watersheds. These features indicate a relatively local DOC origin, likely related to the idiosyncratic connections with organic soils proximal to the water body. Land cover features that apparently should be relevant for DOC (Gergel et al. 1999), such as the wetland percentage in the watershed, did not significantly influence our case.

In boreal watersheds, stream DOC originates predominantly from wetland sources during low flow conditions and from forested areas during high flow (Laudon et al. 2011), and detailed hydrology is becoming an essential component of DOC regulation. In the Cajas Massif, extreme values were achieved in small ponds, which are sometimes marginal to other water bodies. As these systems are very shallow, they are not fed with subsoil water but by water draining from immediate surface soils lacking buffering capacity. Consequently, these ponds had lower pH values (~5). Comparing across lake districts with significantly different average DOC levels (Fig. 7), Cajas' lakes align with high DOC lake districts (e.g., Greenland) in the relationship between divalent cation levels (or alkalinity) and pH. In these high DOC lake districts, the average pH was lower at the same alkalinity than in low DOC lake districts, showing the relevance of organic acids in providing acidity. Although the direct correlation between pH and DOC is low in Cajas

waters, DOC becomes a significant parameter explaining residuals between pH and hardness; therefore, a better fit was obtained with multiple regression ($\text{pH} = 6.37 + 0.0012 \text{ hardness} - 0.026 \text{ DOC}$; $R^2 = 0.46$).

Nevertheless, paludification is not a generalized feature in Cajas lakes and ponds, and a wide range from clear to brownish water was found. Indeed, the apparent color is related to organic matter and metal content, yet there is no strong correlation between the latter two, indicating different sources. The chelation of metals may occur in high DOC systems, but there are lakes with high iron content and low DOC in the Cajas Massif. The organic and metal contents in the Cajas lakes do not share the same main drivers. Compared to iron levels, the drivers' low DOC explanatory capability necessitates an ad hoc investigation of DOC composition and sources in the páramo lakes.

High iron availability

Iron levels are generally high; however, similar to DOC, the smaller the water body and its watershed, the higher the probability of finding elevated values. The differences between the several geological formations were significant and reflect the idiosyncrasies of the volcanism in each, with rhyolite bedrock resulting in increased iron levels. Nevertheless, the driver with more influence was the proportion of wetlands in the watershed. Water in wetlands may achieve lower pH and redox potential, thus facilitating iron solubility. Lake surface layers are usually well-oxygenated and foster iron precipitation, evident in some colorful lake littoral beds (Fig. 2f). Some iron may remain in colloidal form, as measured concentrations often indicate oversaturation.

Interestingly, total phosphorus was associated with iron and manganese in the factorial analyses. Therefore, some iron sources may also provide essential nutrients for primary production. Apatite-bearing iron deposits can be associated with magmatic-hydrothermal

events (Allen et al. 1996). Our study considered only lake surface samples. Although dominant cations may change little throughout the water column, this is not the case for metals, whose solubility depends on redox conditions. Because of the persistent stratification, many of these lakes show oxygen depletion in deep layers (Steinitz-Kannan et al. 1983). These layers provide an environment for reduced metal forms and other reduced compounds, such as ammonium, which are undetected in surface waters. The anoxic conditions also facilitate phosphate solubility; therefore, the correlation between iron and phosphorus is possible because of watershed sources or in-lake processes.

Ecological implications

Main ion composition and dissolved organic matter are two primary factors influencing the biota distribution in high-mountain lakes (Kernan et al. 2009). The chemical variation found in Cajas Massif lakes and ponds is comparable to that of all the European mountain ranges (Fig. 7). Therefore, a small area and relatively homogeneous bedrock provide a variety of aquatic chemical niches that is equivalent to large territories of contrasting bedrock. This remarkable feature might foster species richness in relatively small territories of aquatic organisms that are sensitive to cation composition. The Cajas alkalinity range includes the two ecological thresholds (i.e., ~ 200 and $\sim 1000 \mu\text{eq L}^{-1}$) identified in European mountain ranges in terms of community composition (Catalan et al. 2009a). Diatoms and some crustaceans show this non-linear community response to the alkalinity gradient, which will be interesting to confirm in this far-flung lake district, which shares with European ranges many diatom species (Benito et al. 2018), but not crustaceans (Catalan and Donato-Rondón 2016).

In these volcanic environments, a biologically interesting factor is the Ca:Mg ratio variation (Fig. 3), which is probably related to variations in andesite plagioclase and hornblende proportions. The biological influence of the dominant divalent cation type has been

barely explored as a driver of species segregation in aquatic mountain ecosystems, probably because of the lack of a balanced number of sites. Organisms with carbonate shells (e.g., ostracods, mollusks, etc.) are candidates to respond to this factor, as found in other aquatic ecosystems (Dussart 1976; Chivas et al. 1986).

Soils largely depleted in cations enhance the chemical contrast between lakes and ponds. Small and shallow ponds may lack the inflow of water circulating below the soils; consequently, some show the most acidic water or high DOC content, favoring biotic differentiation (Catalan et al. 2009a). We considered many ponds in our study, but many smaller ones exist in the area (Mosquera et al. 2017a); thus, more extreme pH and DOC conditions can be expected in some of them. DOC and TOC levels in the Cajas massif are higher than in temperate high-mountain lakes and comparable to Nordic mountain lakes and tundra lakes (Camarero et al. 2009). However, these high-latitude lakes freeze during winters, a feature non-present in the páramo that may have driven adaptation in other directions. In this regard, tropical high-mountain lakes are unique. Apart from the high average level, DOC has a wide range, making it a possible axis of non-linear species segregation that might include a wide range of organisms (e.g., rotifers, crustaceans, and chironomids), as has been observed in temperate high-mountain lakes with narrower DOC ranges (Catalan et al. 2009a).

Metals provide a further environmental gradient for biodiversity enhancement, which is not necessarily linked to the organic matter content of water. Vertical redox gradients have been observed in these tropical lakes (Steinitz-Kannan et al. 1983), but specific investigations concerning species adaptations are lacking. Furthermore, horizontal redox gradients from lakes to neighboring wetlands also likely foster species segregation.

The high chemical variability in tropical high-mountain lakes makes them ideal as global change sentinel lakes; some are more

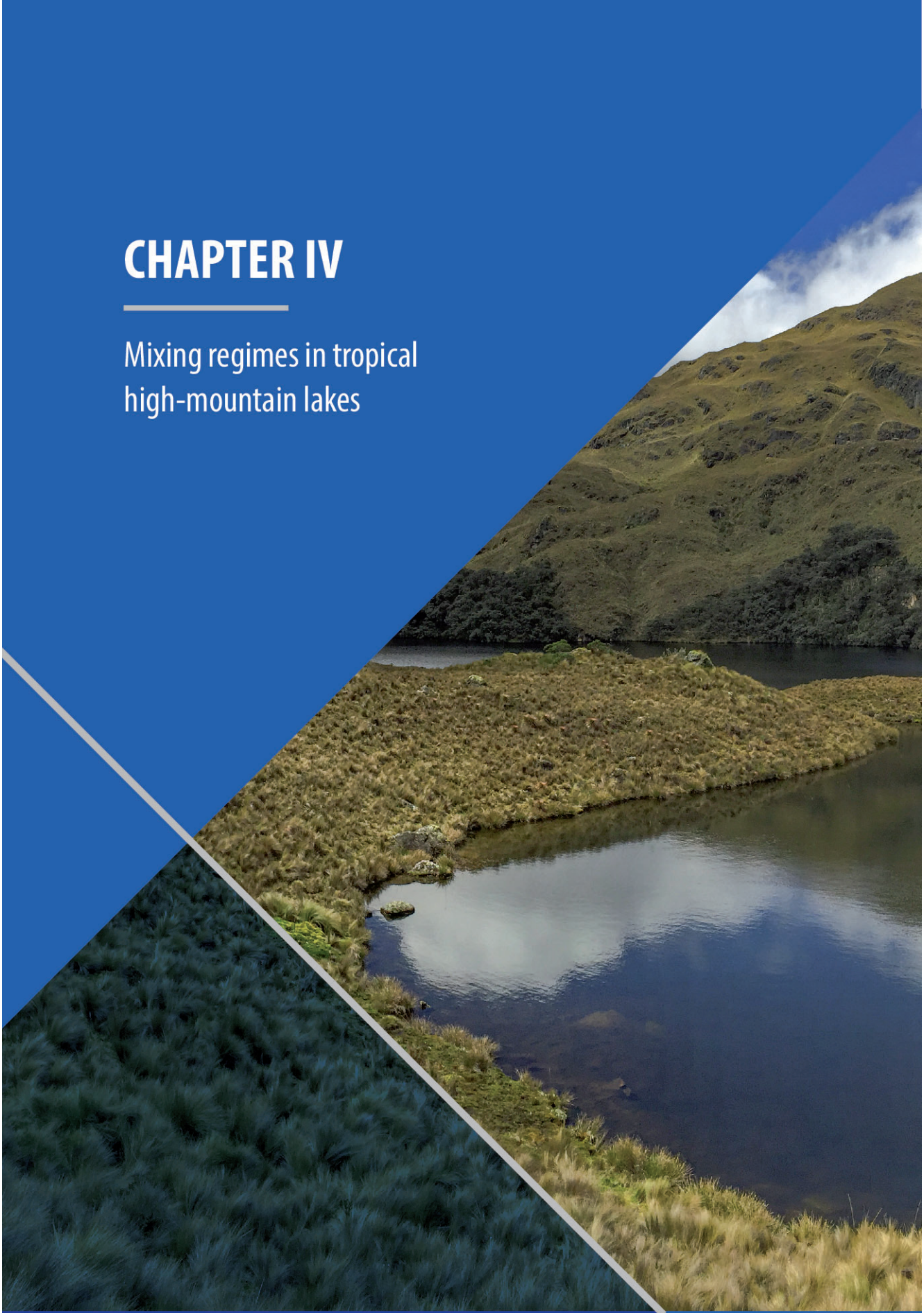
susceptible to acidic or dust deposition, while others are better suited to temperature changes impacting redox conditions. In addition, the long, independent chemical gradients offer the possibility of developing local calibration sets for paleoenvironmental reconstructions using indicator organisms, particularly diatoms (Rivera-Rondón and Catalan 2020). Given the high lake heterogeneity, surveillance and reconstructions may require a thoughtful selection of lakes for making meaningful inferences.

3.5 Acknowledgments

This research was conducted in the context of the Project “Análisis de la variación temporal de las características físico-químicas y biológicas de los lagos del Parque Nacional Cajas (PNC)” financed by the Research Directorate (DIUC) of the University of Cuenca, Ecuador, and the Municipal Public Enterprise of Telecommunications, Drinking Water, Sewerage and Sanitation of Cuenca, Ecuador (ETAPA EP). J.C. contribution was funded by the Spanish Government research grand “Alkaldia. PID2019-111137GB-C21. Ministerio de Ciencia y Tecnología”. Chemical analyses were performed in the Environmental Laboratories, ETAPA EP, Ecuador. We thank Julissa Lucero from the Subgerencia de Gestión Ambiental ETAPA EP, for her assistance in the development of the land cover digital map used in this study. Research permissions in the Cajas NP by ETAPA EP and Ministerio del Ambiente, Agua y Transición Ecológica (MATEE) are acknowledged (ETAPA 003_SGA_2015_PNC_BD_VA_Hampel, MAE-DPACÑ-2015-0243, 189-2018-DPAA/MA, and 217-2020-DPAA/MA).

CHAPTER IV

Mixing regimes in tropical
high-mountain lakes



Tropical high-mountain lakes have traditionally been considered polymictic. However, this view was based on limited information and the consideration that the daily scale involves more weather variation than the seasonal. Based on an annual 10-min sampling time series of thermistor chains in ten Cajas National Park (Ecuador) lakes, the present study shows that most of these lakes are resistant to wind and daily temperature oscillations during the great part of the year, showing a warm monomictic mixing regime. The overturn of the entire water column and persistent daily instability generally only occur between July and September, coinciding with the cloudiness and wind intensity increase and air temperature drop in the region associated with the intertropical synoptic meteorological fluctuations. The duration of the stable period influences the development of oxygen-deficient deep layers. Despite the long water column stability periods, there is no formation of a seasonal thermocline but the development of a stepwise density structure from top to bottom. Short-wave radiation usually counterbalances the negative buoyancy flux associated with net long-wave radiation, evaporation, and sensible heat flux, providing net buoyancy. Quasi-periodic (1-2 weeks) increases in wind and cloudiness mix the upper layers (2-3 m), resulting in the progressive structuring in layers delimited by weak thermoclines every few meters. The weekly scale variation is reflected in the katabatic circulation relevance (NW-SE), which develops over the lake district and interferes with the predominant eastern winds. The duration of the stable period declines with altitude, and the highest lakes (> 4000 m a.s.l) may show permanent low water-column instability, displaying the polymictic regimes once thought as the more general pattern. During the “few cold months,” the water column’s low stability in all lakes facilitates the easy mixing from top to bottom in a few hours. Wavelet cross-correlation analyses indicated a high thermal daily, weekly and seasonal coherence among lakes, which weakens during the cold months. Consequently, the mixing regimes described in the study represent the hundreds of lakes in the region and, likely, other tropical high-mountain lakes in regions of similar climates.

4.1 Introduction

Most tropical high-mountain lakes are ice-free throughout the year. Therefore, they do not show the dimictic mixing pattern typically found in temperate high-mountain lakes (Catalan and Donato-Rondón 2016). Indeed, they have been traditionally considered polymictic, although based on a few observations during limited periods of the year (Löffler 1964; Steinitz-Kannan et al. 1983). A view fostered by early expert conjectures (Hutchinson and Löffler 1956), which expected that most tropical lakes were polymictic. This early assumption has long been refuted for low-land tropical lakes because field evidence showed warm monomictic regimes (Lewis Jr. 1983). However, despite the presence of low oxygen values in the deep layers already warned to be cautious about the apparent lack of stable physical stratification (Steinitz-Kannan 1979), the polymixis view is still widely assumed (Steinitz-Kannan 1997). Some studies have shown stable water columns during extended periods of the year in the 1990s (Donato-R 2010; Catalan and Donato-Rondón 2016) and more recently (Michelutti et al. 2016; Van Colen et al. 2017). These recent year-long series have been interpreted as an indication of climate change imposing changes in the mixing regime (Michelutti et al. 2015a; Michelutti et al. 2015b). The lack of precise physical consideration, historical data from the same sites, and the observations in the 1970-1990s challenge these conjectures.

The surface temperature in many tropical high-mountain lakes is similar to that in temperate high-mountain lakes during summer (Catalan and Donato-Rondón 2016). However, the deep layers are much warmer in the tropics, reducing the overall density gradient in the water column. The lack of strong gradients, top-to-bottom, and marked seasonal thermocline has been the basis for assuming low stability of the water column in front of winds and diel air-temperature oscillations and, consequently, inferring polymictic regimes (Hutchinson and Löffler 1956). However, most high-mountain lakes are relatively deep compared to their surface area

due to their glacial origin, and this high aspect ratio could facilitate that relatively-weak density gradients result in stable water columns. Consequently, we designed an experimental field observation to elucidate between two alternative hypotheses (i.e., polymixis vs. warm monomixis) considering the relevant time scales, lake size, and altitudinal variation.

We selected ten high-mountain lakes in the Cajas Massive (Andes, Ecuador), covering the altitudinal gradient in the area and including a similar number of relatively shallow (< 20 m) and deep (> 30 m) lakes. A thermistor chain, sampling every 10 min, was deployed in each lake, and vertical profiles were performed monthly to have snapshots of higher vertical resolution. These data were the basis for investigating each lake's thermal cycle, the water column's stability, and the eventual annual mixing regime. Furthermore, using measurements from a weather station on the shore of one of the lakes, we estimated the thermal and momentum fluxes and evaluated the mechanical bases of the observed patterns. Finally, we analyzed the thermal response coherence between lake pairs using wavelet cross-correlation to assess whether these observations in relatively few lakes can represent the tendencies in the abundant Cajas massif lakes and other lake districts under similar contexts.

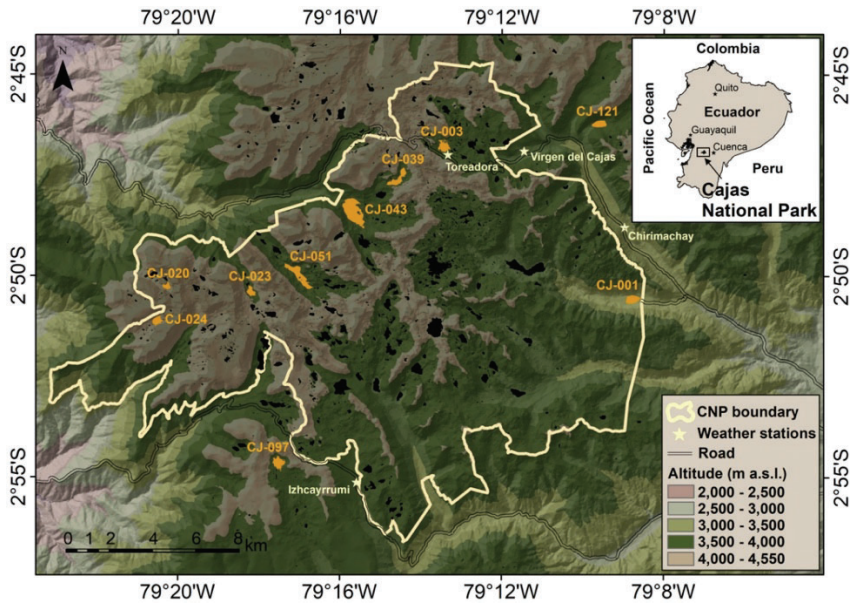


Figure 1. Distribution of the study lakes in the Cajas Massif. Lake codes correspond to those used in Mosquera et al. (2017b) and Table 1. The limits of the Cajas National Park are indicated.

Table 1. Geographical and geomorphological characteristics of the study lakes.

Code*	Name	Latitude	Longitude	Altitude (m a.s.l.)	Maximum depth (m)	Mean depth (m)	Area (m ²)	Volume (m ³)	Watershed area (km ²)
CJ-001	Llaviucu	2° 50' 35.6" S	79° 8' 46.1" W	3152	16.5	8.6	188,867	1,615,853	47.7
CJ-003	Toreadora	2° 46' 45.9" S	79° 13' 26.1" W	3917	29.2	11.3	193,217	2,185,530	5.3
CJ-020	Yantahuaico-3	2° 50' 17.0" S	79° 20' 14.2" W	4112	19.0	8.3	72,844	606,819	1.2
CJ-023	Atugyacu Grande	2° 50' 26.7" S	79° 18' 12.3" W	3969	34.1	16.6	113,431	1,880,171	4.5
CJ-024	Estellascocha	2° 51' 8.0" S	79° 20' 31.7" W	4128	41.9	20.0	122,109	2,440,702	1.5
CJ-039	Larga	2° 47' 41.4" S	79° 14' 40.1" W	3940	47.7	17.5	234,689	41,143,48	3.5
CJ-043	Luspa	2° 48' 17.4" S	79° 15' 45.6" W	3776	65.3	28.9	774,775	22,369,167	19.3
CJ-051	Sunincocha Grande	2° 49' 49.7" S	79° 17' 7.0" W	3842	61.0	19.9	403,522	8,013,226	10.4
CJ-097	Jigeno	2° 54' 42.7" S	79° 17' 31.4" W	3969	25.0	7.8	211,926	1,662,359	1.7
CJ-121	Dos Chorreras	2° 46' 12.5" S	79° 9' 36.9" W	3690	18.2	9.4	164983.7	1,555,441	7.0

* Codes correspond to those used in the lake inventory by Mosquera et al. (2017b)

4.2 Material and methods

Study sites

The study lakes are situated in the Cajas Massif of the Andes of Southern Ecuador. Based on previous lake morphometry information (Mosquera et al. 2017a), ten lakes located in the Cajas National Park (CNP) or immediate surroundings were selected (Fig. 1). The selection covered a wealth of the main altitudinal (3152-4128 m a.s.l), depth (16.5 - 65.3 m) and size (7 - 77 ha) gradients within the lake district (Table 1), excluding the small (<1 ha) lakes and ponds. Bedrock corresponds to a complex imbricate layering of volcanic formations of varying ages (7-37 Ma) influencing water chemistry variation (Mosquera et al. 2022). Part of the Late Pleistocene glaciation footprint is a large number and density of relatively small lakes (i.e., 5955) between 3146 to 4424 m a.s.l. (Mosquera et al. 2017a). The mean annual precipitation in the Cajas Massif ranges from 900 to 1400 L m⁻², peaking at 3400 m a.s.l. Precipitation occurs primarily as drizzle during about 88% of the year, resulting in a wet and usually foggy páramo landscape (Padrón et al. 2015). Fog interception can increase conventional rainfall by >25% (Rollenbeck et al. 2011). Seasonal and interannual rainfall variability corresponds to the equatorial Andes (5° S-1° N) characterized by a bimodal regime with wet periods from February to April and October to November (Segura et al. 2019). Air temperature shows low seasonal variation with colder months from June to October. Temperature oscillations can be substantial during daytime, between 6-18 °C around 3100 m a.s.l, and 3-6 °C at about 4000 m (Bandowe et al. 2018). Typically, a cloudy day show an 80% reduction on short-wave radiation at grown level respect to a clear sky day (Carrillo-Rojas et al. 2016).

Meteorological data

Meteorological data were available from four automatic weather stations (AWSs) run by the University of Cuenca and ETAPA EP (Fig. 1). Three were considered for a general assessment of the weather variation in the area because they were not located near any study lake. The station at the shoreline of Lake Toreadora (CJ-003) enabled the calculation of heat and momentum fluxes for this lake. The Toreadora AWS is located over a tussock grass ground, within the same open-air geometry of the lake, at a 168-m distance and 44-m above the lake surface, including the mast height. The AWS was equipped with sensors for air temperature (T_A , °C, Campbell CS-215, accuracy, ± 0.3 °C), relative humidity (H_r , 0-1, Radiation Shield, $\pm 2\%$), atmospheric pressure (P_A , Pa, Vaisala PTB110, ± 0.3 hPa), short-wave solar radiation (R_S , $W\ m^{-2}$, Campbell CS300 pyranometer, wavelength range: 360-1120 nm, $\pm 5\%$ daily total), net radiation (R_N , $W\ m^{-2}$, Kipp & Zonen NR Lite2, wavelength range: 200 nm to 100 μm and rainfall (Texas TE525MM rain gage, $\pm 1\%$), wind direction and speed (W_D - W_S , Met-One 034B, $\pm 0.11\ m\ s^{-1}$). Data were sampled every second and recorded at five minutes-average. Incident long-wave radiation on the lake surface (R_{Lin} , $W\ m^{-2}$) was estimated considering R_N , R_S , a 0.23 albedo assumed for the low tussock grass ground where the AWS is located (Vásquez et al. 2022), and an outgoing long-wave emission at air temperature estimated with the Stephen-Boltzman equation (see below).

Measurements

Temperature time series were obtained using thermistor chains composed of HOBO® thermistors (U22-001, accuracy: ± 0.21 °C, resolution: 0.02 °C; Onset Computer Corporation, Bourne, MA). The chains were deployed from a buoy moored in the lake's deepest point. Thermistors were placed at depths corresponding to about 100, 75, 50, 25, 15, and $<5\%$ of the lake's relative volume (Table S1). Some thermistors (15, 25%) were omitted in the shallowest lakes. Measurements were recorded at 10-min intervals from the beginning of March 2019 to the end of March 2020.

Conductivity, temperature, and dissolved oxygen 20-cm resolution profiles were performed monthly in the deepest point of each lake using a YSI EXO 1 (YSI Inc., a Xylem brand, Yellow Springs, OH, USA) multiparameter sonde. Monthly oxygen and temperature profiles were also available for 1996-2020 and were used to show that the mixing regimes observed were consistent over the years.

Thermal variation

Probability density functions for each thermistor were estimated using the `geom_density` function from the `ggplot2` R package to characterize temperature variation throughout the study period. The time series obtained with the thermistors were interpolated at 1-m intervals. It was assumed isothermy from the upper thermistor to the lake surface and from the lower thermistor to the bottom. Based on detailed volume resolution bathymetries for each lake (Mosquera et al. 2017a) and the interpolated temperature series, we calculated the time series of the lake's total heat content (GJ m^{-2}), $Q_L = \int T_z C_p \rho_z V_z$, where t_z is temperature ($^{\circ}\text{C}$) at depth z ; C_p , water specific heat ($4186 \text{ J kg}^{-1} \text{ }^{\circ}\text{C}^{-1}$); ρ_z , density (kg m^{-3}); and V_z , volume (m^3). Cross wavelet analyses were used to evaluate the coherence of heat content changes among pairs of lakes (Grinsted et al. 2004) using the *biwavelet* R package.

Water column stability

Water density was computed from temperature and conductivity following Boehrer and Schultze (2010) (see Supplementary material for details). The Schmidt (1928) stability ($St, \text{J m}^{-2}$) that estimates the energy required to thoroughly mix a stratified lake with a given vertical density distribution was used to characterize the water column stability (Kirillin and Shatwell 2016), $St = \frac{g}{A_0} \int_0^{z_{max}} (z - z_V) \rho_z A_z dz$, where g is gravity acceleration; A_z , the horizontal cross-sectional area at depth z ; and z_V , is the center of the volume of the lake, defined as $z_V = \frac{1}{V} \int_0^{z_{max}} z A_z dz$; V being the lake volume.

The monthly temperature profiles were used for a higher resolution assessment of the vertical structure of the density stratification assessed using the buoyancy frequency (N , cph), $N^2 = -\frac{g}{\rho} \frac{d\rho}{dz}$. N indicates the maximum frequency for an internal wave propagating in the specific stratification. The stronger the gradient, the higher the frequency. In the same profiles, the Lake Number (L_N) was used for evaluating the resistance to wind mixing (Imberger and Patterson 1990). $L_N = \frac{2 St z_t}{L \rho_0 u_*^2 z_V}$; where z_t (m) is the depth where N^2 is maximum; L , lake length; and u_* , the surface wind shear velocity (m s^{-1}), $u_*^2 = \frac{\rho_a}{\rho_0} C_D U_a^2$, ρ_a being the air density (kg m^{-3}); C_D , a drag coefficient (0.0013); and U_a^2 , wind velocity at some characteristic height (a) above the lake. Although L_N was initially developed under a two-compartment consideration, it has also proven helpful in complex stratification patterns (Kirillin and Shatwell 2016). Because of the lack of weather stations at each site, we calculated L_N under different wind assumptions using the wind probability distribution based on the whole set of measurements in the four AWSs in the area.

Surface fluxes and mixing layer

Toreadora lake and AWS measurements were used to evaluate the heat and momentum fluxes throughout the changing conditions of the study period. Short-wave radiation at the lake surface was estimated considering a constant albedo ($a = 5\%$), $R_S(0) = R_S(1-a)$. The net surface heat flux omitting short-wave radiation (S , W m^{-2}) was estimated as $S = R_{L\text{in}} - R_{L\text{out}} + E + H$, where $R_{L\text{out}}$, E , and H were water long-wave radiation emission, latent heat, and sensible heat exchange, respectively. Fluxes toward lake water were considered positive. $R_{L\text{out}}$ was determined by $R_{L\text{out}} = \epsilon_w \sigma T_s^4$, being ϵ_w , water emissivity (0.97); σ , the Stephen-Boltzman constant ($5.67 \times 10^{-8} \text{ W m}^{-2} \text{ K}^{-4}$), and T_s , the surface lake temperature ($^\circ\text{K}$). Latent heat flux $E = p_a L_V C_E U_a (q_s - q_a)$, where p_a was air density; L_V , latent heat of evaporation, calculated following (Sharqawy et al. 2010); C_E , a transfer coefficient (0.00154); q_s , specific humidity at saturation pressure at T_s ; and q_a , specific humidity of the air. Sensible heat flux

$H = p_a C_{pa} C_H U_a (T_s - T_a)$, being C_{pa} , air specific heat ($1.01 \text{ J kg}^{-1} \text{ }^\circ\text{C}^{-1}$); C_H , a transfer coefficient (0.00154); and T_a , air temperature. The surface mixed layer was evaluated using the Imberger (1985) approach. The buoyancy flux (B , $\text{m}^2 \text{ s}^{-3}$) was estimated as $B = g \alpha H^* / (C_{pw} \rho_0)$, being α the thermal expansion coefficient; C_{pw} , the specific heat of water ($\text{J kg}^{-1} \text{ }^\circ\text{C}^{-1}$), and H^* , the effective heat flux (W m^{-2}), which was calculated as $H^* = S + R_S(0) + R_S(h) - \frac{2}{h} \int_h^0 R_S(z) dz$ following MacIntyre et al. (2002). The mixed layer thickness (h , m) was defined as the first depth where the temperature difference was $> 0.02 \text{ }^\circ\text{C}$ relative to the temperature measured at 0.2 m . The penetration of short-wave radiation was assumed to follow an exponential decay with an extinction coefficient γ , $R_S(z) = R_S(0) e^{-\gamma z}$. The coefficient was approximated using Secchi disk depth (z_{Secchi}) and the empirical relationship for brown waters, $\gamma z_{\text{Secchi}} = 1.94$ (Reinart et al. 2003). The penetrative convection velocity (w^* , m s^{-1}) was estimated as $w^* = (B h)^{1/3}$. The turbulent kinetic energy flux (F_k) includes penetrative convection and shear components; it should be proportional to a combination of w^* and u^* , $F_k \sim 0.5 (w^{*3} + 1.33 u^{*3})$ as used in MacIntyre et al. (2002) based on (Kim 1976) parametrization. Using this approach, we estimated the relative contribution of penetrative convection to turbulent mixing ($f_c = w^{*3} / (w^{*3} + 1.33 u^{*3})$).

4.3 Results

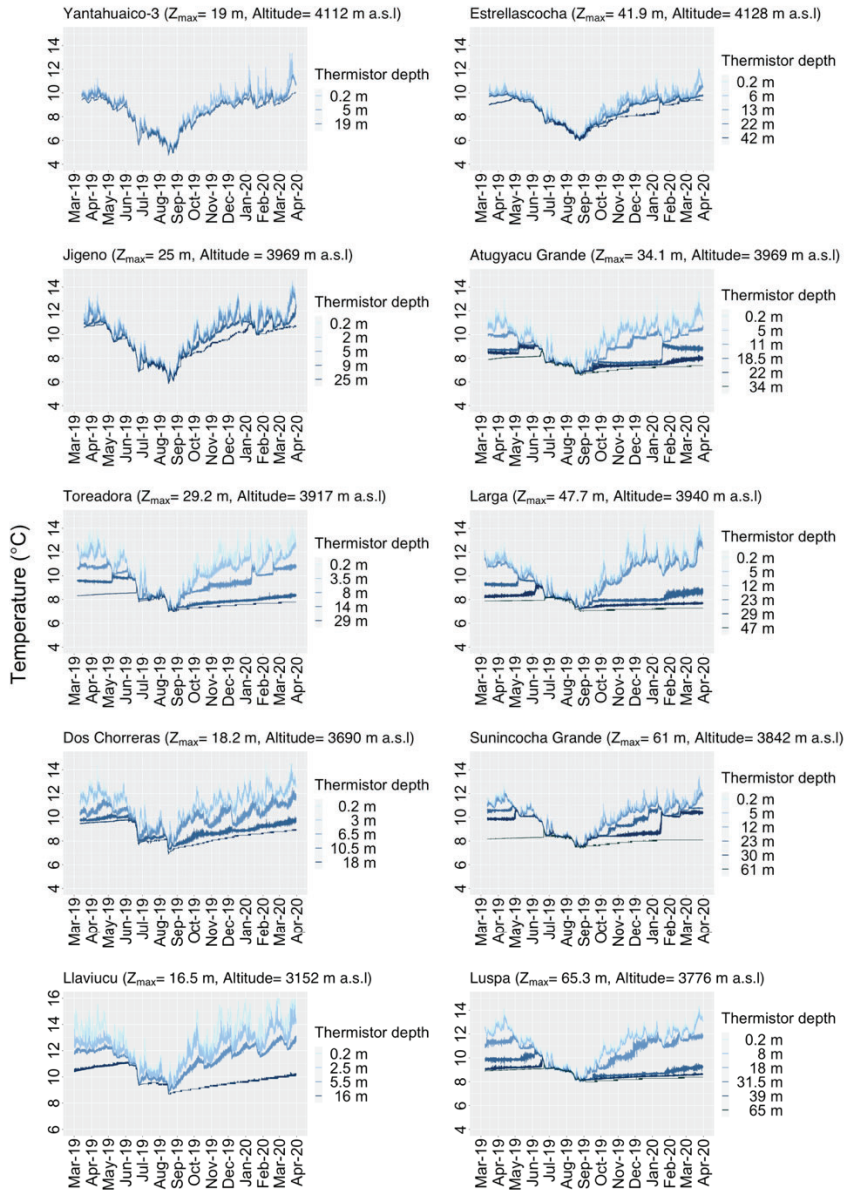


Figure 2a. Thermistor time series for the study lakes in the Cajas Massif (Ecuador).

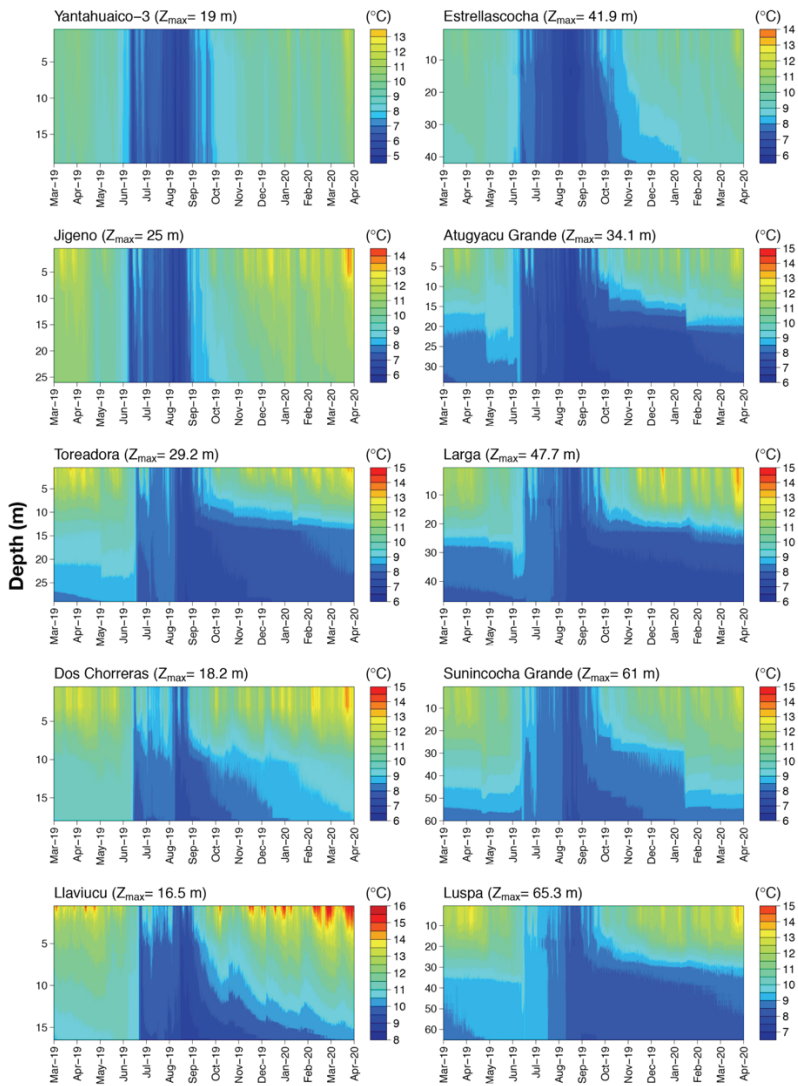


Figure 2b. Isotherm time series for the study lakes.

Temperature variation

The direct plotting of the thermistor measurements (Fig. 2a) showed that, for most lakes, isothermy was only present episodically from June to September (Fig. 2b). Therefore, the seasonal variation included about nine months of stratification and three months of occasional mixing. Only above ~3950 m a.s.l, this pattern was progressively lost. And, only in the high elevation and relatively shallow lake Yantahuaico-3, there was not a long phase of stratification.

The highest surface temperature in the study lakes ranged between 11.2 and 16 °C, typically around 13 °C, and varied mainly according to elevation, declining 3.5 °C per 1000 m ($R^2=0.81$, $p<0.003$). The lowest values in the deep layers varied less among lakes (range, 5-8.5 °C, mean 6.8 °C) and showed a combination of altitude (3.7 °C per 1000 m) and lake depth influence (3 °C per 10 m lower in shallow lakes at the same altitude) ($R^2=0.92$, $p<0.0001$). The temperature range that a lake experienced across the year was typically 6.4 °C (4.8-8 °C), with less variation the deeper the lake (0.04 °C/m, $R^2 = 0.65$, $p<0.02$).

The temperature distribution across the year (Fig. 3) based on the thermistor 10-min measurements summarize the thermal variation at different water column layers. The comparison between the upper and lower thermistor distributions illustrates the variation within and between lakes. Most lakes below 4000 m a.s.l (Llaviucu, Luspa, Dos Chorreras, Sunincocha Grande, Toreadora, Larga, and Atugyacu Grande) shared similar temperature density distributions.

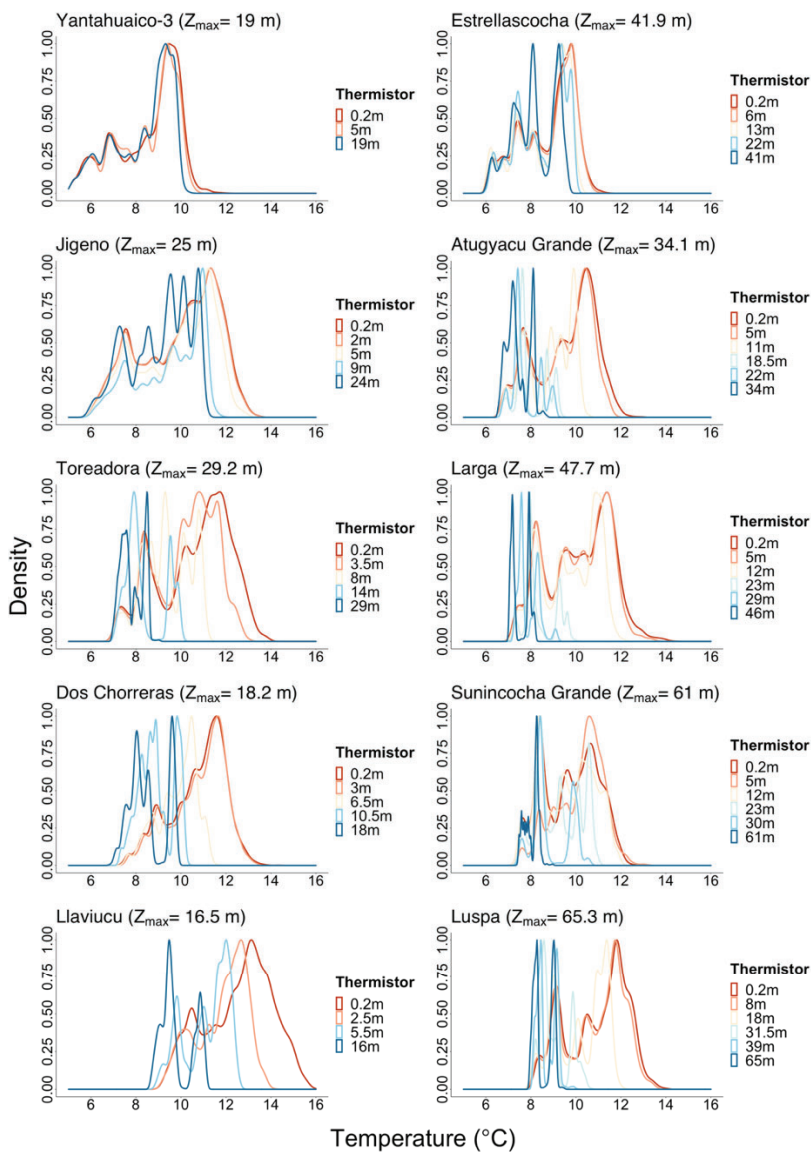


Figure 3. Frequency distributions of the temperature values for each thermistor and lake.

The deepest thermistor showed a marked bimodal distribution, with about two degrees difference between the modes (Fig. 3). The two peaks correspond to the two stratification periods sampled during the study (Fig. 2b), therefore, suggesting an interannual variation during the cooling phases, that was retained in the deepest layers during the following stratification period. Some smaller peaks slightly altered the bimodal distribution in some lakes due to stepwise cooling. The bimodal pattern of deep temperature was lost in the highest lakes, becoming multimodal.

In contrast, the surface temperature density distribution showed a largely skewed unimodal distribution with modal values close to the highest values (Fig. 3). Secondary peaks were more or less relevant depending on the lake. However, the most important secondary peak was always at the lower temperature part of the distribution. The two main peaks in the distribution differ between 3-4 °C and indicate a short and cold period, 7-10 °C, and a long and warmer period, 9 to 13 °C depending on the altitude. The thermistors at intermediate depths showed multimodal temperature density distributions, reflecting transitions from the surface to the deep layer temperature distributions. The higher the lakes, the lower the differences between the temperature density distributions at different depths. Above 4000 m a.s.l, the distributions were very similar across depths, particularly in Yantahuaico-3 lake, where they were identical (Fig. 3).

Despite higher or lower thermal differentiation across the water column, the heat content in the lakes reflected a warm/long period and a cold/short period (Fig. 4), with progressive or steeper transitions between them, depending on the lake. On average, the warmer period showed a ~40% higher heat content than the cold period in the lakes above 4000 m a.s.l and ~30% in those below.

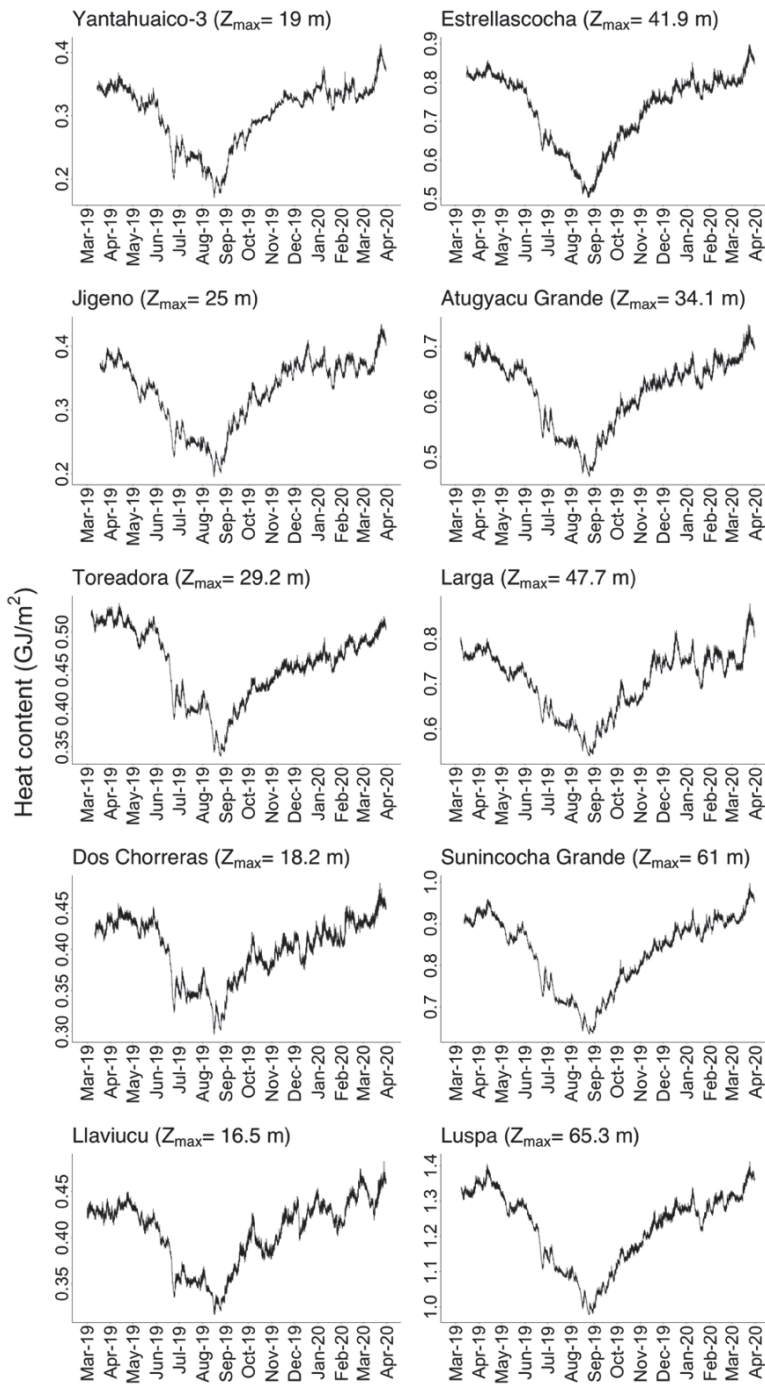


Figure 4. Heat content across the year in the study lakes.

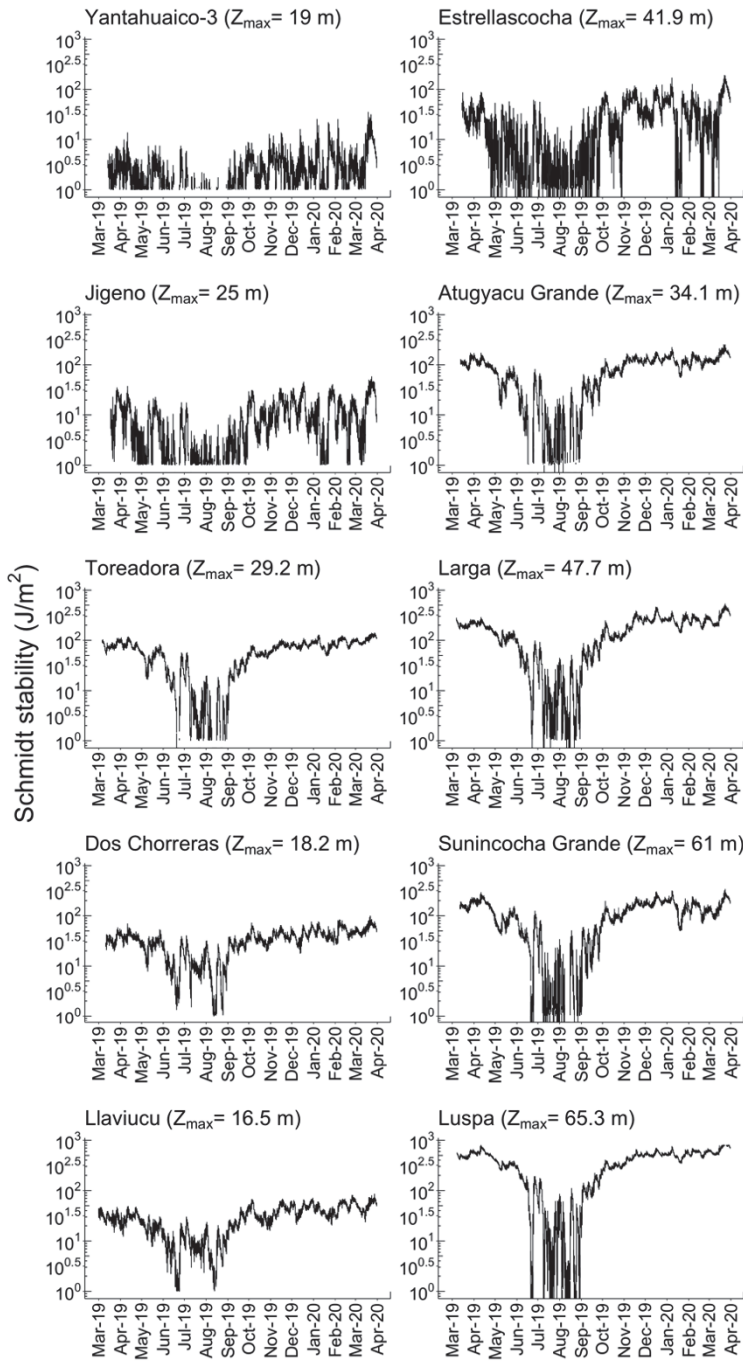


Figure 5. Variation of the water column Schmidt stability across the year in the study lakes.

Water column stability

Although lake cooling and warming proceeded progressively for periods of some months in most lakes, the water column stability experienced sharp transitions, defining two well-differentiated periods of stability and instability as shown by Schmidt stability (Fig. 5). The Schmidt stability considers the volume development of the lakes basin in addition to the density stratification. Seven out of the ten lakes studied showed a well-defined pattern of stable stratification throughout most of the year and a shorter period of instability from late June to mid-September. The three lakes at higher elevations did not show this clear seasonal pattern. Specifically, Lake Yantahuaico-3 showed instability throughout the year, whereas the deeper lakes Jigeno and Estrellascocha showed some long periods of stability from October to November, occasionally shortly interrupted by instability days.

Based on the monthly vertical temperature profiles, the buoyancy frequency distribution across the water column (Fig. 6) indicated that the stability was due to a stepwise distribution from top to bottom of relatively mild density gradients. The water column structure consisted of numerous 1 to 3-m thick layers separated by weak thermoclines. In some lakes and periods, the most substantial gradients accumulated below the first few meters depth for about 5-10 m, but without showing well-defined epilimnion, metalimnion, and hypolimnion compartments.

During the stability period, L_N indicated that the water column structure in most lakes was stable against the common and the strongest winds recorded in the area (Fig. 7). Likely, the L_N cutoff is closer to a value of 10, rather than the original thought value of 1. Otherwise, the observed complete mixing could hardly occur during the unstable period (Fig. 7a).

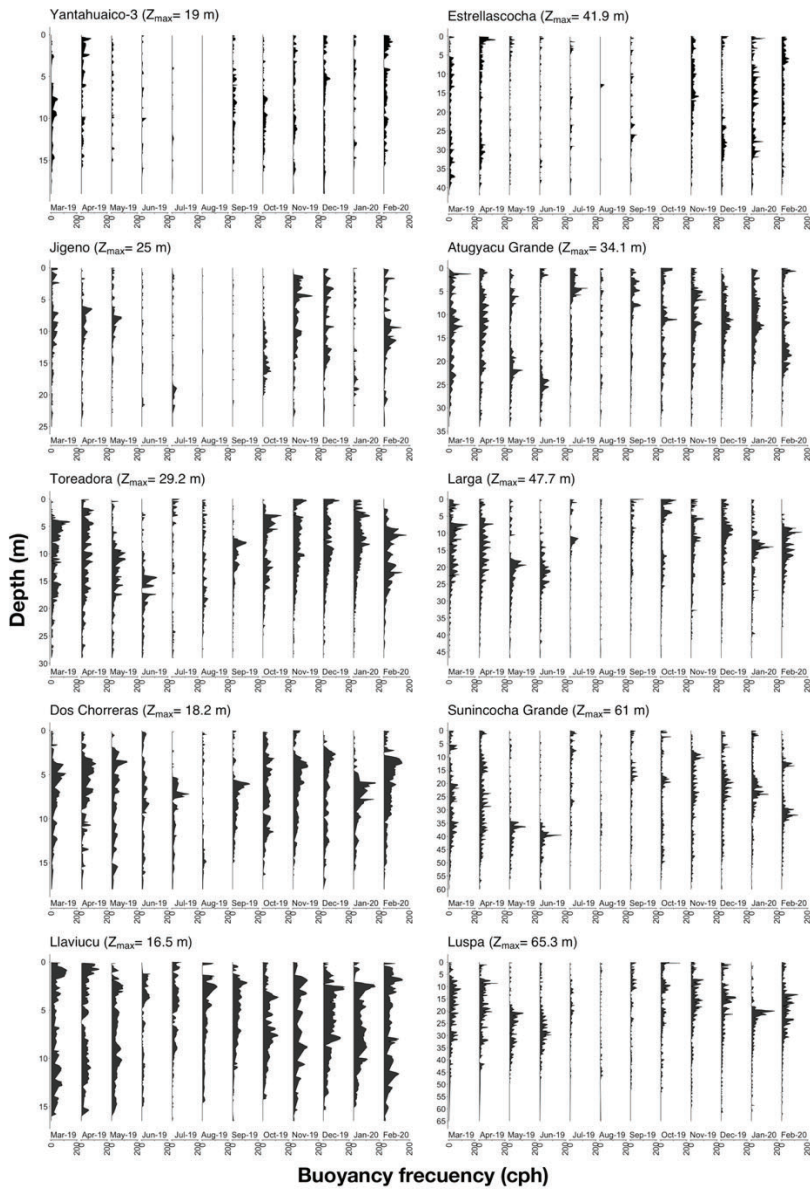


Figure 6. Buoyancy frequency (N) distribution across the year in the study lakes.

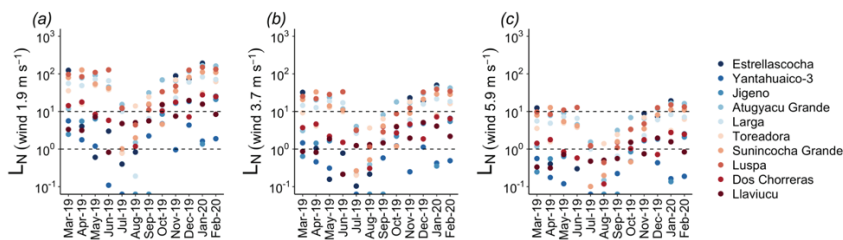


Figure 7. Stability of the water column against wind intensity. The adimensional Lake number (L_N) indicates that wind action can mix the water column when $L_N < 1$ if the wind persists sufficiently longer. L_N for each lake and profile in Fig. 6 is calculated according to the standard (a), unlikely (b), and very unlikely wind intensity (c), which correspond respectively to the median, 95, and 99 percentiles of the whole set of wind intensity measurements in the four AWS during the study period.

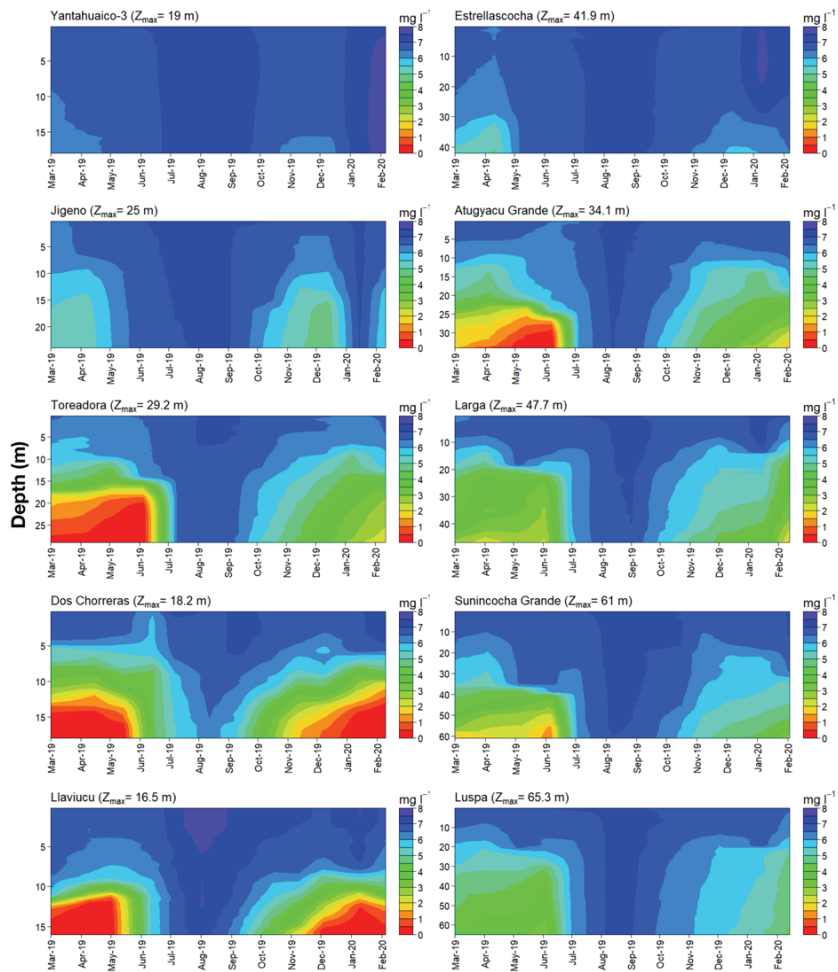


Figure 8. Oxygen distribution across the study lakes based on monthly profiles.

The highest altitude lakes could be mixed by extreme winds at any time and were easily mixed during the coldest period, even by low winds (e.g., $\sim 1 \text{ m s}^{-1}$). In summary, the L_N calculations supported that complete lake mixing can hardly occur in most of these lakes during prolonged periods. The vertical oxygen distribution also evidenced this water column stability and seasonal lake mixing patterns (Fig. 8).

Coherence among lakes

The lake pair-wise cross-wavelet analyses showed an elevated coherence among lakes at daily, weekly and seasonal scales (Fig. S1 and S2). The dominant pattern in the pair-comparisons was a high daily coherence, similar weekly-biweekly coherence, and a slightly lower seasonal coherence (Fig. 9a). Similar to this pattern but losing coherence during the coldest months (Fig. 9b) occurred between lakes at intermediate altitudes and those in the extremes. For instance, Lake Toreadora lost coherence during the cold months with those at much higher (i.e., Yantahuaico-3, Estrellascocha) and lower altitudes (Llaviucu). A third main pattern occurred when comparisons were made with Lake Luspa, for which cross-correlation was weaker at daily scales than at the other two coherence peaks (Fig. 9c). Luspa is the deepest lake in the data set, a fact that could explain higher inertia for daily fluctuations than the shallower lakes.

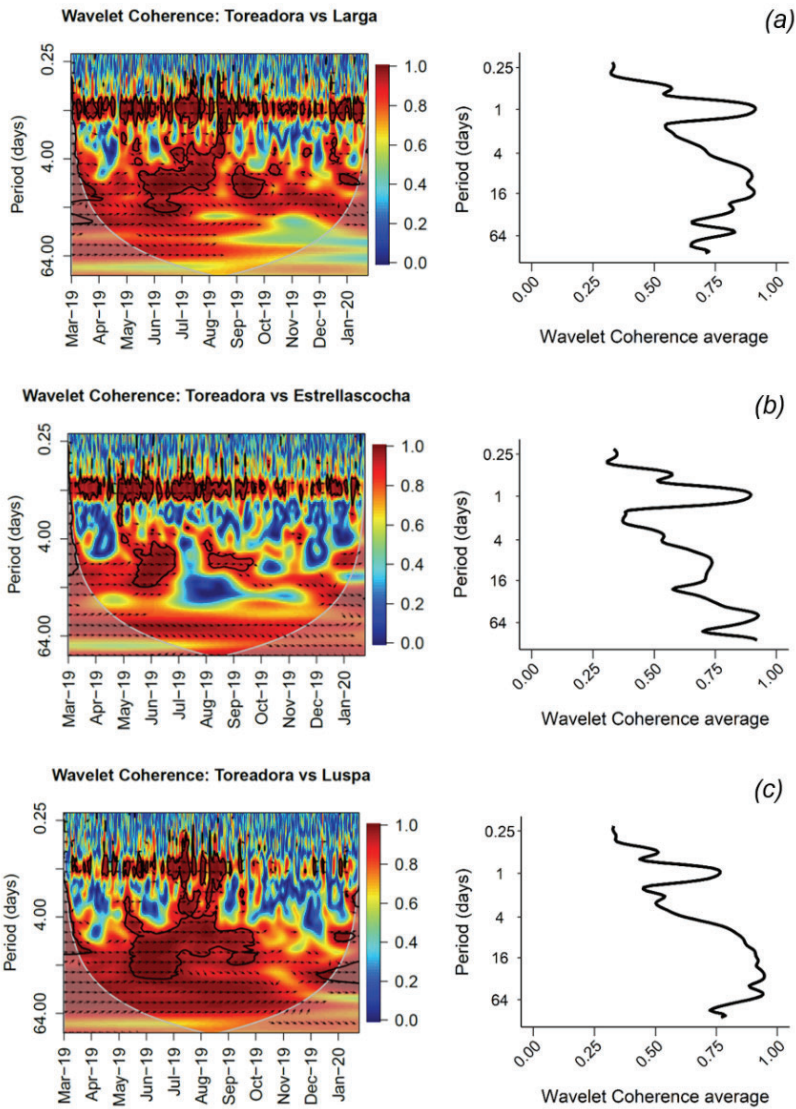


Figure 9. Selected cross-wavelet diagrams to illustrate the tree types of coherence found among lake pairs. The complete set of pair comparisons can be found in the Supplementary information (Fig. S1, S2).

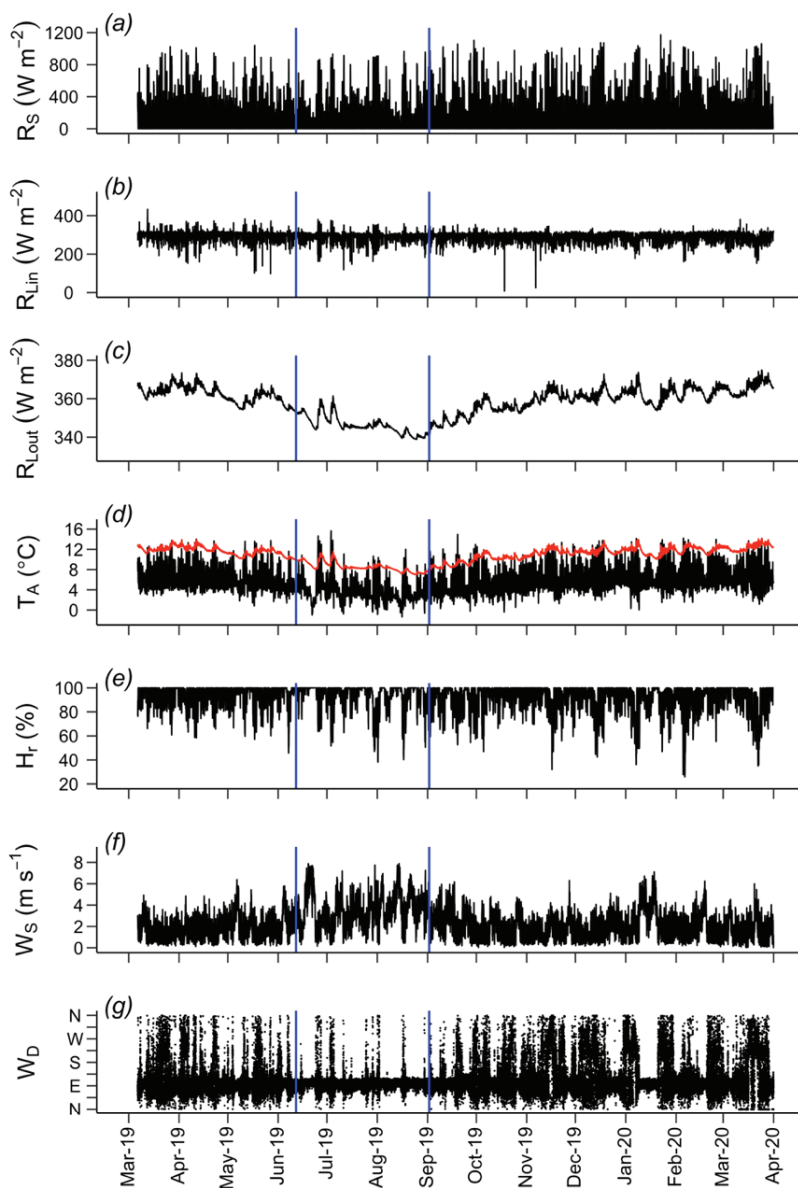


Figure 10. Meteorological forcing components in Lake Toreadora. (a) Short-wave radiation. (b) Incident long-wave radiation. (c) Outgoing long-wave emission. (d) Air temperature (red line is the lake surface temperature). (e) Relative humidity. (f) Wind speed. (g) Wind direction. The period of low Schmidt stability from June to September is indicated across panels (blue lines).

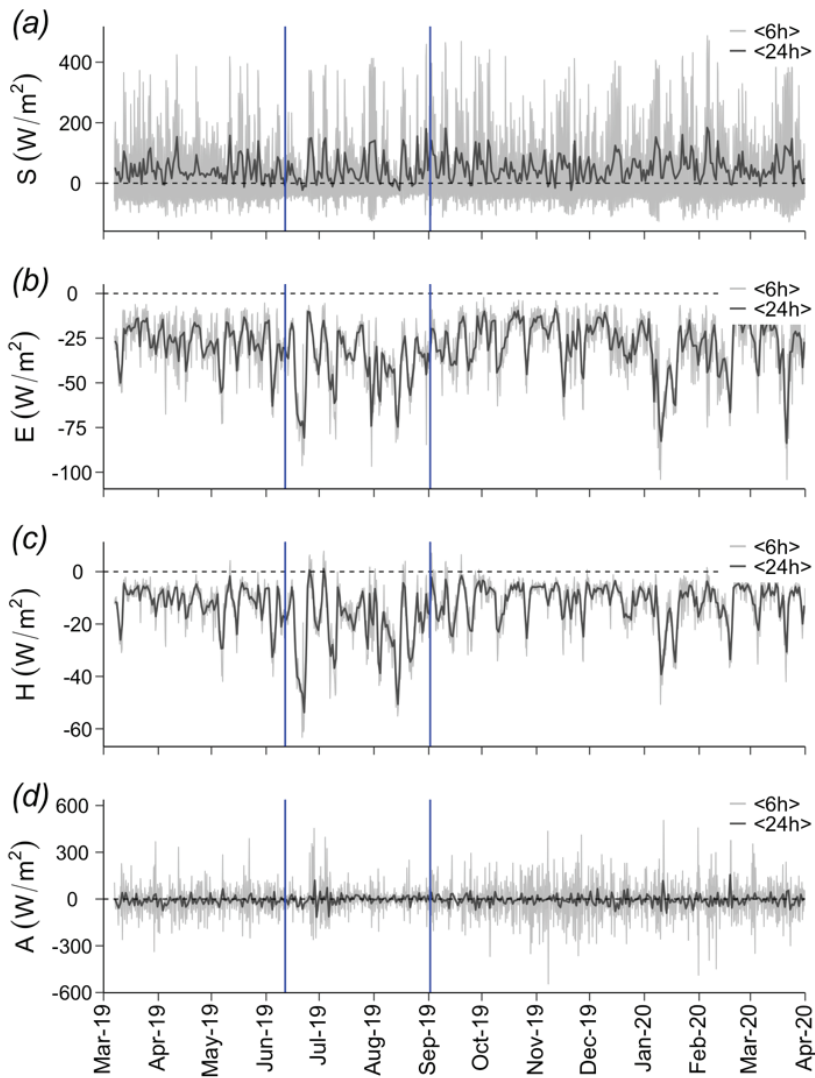


Figure 11. Heat flux components in Lake Treadora. (a) Radiative flux; balance between short-wave and long-wave in and out fluxes. (b) Heat flux associated with evaporation. (c) Sensible heat flux. (d) Advective heat flux estimated by the difference between the sum of the other heat flux components and the heat change in the lake's total heat content. The period of low Schmidt stability from June to September is indicated across panels (blue lines). The series show six, $\langle 6h \rangle$; and twenty-four hours $\langle 24h \rangle$ moving averages of the recorded signals.

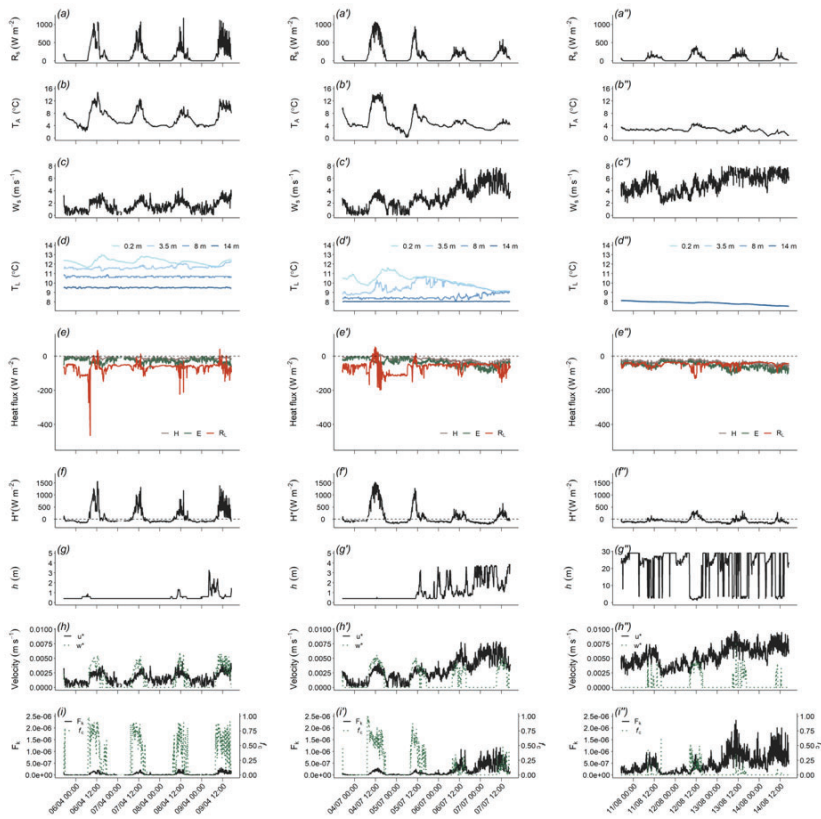


Figure 12. Some daily-scale time windows to illustrate the dominant processes during the stability period (15-18 April 2019, a-i), the transition to instability (6-9 July 2019, a'-i'), and an extreme situation of instability (11-14 August 2019, a''-i'') indicating the weather conditions and thermal and kinetic fluxes in Lake Toreadora. (a) SW, short-wave radiation; (b) T_a , air temperature; (c) WS, wind speed; (d) T_L , lake temperature at 0.2, 3.5, 8, and 14 m depth; (e) Surface heat fluxes (long-wave, evaporative, and sensible heat); (f) Effective heat flux at the surface layer; (g) mixing layer thickness; (h) convective and shear velocity; (i) mechanical energy flux and the fraction derived from the buoyancy flux.

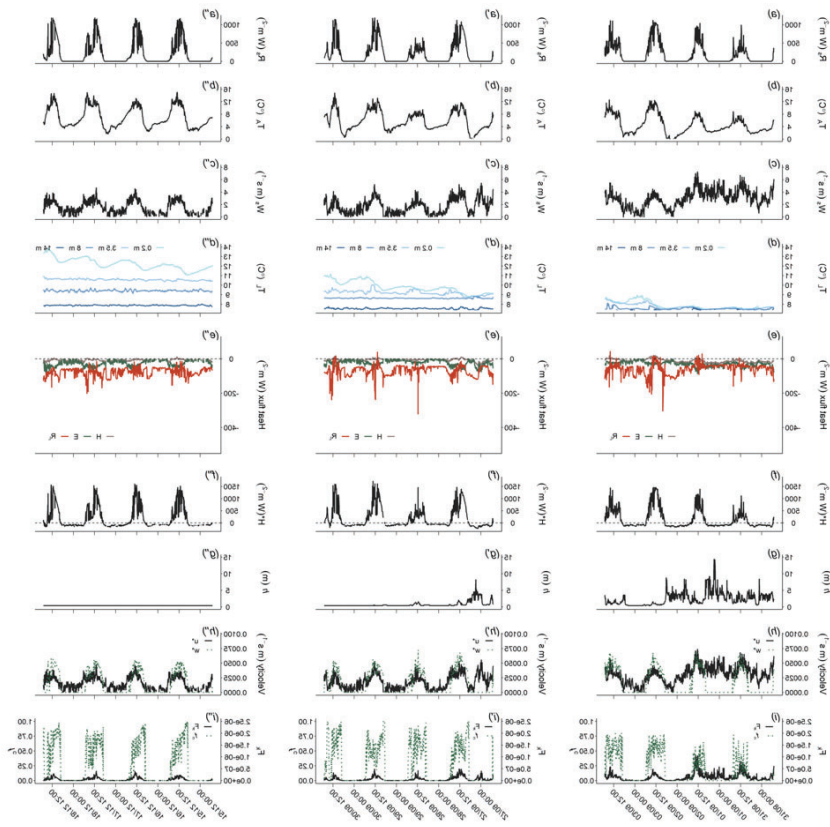


Figure 13. Some daily-scale time windows to illustrate the dominant processes during the end of the mixing period and the transition to stability (August 31 to September 3, 2019; a-i), increased stability (27-30 October 2019, a'-i') and an extreme situation of high stability (15-18 December 2019, a''-i'') indicating the weather conditions and thermal and kinetic fluxes in Lake Toredora. (a) SW, short-wave radiation; (b) T_a , air temperature; (c) WS, wind speed; (d) T_L , lake temperature at 0.2, 3.5, 8, and 14 m depth; (e) Surface heat fluxes (long-wave, evaporative, and sensible heat); (f) Effective heat flux at the surface layer; (g) mixing layer thickness; (h) convective and shear velocity; (i) mechanical energy flux and the fraction derived from the buoyancy flux.

Heat and momentum exchange

The mechanisms driving the observed daily, weekly, and seasonal patterns were investigated in Lake Toreadora, where the AWS was near the lake. The seasonal changes in the driving meteorology between the stable and unstable periods comprised a decline of 1.6 °C in average air temperature and radiation (13.4 W m^{-2}) and an increase in wind intensity (1.2 m s^{-1}), with a shift of the whole wind speed distribution upwards (Fig. 10, S3). Consequently, the latent heat and sensible heat outfluxes increased, and there was little change in the radiative balance (Fig. 11).

The marked increase in wind intensity enhanced momentum transfer during the unstable period. Zooming on few-day windows facilitates visualizing the dominant processes and their characteristics during specific periods (Fig. 12, 13). During the stability period (Fig. 12 a-i, 13 a''-i''), alternating clear and cloudy days with low winds generated buoyancy gains and losses, affecting only the upper meters. The thickness of the mixed layer was usually $<1 \text{ m}$, with episodic increases to 2-3 m during low irradiance and higher wind.

Irradiance penetration was relatively low (Van Colen et al. 2017), which causes buoyancy gain in the upper layer that counteracts negative heat fluxes by evaporation and sensible heat flow towards colder air. Only on cloudy and windy days, turbulent mixing deepened the surface mixed layer by the combined action of convective and wind-shear turbulent mixing. Because wind enhances evaporation and heat transfer, convection contribution to turbulent fluxes is often higher than shear contribution (Fig. 12 h).

The surface dynamics during the long stability period did not affect most of the lake volume. However, when colder and windier days increase the transition to the unstable situation, the mixing quickly progressed because daily buoyancy gains did not compensate for night losses (Fig. 12 a'-i'). Thick upper mixed layers became common, effective heat loss predominated most of the day, and

turbulent penetration was dominated by shear velocity (Fig. 12 h'). During the instability period, in the most extreme situations, air temperature hardly reached 4 °C, radiation was low ($<250 \text{ W m}^{-2}$), and the wind speed was high ($> 6 \text{ m s}^{-1}$, Fig. 12 a''-i''). The whole water column could be mixed in a few hours by mostly wind shear. However, this highly unstable situation lasted for a short period, and when meteorological forcing recovered the usual year-long values, the water column stability quickly recovered (Fig. 13).

Seasonal and daily fluctuations were evident in the raw thermistor data and derived calculations. However, the cross-wavelet analyses showed the weekly scale as another relevant focus of variation in the thermal structure of the lakes. Indeed, oscillations at this scale were evident in the wind direction (Fig. 10b). The wind direction in Toreadora was primarily dominated by winds from the East (Fig. S4). However, there was a minor contribution from winds of the West, which, interestingly, were not distributed randomly. The appearance of western winds oscillated quasi-periodically (Fig. 10b); they were common for about one week, and the wind shift stopped during another. Close inspection indicated that when western winds occurred, they predominantly started after noon and lasted until sunrise (Fig. S5). This pattern suggests that they were related to katabatic processes, which will agree with the absence of the wind direction change during the cold months when easterlies are stronger (Fig. 10b).

Interannual variability

Although the high-resolution study of the ten lakes was limited to one year, there are existing monthly profiles for Lake Toreadora to evaluate the interannual persistence of the observed patterns (Fig. 14). The patterns were consistently similar for the period 1996-2020, including the long-stratification period and the shorter instability phase during July and August, with transition months in June and September. The oxygen profiles mimicked the temperature patterns, although oxygen was not fully homogenized across the water

column as temperature during July and August. There are a few mg L^{-1} differences between the surface and bottom, possibly due to the lower diffusivity of oxygen molecules compared to thermal diffusivity and high oxygen demand in the lake's deep layers.

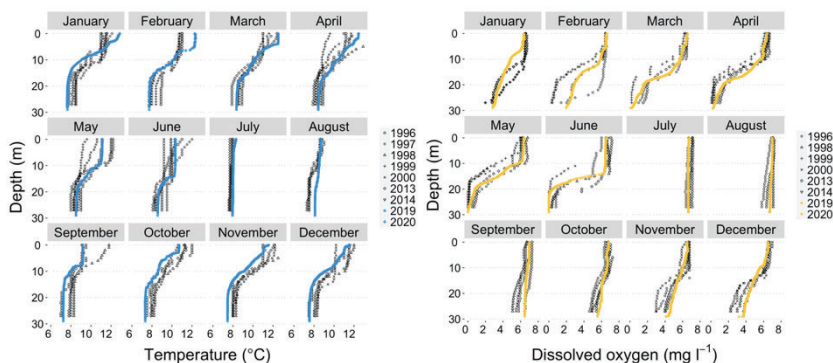


Figure 14. Monthly temperature and oxygen profiles in Lake Toreadora from 1996 to 2020. Profiles from the thermistor study (2019 -2020) are highlighted in color.

4.4 Discussion

Our results provide a robust assessment of the mixing regimes in tropical high-mountain lakes and show that long-year polymixis is not a general feature of these lakes, as traditionally suggested (Löffler 1964; Steinitz-Kannan et al. 1983) and challenged by some recent observations (Catalan and Donato-Rondón 2016; Michelutti et al. 2016). A warm monomictic regime is the most extended pattern. Polymixis occurs only during a limited period of the year (2-3 months). In our study, the all-year-long polymictic regime is limited to the highest (~ 4.000 m a.s.l.) and relatively shallow lakes (< 20 m, maximum depth) lakes. This polymictic pattern also has been found in Perú's Andean lakes located > 4.000 m a.s.l (Michelutti et al. 2019).

Oxygen profiles confirmed the water column's stability throughout many months of the year, and the pluriannual profile series indicated the consistency of the general patterns found, at least for the last three decades. Therefore, high-mountain tropical lakes commonly should show a warm monomictic regime unless they are located at elevations higher than typical for most lakes (e.g., >4000 m a.s.l.) or are shallow. The depth issue should be investigated with further detail as all lakes were > 8 m mean depth in the study set. In high mountain landscapes, water bodies below this mean depth are abundant (dominant) with diffuse limits between what can be denominated a lake, a pond, or a wetland, particularly if they are directly connected to the fluvial network (Mosquera et al. 2017a). The study lake set characterizes the water bodies that undoubtedly will be considered lakes and place them in warm monomictic regimes as low-land tropical lakes have been situated before (Lewis 1996), with the difference of a thermal range of about 10 °C below.

Thermal overall variation within and among lakes was relatively low compared to temperate high-mountain lakes (Catalan et al. 2002). Surface temperature does not markedly differ from summer surface temperature in many high-mountain lake districts (10-15 °C), but the main difference occurs in the deep layers, which hardly achieve values below 6-8 °C. There is no development of a marked seasonal thermocline, dividing the lakes into two clear compartments, a feature that could suggest a lack of water column stability in front of night penetrative convection and wind shear stress. Indeed, the daily scale dominates thermal variation in most lakes throughout the year and provides thermal coherence between them, as shown by the cross-wavelet analyses. However, during most of the year, the daily meteorological fluctuations cannot counteract the stabilizing buoyancy gain provided by short-wave radiation. Consequently, only a relatively shallow upper layer is mixed daily, and the water column shows general stability.

The density gradients across the water column are relatively weak. The overall thermal difference from top to bottom is 5-6 °C. The water column stability is provided by the cumulative effect of many relatively thin layers (a few meters thick) and the lake volume development. The stepwise gradient develops due to alternating high buoyancy gain during the clear sky days and turbulent mixing in windy and cloudy days. Inflows may also play a role in the development of the stepwise structure. The few recorded data on inlets commonly show lower temperature values than the lake's surface. The role of advection transport in the hydrodynamics of these lakes should be studied further, provided that streams likely show short-time temperature fluctuations. It should be noted that wind intensity is low in the area. Although easterlies largely predominate, the intensity is hampered by the Andean Eastern ridge. High-intensity winds common in other mountains rarely occur. Perhaps, this specificity contributed to the misconception about the polymictic character of these lakes. However, L_N calculations using wind intensity in the 8-10 m s⁻¹ range still show values >1 for many lakes, although lower than 10, which seems to be a more appropriate value as a switch indicator for mixing.

Although the daily variation in meteorological forcing in the tropics is more considerable than the seasonal variation, this does not mean that seasonality is not present. In the equatorial region, there are two solar summers (sun in the zenith) and two solar winters (sun position over one of the tropics). However, the second solar winter (December-January) is meteorologically absent because it coincides with increased extra-terrestrial radiation and extended length of the day that compensates for the lower sun elevation. Conversely, these sun position, intensity, and day length mismatches cause a more extended primary winter in June-July (Emck 2007). Eventually, the weekly scale fluctuations mask the solar fluctuations during the rest of the year. Thus, the year splits into a short cold period (June-September) and a warmer period for the rest of the months. Beyond insolation, the oceanic anticyclones shape the climate in the area.

North and South Atlantic high pressures drive the easterlies that predominate in the area. Both anticyclones gain and lose intensity and extension synchronously, producing greater wind intensities in July-August. Therefore, the unstable water columns in the lakes develop because of lower temperatures and stronger winds associated with the climatic situation described. The transitions between “cold” and “warm” synoptic meteorological forcing periods are relatively quick, and so are they reflected in the Schmidt stability of the lakes despite the heat gain and loss being more progressive. The highest lakes (>4000 m a.s.l) develop weaker gradients during calm situations, which are insufficient to resist weak winds. They do not seem to experience lower short-wave radiations; thus, the reason is probably a combined effect of lower air temperature because of the altitude and stronger winds, as expected from the proximity to the ridge.

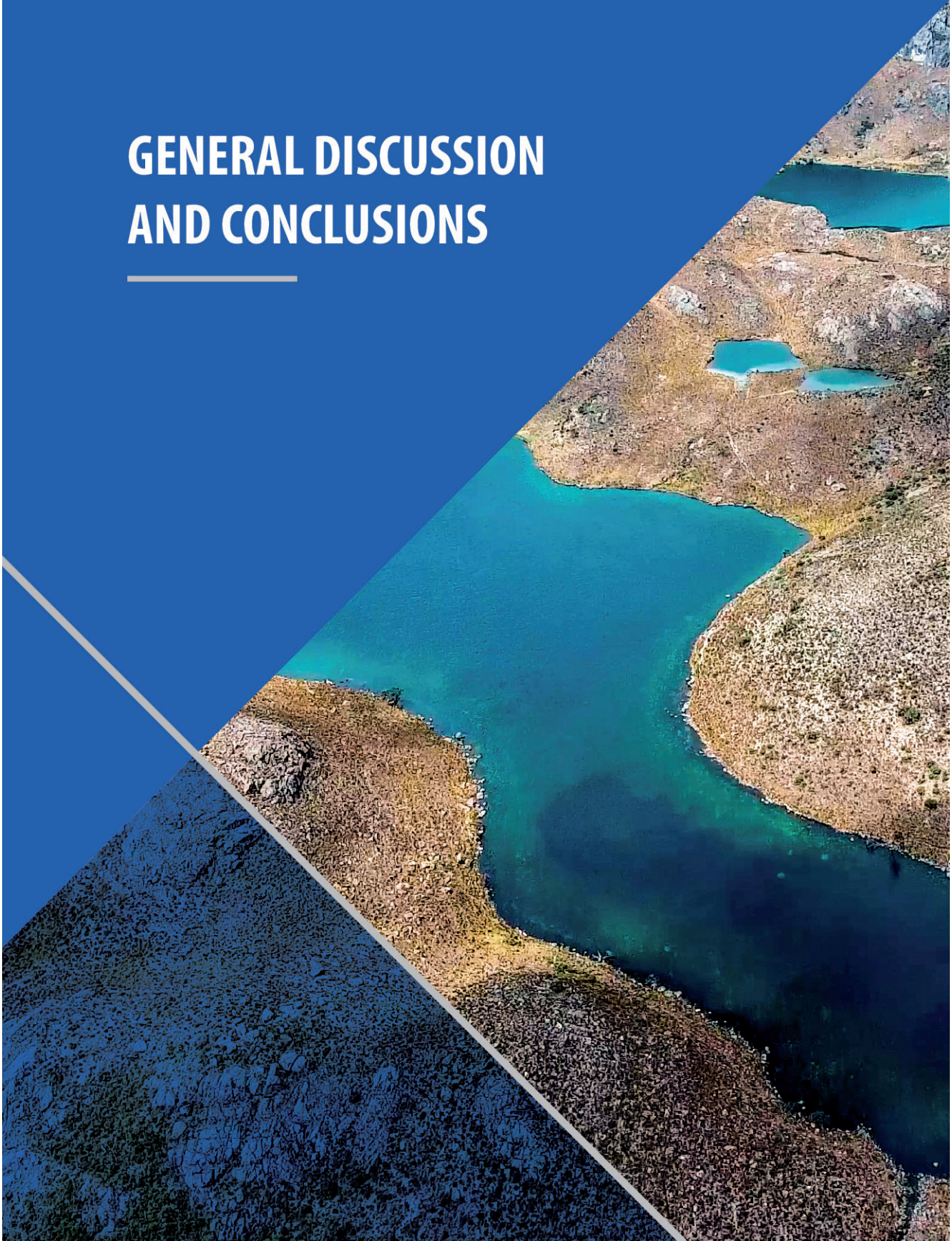
The threshold identified at about 4000 m a.s.l, and also present in the Peruvian lakes, may shift with increasing warming. These lakes could be better sentinels for climate shift than the more abundant and usually studied lower ones. Nevertheless, the cross-wavelet analyses showed a large coherence in the daily and seasonal variability among the lakes, which makes most of them representative for studying past (Schneider et al. 2018) or current climate changes of this tropical region (Michelutti et al. 2016) if interpreted adequately. The conceptual framework should not consider polymixis as the paradigm. Warm monomictic regimes are likely present in many lakes within Holocene climate standards.

The weekly fluctuations coherence among lakes was initially unexpected because oscillations at this scale were thought as part of the weather noise imposed on the stronger daily and seasonal variation. The coherence indicates a common driving mechanism. The quasi-biweekly rhythmicity in the wind direction change from the overwhelming dominant eastern to western in the late evening

was associated with katabatic downslope flows, which can develop in wide valleys in the presence of weak synoptic winds (Princevac et al. 2008). The study lakes' area shows a general elevation decline from NW to SE. Therefore, the wind flow tendency over this slope may interact with the synoptic easterlies, with episodic changes in direction. Interestingly, this interaction produces a quasi-periodic oscillation with about one week in which the shift to western wind occurs on daily bases and about one week that it does not occur. This pattern and the western shift vanish during the “cold” period when the eastern wind intensity is higher. Therefore, the apparent katabatic oscillation is probably driven by oscillations in the Eastern wind intensity, which may interfere with the katabatic wind development. Weekly-scale oscillations have also been described for low land tropical lakes (Lewis Jr. 1983) and can be related to intraseasonal oscillations associated with the particular drivers of South American climate (Liebmann et al. 1999; Alvarez et al. 2014), which discussion is beyond the scope of this study.

Provided the coherence among the lakes studied, the conclusions raised can confidently be extrapolated to the whole Cajas lake district. Could they be extended to other tropical high-mountain lake districts? There are not many studies to compare. Extensive surveys in the páramo lakes of Colombia performed in the 1990s (Donato-R 2010) and late 2010s showed similar oxygen and temperature profiles (Zapata et al. 2021), and the annual cycle in Lake Cumbal (Colombian Andes), the same mixing regime that described in Cajas (Catalan and Donato-Rondón 2016). The similitude makes sense because, although distant, the lake district is under similar synoptic climatic conditions. Tropical high-mountain areas in other parts of the world should share similar solar forcing but may be submitted to different wind circulation conditions and intensities. Indeed, Löffler (1964) already showed summer temperature profiles for African high-mountain lakes that suggest stratification. In any case, we may conclude that polymictic regimes cannot be further presented as the paradigm for lakes in tropical mountains.

GENERAL DISCUSSION AND CONCLUSIONS



5. General Discussion

This thesis constitutes one of the first studies of the Andean tropical zones in which aspects of the limnology of an entire lacustrine system, such as the Cajas Massif in southern Ecuador, are broadly addressed. The thesis' results come from a large set of lakes, in contrast to the few-lakes traditional studies in this planet region. This thesis offers a broad vision of Andean tropical limnology and highlights the importance of the geomorphology of lake basins and altitude in conditioning other aspects, such as the water chemical composition and the physical functioning of water masses.

Generally, the limnology of tropical zones is associated with flood lakes in low areas, such as those formed by abandoned meanders in tropical forests. This perception is primarily due to the high abundance of this type of water masses and has created a historical, scientific bias, particularly comparing tropics and temperate zones. Indeed, there is a large variety of lakes in the tropics: flatland lakes, ancient tertiary lakes, high-mountain lakes, valley lakes, lakes in tropical rainforests, artificial lakes, and subtropical lakes, among others. The small lakes located at high altitudes in tropical mountain ranges constitute one of the most differentiated cases (Nilssen, 1984). Altitude correlates with several strong environmental gradients that considerably model limnological functioning (Lewis Jr., 1987; Ramírez et al., 2020).

In the tropical limnology literature, it is stated that tropical high-mountain lakes of glacial origin are not as abundant as in temperate zones and are relatively less abundant than other lake types in the tropical context (Lewis Jr., 1996 and 2000). However, this lower relative abundance does not justify the low attention paid to them. Very little has been inventoried in the lake districts in the tropical mountains worldwide. Besides, lakes smaller than 0.001 km² have not been part of global inventories (Downing et al., 2006) despite their high abundance, especially in glacial landscapes (Hanson et al.,

2007). In South America, glaciation has formed hundreds of lake districts distributed along the Andes (Rodbell et al., 2008). These lake districts harbor a high abundance of lakes, as in the case of the Cajas Massif (14.7 water bodies per km²), a density comparable to that of European mountain ranges (Chapter 2). In the tropical Andes, this lake abundance has an added and direct value for the large populations that live there because they are a direct source of water for human consumption, irrigation, fish production, and hydroelectricity. Due to the accelerated impact of global change in the Andean mountains and the increase in human pressures on this resource, the deterioration, transformation (damming), and, in some cases, the loss (due to mining activities) of the lake districts are continuous.

The results of the lake abundance and size analysis of the Cajas Massif are framed within an altitudinal range that does not exceed 4500 m a.s.l. in the western cordillera of the Andes, showing a unimodal lacustrine distribution where the highest density occurs at 3936 m a.s.l. However, in other tropical Andean mountains where the altitude exceeds 4500 m a.s.l., the existence of a bimodal distribution is observed with a first mode at a lower altitude than Cajas (3700 m a.s.l.) and a second mode with a peak less than 4300 m, possibly related to different erosive phases of the glaciation (Zapata et al., 2021). This type of distribution is not observed in the mountain chains of the temperate zones, likely due to the restriction of altitude in some ranges (Del Castillo, 2003) and because Asian ranges have not been studied in detail in that sense. It would be interesting to extend the inventories of the lake districts to the mountainous chains in the Andes of Peru (Cordillera Blanca, Cordillera Vilcanota, among others), where there is an altitude continuum from 4000 to 6000 m a.s.l. and active glaciation.

In mountain ranges, altitude constrains the size of lakes compared to those in lowlands since, at higher altitudes, there is less area available for forming large lakes. The lakes of the Cajas Massif show

similarity in the aspect ratio with the alpine lakes of temperate zones (Chapter 2). This pattern was not to be the same in the mountain ranges of the Colombian Andes, whose morphology is shallower, similar to sub-arctic lakes (Catalan & Donato Rondón, 2016; Zapata et al., 2021). Although there are still no complete morphological descriptions of other lake systems in the tropical Andes, individual descriptions show the existence of lakes with areas and depths greater than those reported in Cajas (Steinitz-Kannan et al., 1983; Michelutti et al., 2019). In the satellite images of Google Earth, it is easy to identify the existence of lakes with a large area (> 100 ha) in the páramos of central and northern Ecuador, especially in Peru's mountain ranges. In general, the results show that lake systems of glacial origin could be more represented than previously described in an Andean landscape context, showing many geomorphological similarities with other glacial regions of the planet. Let us consider the factors that most influence the limnological variation of Andean tropical lakes based on the results in the Cajas Massif:

5.1 Altitude

The tropical mountains of the Andes show a wide range of altitude from 3000 to ~5100 m a.s.l. In the Cajas Massif, we can distinguish three well-differentiated altitudinal belts concerning the lacustrine system. The first corresponds to the lakes between 3000 to 3500 m a.s.l., generally valley lakes formed by terminal moraines and likely surrounded by forest formations. The forest line does not have the same altitude across the tropical Andes; it changes from 3500 to 3800 m a.s.l. Second, the lakes above the forest line that are within the “páramo” biome. And finally, those lakes at the headwaters of the watersheds, in the “superpáramo,” within sparsely vegetated areas with rocky soils that are still covered by ice in some parts of the tropical Andes. In the case of the Cajas Massif, this limit is above 4000 m a.s.l. However, in other lake complexes, it could be higher. The little existing limnological information prevents precise

conjectures about these divisions and generally groups all the lakes as “Paramo de los Altos Andes” lakes (Steinitz-Kannan et al., 1983). Soil development, vegetation, bedrock exposure, the presence of glaciers, and atmospheric deposition change with altitude. Therefore, the allochthonous contribution of chemical compounds to the lakes likely will vary with elevation. For instance, it could be expected that the allochthonous contribution of dissolved organic carbon (DOC) would be higher with increasing soil development (Buytaert et al., 2005). The DOC variability should modify the water transparency for both PAR and UV light. (Van Colen et al., 2017; Aguilera et al., 2013; Laurion et al., 2000). Furthermore, catchments at higher altitudes show rockier substrates, more exposed to weathering, which could increase the ionic and phosphorous charge and decrease the nitrogen in the water, and in the higher lake districts that are fed by glacial melting, high values of conductivity, phosphorus, DOC and turbidity could be found (Barta et al., 2018; Michelutti et al., 2019). Surprisingly, in our water chemistry models, altitude was not a significant driver for chemical variability except for iron. This lack of relationship could be due to the relatively low altitudinal range in the Cajas Massif; almost all lakes were below 4000 m a.s.l (Chapter 3). On the other hand, atmospheric deposition studies in the Cajas Massif have shown that the greatest deposition of pollutants occurs at 3400 m a.s.l. and not in the highest parts (4130 m a.s.l (Bandowe et al., 2018; Schneider et al., 2021), atmospheric deposition is one aspect not considered in our study that might have some influence in the variation observed.

Altitude showed a substantial effect on the mixing patterns of the lakes of the Cajas Massif. The warm monomictic regime was the most widespread (Chapter 4), as also reported for the mountain lake districts of Colombia (Zapata et al., 2021; Catalan & Donato Rondón, 2016), ruling out polymyxis as has traditionally been suggested for these tropical areas (Löffler 1964; Steinitz-Kannan et al., 1983). However, the lakes that are at higher altitudes (> 4000 m a.s.l.) and relatively shallow (<20 m, maximum depth) showed an

annual polymictic regime similar to that reported by Michelutti et al. (2019) for relatively shallow lakes above 4800 m a.s.l. (range 4778–5107) in the Vilcanota mountain range in the Peruvian Andes.

5.2 Lake size

The area and the depth have very relevant effects on mountain lakes. In European alpine lakes, the lake size has been identified as an environmental variable determining the assemblages of diatom, rotifers, chydorids, planktonic crustaceans, and chironomids (Catalan et al., 2009). In the case of the lakes of the Cajas massif, mean depth and the ratio between watershed and lake areas significantly influence the water chemistry (Chapter 3). The smaller and shallower lakes are most organic ($>$ DOC, TP, and NH_4^+), less mineralized ($<$ conductivity and Ca^{2+}), and show higher metal levels (e.g., aluminum and iron). These characteristics should determine different biological communities compared to larger lakes. Shallower systems in other tropical areas of the Andes (Colombia, Peru, and Bolivia) have shown the same organic ranges (DOC range: 0.15 - $>$ 21 mg/l) as the lakes of the Cajas Massif (Zapata et al., 2021; Michelutti et al., 2019) and low transparency with high UV-A light attenuation coefficients due to high DOC contents (Aguilera et al., 2013).

5.3 Bedrock

In general, the lithology of the mountain lake districts in the Andes is the product of active volcanism, which produces lava flows that overlap unevenly and heterogeneously over time, complemented more locally by hydrothermal processes that reach the surface creating substrate patches that differ from the dominant rock. This variability of volcanic bedrock provides highly diverse chemistry in relatively small areas, with calcium being the most common and dominant cation (Chapter 3). This variability has also been reported in other Andean lake districts (Zapata et al., 2021; Michelutti et al.,

2019; Steinitz-Kannan et al., 1983) and, generally, the acid neutralizing capacity (ANC) of the lakes. Tropical mountain lakes of the Andes exceed the two European thresholds (ANC 200 and 1000 $\mu\text{eq L}^{-1}$) established for European mountain lakes, so their sensitivity to acidification is lower (Catalan et al., 2009).

5.4 Wetlands

The proportion of wetlands in the lake catchment of tropical mountain systems is a significant factor influencing water chemistry, especially in shallow and small systems. The models of the lakes of the Cajas Massif showed a positive relationship between the levels of nutrients and metals (iron, manganese, nitrate, phosphorus, and DOC) and the proportion of wetlands in the catchment (Chapter 3). Possibly the explanation is that water in wetlands has an acidic pH and a lower redox potential, which facilitate the solubility of the organic Matter)-Al(Fe)-phosphate complexes characteristic of tropical mountain soils (Van Colen et al., 2017; Sanchez-Murillo et al., 2022). This effect is more critical in smaller lakes (ponds and shallow lakes) because wetland areas appear as patches that are generally not extensive in a large grassland matrix. So, for large and deep systems, the occupation of wetlands in the catchment is generally low and not directly attached to the water body. Therefore, the effects of the runoff from wetlands to the lake might not be noticeable in the final chemistry.

5.5 Anoxic layers

A characteristic of tropical mountain lakes that differentiates them from temperate mountain lakes is the presence of a thick deep anoxic layer (Chapter 4). This anoxia is more related to the stable annual stratification (9 months) and to the high oxygen demand determined by the allochthonous loads of organic matter than to the lake's productivity since lakes are essentially oligotrophic or ultraoligotrophic. The anoxia should influence the biogeochemical

pathways in many ways; for instance, becoming a reservoir of ammonium and generating a great denitrification potential around the oxycline coupled with nitrification. Consequently, nitrogen losses from the aquatic system could be high, and nitrogen fixation could become a crucial process to maintain the activity of the aquatic ecosystem (Catalan & Donato Rondón, 2016). Similarly, anoxia can facilitate the solubility of phosphorus and metals, providing a more significant internal load of nutrients, the thicker and stronger the redox gradient, which could influence productivity throughout the year by diffusion (Donato-Rondon, 2010). The functional role of these deep anoxic layers is a subject that merits further research.

6. Conclusions

Chapter 2

- The shape of the distribution of the lake-area abundance from the Cajas Massif is similar to those found in other high-mountain lake districts of glacial origin. It appears as a general feature that the mountain lake distribution differs at both ends from a power law relationship. The deviation in the large-size lake extreme has been attributed to the restriction imposed by altitude, and additional factors like periglacial processes, steep slopes, thin soils, and torrential stream flows that may have enhanced the lake filling.
- The Cajas Massif lakes show shorelines with a fractal dimension $D=1.08$, similar to Earth's lakes $< 4.7 \text{ km}^2$, with no clear departure from this scaling along the lake-size range. One can conclude that the interaction with terrestrial systems and littoral environments in these lakes scale similarly throughout the lake-size range.
- One of the consequences of the biased distribution of the lake-area abundance is that within the Cajas Massif—and probably in similar mountain lake districts—most of the lentic water surface is in midsize lakes and not in ponds. About 50% and more than 85% of the water surface area is on lakes $>10^5$ and $>10^4 \text{ m}^2$, respectively. It is particularly relevant in the context of gas emissions and watershed fluvial network dynamics. Ponds may be of interest for the metacommunity dynamics of some aquatic organisms restricted or with a preference for these systems.
- Significant scattering in some parts of the lake-size gradient (e.g., 10^4 to 10^5 m^2) indicates variations in the geomorphological process configuring the current lake basins. Several particularities point to a differential lake filling as the cause of

the high depth (volume) variation at this mid-lake-size range. The markedly less noisy relationship between area and perimeter than between area and volume indicates that there has been a transformation of the lake bottoms processes posterior to the lake formation.

- Despite the likely profound transformation of some of the Cajas Massif lakes after the excavation of the basin, the general pattern of lake basin formation, illustrated by the patterns between lake area and the maximum depth, still agrees with that from alpine lakes in European ranges and differ from those in subarctic areas. In the latter region, lakes are much wider with respect to depth than in high mountains.
- The dynamics of these relatively shallow lakes, with high water renewal, are mainly dominated by what happens in the watershed and associated stream transport; therefore, they are excellent for reconstructing extreme rainfall events and vegetation and land use changes.

Chapter 3

- High mountain lakes in volcanic basins can present extremely variable water chemistry in relatively small areas, comparable to that in large mountain ranges, where the substrate includes plutonic, metamorphic, and carbonate bedrock changing over large areas.
- The high correlation of calcium with alkalinity and conductivity indicates that partial aluminosilicate dissolution is the primary source of cations in these lakes. Water alkalinity generation primarily occurs in the subsoil saprolite, which explains why water hardness increases with watershed and lake size.

- Complementary weathering processes beyond the predominant cation source could be found in high mountain lakes in volcanic basins. Silica levels indicate complete aluminosilicate dissolution and are associated with monovalent cations (sodium) and sulfate. Likely, they are associated with former hydrothermal processes of active volcanism, which may enhance albitization.
- Average and extreme DOC and iron levels are higher in the Cajas Massif lakes than in temperate mountain lake districts and similar to some boreal areas. Small lakes and ponds record the higher values related possibly to the idiosyncratic connections with organic soils surrounding the water body. The organic and metal contents do not share the same main drivers. Paludification, nevertheless, is not a generalized feature in Cajas lakes and ponds, and a wide range of clear to brownish waters are present.
- The chemical variation (main ion composition, dissolved organic matter, and metals) found in the Cajas Massif lakes and ponds is comparable to that of all the European mountain ranges. Therefore, tropical high mountain lakes provide a variety of aquatic chemical niches in relatively small territories that might foster species richness of aquatic organisms that are sensitive to a specific water chemical composition.

Chapter 4

- Mixing regimes in tropical high-mountain lakes show that a warm monomictic regime is the most extended pattern, not annual polymixis, as traditionally suggested. Polymixis occurs only during a limited period of the year (2-3 months). The all-year-long polymictic regime is limited to the highest (~4.000 m a.s.l.) and relatively shallow lakes (<20 m, maximum depth) lakes.

- The density gradients across the water column in tropical high-mountain lakes are relatively weak compared to temperate high-mountain lakes. Nevertheless, the water column stability is provided by the cumulative effect of many relatively thin layers (a few meters thick) and the lake volume development. This stepwise gradient develops due to alternating high buoyancy gain during the clear sky days and turbulent mixing in windy and cloudy days.

REFERENCES

- Aguilera X., Lazzaro X., Coronel JS. 2013. Tropical high-altitude Andean lakes located above the tree line attenuate UV-A radiation more strongly than typical temperate alpine lakes. *Photochem. Photobiol. Sci.* **12**:1649-1657.
- Ambrosetti, W., and Barbanti, L. 2002. Physical limnology of Italian lakes. 2. Relationships between morphometric parameters, stability and Birgean work. *Journal of Limnology* **61**: 159-167.
- Alvarez, M. S., C. S. Vera, G. N. Kiladis, and B. Liebmann. 2014. Intraseasonal variability in South America during the cold season. *Clim Dynam* **42**: 3253-3269.
- Allen, R. L., I. Lundstrom, M. Ripa, A. Simeonov, and H. Christofferson. 1996. Facies analysis of a 1.9 Ga, continental margin, back-arc, Felsic Caldera province with diverse Zn-Pb-Ag-(Cu-Au) sulfide and Fe oxide deposits, Bergslagen region, Sweden. *Econ Geol* **91**: 979-1008.
- APHA-AWWA-WEF. 2012. Standard Methods for examination of water and wastewater, 22nd ed. American Public Health Association.
- Armienta, M. A. and others 2008. Water chemistry of lakes related to active and inactive Mexican volcanoes. *J Volcanol Geotherm Res* **178**: 249-258.
- Balslev, H., and Luteyn, J. L. 1992. Paramo, an Andean ecosystem under human influence (Paper presented during the Paramo Symposium held at Aarhus University, Denmark 11-12 June 1991).
- Bandowe, B. A. M. and others 2018. A 150-year record of polycyclic aromatic compound (PAC) deposition from high Andean Cajas National Park, southern Ecuador. *Sci Total Environ* **621**: 1652-1663.
- Barta, B. and others 2018. Glacial-fed and páramo lake ecosystems in the tropical high Andes. *Hydrobiologia*, **813**: 19-32.
- Beamish, R. J., and H. H. Harvey. 1972. Acidification of La Cloche mountain lakes, Ontario, and resulting fish mortalities. *J Fish Res Board Can* **29**: 1131-1143.
- Beiderwieden, E., T. Wrzesinsky, and O. Klemm. 2005. Chemical characterization of fog and rain water collected at the eastern Andes cordillera. *Hydrol. Earth Syst. Sci.* **9**: 185-191.

- Benedetti, M. and others 2002. Chemical weathering of basaltic lava flows undergoing extreme climatic conditions: The water geochemistry record. *Chem Geol* **201**: 1-17.
- Benito, X. and others 2019. Identifying temporal and spatial patterns of diatom community change in the tropical Andes over the last c. 150 years. *J Biogeogr* **46**: 1889-1900.
- Bethke, C. M. 2008. *Geochemical and biogeochemical modeling*, Second ed. Cambridge University Press.
- Boehrer, B., and M. Schultze. 2010. Density stratification and stability, p. 96-106. In G. E. Likens [ed.], *Lake ecosystem ecology: a global perspective*. Elsevier.
- Borja, P., and P. Cisneros. 2009. Estudio edafológico. Informe del II año del proyecto "Elaboración de la línea base en hidrología de los páramos de Quimsacocha y su área de influencia", p. 104.
- Boy, J., and W. Wilcke. 2008. Tropical Andean forest derives calcium and magnesium from Saharan dust. *Global Biogeochem Cy* **22**: GB1027.
- Bradley, R. S., M. Vuille, H. F. Diaz, and W. Vergara. 2006. Threats to water supplies in the tropical Andes. *Science* **312**: 1755-1756.
- Buytaert, W. and others 2006. Human impact on the hydrology of the Andean páramos. *Earth-Sci Rev* **79**: 53-72.
- Buytaert, W., J. Sevink, B. De Leeuw, and J. Deckers. 2005. Clay mineralogy of the soils in the south Ecuadorian páramo region. *Geoderma* **127**: 114-129.
- Cael, B. B., A. J. Heathcote, and D. A. Seekell. 2017. The volume and mean depth of Earth's lakes. *Geophys Res Lett* **44**: 209-218.
- Cael, B. B., and D. A. Seekell. 2016. The size-distribution of Earth's lakes. *Sci Rep* **6**: 29633.
- Cael, B. B., Biggs, J., and Seekell, D. A. 2022. The size-distribution of earth's lakes and ponds: Limits to power-law behavior. *Front. Environ. Sci.* **10**: 888735.
- Camarero, L., and Catalan, J. 1996. Variability in the chemistry of precipitation in the Pyrenees (northeastern Spain): Dominance of storm origin and lack of altitude influence. *Journal of Geophysical Research: Atmospheres* **101**: 29491-29498.

- Camarero, L. and others 2009. Regionalisation of chemical variability in European mountain lakes. *Freshw Biol* **54**: 2452-2469.
- Carrillo-Rojas, G., B. Silva, M. Córdova, R. Célleri, and J. Bendix. 2016. Dynamic mapping of evapotranspiration using an energy balance-based model over an Andean páramo catchment of Southern Ecuador. *Remote Sensing* **8**: 160.
- Catalan, J., E. Ballesteros, E. Gacia, A. Palau, and L. Camarero. 1993. Chemical composition of disturbed and undisturbed high-mountain lakes in the Pyrenees - a reference for acidified sites. *Water Res* **27**: 133-141.
- Catalan, J. and others 2006. High mountain lakes: extreme habitats and witnesses of environmental changes. *Limnetica* **64**: 123-145.
- Catalan, J. and others 2009a. Ecological thresholds in European alpine lakes. *Freshw Biol* **54**: 2494-2517.
- Catalan, J., C. J. Curtis, and M. Kernan. 2009b. Remote European mountain lake ecosystems: regionalisation and ecological status. *Freshw Biol* **54**: 2419-2432.
- Catalan, J., and J. C. Donato-Rondón. 2016. Perspectives for an integrated understanding of tropical and temperate high-mountain lakes. *J Limnol* **75(s1)**: 215-234.
- Catalan, J. and others 2013. Global change revealed by palaeolimnological records from remote lakes: A review. *J Paleolimnol* **49**: 513-535.
- Catalan, J. and others 2002. Seasonal ecosystem variability in remote mountain lakes: implications for detecting climatic signals in sediment records. *J Paleolimnol* **28**: 25-46.
- Celleri, R., P. Willems, W. Buytaert, and J. Feyen. 2007. Space-time rainfall variability in the Paute basin, Ecuadorian Andes. *Hydrol Process* **21**: 3316-3327.
- Coblentz, D., and P. L. Keating. 2008. Topographic controls on the distribution of tree islands in the high Andes of south-western Ecuador. *J Biogeogr* **35**: 2026-2038.
- Colinvaux, P. A., M. B. Bush, M. SteinitzKannan, and M. C. Miller. 1997. Glacial and postglacial pollen records from the Ecuadorian Andes and Amazon. *Quaternary Res* **48**: 69-78.
- Crespo, P. J. and others 2011. Identifying controls of the rainfall-runoff response of small catchments in the tropical Andes (Ecuador). *J Hydrol* **407**: 164-174.

- Cruz, J. V., R. M. Coutinho, M. R. Carvalho, N. Oskarsson, and S. R. Gislason. 1999. Chemistry of waters from Furnas volcano, Sao Miguel, Azores: fluxes of volcanic carbon dioxide and leached material. *J Volcanol Geotherm Res* **92**: 151-167.
- Chivas, A. R., P. de Deckker, and J. M. G. Shelley. 1986. Magnesium content of non-marine ostracod shells: A new palaeosalinometer and palaeothermometer. *Palaeogeogr Palaeoclimatol Palaeoecol* **54**: 43-61.
- Degefu, F., and Schagerl, M. 2015. Zooplankton abundance, species composition and ecology of tropical high-mountain crater Lake Wonchi, Ethiopia. *J. Limnol.* **74**: 324-334.
- de Mendoza, G., W. Traunspurger, A. Palomo, and J. Catalan. 2017. Nematode distributions as spatial null models for macroinvertebrate species richness across environmental gradients: a case from mountain lakes. *Ecol Evol* **on-line first doi: 10.1002/ece3.2842**.
- Del Castillo, M. 2003. Morfometría de los lagos: Una aplicación a los lagos del Pirineo (Doctoral dissertation, PhD. Thesis, University of Barcelona (in Spanish)).
- Di Figlia, M. G., A. Bellanca, R. Neri, and A. Stefansson. 2007. Chemical weathering of volcanic rocks at the island of Pantelleria, Italy: Information from soil profile and soil solution investigations. *Chem Geol* **246**: 1-18.
- Donato-R, J. 2010. Phytoplankton of Andean lakes in Northern Southamerica (Colombia). Composition and distribution factors. A.R.G. Gantner Verlag K.G.
- Dormann, C. F. and others 2018. Model averaging in ecology: a review of Bayesian, information-theoretic, and tactical approaches for predictive inference. *Ecol Monogr* **88**: 485-504.
- Downing, J. A. and others 2006. The global abundance and size distribution of lakes, ponds, and impoundments. *Limnol Oceanogr* **51**: 2388-2397.
- Downing, J. A. 2009. Global limnology: Up-scaling aquatic services and processes to planet Earth. *Internationale Vereinigung für theoretische und angewandte Limnologie: Verhandlungen* **30**: 1149-1166.
- Dunkley, P., and A. Gaibor. 2009. Mapa geológico Cordillera Occidental 2o-3o. Hoja geológica Cuenca -NVF 53. In I. G. M. d. Ecuador [ed.]. Servicio Geológico Nacional. Ministerio de Minas y Petróleos. República de Ecuador.

- Dupre, B. and others 2003. Rivers, chemical weathering and Earth's climate. *C R Geosci* **335**: 1141-1160.
- Dussart, G. 1976. The ecology of freshwater molluscs in North West England in relation to water chemistry. *J Molluscan Stud* **42**: 181-198.
- Eggermont, H., J. M. Russell, G. Schettler, K. Van Damme, I. Bessems, and D. Verschuren. 2007. Physical and chemical limnology of alpine lakes and pools in the Rwenzori Mountains (Uganda-DR Congo). *Hydrobiologia* **592**: 151-173.
- Eldrandaly, K. A., and M. S. Abu-Zaid. 2011. Comparison of six GIS-based spatial interpolation methods for estimating air temperature in Western Saudi Arabia. *J Environ Inform* **18**: 38-45.
- Emck, P. 2007. A climatology of South Ecuador, with special focus on the major Andean ridge as Atlantic-Pacific divide. Friedrich-Alexander-Universität Erlangen-Nürnberg.
- Engvik, A. K., A. Putnis, J. D. Fitz Gerald, and H. k. Austrheim. 2008. Albitization of granitic rocks: the mechanism of replacement of oligoclase by albite. *Canad Mineral* **46**: 1401-1415.
- Fabian, P., M. Kohlpaintner, and R. Rollenbeck. 2005. Biomass burning in the Amazon-Fertilizer for the mountaineous rain forest in Ecuador *Environ Sci Pollut R* **12**: 290-296.
- Fee, E. J. 1992. Effects of lake size on phytoplankton photosynthesis. *Can J Fish Aquat Sci* **49**: 2445-2459.
- Franke, R. 1982. Smooth interpolation of scattered data by local thin plate splines. *Comput Math Appl* **8**: 273-281.
- Franke, R., and G. Nielson. 1980. Smooth interpolation of large sets of scattered data. *Int J Numer Meth Eng* **15**: 1691-1704.
- Gergel, S. E., M. G. Turner, and T. K. Kratz. 1999. Dissolved organic carbon as an indicator of the scale of watershed influence on lakes and rivers. *Ecol Appl* **9**: 1377-1390.
- Grimalt, J. O. and others 2001. Selective trapping of organochlorine compounds in mountain lakes of temperate areas. *Environ Sci Technol* **35**: 2690-2697.
- Grinsted, A., J. C. Moore, and S. Jevrejeva. 2004. Application of the cross wavelet transform and wavelet coherence to geophysical time series. *Nonlin. Processes Geophys.* **11**: 561-566.

- Gunkel, G. 2000. Limnology of an equatorial high mountain lake in Ecuador, Lago San Pablo. *Limnologica* **30**: 113-120.
- Gunkel, G., and Beulker, C. 2009. Limnology of the Crater Lake Cuicocha, Ecuador, a cold water tropical lake. *Int. Rev. Hydrobiol.* **94**: 103-125.
- Hakanson, L. 1981. *A Manual of Lake Morphometry*. Springer Berlin Heidelberg.
- Hanselman, D., and B. Littlefield. 1998. *Mastering MATLAB 5: A Comprehensive Tutorial and Reference*. Prentice-Hall Inc.
- Hansen, B. C. S., D. T. Rodbell, G. O. Seltzer, B. Leon, K. R. Young, and M. Abbott. 2003. Late-glacial and Holocene vegetational history from two sites in the western Cordillera of southwestern Ecuador. *Palaeogeography Palaeoclimatology Palaeoecology* **194**: 79-108.
- Hanson, P. C., S. R. Carpenter, J. A. Cardille, M. T. Coe, and L. A. Winslow. 2007. Small lakes dominate a random sample of regional lake characteristics. *Freshw Biol* **52**: 814-822.
- Hobbs, W. O. and others 2010. Quantifying recent ecological changes in remote lakes of North America and Greenland using sediment diatom assemblages. *Plos One* **5**: e10026.
- Hohenegger, C., B. Alali, K. R. Steffen, D. K. Perovich, and K. M. Golden. 2012. Transition in the fractal geometry of Arctic melt ponds. *Cryosphere* **6**: 1157-1162.
- Hungerbühler, D. and others 2002. Neogene stratigraphy and Andean geodynamics of southern Ecuador. *Earth-Sci Rev* **57**: 75-124.
- Hutchinson, G. E. 1957. *A treatise on limnology*. Vol. I. Geography, physics and chemistry. John Willey & Sons. Inc. New York, 1015.
- Hutchinson, G. E., and H. Löffler. 1956. The thermal classification of lakes. *Proc Natl Acad Sci U S A* **42**: 84-86.
- Imberger, J. 1985. The diurnal mixed layer1. *Limnol Oceanogr* **30**: 737-770.
- Imberger, J. 2012. *Environmental fluid dynamics: flow processes, scaling, equations of motion, and solutions to environmental flows*. Academic Press.
- Imberger, J., and J. C. Patterson. 1990. Physical Limnology. *Advances in Applied Mechanics* **27**: 303-471.
- Jacobsen, D., and O. Dangles. 2017. *Ecology of high altitude waters*. Oxford University Press.

- Kamenik, C., R. Schmidt, G. Kum, and R. Psenner. 2001. The influence of catchment characteristics on the water chemistry of mountain lakes. *Arct Antarct Alp Res* **33**: 404-409.
- Kernan, M. and others 2009. Regionalisation of remote European mountain lake ecosystems according to their biota: environmental versus geographical patterns. *Freshw Biol* **54**: 2470-2493.
- Kim, J.-W. 1976. A Generalized Bulk Model of the Oceanic Mixed Layer. *Journal of Physical Oceanography* **6**: 686-695.
- Kirillin, G., and T. Shatwell. 2016. Generalized scaling of seasonal thermal stratification in lakes. *Earth-Sci Rev* **161**: 179-190.
- Kopáček, J., J. Hejzlar, E. Stuchlik, J. Fott, and J. Vesely. 1998. Reversibility of acidification of mountain lakes after reduction in nitrogen and sulphur emissions in Central Europe. *Limnol Oceanogr* **43**: 357-361.
- Kopáček, J. and others 2017. Climate change increasing calcium and magnesium leaching from granitic alpine catchments. *Environ Sci Technol* **51**: 159-166.
- Laudon, H. and others 2011. Patterns and dynamics of dissolved organic carbon (DOC) in boreal streams: The role of processes, connectivity, and scaling. *Ecosystems* **14**: 880-893.
- Laurion, I., Ventura, M., Catalan, J., Psenner, R., and Sommaruga, R. 2000. Attenuation of ultraviolet radiation in mountain lakes: Factors controlling the among-and within-lake variability. *Limnol Oceanogr* **45**: 1274-1288.
- Lehner, B., and P. Doll. 2004. Development and validation of a global database of lakes, reservoirs and wetlands. *J Hydrol* **296**: 1-22.
- Lewis Jr., W. M. 1983. Temperature, heat, and mixing in Lake Valencia, Venezuela. *Limnol Oceanogr* **28**: 273-286.
- Lewis Jr, W. M. 1987. Tropical limnology. *Annu Rev Ecol Evol Syst* **18**: 159-184.
- Lewis, W. M. 1996. Tropical lakes: How latitude makes a difference, p. 43-64. In F. Schiemer and K. T. Boland [eds.], *Perspectives in Tropical Limnology*. SPB Academic Publishing.
- Lewis Jr, W. M. 2000. Basis for the protection and management of tropical lakes. *Lakes Reserv.: Res. Manag.* **5**: 35-48.

- Lewis Jr, W. M. 2011. Global primary production of lakes: 19th Baldi Memorial Lecture. *Inland Waters* **1**: 1-28.
- Liebmann, B., G. Kiladis, J. Marengo, T. Ambrizzi, and J. Glick. 1999. Submonthly Convective Variability over South America and the South Atlantic Convergence Zone. *J Climate* **12**.
- Löffler, H. 1964. The limnology of tropical high-mountain lakes. *Verhandlungen Internationalen Vereinigung Limnologie* **15**: 176-193.
- Logue, J., N. Mouquet, H. Peter, H. Hillebrand, and G. Metacommunity Working. 2011. Empirical approaches to metacommunities: a review and comparison with theory. *Trends Ecol Evol* **26**: 482-491.
- Luteyn, J. L. 1992. Páramos: why study them?, p. 1-14. In H. Balslev and J. L. Luteyn [eds.], *Páramo: An Andean ecosystem under human influence*. Academic Press.
- MacIntyre, S., J. R. Romero, and G. W. Kling. 2002. Spatial-temporal variability in surface layer deepening and lateral advection in an embayment of Lake Victoria, East Africa. *Limnol Oceanogr* **47**: 656-671.
- Makowski Giannoni, S., K. Trachte, R. Rollenbeck, L. Lehnert, J. Fuchs, and J. Bendix. 2016. Atmospheric salt deposition in a tropical mountain rainforest at the eastern Andean slopes of south Ecuador – Pacific or Atlantic origin? *Atmos. Chem. Phys.* **16**: 10241-10261.
- Marchetto, A. and others 1995. Factors affecting water chemistry of Alpine lakes. *Aquat Sci* **57**: 81-89.
- Massabuau, J. C., B. Fritz, and B. Burtin. 1987. Acidification of fresh-waters (pH-less-than-or-equal-to-5) in the Vosges mountains (Eastern France). *C.R. Acad. Sci. Paris, Sciences de la vie / Life Sciences* **305**: 121-124.
- Matson, P., Mcdowell, W., Townsend A., and Vitousek, P. 1999. The globalization of N deposition: ecosystem consequences in tropical environments. *Biogeochemistry* **46**: 67-83.
- Matsukura, Y., T. Hirose, and C. T. Oguchi. 2001. Rates of chemical weathering of porous rhyolites: 5-year measurements using the weight-loss method. *Catena* **43**: 341-347.
- Michelutti, N., C. Cooke, W. Hobbs, and J. Smol. 2015a. Climate-driven changes in lakes from the Peruvian Andes. *J Paleolimnol*: 1-8.

- Michelutti, N., A. L. Labaj, C. Grooms, and J. P. Smol. 2016. Equatorial mountain lakes show extended periods of thermal stratification with recent climate change. *J Limnol* **75**: 403-408.
- Michelutti, N., P. M. Tapia, A. L. Labaj, C. Grooms, X. Wang, and J. P. Smol. 2019. A limnological assessment of the diverse waterscape in the Cordillera Vilcanota, Peruvian Andes. *Inland Waters* **9**: 395-407.
- Michelutti, N., A. P. Wolfe, C. A. Cooke, W. O. Hobbs, M. Vuille, and J. P. Smol. 2015b. Climate change forces new ecological states in tropical Andean lakes. *Plos One* **10**: e0115338.
- Ministerio del Ambiente del Ecuador (MAE). 2007. Plan Estratégico del Sistema Nacional de Áreas Protegidas del Ecuador 2007-2016. Informe Final de Consultoría. Proyecto GEF: Ecuador Sistema Nacional de Áreas Protegidas (SNAP-GEF). REGAL-ECOLEX. Quito.
- Moiseenko, T., N. Gashkina, M. Dinu, T. Kremleva, and V. Khoroshavin. 2013. Aquatic geochemistry of small lakes: Effects of environment changes. *Geochemistry Int* **51**: 1031–1148.
- Molina, A., V. Vanacker, M. D. Corre, and E. Veldkamp. 2019. Patterns in soil chemical weathering related to topographic gradients and vegetation structure in a high Andean tropical ecosystem. *J Geophys Res Earth Surf* **124**: 666-685.
- Morán-Reascos, D. 2017. Analysis of mineralization extension continuity around the Loma Larga high-sulphidation system. Master Thesis. Universidad Central de Ecuador.
- Moser, K. A. and others 2019. Mountain lakes: Eyes on global environmental change. *Glob Planet Change* **178**: 77-95.
- Mosquera, P. V., H. Hampel, R. F. Vázquez, M. Alonso, and J. Catalan. 2017a. Abundance and morphometry changes across the high-mountain lake-size gradient in the tropical Andes of Southern Ecuador. *Water Resour Res* **53**: 7269-7280.
- . 2017b. Abundance and morphometry changes across the high mountain lake-size gradient in the tropical Andes of Southern Ecuador. *Dryad Dataset* . doi: 10.5061/dryad.sn058.
- Mosquera, P. V., H. Hampel, R. F. Vázquez, and J. Catalan. 2022. Water chemistry variation in tropical high-mountain lakes on old volcanic bedrocks. *Limnol Oceanogr* **67**: 1522–1536.

- Murphy, J., and J. P. Riley. 1962. A modified single solution method for the determination of phosphate in natural waters. *Anal Chim Acta* **27**: 31-36.
- Nauwerck, A. 1994. A survey on water chemistry and plankton in high-mountain lakes in Northern Swedish Lapland. *Hydrobiologia* **274**: 91-100.
- Nilssen, J. P. 1984. Tropical lakes—functional ecology and future development: The need for a process-orientated approach. *Hydrobiologia*, **113**: 231-242.
- O'Reilly, C. M. and others 2015. Rapid and highly variable warming of lake surface waters around the globe. *Geophys Res Lett* **42**: 10,773-710,781.
- Ohba, T., and Y. Kitade. 2005. Subvolcanic hydrothermal systems: Implications from hydrothermal minerals in hydrovolcanic ash. *J Volcanol Geotherm Res* **145**: 249-262.
- Oñate-Valdivieso, F. and others 2018. Temporal and spatial analysis of precipitation patterns in an Andean region of southern Ecuador using LAWR weather radar. *Meteorol Atmospheric Phys* **130**: 473-484.
- Padrón, R. S., B. P. Wilcox, P. Crespo, and R. Céleri. 2015. Rainfall in the Andean páramo: New insights from high-resolution monitoring in Southern Ecuador. *J Hydrometeorol* **16**: 985-996.
- Peters, T. and others. 2013. Environmental changes affecting the Andes of Ecuador. In *Ecosystem services, biodiversity and environmental change in a tropical mountain ecosystem of South Ecuador* (pp. 19-29). Springer, Berlin, Heidelberg.
- Post, D. M., M. L. Pace, and N. G. H. Jr. 2000. Ecosystem size determines food-chain length in lakes. *Nature* **405**: 1047-1049.
- Poulenard, J., P. Podwojewski, and A. J. Herbillon. 2003. Characteristics of non-allophanic Andisols with hydric properties from the Ecuadorian páramos. *Geoderma* **117**: 267-281.
- Pozzo, A. and others 2002. Influence of volcanic activity on spring water chemistry at Popocatepetl Volcano, Mexico. *Chem Geol* **190**: 207-229.
- Princevac, M., J. C. R. Hunt, and H. J. S. Fernando. 2008. Quasi-Steady Katabatic Winds on Slopes in Wide Valleys: Hydraulic Theory and Observations. *Journal of the Atmospheric Sciences* **65**: 627-643.

- Psenner, R. 1989. Chemistry of high mountain lakes in siliceous catchments of the Central Eastern Alps. *Aquat Sci* **51**: 1015-1621.
- Psenner, R., and J. Catalan. 1994. Chemical composition of lakes in crystalline basins: a combination of atmospheric deposition, geologic background, biological activity and human action, p. 255-314. In R. Margalef [ed.], *Limnology now: a paradigm of planetary problems*. Elsevier Science B.V.
- Psenner, R., and R. Schmidt. 1992. Climate-driven pH control of remote Alpine lakes and effects of acid deposition. *Nature* **356**: 781-783.
- Ramírez, A., Caballero, M., Vázquez, G., and Colón-Gaud, C. 2020. Preface: recent advances in tropical lake research. *Hydrobiologia*, **847**: 4143-4144.
- Ramsay, P. M., and E. R. B. Oxley. 1997. The growth form composition of plant communities in the Ecuadorian paramos. *Plant Ecol* **131**: 173-192.
- Reinart, A., A. Herlevi, H. Arst, and L. Sipelgas. 2003. Preliminary optical classification of lakes and coastal waters in Estonia and south Finland. *J Sea Res* **49**: 357-366.
- Renka, R. J. 1988. Multivariate interpolation of large sets of scattered data. *ACM Trans Math Softw* **14**: 139-148.
- Rivera-Rondón, C. A., and J. Catalan. 2020. Diatoms as indicators of the multivariate environment of mountain lakes. *Sci Total Environ* **703**: 135517.
- Rivera Rondon, C. A., A. M. Zapata, and J. C. Donaton Rondón. 2010. Estudio morfométrico del lago Guatavita (Colombia). *Acta Biol Colomb* **15**: 131-144.
- Rodbell, D. T., G. O. Seltzer, D. M. Anderson, M. B. Abbott, D. B. Enfield, and J. H. Newman. 1999. A 15,000 year record of El Niño-driven alluviation in southwestern Ecuador. *Science* **283**: 516-520.
- Rodbell, D. T., Seltzer, G. O., Mark, B. G., Smith, J. A., and Abbott, M. B. 2008. Clastic sediment flux to tropical Andean lakes: records of glaciation and soil erosion. *Quaternary Sci Rev*, **27**: 1612-1626.
- Rodbell, D. T., J. A. Smith, and B. G. Mark. 2009. Glaciation in the Andes during the Lateglacial and Holocene. *Quaternary Sci Rev* **28**: 2165-2212.
- Rogora, M., A. Marchetto, and R. Mosello. 2001. Trends in the chemistry of atmospheric deposition and surface waters in

- the Lake Maggiore catchment. *Hydrology and Earth System Sciences* **5**: 379-390.
- Rollenbeck, R., J. Bendix, and P. Fabian. 2011. Spatial and temporal dynamics of atmospheric water inputs in tropical mountain forests of South Ecuador. *Hydrol Process* **25**: 344-352.
- Sánchez-Murillo, R. and others. Exploring Dissolved Organic Carbon Variations in a High Elevation Tropical Peatland Ecosystem: Cerro de la Muerte, Costa Rica. *Front. Water* **3**: 742780.
- Sarmiento, H. 2012. New paradigms in tropical limnology: the importance of the microbial food web. *Hydrobiologia* **686**: 1-14.
- Schmidt, W. 1928. Über die temperatur- und stabilitätsverhältnisse von seen. *Geografiska Annaler* **10**: 145-177.
- Schneider, T., H. Hampel, P. V. Mosquera, W. Tylmann, and M. Grosjean. 2018. Paleo-ENSO revisited: Ecuadorian Lake Pallacocha does not reveal a conclusive El Niño signal. *Glob Planet Change* **168**: 54-66.
- Schneider, T. and others. 2021. 250-year records of mercury and trace element deposition in two lakes from Cajas National Park, SW Ecuadorian Andes. *Environ. Sci. Pollut. Res.* **28**: 16227-16243.
- Seekell, D. A., and M. L. Pace. 2011. Does the Pareto distribution adequately describe the size-distribution of lakes? *Limnol Oceanogr* **56**: 350-356.
- Seekell, D. A., M. L. Pace, L. J. Tranvik, and C. Verpoorter. 2013. A fractal-based approach to lake size-distributions. *Geophys Res Lett* **40**: 517-521.
- Segura, H. and others 2019. New insights into the rainfall variability in the tropical Andes on seasonal and interannual time scales. *Clim Dynam* **53**: 405-426.
- Sharqawy, M. H., J. H. Lienhard, and S. M. Zubair. 2010. Thermophysical properties of seawater: a review of existing correlations and data. *Desalination and Water Treatment* **16**: 354-380.
- Smol, J. P. 2012. A planet in flux: How is life on Earth reacting to climate change? *Nature* **483**: S12-S15.
- Sorvari, S., A. Korhola, and R. Thompson. 2002. Lake diatom response to recent Arctic warming in Finnish Lapland. *Global Change Biol* **8**: 171-181.

- Steffen, W., W. Broadgate, L. Deutsch, O. Gaffney, and C. Ludwig. 2015. The trajectory of the Anthropocene: The Great Acceleration. *Anthr Rev* **2**: 81-98.
- Steinitz-Kannan, M. 1979. Comparative limnology of Ecuadorian lakes: a study of species number and composition of plankton communities of the Galapagos islands and the Equatorial Andes. The Ohio State University.
- . 1997. The lakes in Andean protected areas of Ecuador. *The George Wright Forum* **14**: 33-43.
- Steinitz-Kannan, M., P. A. Colinvaux, and R. Kannan. 1983. Limnological studies in Ecuador 1. A survey of chemical and physical properties of Ecuadorian lakes. *Arch Hydrobiol Suppl* **65**: 61-105.
- Steinitz-Kannan, M., C. Lopez, D. Jacobsen, and M. D. Guerra. 2020. History of limnology in Ecuador: a foundation for a growing field in the country. *Hydrobiologia* **847**: 4191–4206.
- Sun, Z. and others 2020. Sodium-rich volcanic rocks and their relationships with iron deposits in the Aqishan–Yamansu belt of Eastern Tianshan, NW China. *Geosci Front* **11**: 697-713.
- Van Colen, W. R. and others 2017. Limnology and trophic status of glacial lakes in the tropical Andes (Cajas National Park, Ecuador). *Freshw Biol* **62**: 458-473.
- Vásconez, P. and others. 2011. Páramo. Paisaje estudiado, habitado, manejado e institucionalizado. *EcoCiencia/AbyaYala/ECOBONA*. Quito.
- Vásquez, C., R. Céleri, M. Córdova, and G. Carrillo-Rojas. 2022. Improving reference evapotranspiration (ET_o) calculation under limited data conditions in the high Tropical Andes. *Agric Water Manag* **262**: 107439.
- Vázquez, R. F., and J. Feyen. 2007. Assessment of the effects of DEM gridding on the predictions of basin runoff using MIKE SHE and a modelling resolution of 600 m. *J Hydrol* **334**: 73-87.
- Vivoni, E. R., V. Y. Ivanov, R. L. Bras, and D. Entekhabi. 2005. On the effects of triangulated terrain resolution on distributed hydrologic model response. *Hydrol Process* **19**: 2101-2122.
- Vuille, M., R. S. Bradley, and F. Keimig. 2000. Climate Variability in the Andes of Ecuador and Its Relation to Tropical Pacific and Atlantic Sea Surface Temperature Anomalies. *J Climate* **13**: 2520-2535.

- Wetzel, R. G. 2001. *Limnology: lake and river ecosystems*. Gulf Professional Publishing.
- White, A. F. and others 1998. Chemical weathering in a tropical watershed, Luquillo mountains, Puerto Rico: I. Long-term versus short-term weathering fluxes. *Geochim Cosmochim Acta* **62**: 209-226.
- White, A. F., and S. L. Brantley. 1995. Chemical weathering rates of silicate minerals: An overview, p. 1-22. In A. F. White and S. L. Brantley [eds.], *Chemical weathering rates of silicate minerals*. *Reviews in Mineralogy*. De Gruyter.
- . 2003. The effect of time on the weathering of silicate minerals: why do weathering rates differ in the laboratory and field? *Chem Geol* **202**: 479-506.
- Wise, S. 2000. Assessing the quality for hydrological applications of digital elevation models derived from contours. *Hydrol Process* **14**: 1909-1929.
- Wolfe, A.P., Baron, J.S., and Cornett, R.J. 2001. Anthropogenic nitrogen deposition induces rapid ecological changes in alpine lakes of the Colorado Front Range (USA). *J. Paleolimnol.* **25**: 1–7.
- Yang, H. D., D. R. Engstrom, and N. L. Rose. 2010. Recent Changes in Atmospheric Mercury Deposition Recorded in the Sediments of Remote Equatorial Lakes in the Rwenzori Mountains, Uganda. *Environ Sci Technol* **44**: 6570-6575.
- Zapata, A., C. A. Rivera-Rondón, D. Valoyes, C. L. Muñoz-López, M. Mejía-Rocha, and J. Catalan. 2021. Páramo lakes of Colombia: An overview of their geographical distribution and physicochemical characteristics. *Water* **13**: 2175.

SUPPORTING INFORMATION

This section comprises supporting information for Chapter 2, Chapter 3 and Chapter 4.

APPENDIX A

Chapter 2

Introduction

The details of the digital bathymetry methods are provided in **Text S1**, and **Figure S1** and the lakes covered by the bathymetry survey in the Cajas National Park are listed in **Table S1**. Four more figures supporting the main text are also included. **Figure S2** shows the altitudinal distribution of the high mountain water bodies of the Cajas Massif. **Figure S3** illustrates some lake shapes across the shoreline development (DL) gradient. **Figure S4**, the volume-area relationship considering two lake morphologies. And, **Figure S5**, the maximum depth (Z_{\max}), mean depth (Z_{mean}) and relative depth (Z_r) distribution among the Cajas National Park lakes.

Text S1. Digital bathymetry method

The process to produce the digital bathymetry of the studied lakes and the derived geomorphological products included: (i) in-situ gathering and office processing of the surveying data so that any incongruence could be filtered out; (ii) preparing the information with the right digital format for the forthcoming steps; (iii) selecting and applying an interpolation algorithm to obtain the bathymetric surface (i.e. the digital bathymetric model) of every surveyed lake; and (iv) obtaining the required geomorphological products derived from the digital bathymetric models of the lakes. For most of these processes, specific-task subroutines were programmed, particularly with PERL (Practical Extracting and Reporting Language) and Matlab®.

The first step included the integration of the depth data collected in the field with the data derived from the digitalization of the orthophotos (i.e. boundaries of the lakes associated with zero-depth)

so that the feasible bounds of the following interpolation process could be defined properly (besides adding additional zero-depth data for the interpolation process). For filtering out some potential pitfalls of the data collected in the field, these lake boundaries as well as other relevant spatial information, together with field annotations, were contrasted with the aid of geographical information systems (GIS) (ArcGis® and IDRISI® Selva).

In the second step, suitable specific-task subroutines, usually programmed with PERL, were used so as to get the different data saved with the right format, as a function of the software that was used later for the interpolation process, particularly Surfer® 13.0.

The third step was obtaining the digital bathymetric model of the surveyed lakes. It included assessing an appropriate interpolation algorithm for the current study, by judging the depth accuracy of the resulting interpolation product (i.e. the bathymetric model of a given lake).

For some of the studied lakes, the implemented quality assessment process considered a visual comparison (Figure S1) of the results of the different alternative interpolation methods. Through this visual analysis, some of the methods were already discarded. In a second approach, similarly to what is typically done in topographic studies (Vázquez and Feyen, 2007), the accuracy assessment was based on the comparison of the depths modelled with a set of field observations (quality control data set), selected randomly from the set of total field observations. It is important to note that the data of this randomly selected set of observations were not included in the interpolation process itself but, instead, they were only used for quality assessment purposes; that is, only 80 % of the available information was used for deriving the interpolated bathymetric surfaces.

For a particular interpolation method, the depths comparison was characterised using residuals, that is, the depth difference between the interpolation model and the quality control data set (at the spot locations of these control quality data). This comparison was further aggregated to a single measure depicting the elevation difference between the interpolation product and the quality control data: the Mean Absolute Error (MAE), which is the average of the absolute

values of all of the residuals for a particular interpolation product and a particular lake. Absolute values were used to avoid residuals of similar magnitude, but of opposite sign, cancelling to each other, as such, giving the false sensation of low depth discrepancies (Vázquez and Feyen 2007). For a particular tested interpolation algorithm, the quality of the method was assessed through a frequency distribution (empirical) function of the MAE, calculated considering the respective interpolation products of all of the studied lakes; so that, the outcome of the quality assessment is a plot of frequency distributions of the MAE as a function of the interpolation method (Figure S1c).

In total, ten interpolation methods were tested (Franke and Nielson 1980; Franke 1982; Renka 1988; Hanselman and Littlefield 1998; Wise 2000; Vivoni et al. 2005; Vázquez and Feyen 2007; Eldrandaly and Abu-Zaid 2011), namely, (1) Inverse Distance to a Power, (2) Kriging Standard, (3) Minimum Curvature, (4) Modified Shepard's Method, (5) Natural Neighbour, (6) Nearest Neighbour, (7) Polynomial Regression, (8) Radial Basis Functions, (9) Triangular Interpolation Network (TIN) combined with linear interpolation along the edges of the triangles, and (10) Moving Average.

Finally, in the fourth step, the most suitable interpolation method was applied to obtain the digital bathymetric model of each lake surveyed. Given the significant number of lakes considered in the current study, the interpolation and quality control analyses were carried out automatically, using (i) the programming framework that Surfer® enables by mean of Visual Basic; and (ii) PERL specific-purpose subroutines.

The outcome of the quality assessment on the products of the ten different interpolation methods considered in this study is depicted in Figure S1c, in the form of ten frequency distribution curves. For a given interpolation method, every dot in the respective distribution curve represents the quality (measured by the MAE) of the bathymetric surface of one of the study lakes obtained by applying the method to the available observations. The figure depicts that indeed these distribution curves enable characterising the differences (and similitudes) among the different interpolation methods since differences (and similitudes) among these curves are systematic. Further, the quality of the products of a given interpolation method,

characterized herein by the MAE, shapes the evolution of the respective distribution curve so that better interpolation methods have associated distributions that evolve in a relatively short MAE range, whilst methods that are not that suitable have associated distributions that are spanning (much) longer MAE ranges (Figure S1c).

The analysis shows that the best interpolation methods for the conditions of the current study were: (2) Kriging Standard, (3) Minimum Curvature, (5) Natural Neighbour, (6) Nearest Neighbour and (9) TIN with Linear Interpolation, given that the differences among their respective distributions are only marginal and that the associated MAE range is the shortest possible (about 2 m). Thus, we use the Standard version of the Kriging interpolation method for the bathymetry digital development. Nevertheless, statistically, there is not any advantage in using this interpolation method over the other methods with similar MAE distributions in Figure S1c. Indeed, even the simple and traditional (1) Inverse Distance to a Power method performs acceptably compared to methods 2, 3, 5, 6 and 9 (Figure S1c).

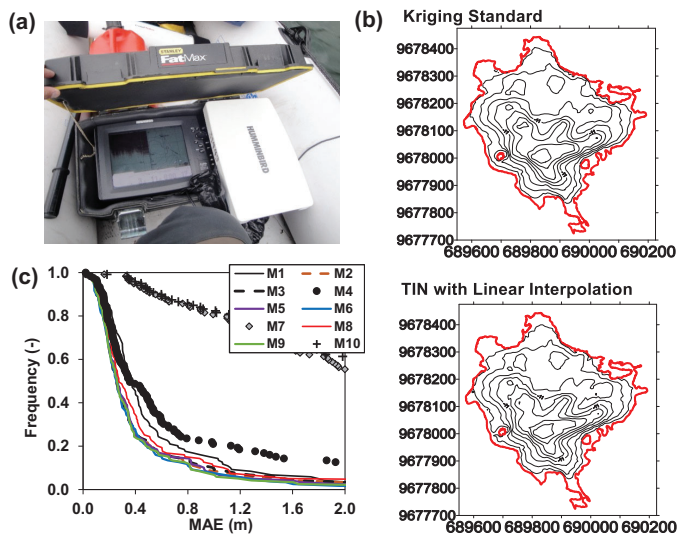


Figure S1. Process followed to define the digital bathymetry of the studied lakes: (a) sonar used for the surveying; (b) graphical assessment of the quality of the interpolation methods applied on the observed bathymetric data; and (c) statistical evaluation of the quality of the interpolation

methods (i.e., frequency distributions of the mean absolute error, MAE, as a function of the interpolation method).

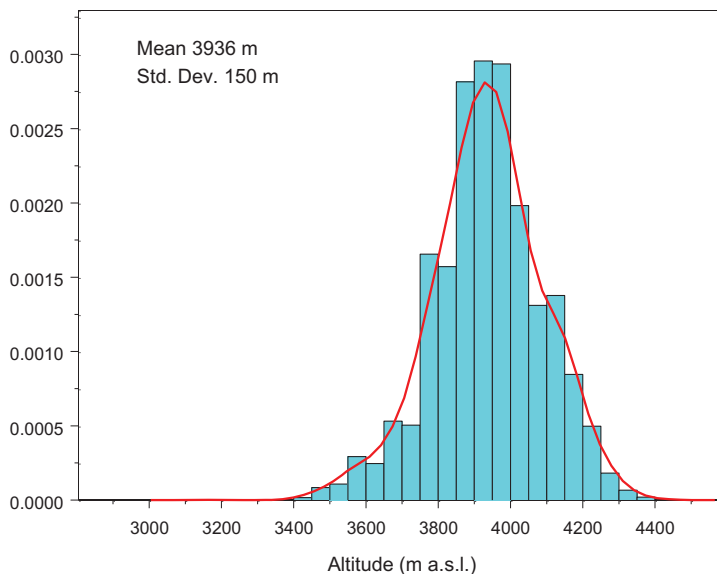


Figure S2. Altitudinal distribution of the high-mountain lakes of the Cajas Massif.

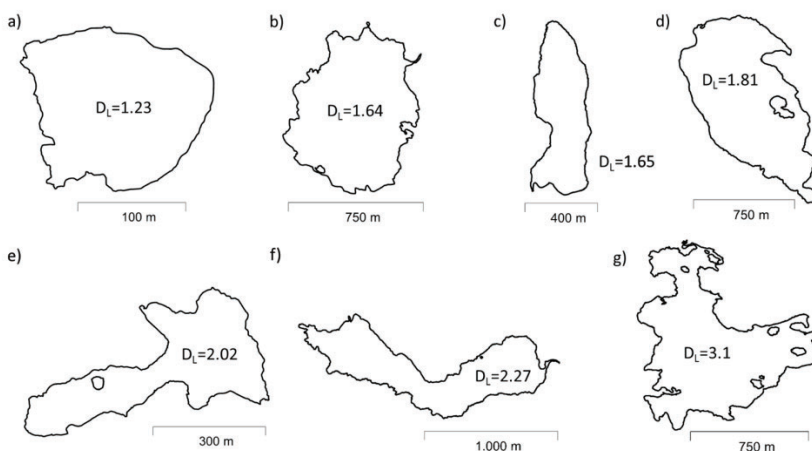


Figure S3. Some examples of the lake shapes and their corresponding shoreline development (DL) in the Cajas National Park. a) Laguna de la

Cascada , b) Lagartococha , c) Angas , d) Luspa , e) Burín Grande , f) Mamamag , and g) Osohuayco.

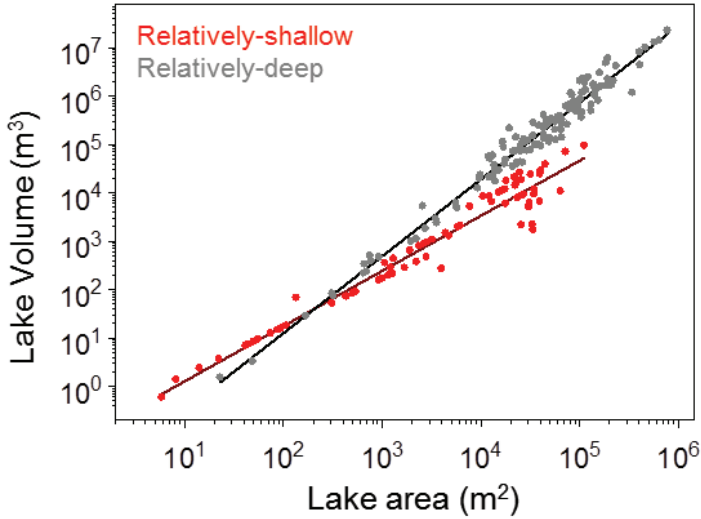


Figure S4. The volume-area relationship for the lakes of the Cajas Massif based on a survey of 202 lakes and ponds in the Cajas National Park and assuming two lake morphologies. The lakes were initially classified into two groups (relatively deep (*rd*) and relatively shallow (*rs*)) according to the positive or negative residuals with respect equation (3) in the main text. Then an allometric equation was fit to each group. The new equations were applied to the whole set, and the lakes were reclassified into two groups according to the lowest residual of the two equations. A new fitting with the new two groups was performed, and then a new reclassification. This procedure was repeated until there were no changes in the classification. The resulting equations were:

$$V_{rd} = 0.0084 A_{rd}^{1.59} \quad r^2 = 0.97 \quad n = 130$$

$$V_{rs} = 0.0929 A_{rs}^{1.14} \quad r^2 = 0.96 \quad n = 72$$

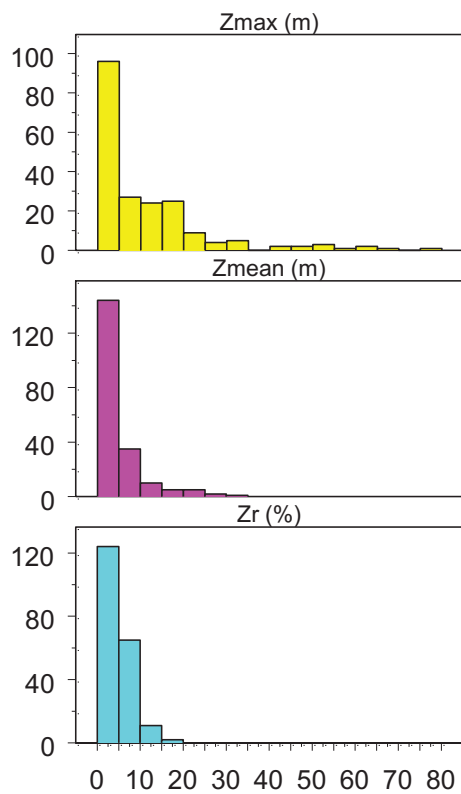


Figure S5. Distribution of the maximum depth (Z_{\max}), mean depth (Z_{mean}) and relative depth (Z_r) among the Cajas National Park lakes.

Table S1 List of the water bodies of the Cajas National Park included in the bathymetry survey

Code	Name	Latitude	Longitude	Altitude (m a.s.l.)
CJ-001	Llaviucu	2° 50' 35.584" S	79° 8' 46.136" W	3152
CJ-002	Patoquinas	2° 46' 54.316" S	79° 12' 30.998" W	3800
CJ-003	Toreadora	2° 46' 45.871" S	79° 13' 26.144" W	3917
CJ-004	Illincocha	2° 46' 44.674" S	79° 13' 52.401" W	3983
CJ-005	Chica Toreadora	2° 46' 29.042" S	79° 13' 48.313" W	3984
CJ-006	Piñancocha	2° 45' 13.787" S	79° 13' 55.515" W	4221
CJ-007	Fondococho	2° 45' 35.329" S	79° 14' 10.861" W	4127
CJ-008	Pallcacocho	2° 46' 15.057" S	79° 13' 57.561" W	4046
CJ-009	Riñoncocha	2° 45' 58.862" S	79° 13' 46.836" W	4034
CJ-010	Toreador	2° 45' 53.128" S	79° 13' 22.564" W	3927
CJ-011	Ataudcocha	2° 46' 15.415" S	79° 12' 52.294" W	3882
CJ-012	Tintacocho	2° 50' 58.385" S	79° 17' 39.274" W	4033
CJ-013	Del Diablo	2° 50' 39.448" S	79° 17' 45.972" W	4063
CJ-014	Contrahierba	2° 50' 47.165" S	79° 18' 8.754" W	4004
CJ-015	Totorilla	2° 50' 5.796" S	79° 19' 21.697" W	4090
CJ-016	Cristales	2° 50' 27.292" S	79° 19' 5.25" W	4148
CJ-017	Yanacocho de Jerez	2° 50' 18.087" S	79° 19' 33.27" W	4159
CJ-018	Yantahuaico 1	2° 50' 0.697" S	79° 20' 37.242" W	4075

Supporting Information

CJ-019	Yantahuaico 2	2° 50' 4.024" S	79° 20' 19.202" W	4110
CJ-020	Yantahuaico 3	2° 50' 16.909" S	79° 20' 14.198" W	4112
CJ-021	Marmolcocha	2° 46' 53.399" S	79° 13' 9.881" W	3926
CJ-022	Unidas	2° 46' 17.781" S	79° 13' 7.02" W	3861
CJ-023	Atugyacu Grande	2° 50' 26.725" S	79° 18' 12.249" W	3969
CJ-024	Estrellascocha	2° 51' 8.014" S	79° 20' 31.706" W	4128
CJ-025	Negra de Jerez	2° 51' 19.484" S	79° 19' 9.092" W	4045
CJ-026	Atascaderos	2° 51' 20.023" S	79° 19' 21.913" W	4038
CJ-027	Pailascocha de Jerez	2° 51' 39.945" S	79° 19' 42.445" W	3970
CJ-028	Atugloma	2° 51' 31.146" S	79° 18' 52.109" W	4141
CJ-029	Angas	2° 52' 1.014" S	79° 17' 56.213" W	3886
CJ-030	Dublaycocha	2° 51' 36.005" S	79° 17' 51.749" W	3915
CJ-031	S/N	2° 52' 11.2" S	79° 17' 32.173" W	4023
CJ-032	Estrellascocha	2° 54' 47.902" S	79° 15' 13.615" W	3818
CJ-033	Lagunaloma o Verdecocha	2° 53' 12.162" S	79° 18' 27.871" W	3837
CJ-034	Napalé Vía	2° 53' 38.702" S	79° 17' 28.384" W	3945
CJ-035	Tinguercocha 1	2° 53' 11.919" S	79° 17' 34.608" W	3895
CJ-036	Ingacasa	2° 51' 31.179" S	79° 16' 19.544" W	3977
CJ-037	Ingacocha 1	2° 51' 39.453" S	79° 16' 1.497" W	3958
CJ-038	Chachacomes	2° 51' 18.704" S	79° 15' 54.082" W	4000
CJ-039	Larga	2° 47' 41.422" S	79° 14' 40.103" W	3940

CJ-040	Negra	2° 47' 0.622" S	79° 14' 33.915" W	4043
CJ-041	Cardenillo	2° 46' 56.252" S	79° 14' 49.979" W	4104
CJ-042	Togllacocho	2° 48' 0.985" S	79° 14' 59.984" W	3859
CJ-043	Luspa	2° 48' 17.395" S	79° 15' 45.61" W	3776
CJ-044	Tinguercocha 2	2° 53' 10.185" S	79° 17' 50.735" W	3888
CJ-045	Cucheros	2° 47' 34.028" S	79° 12' 7.595" W	3887
CJ-046	Canutillos Grande	2° 49' 10.558" S	79° 15' 25.102" W	3851
CJ-047	Canutillos chica 2	2° 49' 50.577" S	79° 15' 9.534" W	3942
CJ-048	Canutillos chica 1	2° 49' 40.139" S	79° 15' 17.255" W	3934
CJ-049	Osohuayco	2° 49' 48.808" S	79° 13' 37.361" W	3856
CJ-050	Mamamag / Taitachugo	2° 49' 44.619" S	79° 11' 38.063" W	3543
CJ-051	Sunincocha Grande	2° 49' 49.679" S	79° 17' 7.03" W	3842
CJ-052	Burín Grande	2° 48' 28.58" S	79° 12' 44.938" W	3891
CJ-053	Burín Chico 1	2° 48' 38.229" S	79° 12' 53.017" W	3872
CJ-054	Burín Chico 2	2° 48' 19.537" S	79° 13' 10.69" W	3900
CJ-055	El Ocho	2° 47' 57.211" S	79° 12' 52.691" W	3991
CJ-056	3ra de Sunincocha	2° 49' 21.461" S	79° 17' 33.718" W	3808
CJ-057	Las Chorreras	2° 49' 12.401" S	79° 17' 5.563" W	4079
CJ-058	2da de Sunincocha	2° 49' 7.169" S	79° 17' 55.949" W	3768
CJ-059	Quinuascocha	2° 50' 15.991" S	79° 16' 6.997" W	3894
CJ-060	Potro muerto	2° 50' 6.73" S	79° 16' 18.343" W	3897

Supporting Information

CJ-061	Culebrillas	2° 49' 45.304" S	79° 16' 37.056" W	3955
CJ-062	Cueva Escrita	2° 50' 49.7" S	79° 16' 16.724" W	4019
CJ-063	Llipus loma	2° 50' 59.438" S	79° 15' 58.223" W	4023
CJ-064	Llipus loma 3	2° 50' 38.607" S	79° 16' 22.342" W	4001
CJ-065	Llipus loma 2	2° 50' 42.737" S	79° 16' 19.293" W	4007
CJ-066	Negra	2° 47' 29.339" S	79° 14' 57.895" W	3973
CJ-067	Azul	2° 47' 17.374" S	79° 14' 46.225" W	4043
CJ-068	Pampeada Grande	2° 46' 4.85" S	79° 15' 56.877" W	4121
CJ-069	Pampeada Chica	2° 45' 55.309" S	79° 16' 17.643" W	4158
CJ-070	Del Rayo	2° 46' 7.585" S	79° 16' 19.826" W	4149
CJ-071	Cuchichaspana	2° 50' 14.266" S	79° 15' 45.534" W	3962
CJ-072	Cuchichaspana Chica	2° 50' 25.562" S	79° 14' 37.626" W	3972
CJ-073	Piedra Blanca o Llaviucu	2° 50' 14.636" S	79° 15' 35.834" W	3950
CJ-074	Ojo de Osohuaico	2° 50' 10.497" S	79° 13' 42.055" W	3878
CJ-075	Patos Colorados	2° 50' 12.043" S	79° 13' 10.648" W	3946
CJ-076	Lagartococha	2° 51' 20.322" S	79° 13' 40.233" W	4001
CJ-077	Anexo Osohuayco	2° 50' 0.759" S	79° 13' 39.253" W	3871
CJ-078	Ingacochoa 2	2° 51' 40.377" S	79° 16' 10.206" W	3959
CJ-079	J	2° 52' 0.997" S	79° 15' 57.288" W	3919
CJ-080	Martillo	2° 51' 16.491" S	79° 16' 16.199" W	3977
CJ-081	Apicochoa 1	2° 47' 14.254" S	79° 12' 40.874" W	3924

CJ-082	Apicocha 2	2° 47' 9.61" S	79° 12' 48.133" W	3924
CJ-083	Apicocha 3	2° 47' 3.046" S	79° 12' 55.88" W	3916
CJ-084	Cascarilla 1	2° 52' 0.094" S	79° 16' 45.694" W	4008
CJ-085	Cascarilla 2	2° 51' 49.49" S	79° 16' 51.182" W	4002
CJ-086	Cascarilla 3	2° 52' 34.23" S	79° 16' 36.48" W	3984
CJ-087	Chica luspa 1	2° 48' 35.76" S	79° 15' 5.145" W	3806
CJ-088	Chica luspa 2	2° 48' 39.979" S	79° 14' 56.106" W	3818
CJ-089	Trensillas	1° 48' 37.684" S	31° 7' 47.755" W	3997
CJ-090	Chullacocha	3° 1' 22.439" S	79° 13' 20.954" W	3787
CJ-091	Quimsacocha 1	3° 3' 12.64" S	79° 14' 43.933" W	3827
CJ-092	Quimsacocha 2	3° 3' 3.29" S	79° 14' 59.297" W	3827
CJ-093	Vado de los Arrieros 1	2° 51' 54.074" S	79° 14' 39.172" W	3814
CJ-094	Vado de los Arrieros 2	2° 51' 25.312" S	79° 14' 49.285" W	3820
CJ-095	Botacocha	2° 51' 38.827" S	79° 14' 31.554" W	3839
CJ-096	Carpahuayco	2° 50' 42.632" S	79° 14' 48.799" W	3917
CJ-097	Jigeno	2° 54' 42.645" S	79° 17' 31.396" W	3969
CJ-098	De Patos	2° 54' 8.287" S	79° 16' 40.515" W	3971
CJ-099	De la Cascada	2° 45' 48.633" S	79° 12' 58.808" W	3967
CJ-100	Cardenillo	2° 45' 25.534" S	79° 12' 46.573" W	4137
CJ-101	Derrumbo Amarillo	2° 45' 52.536" S	79° 12' 35.558" W	4036
CJ-102	Perro Grande	2° 45' 37.052" S	79° 13' 47.775" W	4000

Supporting Information

CJ-103	Chica Ventanas	2° 52' 31.268" S	79° 15' 32.668" W	3856
CJ-104	Bejuco	2° 52' 57.996" S	79° 14' 30.203" W	3628
CJ-105	Tintacocha	2° 52' 42.586" S	79° 15' 4.32" W	3679
CJ-106	Ventanas	2° 52' 47.451" S	79° 15' 56.312" W	3913
CJ-107	Chusalongo 1	2° 55' 48.502" S	79° 14' 42.631" W	3778
CJ-108	Chusalongo 2	2° 55' 38.583" S	79° 14' 48.702" W	3794
CJ-109	Chusalongo 3	2° 55' 45.875" S	79° 14' 28.227" W	3780
CJ-110	Chusalongo 4	2° 55' 56.395" S	79° 14' 31.578" W	3764
CJ-111	Del Sharo	2° 46' 1.264" S	79° 16' 38.548" W	4253
CJ-112	Negra	2° 46' 8.977" S	79° 16' 36.627" W	4228
CJ-113	De Patos Blancos	2° 45' 40.312" S	79° 16' 24.755" W	4210
CJ-114	Juan Pasana	2° 45' 30.525" S	79° 16' 33.057" W	4294
CJ-115	Chica Hunanchi	2° 51' 58.855" S	79° 13' 54.419" W	3874
CJ-116	Hunanchi	2° 52' 19.022" S	79° 14' 4.328" W	3834
CJ-117	Verdes	2° 51' 33.277" S	79° 12' 57.346" W	3886
CJ-118	Estrellascocha 2	2° 55' 10.523" S	79° 15' 11.119" W	3769
CJ-119	Estrellascocha 3	2° 55' 4.383" S	79° 14' 58.274" W	3802
CJ-120	Estrellascocha 4	2° 55' 15.687" S	79° 15' 23.674" W	3761
CJ-121	Dos Choreras	2° 46' 12.542" S	79° 9' 36.858" W	3690
CJ-122	Taquiurco	2° 46' 44.076" S	79° 11' 57.279" W	3623
CJ-123	Barros	2° 46' 38.203" S	79° 12' 10.108" W	3815

CJ-124	Charco-Anex-Barros	2° 46' 41.038" S	79° 12' 11.82" W	3824
CJ-125	Humedal Totora	2° 46' 44.464" S	79° 12' 17.448" W	3824
CJ-126	Charco Pardo Anex Humedal	2° 46' 44.174" S	79° 12' 19.358" W	3832
CJ-127	Barros 2	2° 46' 18.392" S	79° 12' 19.624" W	3871
CJ-128	Barros 3	2° 46' 24.609" S	79° 12' 18.675" W	3873
CJ-129	Charca Anexo Barros 3	2° 46' 28.025" S	79° 12' 17.181" W	3863
CJ-130	Charca 2 Anexo Barros 3	2° 46' 28.48" S	79° 12' 17.018" W	3859
CJ-131	Totoras	2° 46' 50.554" S	79° 12' 40.424" W	3810
CJ-132	Verdecocha	2° 48' 54.131" S	79° 9' 35.117" W	3659
CJ-133	San Antonio 1	2° 49' 17.978" S	79° 10' 7.034" W	3846
CJ-134	San Antonio 2	2° 49' 34.423" S	79° 10' 10.925" W	3721
CJ-135	Patococha 1	2° 48' 34.226" S	79° 10' 27.498" W	3841
CJ-136	Charca Anexo Pato 2	2° 48' 21.486" S	79° 10' 19.586" W	3801
CJ-137	Patococha grande 1	2° 48' 22.024" S	79° 10' 9.873" W	3783
CJ-138	Charca Anexo Patococha 1	2° 48' 11.467" S	79° 10' 3.512" W	3754
CJ-139	Lago Anexo Estrellascocha 1	2° 51' 5.881" S	79° 20' 19.729" W	4125
CJ-140	Charca Anexo Estrellascocha 1	2° 51' 9.305" S	79° 20' 23.933" W	4116
CJ-141	Estrellascocha 2	2° 51' 20.09" S	79° 20' 52.508" W	4074
CJ-142	Estrellascocha 3	2° 51' 15.583" S	79° 20' 42.283" W	4092
CJ-143	Estrellascocha 4	2° 51' 19.298" S	79° 20' 45.192" W	4088
CJ-144	Charca Anexo Estrellascocha 4	2° 51' 18.876" S	79° 20' 45.937" W	4095

Supporting Information

CJ-145	Lago somero anexo Estrella 2	2° 51' 28.681" S	79° 20' 49.55" W	4073
CJ-146	Estrellas 5	2° 51' 22.036" S	79° 20' 47.034" W	4084
CJ-147	Lago somero anexo Yantahuaico 1	2° 50' 7.428" S	79° 20' 31.696" W	4085
CJ-148	Lago somero anexo Yantahuaico 4	2° 50' 7.787" S	79° 20' 32.019" W	4086
CJ-149	Cocha totorilla 1	2° 50' 4.336" S	79° 19' 47.213" W	4223
CJ-150	Cocha totorilla 2	2° 50' 4.435" S	79° 19' 48.41" W	4229
CJ-151	Cocha totorilla 3	2° 50' 4.274" S	79° 19' 49.479" W	4232
CJ-152	Cocha totorilla 4	2° 50' 20.934" S	79° 19' 21.351" W	4169
CJ-153	Cocha Jerez 1	2° 51' 23.571" S	79° 19' 21.52" W	4040
CJ-154	Cocha Jerez 2	2° 51' 17.444" S	79° 19' 16.769" W	4029
CJ-155	Cocha Jerez 3	2° 51' 16.337" S	79° 19' 16.35" W	4036
CJ-156	Cocha totorilla 5	2° 49' 46.18" S	79° 19' 31.568" W	4078
CJ-157	Culebrillas	2° 25' 25.25" S	78° 51' 38.535" W	3901
CJ-158	Paredones	2° 25' 36.083" S	78° 51' 35.508" W	3946
CJ-159	Charca anostraceos	2° 47' 2.928" S	79° 14' 51.944" W	4131
CJ-160	Charca L2	2° 47' 2.359" S	79° 14' 41.261" W	4070
CJ-161	Lago somero anexo L2	2° 47' 2.23" S	79° 14' 42.427" W	4071
CJ-162	Lago somero anexo larga	2° 47' 34.331" S	79° 14' 44.257" W	3955
CJ-163	Lago somero anexo luspa	2° 48' 12.803" S	79° 15' 22.306" W	3819
CJ-164	Charca anostraceos 2	2° 48' 1.836" S	79° 15' 46.96" W	3804
CJ-165	AN-CH001	2° 52' 22.047" S	79° 17' 57.639" W	3884

CJ-166	Charca anostraceos anexo angas	2° 52' 22.346" S	79° 18' 1.685" W	3881
CJ-167	Lago Azul	2° 52' 56.986" S	79° 17' 19.412" W	3974
CJ-168	Charca Anexo a tinguercocha 1	2° 53' 10.27" S	79° 17' 20.72" W	3894
CJ-169	Las Chorreras 2	2° 49' 10.655" S	79° 16' 51.806" W	4085
CJ-170	Mangacochoa 1	2° 49' 52.989" S	79° 16' 16.097" W	4009
CJ-171	Mangacochoa 2	2° 49' 49.301" S	79° 16' 10.048" W	3995
CJ-172	Mangacochoa 3	2° 49' 52.261" S	79° 16' 8.619" W	4009
CJ-173	Charca SU 1	2° 49' 49.433" S	79° 16' 33.294" W	3966
CJ-174	Ira de Sunincocha	2° 48' 54.454" S	79° 18' 5.195" W	3752
CJ-175	Charco 1 anexo Ingacochoa 1	2° 51' 19.642" S	79° 16' 32.674" W	4046
CJ-176	Lago somero 2 anexo a Ingacasa	2° 51' 15.586" S	79° 16' 41.519" W	4045
CJ-177	Charco 3 anexo a Ingacasa	2° 51' 22.125" S	79° 16' 38.693" W	4007
CJ-178	Lago somero anexo a Ingacochoa 2	2° 51' 42.128" S	79° 15' 44.042" W	3960
CJ-179	Lago somero 2 anexo a Ingacochoa 2	2° 51' 41.357" S	79° 15' 50.81" W	3975
CJ-180	Lago somero 3 anexo a Ingacochoa 2	2° 51' 37.646" S	79° 15' 50.654" W	3984
CJ-181	Charco 1 anexo a tintacochoa	2° 52' 42.367" S	79° 12' 23.534" W	3705
CJ-182	Hato de Chocar	2° 52' 10.414" S	79° 12' 12.123" W	3706
CJ-183	Lago somero Hato de Chocar 1	2° 52' 22.521" S	79° 12' 9.74" W	3703
CJ-184	Totoracochoa	2° 52' 55.054" S	79° 11' 36.535" W	3583
CJ-185	Hato de chocar 2 o Tintacochoa	2° 52' 31.435" S	79° 12' 26.789" W	3968
CJ-186	Chuspihuaycu	2° 51' 36.54" S	79° 11' 19.014" W	3578

Supporting Information

CJ-187	Perro chico	2° 45' 41.136" S	79° 13' 36.212" W	3950
CJ-188	L-SU1	2° 50' 9.413" S	79° 16' 27.404" W	3886
CJ-189	LSO2	2° 50' 6.975" S	79° 16' 29.739" W	3897
CJ-190	L. somero anexo a Culebrillas	2° 49' 42.518" S	79° 16' 46.255" W	3971
CJ-191	Charco anexo Culebrillas	2° 49' 49.114" S	79° 16' 37.762" W	3957
CJ-192	Charco anexo Culebrillas	2° 49' 50.548" S	79° 16' 38.893" W	3953
CJ-193	Charco anexo Osohuayco	2° 50' 0.99" S	79° 13' 41.228" W	3865
CJ-194	Charco anexo Osohuayco 2	2° 49' 59.753" S	79° 13' 41.359" W	3867
CJ-195	Charco anexo Osohuayco 3	2° 49' 58.971" S	79° 13' 41.166" W	3883
CJ-196	Chico Juan Manuel	2° 50' 12.024" S	79° 12' 37.171" W	3775
CJ-197	Charco anexo Osohuayco 4	2° 49' 59.768" S	79° 13' 51.363" W	3894
CJ-198	Charco anexo Osohuayco 5	2° 50' 2.587" S	79° 13' 42.488" W	3866
CJ-199	Atucpamba 1	2° 52' 1.934" S	79° 18' 45.685" W	4143
CJ-200	Atucpamba 2	2° 51' 55.38" S	79° 18' 38.539" W	4156
CJ-201	Atucpamba 3	2° 51' 53.233" S	79° 18' 40" W	4148
CJ-202	Atucpamba 4	2° 51' 47.079" S	79° 18' 39.329" W	4147

Chapter 3

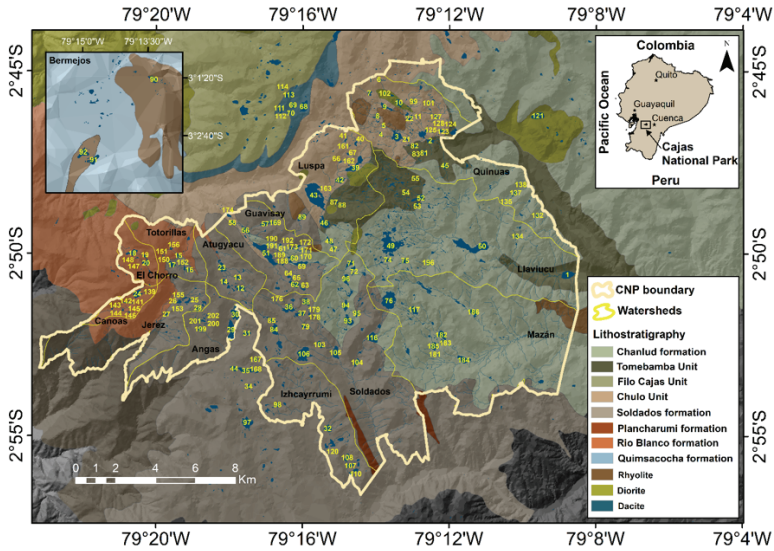


Figure S1. Geological formations in the Cajas Massif study area and main drainage basins. The formation characteristics are summarized in Table S1. The main rhyolite spots and dacite belts associated with the Chulo and Filo Cajas units are highlighted. Drainage watersheds for many waterbodies correspond to a unique formation, but there are cases including several. Even so, lithological variation within a formation may be locally high concerning bedrock composition and material. Geological information based on Dunkley, P., and A. Gaibor. 2009. Mapa Geológico Cordillera Occidental 2°-3°. Hoja geológica Cuenca -NVF 53. . *In* I. G. M. d. Ecuador [ed.]. Servicio Geológico Nacional. Ministerio de Minas y Petróleos. República de Ecuador.

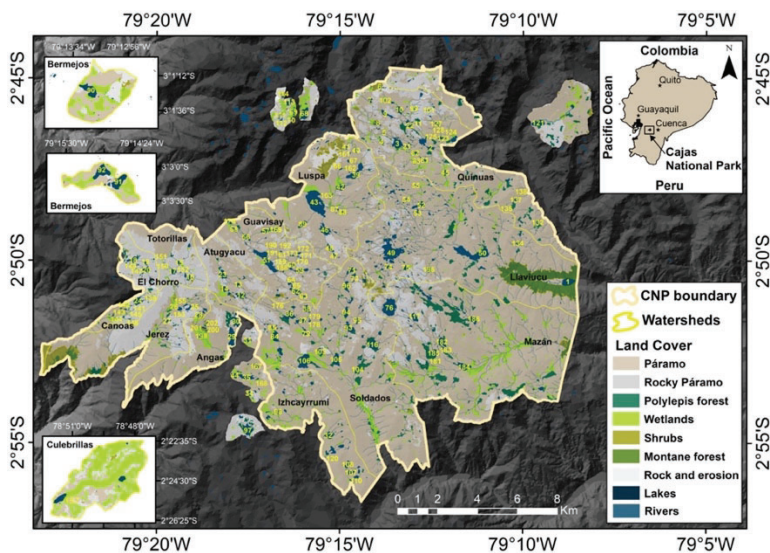


Figure S2. Land cover map produced by digitalization and classification of aerial photographs of the project SIG-Tierras (2010–2014, www.sigtierras.gob.ec). The scale of cartographic digitalization was 1:5000.

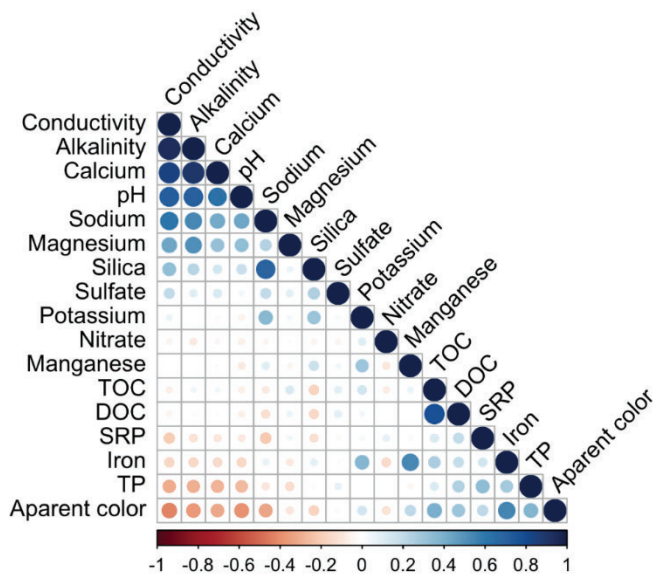


Figure S3. Correlation between water chemistry variables in the study lakes of the Cajas Massif, Ecuador.

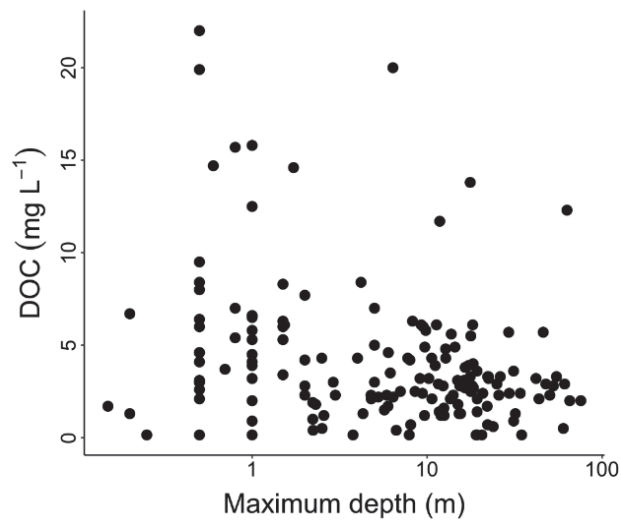


Figure S4. Relationship between water body depth and DOC concentration in the Cajas Massif (Andes, Ecuador).

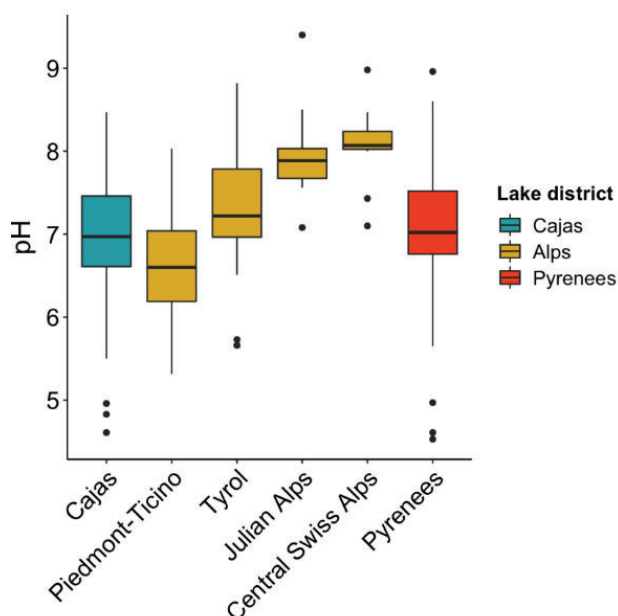


Figure S5. The pH range and distribution in Cajas NP are equivalent to those found in large European mountain ranges (e.g., Pyrenees, Alps). In these ranges, the same variation is achieved only by combining areas of plutonic, metamorphic, and carbonates bedrocks; here illustrated showing pH distributions for different geographical parts of the Alps (Catalan, J., C. J. Curtis, and M. Kernan. 2009. Remote European mountain lake ecosystems: regionalisation and ecological status. *Freshw Biol* 54: 2419-2432).

Table S1. Lithostratigraphy classes in the study area

Geological formation	Layering	Volcanic material	Primary parent rock	Secondary parent rock	Geological period	Age (Ma)	Other features	Lakes in the study
Chulo Unit	Upper: Filo Cajas, Tomebamba, Chanlud	Tuffs, breccia, domes	Rhyolite	Dacite, andesite (dykes)	Late Eocene	37*		28
Filo Cajas Unit	Upper: Chanlud Lower: Chulo	Tuffs, lava, breccia	Dacite	Andesite	Very Late Eocene or Early Oligocene	35*	Rich quartz crystals. Large dacite belt. Locally, rhyolite domes	8
Tomebamba Unit	Upper: Chanlud Lower: Chulo	Tuffs, lapilli	Andesite and dacite		Early Oligocene	34.1±1.3	Tuff secondary alteration with chlorite, epidote, actinolite, calcite, and pyrite	10
Chanlud formation	Upper: Soldados Lower: Chulo, Filo Cajas, Tomebamba	Lava, breccia, tuffs	Andesite	Dacite, rhyodacite, basalt (dykes)	Early Oligocene	33*	Up to 1 km thickness. Intrusive diorites.	30
Rio Blanco formation	Upper: Soldados Lower: Chulo	Lava, ash tuffs, breccia with sandstone	Andesite	Dacite, meladiorite (intrusive)	Early Oligocene	33*	Feldspathic lava with hypersthene and hornblende. Some	15

Supporting Information

Soldados formation	Upper: Plancharumi Lower: Chanlud, Rio Blanco	Ash tuffs, lapilli	Dacite	Andesite	Late Oligocene	29.8±1.2	underwater deposited. Rich in feldspar and quartz. Chlorite lapilli	70
Plancharumi formation	Upper: Quimsacocha	Tuffs, breccia, sandstone, lava, lapilli	Rhyolite		Late Oligocene	25.7±1.1		
Quimsacocha formation	Lower: Plancharumi, Turi (8-9 Ma)	Lava, breccia	Andesite		Late Miocene	<8*		3
Cisarán formation	Lower: Turi	Lava	Andesite	Dacite	Late Miocene	6.9±0.7		1
Intrusive rocks			Diorite			10-30*	Intrusive bodies occur across several formations. Some contemporary of the volcanic rocks and others much younger	

Mainly based on Dunkley and Gaibor (2009), see Fig. S2 legend.

* Estimated age by relative stratigraphic position

Table S2. Summary of the land cover relative abundance in

Land cover class	Minimum	1 st Quartile	Median	Mean	3 rd Quartile	Maximum
Páramo	0	31	50	45	60	95
Shrubs	0	0.005	1.9	3.9	4.8	47
<i>Polylepis</i> forest	0	0	0.75	2.4	2.9	27
Rocky páramo	0	7.1	22	27	40	93
Eroded land	0	0	0.09	2.6	2.7	45
Bare rock	0	0	0	2.1	0.7	32
Wetlands	0	1.9	5.6	7.3	9.3	48
Waterbodies	0	5.4	8.1	9.9	12	37

Note: Montane evergreen forest was only present in Lake Llaviucu (8.2%), located at a lower altitude (i.e., 3152 m a.s.l.).

Chapter 4

Table S1. Thermistor deployment depth according to cumulative relative lake volume.

Lake / Volume (%)	Depth (m)					
	~100	75	50	25	15	<5
Llaviucu	0.2	2.5	5.5	-	-	16
Toreadora	0.2	3.5	8	14	-	29
Yantahuaico-3	0.2	-	5	-	-	19
Atugyacu Grande	0.2	5	11	18.5	22	34
Estrellascocha	0.2	6	13	22	-	42
Larga	0.2	5	12	23	29	47
Luspa	0.2	8	18	31.5	39	65
Sunincocha Grande	0.2	5	12	23	30	61
Jigeno	0.2	2	5	9	-	25
Dos Chorreras	0.2	3	6.5	10.5	-	18

Equations used for water density, ρ (kg m^{-3})

- 1) Temperature related density, $\rho_T = 999.8429 + 0.001 (0.059385 T^3 - 8.56272 T^2 + 65.4891 T)$
- 2) Conductivity related density, $\rho_K = 0.67 \times 10^{-3} K_{20}$
- 3) $\rho = \rho_T + \rho_K$

where T is water temperature ($^{\circ}\text{C}$) and K_{20} , water conductivity at 20 $^{\circ}\text{C}$ (mS cm^{-1})

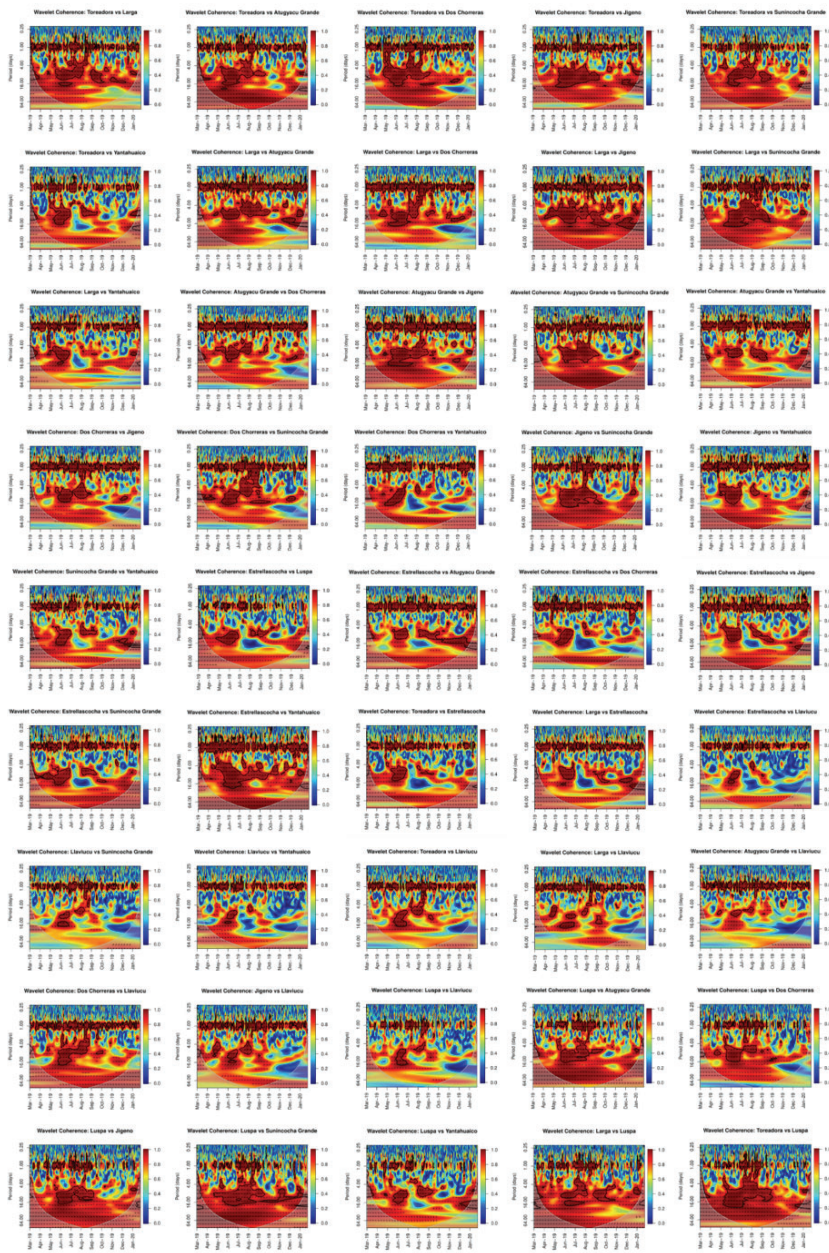


Figure S1. Cross-wavelet analyses between heat flux fluctuations of lake pairs.

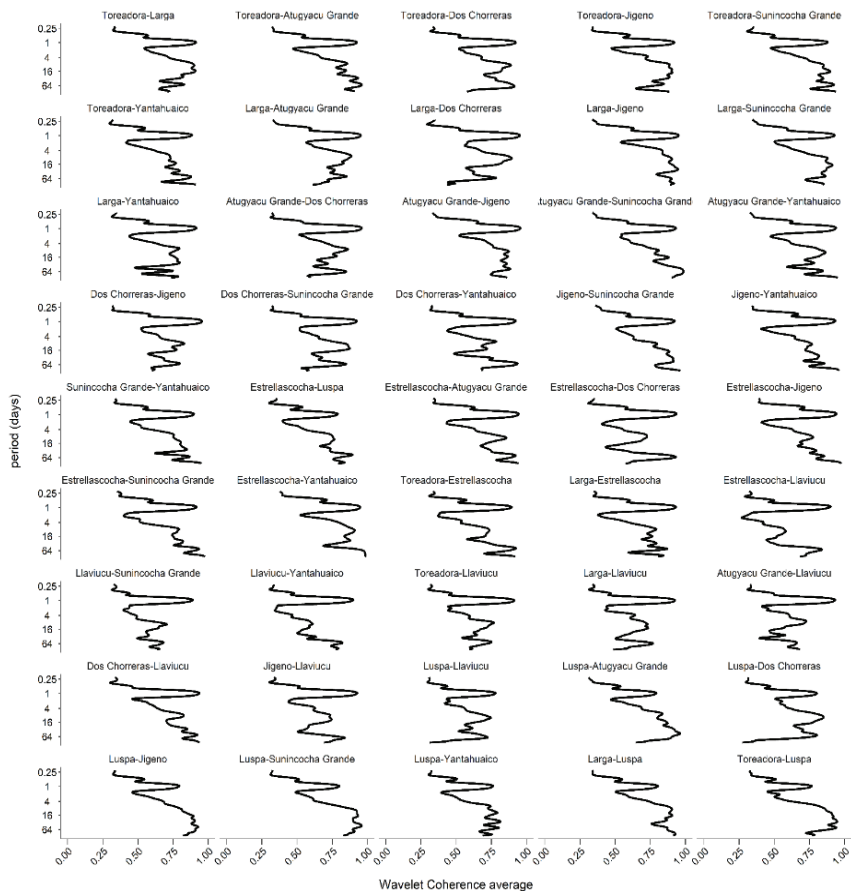


Figure S2. Averaged coherence across temporal scales for lake pairs cross-wavelet comparisons in Fig. S1.

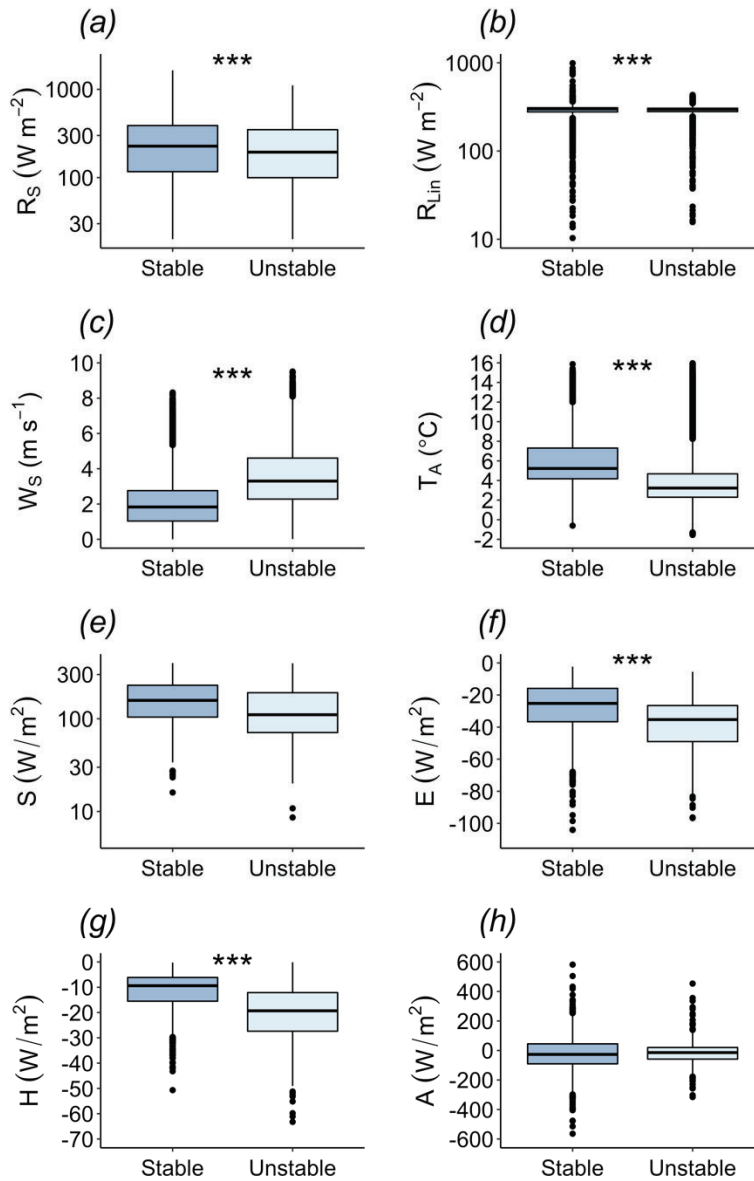


Figure S3. Weather components comparison between the stable and unstable periods in Lake Toreadora.

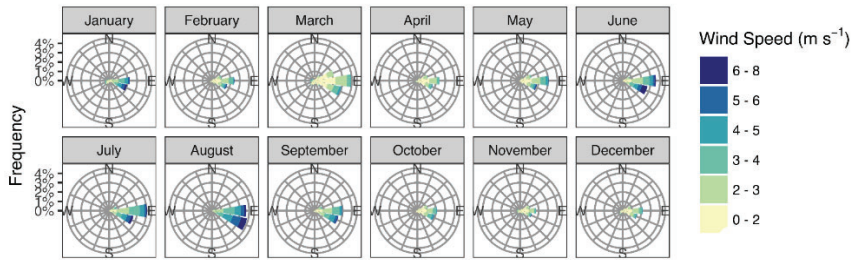


Figure S4. Monthly wind direction and speed distribution in Lake Toreadora.

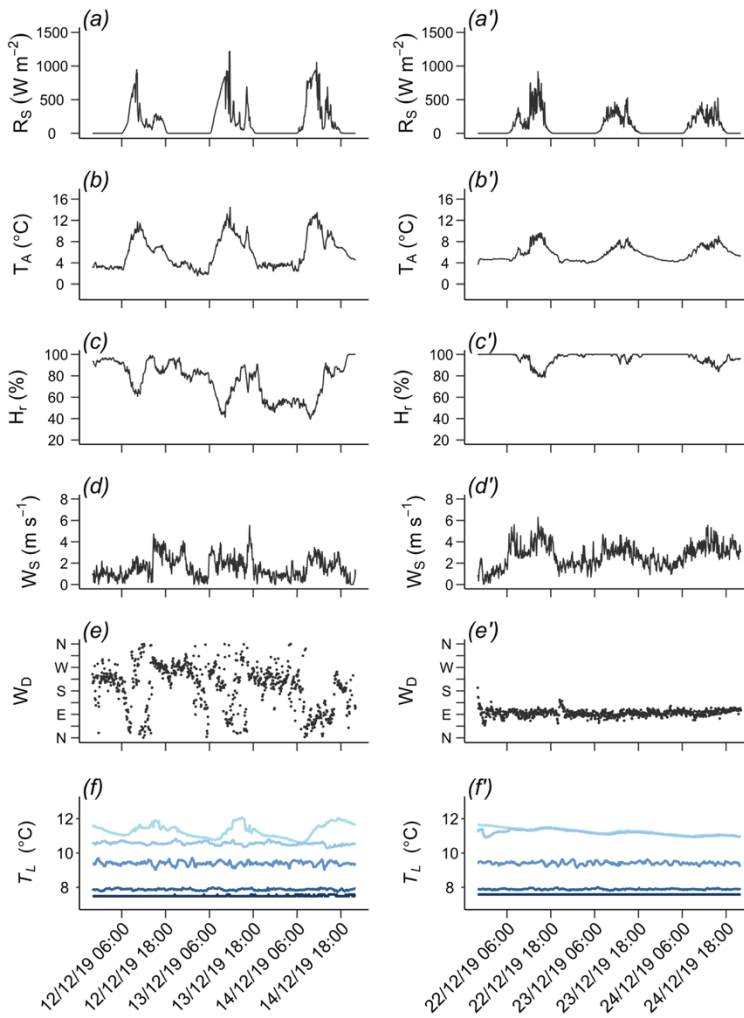


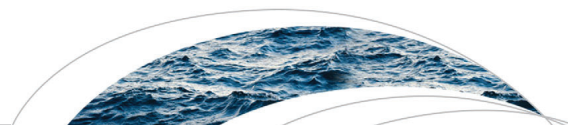
Figure S5. Weather components comparison between days with wind direction shift towards west (a-f) and days with persistent east wind direction (a'-f').

APPENDIX B

This appendix provides the original publication of Chapter 2 and Chapter 3.

Mosquera, P. V., H. Hampel, R. F. Vázquez, M. Alonso, and J. Catalan. 2017a. Abundance and morphometry changes across the high-mountain lake-size gradient in the tropical Andes of Southern Ecuador. *Water Resour Res* 53: 7269-7280. <https://doi.org/10.1002/2017WR020902>

Mosquera, P. V., H. Hampel, R. F. Vázquez, and J. Catalan. 2022. Water chemistry variation in tropical high-mountain lakes on old volcanic bedrocks. *Limnol Oceanogr* 67: 1522–1536. <https://doi.org/10.1002/lno.12099>



RESEARCH ARTICLE

10.1002/2017WR020902

Special Section:

Responses to Environmental Change in Aquatic Mountain Ecosystems

Key Points:

- The tropical high-mountain lakes show power-law lake-size distributions truncated at both ends similar to those found in temperate ranges
- The marked relief limits the size of the largest lakes at high altitudes, whereas ponds are particularly prompt to a complete infilling
- Lake volume scales to lake area according to a larger coefficient than found in other lake areas of glacial origin but gentle relief

Supporting Information:

- Supporting Information S1

Correspondence to:

J. Catalan,
j.catalan@creaf.uab.cat

Citation:

Mosquera, P. V., H. Hampel, R. F. Vázquez, M. Alonso, and J. Catalan (2017), Abundance and morphometry changes across the high-mountain lake-size gradient in the tropical Andes of Southern Ecuador, *Water Resour. Res.*, 53, 7269–7280, doi:10.1002/2017WR020902.

Received 6 APR 2017

Accepted 20 JUL 2017

Accepted article online 26 JUL 2017

Published online 23 AUG 2017

Abundance and morphometry changes across the high-mountain lake-size gradient in the tropical Andes of Southern Ecuador

Pablo V. Mosquera^{1,2} , Henrietta Hampel^{3,4} , Raúl F. Vázquez^{4,5} , Miguel Alonso² , and Jordi Catalan⁶ 

¹Subgerencia de Gestión Ambiental de la Empresa Pública Municipal de Telecomunicaciones, Agua potable, Alcantarillado y Saneamiento (ETAPA EP), Cuenca, Ecuador, ²Departament de Biologia Evolutiva, Ecologia i Ciències Ambientals, Universitat de Barcelona, Barcelona, Spain, ³Facultad de Ciencias Químicas, Universidad de Cuenca, Cuenca, Ecuador, ⁴Facultad de Ingeniería, Universidad de Cuenca, Cuenca, Ecuador, ⁵Laboratorio de Ecología Acuática, Departamento de Recursos Hídricos y Ciencias Ambientales, Universidad de Cuenca, Cuenca, Ecuador, ⁶CREAF - CSIC, Campus UAB, Cerdanyola del Vallès, Spain

Abstract The number, size, and shape of lakes are key determinants of the ecological functionality of a lake district. The lake area scaling relationships with lake number and volume enable upscaling biogeochemical processes and spatially considering organisms' metapopulation dynamics. These relationships vary regionally depending on the geomorphological context, particularly in the range of lake area <math><1\text{ km}^2</math> and mountainous regions. The Cajas Massif (Southern Ecuador) holds a tropical mountain lake district with 5955 water bodies. The number of lakes deviates from a power law relationship with the lake area at both ends of the size range; similarly to the distributions found in temperate mountain ranges. The deviation of each distribution tail does not respond to the same cause. The marked relief limits the size of the largest lakes at high altitudes, whereas ponds are prompt to a complete infilling. A bathymetry survey of 202 lakes, selected across the full-size range, revealed a volume-area scaling coefficient larger than those found for other lake areas of glacial origin but softer relief. Water renewal time is not consistently proportional to the lake area due to the volume-area variation in midsize lakes. The 85% of the water surface is in lakes >math>10^4\text{ m}^2</math> and 50% of the water resources are held in a few ones (~10) deeper than 18 m. Therefore, midlakes and large lakes are by far more biogeochemically relevant than ponds and shallow lakes in this tropical mountain lake district.

1. Introduction

Many ecological processes in lakes scale with size [Fee, 1992; Post *et al.*, 2000]. Lake-size distributions play a pivotal role from biogeochemistry to community ecology; e.g., for upscaling metabolism or emission processes to regional and global contexts or investigating species distribution and metacommunity dynamics. Based on this interest, the estimation of the number of Earth's lakes indicated that they could be power law distributed across the full-size gradient [Downing *et al.*, 2006]. In the initial data sets used, nonetheless, there was a cutoff for small lakes or were operatively underrepresented. Consideration of a broader size range has shown that small lakes deviate from the power law distribution and are less abundant than previously expected, although they still dominate inventories [Cael and Seekell, 2016]. Consequently, there is a current need to investigate the regional patterns of small water bodies (subkilometer scales) and unveil the geomorphological processes that may drive and constrain them.

Remote lakes, defined as those in which human activities in the catchment are not the primary drivers of their dynamics, are of interest for tracking the footprint of global change at regional and planetary scales [Hobbs *et al.*, 2010; Catalan *et al.*, 2013]. Many of these lakes are of glacial origin and located in high mountains all over the planet and Arctic and subarctic regions. They are typically relatively small [Catalan *et al.*, 2009] and thus their abundance may likely deviate from the general Earth's scaling [Cael and Seekell, 2016]. In the case of mountain lakes, the relieve imposes additional topographical limitations that cause deviations from lake-size distributions in flatter regions [Seekell *et al.*, 2013]. There is an increasing relevance of high-mountain lakes in the assessment of global change, including climatic [Smol, 2012; O'Reilly *et al.*, 2015],

pollution aspects [Grimalt *et al.*, 2001; Yang *et al.*, 2010] and the interaction among both [Psenner and Schmidt, 1992]. To increase the reliability and comparability of the observations, it becomes fundamental to develop comprehensive regional mountain lake inventories and characterize the abundance-area distribution across the lake-size gradient. Recent changes in the thermal seasonal patterns in remote lakes are calling attention in the current warming situation [Sorvari *et al.*, 2002; Smol, 2012]. Inevitably, observations are performed on a few sites. The degree by which the observations can be extended to a large number of lakes requires some regional knowledge of the lake basin morphometric scaling. Under a similar external forcing, the physical behavior of lakes depends on to the lake aspect ratio (area versus volume) [Imberger, 2012]. The available data on lake volume distributions are more limited than the lake area ones as the former cannot be easily inferred from remote sensing and GIS modeling as the latter. In practice, it is commonly assumed that the lake volume-area scaling does not change for lakes of similar origin. However, this assumption may not always apply, or dispersion around a general pattern may be high [Cael *et al.*, 2017]. Some lakes may be on watersheds with relief, bedrocks or soils that erode more quickly than others. On the other hand, high-mountain lake districts provide excellent frameworks for the understanding of species distribution in habitats that occur discretely (that is as “islands”) in a matrix of unsuitable leaving space for organisms [de Mendoza *et al.*, 2017]. The metapopulation and metacommunity dynamics of the species highly depend on the abundance, density, and size structure of the habitats [Logue *et al.*, 2011]. One can expect that research on this topic will increasingly take advantage of the high-mountain natural experimental setting.

There is an increasing interest in tropical high-mountain lake systems and climate change [Michelutti *et al.*, 2015a]. The information about these ecosystems is sparser than for mountain lakes in temperate zones [Catalan and Donato-Rondón, 2016]. Particularly, there is still only a partial knowledge of the seasonal and interannual variability in the lake mixing and stratification patterns. If there is any current paradigm, this is based on a few sites of unknown representability for the whole set of lakes. A large group of tropical high-mountain lakes is situated along the Andean range in the equatorial zone (i.e., at Venezuela, Colombia, Ecuador, Peru, and Bolivia), above the tree line, between 3500 and 4500 m asl in the Paramo ecosystem [Gunkel, 2000; Donato-Rondón, 2010]. These lakes play a significant role in the hydrology of the region by regulating the availability and supply of water. Eventually, they feed both the great tributaries of the Amazon and rivers draining to the Pacific Ocean. Part of the water is used for human consumption, industry, irrigation, and electricity generation for millions of people who live in or nearby the Andean range [Luteyn, 1992; Buytaert *et al.*, 2006]. Climate change may result in severe threats for water supply [Bradley *et al.*, 2006]. Despite their relevance as ecosystems and water resources, there is little information available on the limnology of the Andean tropical lakes [Catalan and Donato-Rondón, 2016; Van Colen *et al.*, 2017]. Some of the studies were carried out in the 1980s and 1990s [Steinitz-Kannan *et al.*, 1983; Donato-Rondón, 2010] but knowledge on the hydrogeomorphology of these lakes is extremely scarce [Rivera Rondon *et al.*, 2010].

In Ecuador, most of the high-mountain tropical lakes are situated within national protected areas, out of which, 17 areas are found entirely or partially in the Paramo mountain belt [Steinitz-Kannan, 1997]. Herein, the Cajas National Park (Cajas NP), located in the austral region of Ecuador, contains a large number of lentic systems, which provide drinking water to nearly the 60% of the population of Cuenca, the third largest city in Ecuador. In fact, the National Park is embedded in a large UNESCO Biosphere reserve comprising the entire Cajas Massif. In this area, geomorphological processes occurring at the last glacial period resulted in an exceptionally high density of lakes above 3400 m asl (i.e., 13 lake km⁻²). In this study, we aim at characterizing the lake's morphometry across the full-size gradient and providing scaling relationships for the region and similar tropical high-mountain lake districts in the Andes. We performed an inventory of all the high-mountain lakes of glacial origin in the Cajas Massif and determined their area using GIS information. For a representative lake subset in the Cajas NP, we carried out a bathymetry survey to complete the morphometric characterization. We compare the relationships found with those in other alpine and lowland locations and discuss the results according to current geomorphological theories. The lake abundance and morphometric relationships derived constitute a comparative framework for current and future ecological, biogeochemical and physical research in these lakes and the basis for a more robust geographic upscaling of the processes investigated and informed management of the protected areas.

2. Materials and Methods

2.1. The Region and Study Sites

The studied lakes are situated in the Cajas Massif by the south of Ecuador, between 3°11'26" and 2°40'21" South; and 79°9'09" and 79°17'57" West. An inventory of all the lakes and ponds of glacial origin (5955) was intended for the region, and a representative subset of them (202) was selected within the Cajas NP for a bathymetry survey (Figure 1). For the sake of brevity, we will use "lake" as the general name for water

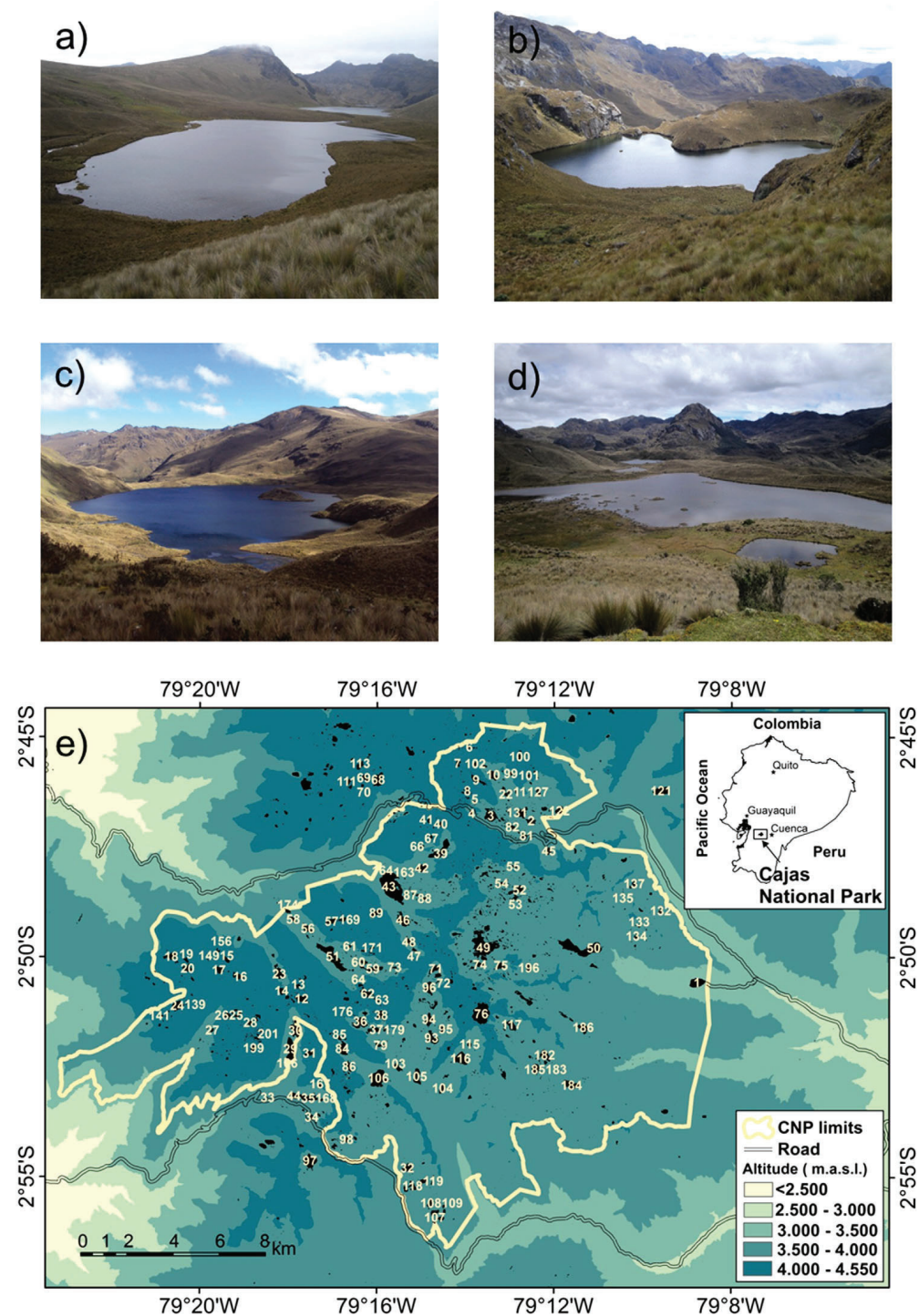


Figure 1. Some representative lake images from the Cajas National Park (CNP) ((a) Cascarilla 3–086, (b) Fondococha-007, (c) Luspa-043, and (d) Apicocha 1–081) and (e) a map with an indication of the lakes included in the bathymetry survey. The numbers refer to identification codes that have been used in the scope of the current study (see supporting information Table S1).

bodies of any size throughout most of the text. The 45% of the area drains to the Pacific Ocean, and the remaining 55% to the Atlantic. The primary bedrock is volcanic (Tarqui formation), including rhyolite, andesite, tuff, pyroclastic, and ignimbrites [Hungerbühler *et al.*, 2002]. The regional geomorphology was shaped by glacier activities until the late Pleistocene when the ice retreated around 17,000–15,000 years ago [Colinvaux *et al.*, 1997; Hansen *et al.*, 2003; Rodbell *et al.*, 2009]. Part of the glacier footprint is a large density of relatively small lakes above 3400 m above the sea level (asl), except Lake Llaviucu located at a lower altitude (3146 m asl) at the backside of a terminal frontal moraine of a large glacial tongue. The main soil types at the region are nonallophanic Andosols and Histosols from volcanic origin [Borja and Cisneros, 2009; Crespo *et al.*, 2011]. Both types present dark colored epipedons characterized by high organic matter content, high porosity, low apparent density (400 kg m^{-3}) and a high water retention capacity (in average, 6 g g^{-1} at a pressure of 1500 kPa), with higher values in the H horizon [Buytaert *et al.*, 2005]. Most of the rainfall is retained in soils and released gradually to the water courses, regulating the hydrology of these ecosystems [Poulenard *et al.*, 2003; Buytaert *et al.*, 2005]. The vegetation in 91% of the total extent of the Cajas NP and about 50% of the massif is herbaceous with a dominating presence of the genera *Stipa* and *Calamagrostis* [Ramsay and Oxley, 1997]. Concerning woody vegetation, only *Polylepis* species are present above the 3400 m asl. Lower altitudes—below the alpine lake inferior limit—are covered by the high-mountain forest (“bosque montano”). At present, the main impacts of land use and human activities on vegetation are tourism, fishery, grazing, and localized burning of the vegetation. Annual precipitation is between 900 and $1600 \text{ L m}^{-2} \text{ yr}^{-1}$ with contrasting seasons and high variation from year to year [Vuille *et al.*, 2000; Celleri *et al.*, 2007; Padrón *et al.*, 2015]. High rainfall causes enhanced soil erosion with deposition of light-colored clastic laminae in the sediments of some lakes [Rodbell *et al.*, 1999].

2.2. Lake Inventory and Area, and Perimeter Estimation

The boundaries of each lake were generated by heads-up digitalization of the aerial photographs of the project SIG-Tierras (2010–2014, www.sigtierras.gob.ec/) for the zone of the Cajas Massif. The images were orthorectified and georeferenced and had a spatial resolution of $30 \times 30 \text{ cm}^2$. Only one digitizer performed the manual task, for consistency, and several people repeatedly checked for omissions and mistakes. ArcGIS 10.0 (ESRI Inc., Redlands, CA, USA) was used with a screen zoom of the photographs always below a scale of 1:200. The scale of cartographic digitalization was 1:5000. The area and perimeter of each lake were calculated from the digitized contour shapefile using the ArcGIS 10.0 calculator and the altitude from the raster of the SIG-Tierras digital elevation model that has a spatial resolution of $3 \times 3 \text{ m}^2$.

2.3. Bathymetry Survey and Lake Basin Modeling

A selection of 202 lakes and ponds, covering the full-size gradient, was made to perform a bathymetry survey (supporting information Figure S1) within the Cajas NP (Figure 1). The survey was carried out with the aid of an inflatable rubber boat (Navigator II, RTS, China), approximately 3.5 m long, equipped with a propeller (2 HP, Yamaha, Japan) and an echo sounder Humminbird® model 1198c SI (Eufaula, AL, USA). The previously digitized lake boundary was used as zero-depth reference and for the planning of the number of gridded profiling transects and the spacing between them according to the lake size: for lakes with area $> 0.2 \text{ km}^2$, the transect spacing was around 100 m; for lakes between 0.1 and 0.2 km^2 , around 50 m; and for lakes $< 0.1 \text{ km}^2$, around 25 m. The distance between the bathymetry points not exceeded 5 m. In the shallow lakes and ponds, where the use of the boat was not possible, measurements were taken at several points of the water body using a topographic measuring rod.

The digital bathymetry procedure is described in detail in the supporting information Text S1. The main steps included: (i) integration of the depth data collected in the field with the data derived from the digitalization of the orthophotos (i.e., boundaries of the lakes associated with zero depth); (ii) data preparation according to the demands of the following processing steps; (iii) selection and application of an appropriate interpolation algorithm for each lake, in total, ten interpolation methods were tested [Franke and Nielson, 1980; Franke, 1982; Renka, 1988; Hanselman and Littlefield, 1998; Wise, 2000; Vivoni *et al.*, 2005; Vázquez and Feyen, 2007; Eldrandaly and Abu-Zaid, 2011]; and (iv) production of the digital bathymetric models and geomorphological parameters. Given the number of lakes considered in the bathymetry survey, the interpolation and quality control analyses were carried out automatically, using the programming framework that Surfer® 13.0 enables in conjunction with PERL (Practical Extraction and Report Language) subroutines.

Table 1. Morphometric Descriptors of the 202 Lakes and Ponds Included in the Bathymetry Survey of the Cajas National Park (Ecuador)

Variable	Acronym	Unit	Mean	Median	Minimum	Maximum
Area	A	m ²	58,860	25,708	6	774,775
Perimeter	S	m	1,146	895	10	8,795
Fetch	Fetch	m	324	271	4	1,563
Maximum length	L _{max}	m	341	274	4	2,142
Maximum width	B _{max}	m	175	153	2	956
Mean width	B _{mean}	m	105	92	1	531
Volume	V	m ³	692,717	38,046	0.6	22,369,167
Maximum depth	Z _{max}	m	11.0	6.0	0.2	75.5
Mean depth	Z _{mean}	m	4.2	1.9	0.1	30.6
Shoreline development	D _L		1.6	1.5	1.0	3.1
Volume development	D _V		1.0	1.0	0.4	1.8
Z _{mean} /Z _{max} ratio	Z _{mean} /Z _{max}		0.3	0.3	0.1	0.6
L _{max} /B _{mean} ratio	L _{max} /B _{mean}		3.3	2.9	1.4	9.9
Relative depth	Z _r	%	4.6	4.2	0.1	15.5
Watershed area	A _w	km ²	2	1	0.000015	48
A _w /V ratio	A _w /V		173	12	0.1	10,113
Water renewal time	t _{WR}	Day	167	48	<1	4,261

From the digitalized lake basins several morphometric variables and indicative ratios were determined (Table 1). Fetch, defined as the maximum distance that the wind can travel on the surface of the water before it is intersected, was estimated according to *Hakanson* [1981].

3. Results

3.1. Lake Abundance and Size

In the Cajas Massif, all the lakes of glacial origin are < 1 km² in area. Lake abundance (N) increases with declining area (A). Although the fitting of a scaling factor (b) is significant, the distribution deviates from a true power law at both ends (Figure 2a).

$$N \sim A^b \tag{1}$$

The deviation in the low-size range is not related to a methodological bias as the distribution starts to diverge at values without orthophoto image resolution problems for digitalization [*Seekell and Pace, 2011*]. The distribution is also truncated at the large-size range. This kind of truncation has been attributed to the particular situation of mountain lake districts, where there is a decline of the available surface at higher elevations and, therefore, the probability to find large lakes drops above certain altitude [*Seekell et al., 2013*]. The maximum density of lakes in the Cajas Massif occurs about 3936 m asl and declines symmetrically towards both ends, although without following a normal distribution (supporting information Figure S2). The highest lake is located at 4424 m asl, and the lowest at 3146 m, although the latter is an exception corresponding to a terminal moraine and, in fact, the rest of the lakes are located at elevations > 3400 m asl. If

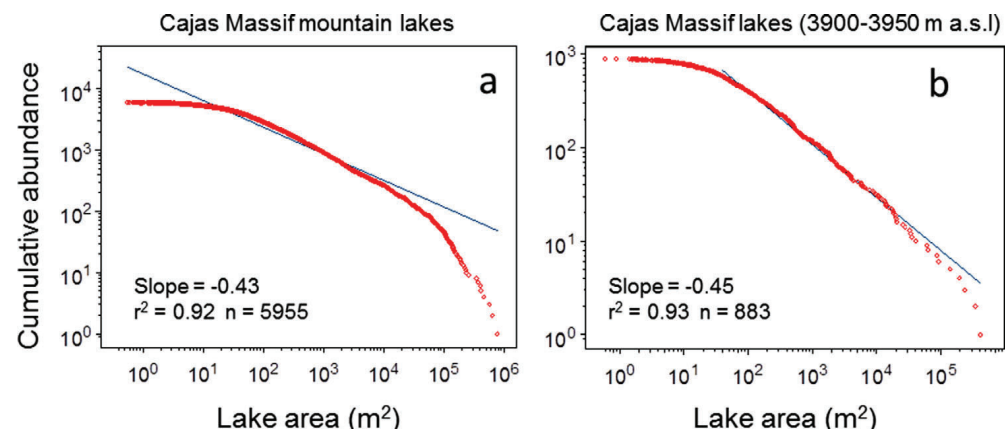


Figure 2. Lake-area distribution in the Cajas Massif (Southern Ecuador). (a) All high-mountain lakes and ponds from the Cajas Massif. (b) Subset of lakes around the average altitude of the lake distribution. The straight line indicates a power law fitting (equation (1)). In Figure 2b, only the right linear range was fitted.

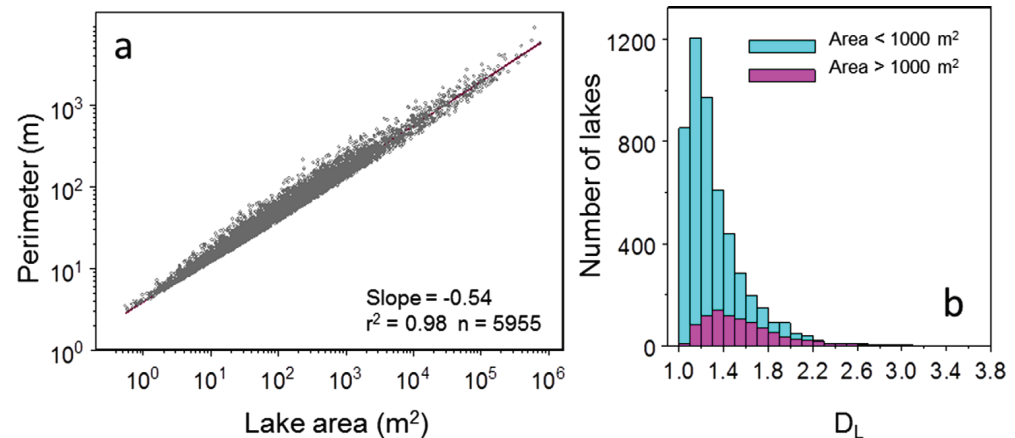


Figure 3. (a) Allometric relationship between the area and the perimeter of the Cajas Massif lakes. (b) Distribution of the shoreline development (D_L) for lakes with size above and below 1000 m^2 , respectively.

one considers only the lakes around the mean altitude of the lakes (Figure 2b), the distribution becomes less bent at the large-size extreme, whereas, at the small-size end, the shape of the distribution scarcely changes respect to the whole lake set. This feature indicates that the deviation of a power law at each extreme does not respond to the same cause. The large lake-size tail of the distribution is much affected by altitude than the small lake-size end. Nevertheless, some restriction to the appearance of large lakes remains as the log-log representation of the tail is still not linear (Figure 2b). The truncation may also happen if the study extent is small, which could be the case with the altitudinal restriction.

3.2. Lake Shape

The complexity of the shoreline geometry is captured by the relationship between the lake area and the perimeter (Figure 3a). The fractal dimension (D), defined as

$$S \sim \sqrt{A}^D \tag{2}$$

is close to one ($D = 1.079$) for the whole lake set of the Cajas Massif, indicating as such that the lake shape, in general, corresponds to polygons scarcely ramified. Through the size range, there is no a significant deviation from this general pattern (Figure 3a).

The shoreline development (D_L) evaluates the departure of the shape from a circle ($D_L = 1$). Most of the lakes show D_L values close to one (Table 1 and Figure 3b). This feature, however, relaxes when the size of the lakes increases as larger lakes tend to be more convoluted than the smaller ones (Figure 3b and supporting information Figure S3).

A few large lakes show elongated subrectangular or sub-circular forms with sinuous shorelines such as Osohuayco ($D_L = 3.1$) and Toreadora ($D_L = 2.6$), both being within the Cajas NP.

3.3. Lake 3-D Shape

The bathymetry survey in the Cajas NP provided the basis for extending the lake shape analysis to a third dimension. There is a general significant allometric relationship between lake area (A, m^2) and volume (V, m^3) that describes the invariance in shape as size changes:

$$V = 0.0107 A^{1.52}, r^2 = 0.93, n = 202 \tag{3}$$

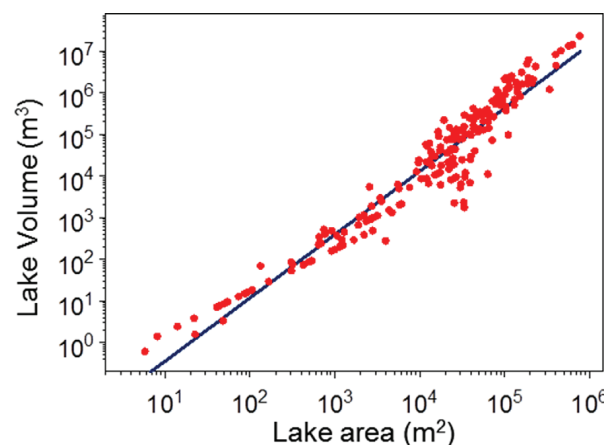


Figure 4. The relationship between area and volume for the lakes of the Cajas Massif based on a survey of 202 lakes and ponds in the Cajas National Park.

The distribution of the deviations from the general relationship (Figure 4) does not appear to be homogeneous across the entire

Cajas NP lakes show low Z_r values (Figure 5b). Only a few lakes show $Z_r > 10\%$; a value considered the threshold for high overexcavation. It can be thought that either the basins were not so much excavated as in other high-mountain ranges, the in-filling process has advanced more or a combination of both considerations. In fact, about 20% of the water bodies show $Z_r < 2\%$, which is considered an indication of being closer to an eventual complete filling. The Z_r patterns do not show any correspondence with the watershed orientation and main river basins distribution. Only at the level of relatively small subbasins, they display a geographical pattern (Figure 6b). Some of these subbasins show a high proportion of water bodies close to filling up (i.e., Canoas, Culebrillas, and Jerez), whereas the highly overexcavated lake basins are scattered over many subbasins, only Atugyacu is particularly rich in these latter lakes.

3.4. Lake Watershed

As could be expected from glacier erosive processes, the larger the watershed, the larger the lake (Figure 6a). However, the tendency is allometric so that the lake's area increases at a lower rate than the respective watershed.

$$A = 1.95 \times A_w^{0.71}, \quad r^2 = 0.86, \quad n = 202 \quad (5)$$

There is not a marked geographical pattern in the lake-size distribution across the main subbasins (Figure 6a). The watershed area and lake volume are the primary determinants of the average water renewal time (t_{WR}) in the lakes of the Cajas NP, provided the relatively homogeneous climate and geological landscape of the area. Under a similar amount of average precipitation, the runoff entering the lakes is proportional to the watershed area, whereas the retention capacity is proportional to the lake volume. Consequently, the morphological dissimilarities among lakes of a similar size result in marked differences in the t_{WR} (Figure 6b). Overall, t_{WR} of a few weeks to a few months largely predominate, and only a few lakes may show average t_{WR} above 1 or several years.

4. Discussion

4.1. Lake-Size Distribution

The shape of the distribution of the lake-area abundance from the Cajas Massif (Figure 2a) is similar to those found in other high-mountain lake districts of glacial origin [Hanson *et al.*, 2007; Seekell and Pace, 2011]. The general features are deviations at both ends from a power law relationship and a slope around -0.5 of a log-log linear fitting (-0.66 , -0.43 , and -0.43 in the Adirondack Mountains, the Northern Highland Lake District, and our study, respectively) [Seekell and Pace, 2011]. It appears as a general feature that the mountain lake distribution differs from a power law, and the scaling slope is well below one; thus not following the two features that characterize the self-similar distribution of lakes $> 1 \text{ km}^2$ in the planet [Lehner and Doll, 2004; Downing *et al.*, 2006; Cael and Seekell, 2016].

The deviation in the large-size lake extreme has been attributed to the restriction imposed by the departure from a flat surface so that the available area declines with altitude and thus the probability for large lakes diminishes [Seekell *et al.*, 2013]. Considering a belt of lakes around the elevation of the highest lake density mitigates this restriction; however, even only fitting the large-size long tail, the slope remains around 0.5 , and the distribution does not significantly fit a power law in the Cajas Massif. It seems, therefore, that there is an additional factor, beyond elevation, modifying the lake-size distribution in high-mountain lake districts. Periglacial processes, steep slopes, thin soils, and torrential stream flows may have enhanced the lake filling, perhaps at an early phase during deglaciation, when retreating glaciers move high amounts of detrital material and stream flows are rich in glacier flour. The large lakes in the central valleys may have been particularly affected by these processes so that their presence in the landscape has been substituted by flat lands of meandering streams or peatlands.

One of the consequences of the biased distribution is that within the Cajas Massif—and probably in similar mountain lake districts—most of the lentic water surface is in midsize lakes and not in ponds (Figure 7a). About 50% and more than 85% of the water surface area is on lakes $> 10^5$ and $> 10^4 \text{ m}^2$, respectively. Biogeochemical processes in these systems are thus particularly relevant in the context of gas emissions and watershed and fluvial network dynamics. On the other hand, the still enormous numbers of ponds may be of interest for the metacommunity dynamics of some aquatic organisms restricted or with a preference for these systems (e.g., amphibians).

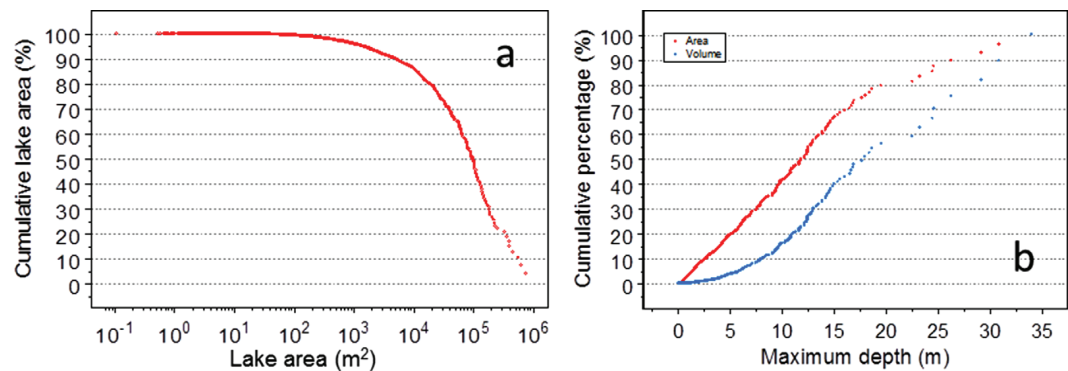


Figure 7. (a) Percentage of cumulative lake area from the largest lake to the smallest pond in the Cajas Massif. (b) Percentage of cumulative lake volume (blue) and lake area (red) with increasing maximum depth in the Cajas Massif as estimated with equations (3) and (5), respectively.

4.2. Lake Basin Morphology

Earth’s lakes $>4.7 \text{ km}^2$ show shorelines with a fractal dimension $D = 1.34$, close to expected predictions ($D = 4/3$) of the percolation theory [Cael and Seekell, 2016]; whereas lakes $<4.7 \text{ km}^2$ depart from this pattern and show $D = 1.00$. The Cajas Massif lakes are close to the last model ($D = 1.08$), in this case in agreement with the general pattern in relatively flat landscapes. There is no clear departure from this scaling along the lake-size range (Figure 3a) as may occur if a subset of lakes or ponds become particularly convoluted [Hohegger et al., 2012]. Nevertheless, the shoreline development ratio (D_L) indicates that the larger the lake there is an increasing probability to become subrectangular and present sinuous shorelines in some cases (Figure 3b), yet the high scattering prevents from a significant departure from the general pattern. The lakes with higher D_L (e.g., >2) may correspond to cases of flooding of several subbasins (supporting information Figure S3). In any case, for most of the lakes, the differences are relatively small. One can conclude that in these lakes the interaction with terrestrial systems and littoral environments scale similarly throughout the lake-size range.

Large scattering in some parts of the lake-size gradient (e.g., 10^4 to 10^5 m^2) indicates some variation in the geomorphological process configuring the current lake basins. Several particularities point to a differential lake filling as the cause of the high depth (volume) variation at this mid lake-size range. (1) The markedly less noisy relationship between area and perimeter than between area and volume indicates that there has been a transformation of the lake bottoms processes posterior to the lake formation; otherwise, the shape heterogeneity in surface usually also correspond with the 3-D variation [Hakanson, 1981]. A comparison of the sediment records and detailed watershed bedrock and soil characteristics could provide the necessary evidence on this issue. Up to now, only the sediments of one of the “relatively shallow” lakes have been cored up to the bedrock (i.e., Pallcacoha) [Rodbell et al., 1999]. The sedimentary record shows a relatively fast accumulation of light-colored inorganic sediment during Late Glacial and a transition to dark organic-rich gyttja at the onset of the Holocene, with lower accumulation rates. The average rates increase again and accelerate up to present by Mid-Holocene. Part of this acceleration may be due to the observed increasing frequency of ENSO events throughout the Holocene. This situation implies torrential rains that produce clastic laminae in the sediment profile. The volcanic bedrock of the watershed erodes easily, and debris flows and talus are abundant and located not far from the lake. However, the accumulation rate of the dark facies also increases. This feature may be due to natural processes, such as aquatic and subaquatic vegetation growth, with higher retention of fine sediment, or to human land perturbation (e.g., fire) as early cultures in the Andes have affected vegetation and soil stability since ancient times [Coblentz and Keating, 2008]. (2) The relative depth of many lakes ($Z_r \ll 10\%$) depart from values typical of overexcavation by glaciers. Assuming that there is no reason for a differential excavation of glaciers in tropical areas, the explanation should rely on an enhanced infilling compared to the temperate zone, which could be related to the soil erodibility and littoral vegetation development both enhanced in tropical volcanic humid regions. (3) The lakes deviating more from the general relationship between lake and watershed area (Figure 6a) also are lakes that are relatively shallow compared to their areas; for example, those in the Canoas subbasin. That is, the filling process may have also contributed to reducing the shoreline, although not as much as it

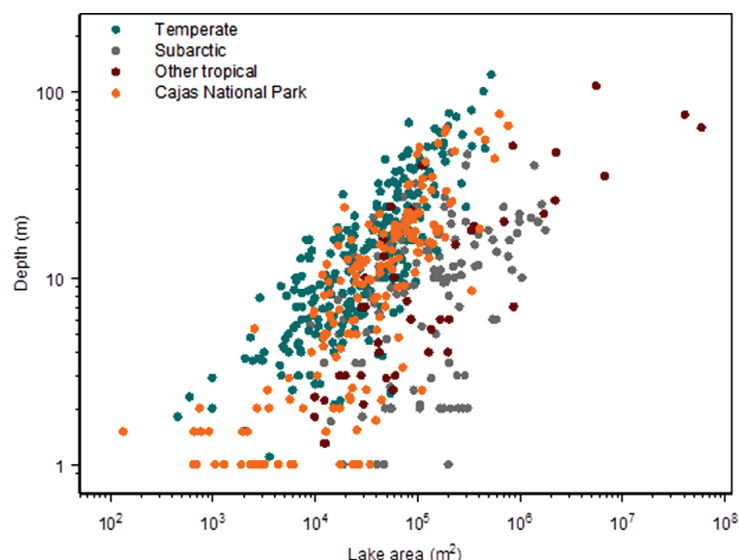


Figure 8. The relationship between lake area and maximum depths for remote lakes. Cajas National Park lakes are compared with a set of European temperate high-mountain lakes, subarctic lakes and tropical high-mountain from other parts of the world, mostly Colombian lakes.

has affected mean depth. (4) Lakes relatively deep and relative shallow for intermediate lake areas can be found in the same subbasins, which indicates that they do not respond to a geographical differentiation of the glacier erosion but rather to strictly nearby site geomorphological particularities.

Despite of the likely profound transformation of some of the Cajas Massif lakes after the excavation of the basin, the general pattern of lake basin formation, illustrated by the patterns between lake area and maximum depth (Figure 8), still agrees with that from alpine lakes in European ranges and differ from those in subarctic

areas. In the latter region, lakes are much larger compared to depth than in high mountains [Catalan *et al.*, 2009]. Glacier excavation in the ice accumulation zones depends on the steepness of the slope of the basin. In this aspect, the Cajas' lakes follow the pattern of some of the high-mountain lakes in the Colombian Andes and differ from others there that are closer to subarctic forms [Catalan and Donato-Rondón, 2016]. Accurate bathymetry surveys comprising a relatively large numbers of high-mountain lakes are not broadly available. It would be interesting to investigate whether the pattern of differential lake filling found in the Cajas NP lakes repeats elsewhere or, alternatively, they are more likely in particular climatic regions (e.g., tropical) and bedrock substrates (e.g., volcanic). Development of littoral and subaquatic vegetation may also play a role, and this could be particularly relevant in tropical high-mountain lakes.

5. Conclusions

Inventories of lake and pond areas are increasingly available at higher spatial resolution and become useful for multiple purposes. Lake-size distributions are the basis for upscaling biogeochemical processes to landscape scales, design research projects that depend on the selection of a few sites, and applying management criteria in protected or land used areas. The three activities require either some categorization of the water bodies or the characterization of the continuum variation. The use of lake surface area, which is broadly available, is not sufficient for an accurate functional classification of the water bodies in the Cajas Massif. At long term, the goal should be to increase the number of maximum depth measurements, at least for those lakes between 7000 and 40,000 m², the range of higher volume-area variation. Then, the use of the corresponding allometric equations can provide acceptable mean depth and lake volume estimations.

Concerning biogeochemical processes, the results presented herein show that lakes rather than ponds cover much more landscape surface and hold an even larger percentage of water volume (Figure 7). About 50% of the water is contained in a few lakes (~10) >18 m depth (Figure 7b). Water bodies <5 m depth, only account for about 5% of the total water stored. Research regarding the water column physical structure, biogeochemical process, and responses to global change merits concentrating in lakes >12 m depth as they hold about 80% of the volume and 50% of the pond and lake surface. However, lake morphology is not the only criteria to take into account. The size of the lake watershed cannot be ignored as they led to renewal times that differ markedly (Figure 6b). The issue becomes particularly critical for lakes with volume >10⁵ m³ as the water renewal times may vary from a few weeks to a few years depending on the watershed size and lake connectivity to the drainage network.

Beyond the identified allometric relationships that allow large-scale estimations and provide criteria for site selection, the detailed bathymetry survey within the Cajas NP constitutes a precise piece of information for research studies and management in the context of climate and other environmental changes. Studies on the thermal structure related to climate change may be preferentially accomplished in the relatively deep lakes, whereas those focusing on watershed transport may select relative-shallow lakes. In any case, all the lakes cannot be accommodated under a similar interpretative umbrella. For instance, in the Cajas NP, paleolimnological studies have been performed in several lakes, some of them referring to climatic and environmental changes during the Holocene and Late Glacial, others addressing current climatic change. The relatively shallow lake Pallcacocha provided a record of El Niño-Southern Oscillation (ENSO) throughout the last 15,000 years by the light-colored clastic laminae produced by storm-induced events [Rodbell *et al.*, 1999]. The dynamics of these relatively shallow lakes, with high water renewal, are mainly dominated by what happens in the watershed and associated stream transport; therefore, they are excellent for reconstruction of extreme rainfall events, vegetation [Hansen *et al.*, 2003] and land use changes. The relatively deep lakes, with water renewal longer than 1 year, are more appropriate for addressing issues related with proxies generated within the lake (e.g., diatom records) that respond to the physical and chemical characteristics of the water column and their changes throughout the year. These changes may also depend on extreme events, but also on more gentle climatic fluctuations and, particularly, interannual tendencies [Michelutti *et al.*, 2015b]. The allometric patterns found in the tropical high-mountain lakes of Southern Ecuador are worth to be investigated in other ranges with the aim of building up a full understanding of the morphometric structure of high-mountain lakes and their implications for biogeochemical and ecological dynamics.

Acknowledgments

The authors express their gratitude to the “Empresa Pública Municipal de Telecomunicaciones, Agua Potable, Alcantarillado y Saneamiento de Cuenca-Ecuador”(ETAPA EP) and the “Universidad de Cuenca”(UC, Ecuador) for funding this study through the project “Caracterización limnológica de los lagos y lagunas del Parque Nacional Cajas,” which was carried out in the Aquatic Ecology Laboratory (LEA) of the UC and directed by HH and RFV. Additionally, M.A. and H.H. were funded by the PROMETEO Project of the Ecuadorian Secretary for Higher Education, Science, Technology and Innovation (SENESCYT). Special thanks go to the assistant Mario Domínguez who worked in the LEA and contributed to the development of the different field sampling campaigns. J.C. was supported by LACUS project funded by the Spanish Government research grant CGL2013–45348-P, Ministerio de Economía y Competitividad. The lake morphology data in this study have been deposited in Dryad [Mosquera *et al.*, 2017].

References

- Borja, P., and P. Cisneros (2009), *Estudio edafológico. Informe del II año del proyecto “Elaboración de la línea base en hidrología de los páramos de Quimsacocha y su área de influencia,”* 104 pp., Universidad de Cuenca, Cuenca, Ecuador.
- Bradley, R. S., M. Vuille, H. F. Diaz, and W. Vergara (2006), Threats to water supplies in the tropical Andes, *Science*, 312(5781), 1755–1756.
- Buytaert, W., J. Sevink, B. De Leeuw, and J. Deckers (2005), Clay mineralogy of the soils in the south Ecuadorian páramo region, *Geoderma*, 127, 114–129.
- Buytaert, W., R. Celleri, B. De Bievre, F. Cisneros, G. Wyseure, J. Deckers, and R. Hofstede (2006), Human impact on the hydrology of the Andean paramos, *Earth Sci. Rev.*, 79(1–2), 53–72.
- Cael, B. B., and D. A. Seekell (2016), The size-distribution of Earth’s lakes, *Sci. Rep.*, 6, 29,633.
- Cael, B. B., A. J. Heathcote, and D. A. Seekell (2017), The volume and mean depth of Earth’s lakes, *Geophys. Res. Lett.*, 44, 209–218, doi: 10.1002/2016GL071378.
- Catalan, J., and J. C. Donato-Rondón (2016), Perspectives for an integrated understanding of tropical and temperate high-mountain lakes, *J. Limnol.*, 75(1s), 215–234.
- Catalan, J., C. J. Curtis, and M. Kernan (2009), Remote European mountain lake ecosystems: Regionalisation and ecological status, *Freshwater Biol.*, 54(12), 2419–2432.
- Catalan, J., et al. (2013), Global change revealed by palaeolimnological records from remote lakes: A review, *J. Paleolimnol.*, 49(3), 513–535.
- Celleri, R., P. Willems, W. Buytaert, and J. Feyen (2007), Space–time rainfall variability in the Paute basin, Ecuadorian Andes, *Hydrol. Processes*, 21(24), 3316–3327.
- Coblentz, D., and P. L. Keating (2008), Topographic controls on the distribution of tree islands in the high Andes of south-western Ecuador, *J. Biogeogr.*, 35(11), 2026–2038.
- Colinvaux, P. A., M. B. Bush, M. SteinitzKannan, and M. C. Miller (1997), Glacial and postglacial pollen records from the Ecuadorian Andes and Amazon, *Quat. Res.*, 48(1), 69–78.
- Crespo, P. J., J. Feyen, W. Buytaert, A. Bücken, L. Breuer, H.-G. Frede, and M. Ramírez (2011), Identifying controls of the rainfall–runoff response of small catchments in the tropical Andes (Ecuador), *J. Hydrol.*, 407(1–4), 164–174.
- de Mendoza, G., W. Traunspurger, A. Palomo, and J. Catalan (2017), Nematode distributions as spatial null models for macroinvertebrate species richness across environmental gradients: A case from mountain lakes, *Ecol. Evol.*, 7, 3016–3028, doi:10.1002/ece3.2842.
- Donato-Rondón, J. C. (2010), *Phytoplankton of Andean Lakes in Northern Southamerica (Colombia). Composition and Distribution Factors*, A.R.G. Gantner Verlag K.G., Ruggell, Liechtenstein.
- Downing, J. A., et al. (2006), The global abundance and size distribution of lakes, ponds, and impoundments, *Limnol. Oceanogr.*, 51(5), 2388–2397.
- Eldrandaly, K. A., and M. S. Abu-Zaid (2011), Comparison of six GIS-based spatial interpolation methods for estimating air temperature in Western Saudi Arabia, *J. Environ. Inf.*, 18(1), 38–45.
- Fee, E. J. (1992), Effects of lake size on phytoplankton photosynthesis, *Can. J. Fish. Aquat. Sci.*, 49, 2445–2459.
- Franke, R. (1982), Smooth interpolation of scattered data by local thin plate splines, *Comput. Math. Appl.*, 8(4), 273–281.
- Franke, R., and G. Nielson (1980), Smooth interpolation of large sets of scattered data, *Int. J. Numer. Meth. Eng.*, 15(11), 1691–1704.
- Grimalt, J. O., et al. (2001), Selective trapping of organochlorine compounds in mountain lakes of temperate areas, *Environ. Sci. Technol.*, 35(13), 2690–2697.
- Gunkel, G. (2000), Limnology of an equatorial high mountain lake in Ecuador, Lago San Pablo, *Limnologica*, 30(2), 113–120.
- Hakanson, L. (1981), *A Manual of Lake Morphometry*, Springer, Berlin.
- Hanselman, D., and B. Littlefield (1998), *Mastering MATLAB 5: A Comprehensive Tutorial and Reference*, Prentice Hall, London, U. K.
- Hansen, B. C. S., D. T. Rodbell, G. O. Seltzer, B. Leon, K. R. Young, and M. Abbott (2003), Late-glacial and Holocene vegetational history from two sites in the western Cordillera of southwestern Ecuador, *Palaeogeogr. Palaeoclimatol. Palaeoecol.*, 194(1–3), 79–108.

- Hanson, P. C., S. R. Carpenter, J. A. Cardille, M. T. Coe, and L. A. Winslow (2007), Small lakes dominate a random sample of regional lake characteristics, *Freshwater Biol.*, *52*(5), 814–822.
- Hobbs, W. O., R. J. Telford, H. J. B. Birks, J. E. Saros, R. R. O. Hazewinkel, B. B. Perren, E. Saulnier-Talbot, and A. P. Wolfe (2010), Quantifying recent ecological changes in remote lakes of North America and Greenland using sediment diatom assemblages, *PLoS One*, *5*(3), e10026.
- Hohenegger, C., B. Alali, K. R. Steffen, D. K. Perovich, and K. M. Golden (2012), Transition in the fractal geometry of Arctic melt ponds, *Cryosphere*, *6*(5), 1157–1162.
- Hungerbühler, D., M. Steinmann, W. Winkler, D. Seward, A. Egüez, D. E. Peterson, U. Helg, and C. Hammer (2002), Neogene stratigraphy and Andean geodynamics of Southern Ecuador, *Earth Sci. Rev.*, *57*(1–2), 75–124.
- Imberger, J. (2012), *Environmental Fluid Dynamics: Flow Processes, Scaling, Equations of Motion, and Solutions to Environmental Flows*, 460 pp., Academic, Oxford, U. K.
- Lehner, B., and P. Doll (2004), Development and validation of a global database of lakes, reservoirs and wetlands, *J. Hydrol.*, *296*(1–4), 1–22.
- Logue, J., N. Mouquet, H. Peter, and H. Hillebrand, and The Metacommunity Working Group (2011), Empirical approaches to metacommunities: A review and comparison with theory, *Trends Ecol. Evol.*, *26*(9), 482–491.
- Luteyn, J. L. (1992), Páramos: Why study them?, in *Páramo: An Andean Ecosystem Under Human Influence*, edited by H. Balslev and J. L. Luteyn, pp. 1–14, Academic, London.
- Michelutti, N., C. Cooke, W. Hobbs, and J. Smol (2015a), Climate-driven changes in lakes from the Peruvian Andes, *J. Paleolimnol.*, *54*, 1–8.
- Michelutti, N., A. P. Wolfe, C. A. Cooke, W. O. Hobbs, M. Vuille, and J. P. Smol (2015b), Climate change forces new ecological states in tropical Andean lakes, *PLoS One*, *10*(2), e0115338, doi:10.1371/journal.pone.0115338.
- Mosquera, P. V., H. Hampel, R. F. Vázquez, M. Alonso, and J. Catalan (2017), Abundance and morphometry changes across the high mountain lake-size gradient in the tropical Andes of Southern Ecuador, Dryad, Durham, N. C., doi:10.5061/dryad.sn058.
- O'Reilly, C. M., et al. (2015), Rapid and highly variable warming of lake surface waters around the globe, *Geophys. Res. Lett.*, *42*, 10,773–710,781, doi:10.1002/2015GL066235.
- Padrón, R. S., B. P. Wilcox, P. Crespo, and R. Céleri (2015), Rainfall in the Andean Páramo: New insights from high-resolution monitoring in Southern Ecuador, *J. Hydrometeorol.*, *16*(3), 985–996.
- Post, D. M., M. L. Pace, and N. G. Hairston Jr. (2000), Ecosystem size determines food-chain length in lakes, *Nature*, *405*, 1047–1049.
- Poulenard, J., P. Podwojewski, and A. J. Herbillon (2003), Characteristics of non-allophanic Andisols with hydric properties from the Ecuadorian páramos, *Geoderma*, *117*(3–4), 267–281.
- Psenner, R., and R. Schmidt (1992), Climate-driven pH control of remote Alpine lakes and effects of acid deposition, *Nature*, *356*(6372), 781–783.
- Ramsay, P. M., and E. R. B. Oxley (1997), The growth form composition of plant communities in the Ecuadorian paramos, *Plant Ecol.*, *131*(2), 173–192.
- Renka, R. J. (1988), Multivariate interpolation of large sets of scattered data, *ACM Trans. Math. Software*, *14*(2), 139–148.
- Rivera Rondon, C. A., A. M. Zapata, and J. C. Donaton Rondón (2010), Estudio morfométrico del lago Guatavita (Colombia), *Acta Biol. Colombiana*, *15*(3), 131–144.
- Rodbell, D. T., G. O. Seltzer, D. M. Anderson, M. B. Abbott, D. B. Enfield, and J. H. Newman (1999), A 15,000 year record of El Niño-driven alluviation in southwestern Ecuador, *Science*, *283*(5401), 516–520.
- Rodbell, D. T., J. A. Smith, and B. G. Mark (2009), Glaciation in the Andes during the Lateglacial and Holocene, *Quat. Sci. Rev.*, *28*(21–22), 2165–2212.
- Seekell, D. A., and M. L. Pace (2011), Does the Pareto distribution adequately describe the size-distribution of lakes?, *Limnol. Oceanogr.*, *56*(1), 350–356.
- Seekell, D. A., M. L. Pace, L. J. Tranvik, and C. Verpoorter (2013), A fractal-based approach to lake size-distributions, *Geophys. Res. Lett.*, *40*, 517–521, doi:10.1002/grl.50139.
- Smol, J. P. (2012), A planet in flux: How is life on Earth reacting to climate change?, *Nature*, *483*, S12–S15.
- Sorvari, S., A. Korhola, and R. Thompson (2002), Lake diatom response to recent Arctic warming in Finnish Lapland, *Global Change Biol.*, *8*(2), 171–181.
- Steinitz-Kannan, M. (1997), The lakes in Andean protected areas of Ecuador, *George Wright Forum*, *14*, 33–43.
- Steinitz-Kannan, M., P. A. Colinvaux, and R. Kannan (1983), Limnological studies in Ecuador 1. A survey of chemical and physical properties of Ecuadorian lakes, *Arch. Hydrobiol. Suppl.*, *65*(1), 61–105.
- Van Colen, W. R., P. Mosquera, M. Vanderstukken, K. Goiris, M.-C. Carrasco, E. Decaestecker, M. Alonso, F. León-Tamariz, and K. Muylaert (2017), Limnology and trophic status of glacial lakes in the tropical Andes (Cajas National Park, Ecuador), *Freshwater Biol.*, *62*(3), 458–473.
- Vázquez, R. F., and J. Feyen (2007), Assessment of the effects of DEM gridding on the predictions of basin runoff using MIKE SHE and a modelling resolution of 600 m, *J. Hydrol.*, *334*(1–2), 73–87.
- Vivoni, E. R., V. Y. Ivanov, R. L. Bras, and D. Entekhabi (2005), On the effects of triangulated terrain resolution on distributed hydrologic model response, *Hydrol. Processes*, *19*(11), 2101–2122.
- Vuille, M., R. S. Bradley, and F. Keimig (2000), Climate variability in the Andes of Ecuador and its relation to Tropical Pacific and Atlantic Sea surface temperature anomalies, *J. Clim.*, *13*(14), 2520–2535.
- Wise, S. (2000), Assessing the quality for hydrological applications of digital elevation models derived from contours, *Hydrol. Processes*, *14*(11–12), 1909–1929.
- Yang, H. D., D. R. Engstrom, and N. L. Rose (2010), Recent changes in atmospheric mercury deposition recorded in the sediments of remote equatorial lakes in the Rwenzori Mountains, Uganda, *Environ. Sci. Technol.*, *44*(17), 6570–6575.

Water chemistry variation in tropical high-mountain lakes on old volcanic bedrocks

Pablo V. Mosquera ^{1,2}, Henrietta Hampel ³, Raúl F. Vázquez ⁴, Jordi Catalan ^{5,6*}

¹Departament de Biologia Evolutiva, Ecologia i Ciències Ambientals, Universitat de Barcelona, Barcelona, Spain

²Subgerencia de Gestión Ambiental de la Empresa Pública Municipal de Telecomunicaciones, Agua potable, Alcantarillado y Saneamiento (ETAPA EP), Cuenca, Ecuador

³Laboratorio de Ecología Acuática, Facultad de Ciencias Químicas, Universidad de Cuenca, Cuenca, Ecuador

⁴Departamento de Ingeniería Civil, Facultad de Ingeniería, Universidad de Cuenca, Cuenca, Ecuador

⁵CREAF, Cerdanyola del Vallès, Spain

⁶CSIC, Cerdanyola del Vallès, Spain

Abstract

Water chemistry and its ecological implications have been extensively investigated in temperate high-mountain lakes because of their role as sentinels of global change. However, few studies have considered the drivers of water chemistry in tropical mountain lakes underlain by volcanic bedrock. A survey of 165 páramo lakes in the Cajas Masif of the Southern Ecuador Andes identified 4 independent chemical variation gradients, primarily characterized by divalent cations (hardness), organic carbon, silica, and iron levels. Hardness and silica factors showed contrasting relationships with parent rock type and age, vegetation, aquatic ecosystems in the watershed, and lake and watershed size. Geochemical considerations suggest that divalent cations (and related alkalinity, conductivity, and pH) mainly respond to the cumulative partial dissolution of primary aluminosilicates distributed throughout the subsurface of watersheds, and silica and monovalent cations are associated with the congruent dissolution of large amounts of secondary aluminosilicates localized in former hydrothermal or tectonic spots. Dissolved organic carbon was much higher than in temperate high-mountain lakes, causing extra acidity in water. The smaller the lakes and their watersheds, the higher the likelihood of elevated organic carbon and metals and low hardness. The watershed wetland cover favored metal levels in the lakes but not organic carbon. Phosphorus, positively, and nitrate, negatively, weakly correlated with the metal gradient, indicating common influence by in-lake processes. Overall, the study revealed that relatively small tropical lake districts on volcanic basins can show chemical variation equivalent to that in large mountain ranges with a combination of plutonic, metamorphic, and carbonate rock areas.

Orogenesis provides crystalline bedrock with low permeability and, consequently, past glacial excavation promoted lake districts on many high mountains around the world (Jacobsen and Dangles 2017). The water chemical composition

*Correspondence: j.catalan@creaf.uab.cat

This is an open access article under the terms of the [Creative Commons Attribution-NonCommercial-NoDerivs](https://creativecommons.org/licenses/by-nc-nd/4.0/) License, which permits use and distribution in any medium, provided the original work is properly cited, the use is non-commercial and no modifications or adaptations are made.

Additional Supporting Information may be found in the online version of this article.

Author Contribution Statement: P.V.M., H.H. and R.F.V. planned the lake survey and provided financial support. P.V.M. performed field sampling, coordinated chemical analyses, and developed the land cover map. P.V.M. and R.F.V. performed GIS analyses and developed the land class mapping. J.C. and P.V.M. performed the data analyses, outlined the manuscript, and wrote the initial draft. All authors provided valuable discussion points and revisions to the manuscript.

of these lakes is driven by atmospheric deposition, geological background, watershed and in-lake biological activity, and human influence (Psenner and Catalan 1994). Crystalline rocks usually lack readily soluble minerals; therefore, lakes and headwaters in mountains show low salt content and low acid-neutralizing capacity, making them sensitive to acidic deposition. As a consequence of the “Great acceleration” (Steffen et al. 2015), emissions of sulfur and nitrogen oxides to the atmosphere caused the acidification of ecosystems in remote areas, including mountains in North America (Beamish and Harvey 1972) and Europe (Massabuau et al. 1987). High-mountain lakes became indicators of the acidification process and its ecological impact (Kopáček et al. 1998; Rogora et al. 2001). Interest in the biogeochemistry and biota of mountain lakes has increased, and as a result, information and knowledge have been accumulating over the last decades (Catalan et al. 2009b). Currently, high-mountain lakes across the globe are considered sentinels of the systemic change of

the planet (Moser et al. 2019). In this context, there is a growing interest in tropical high-mountain lakes (Michelutti et al. 2015; Van Colen et al. 2017; Benito et al. 2019; Steinitz-Kannan et al. 2020; Zapata et al. 2021), which have historically received less attention (Eggermont et al. 2007). Although high-mountain lakes are among the most comparable ecosystems globally, and a common conceptual framework might be used to analyze them (Catalan and Donato-Rondón 2016), tropical high-mountain lake regions have unique environmental characteristics that require special attention. Seasonal weather changes are low, and mean air temperature and rainfall are higher than in temperate high-mountain lake districts (Jacobsen and Dangles 2017).

The chemical composition of water in temperate high-mountain lake districts is primarily related to the bedrock (Psenner 1989; Nauwerck 1994; Marchetto et al. 1995; Kamenik et al. 2001). Although the ionic strength is consistently lower than that of low-land waters, temperate mountain lakes on metamorphic, plutonic, or carbonate rocks may markedly vary in acidity and dominant ions under similar sea salt- and human-influenced atmospheric deposition (Catalan et al. 1993). Mountain lake districts that show considerable chemical variation usually have a high diversity of bedrock composition, common in large massifs and ranges resulting from old collisional orogeny (Camarero et al. 2009). Uplifted and bent sedimentary rock landscapes may include highly metamorphosed materials, which eventually surround intrusive igneous rocks. Slates rich in sulfides may provide highly acidic waters, granitic batholiths have very low ionic levels, whereas carbonate bedrock holds alkaline waters (Marchetto et al. 1995). This broad range of chemical conditions provides niche gradients for species segregation (Catalan et al. 2009a).

Many tropical lake districts are located on volcanic bedrock in young accretionary orogenic belts. Therefore, the chemical diversity that results from weathering could be expected to be lower than in the ranges of high lithologic diversity. Furthermore, alpine areas in temperate zones continuously expose fresh rock to chemical weathering, fostered by cryofracturing of bare rock and unstable slopes. In tropical zones, warmer conditions and high vegetation cover likely diminish the availability of exposed surfaces, with rock weathering relegated to deep subsoils. Soils in tropical high-mountain lake districts have a postglacial origin. Despite their relatively young origin, they are depleted in exchangeable cations because of the high rainfall and relatively warm temperature (Molina et al. 2019). Therefore, we might expect less chemical diversity and lower acid-neutralizing capacity in mountain lakes on tropical volcanic bedrock than in temperate mountain lake districts. However, the limited data available suggests that significant variation may occur (Armienta et al. 2008; Catalan and Donato-Rondón 2016), perhaps related to the higher weatherability of basaltic lithologies compared to granite (Dupre et al. 2003), which may result in higher temporal and spatial heterogeneity of the process over the same substrate.

Consequently, this study aimed to comprehensively analyze the primary drivers of water chemistry variation in a tropical lake district on volcanic bedrock. We performed an extensive survey of the lakes and ponds ($n = 165$) in the Cajas Massif in the Andes of Southern Ecuador and measured the main chemical components of surface waters. The chemical variation was related to lake and watershed morphological characteristics, volcanic geological formations, and land cover. We evaluated the possible mechanisms behind the observed patterns concerning rock weathering in the spatially complex lithology provided by volcanism and a water-saturated cold tropical landscape that fosters organic matter accumulation. Finally, we briefly discuss the potential ecological implications of the chemical variation for constraints and ecological thresholds in species distributions and metacommunity dynamics.

Material and methods

Study sites and sampling

The Cajas Massif in the Southern Ecuador Andes contains approximately 6000 lakes and ponds of glacial origin (Mosquera et al. 2017a). The present study included data from 165 water bodies (Fig. 1), mainly within the Cajas National Park (CNP). Lakes (> 0.5 ha) were selected proportionally to their density in the 2 main hydrological basins of the CNP (western, eastern) and 15 subbasins (Supporting Information Fig. S1). Two other watersheds outside the park were also included to consider the lakes at the highest altitudes. In each subbasin, we sampled the largest lakes and a proportion of the rest ($> 50\%$) based on altitude and size distribution (Table 1). When visiting the lakes, ponds were opportunistically sampled by heuristically selecting those of varying characteristics (e.g., transparency, macrophyte cover). Lake bathymetries are available from all water bodies (Mosquera et al. 2017a). Although the area studied was relatively small (~ 334 km²), it represented the entire Cajas Massif variation in lithology, vegetation, and aquatic ecosystems. The landscape corresponds to páramo ecosystems with surplus water (Carrillo-Rojas et al. 2016). Seasonal and interannual rainfall modes correspond to the equatorial Andes (5°S – 1°N), characterized by a bimodal regime with wet periods from February to April and October to November associated with a westward humidity transport from the equatorial Amazon (Segura et al. 2019) with occasional extreme fluctuations conditioned by the equatorial Pacific (Oñate-Valdivieso et al. 2018; Schneider et al. 2018). Although the Amazonian air masses tend to lose humidity over the eastern flanks of the cordillera, rainfall occurs throughout the year (only $\sim 12\%$ dry days) at the lake district elevation, primarily as drizzle ($\sim 80\%$ duration), with mean annual precipitation in the Cajas Massif from ca. 900–1400 mm, with the maximum around 3400 m a.s.l. (Padrón et al. 2015). Cloud condensation is common, and fog interception can increase conventional rainfall by $> 25\%$ (Rollenbeck et al. 2011).

A lake survey for chemical analysis was carried out during 2014–2015. Lakes with > 1 -m depth (76%) were sampled at

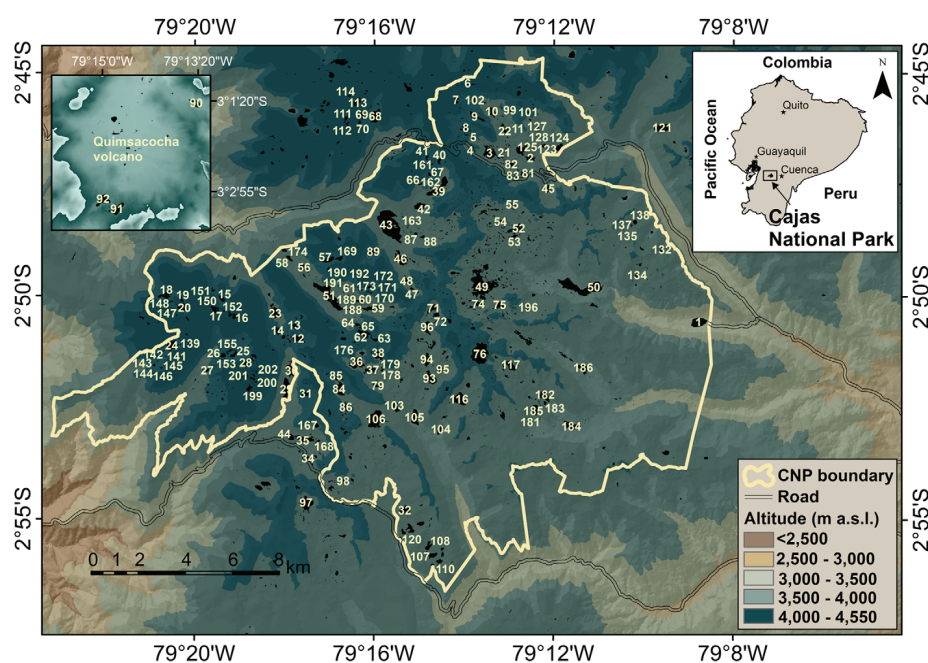


Fig. 1. Location of the study area and lakes. The large majority are located in the Cajas National Park (162), and some are in the Quimsacocha volcano area (3) and Sangay National Park (Culebrillas lake, #157, not shown). Identifiers correspond to codes from Mosquera et al. (2017b).

Table 1. Summary of the physical features of 165 lakes and ponds sampled for this study.

Variable	Unit	Minimum	First quartile	Median	Mean	Third quartile	Maximum
Latitude, N	Degrees	-3.05	-2.86	-2.84	-2.83	-2.80	-2.42
Longitude, E	Degrees	-79.35	-79.29	-79.26	-79.26	-79.23	-78.86
Altitude	m a.s.l.	3152	3856	3958	3945	4043	4294
Maximum depth	m	0.15	1.50	8.25	13	18	76
Mean depth	m	0.05	0.50	2.5	4.8	6.6	30.6
Area	m ²	22	12,177	32,012	68,698	81,331	774,775
Volume	m ³	3.2	6214	72,124	841,645	521,336	22,369,167
Watershed area	km ²	0.00002	0.28	0.98	2.74	2.19	47.70

the deepest point from a dinghy; shallower lakes and ponds were sampled from the shoreline. The upper mixed layer was determined by performing temperature profiles, and water samples were collected using Van Dorn bottles (3 L) every two meters and integrated. Water samples were immediately screened (64- μ m mesh) to remove zooplankton and debris before being cold stored and transported to ETAPA EP labs in the nearby city of Cuenca (Ecuador) for analysis. For nitrate, soluble reactive phosphorus (SRP) and dissolved organic carbon (DOC) samples were filtered using precombusted (450 °C, 4 h) GF/F Whatman[®] (Maidstone) 47-mm \varnothing glass fiber filters and Swinnex[®] (Merck Millipore) syringes.

Chemical analysis

Standard methods for water chemical analyses were followed (APHA-AWWA-WEF 2012). Sodium, potassium, silica, aluminum (only for 2019–2020 samples), iron, and manganese were

determined by inductively coupled plasma spectrometry (SM 3120 B; ICP-OES, Optima 7000 DV, PerkinElmer); calcium and magnesium by ethylenediaminetetraacetic acid (EDTA) titrimetric methods (SM 3500-Ca B and 3500-Mg B); alkalinity by potentiometric titration (SM 2320Bb); sulfate by a turbidimetric method (SM 4500 SO₄²⁻ E); chloride by mercuric nitrate titration (SM 4500-Cl⁻ C); SRP and total phosphorus (TP) following the method of Murphy and Riley (1962), the latter after potassium persulfate digestion; nitrate was reduced to nitrite and determined by colorimetry (SM 4500-NO₃⁻ E); ammonium by the salicylate method (10012, HACH), total organic carbon (TOC), and DOC by acidic digestion (Method 10129, HACH). Conductivity at 20 °C was measured using a YSI-EXO-1 sensor and pH with a WTW 3320 pH meter (Xylem Analytics) equipped with a sensor for low-ionic-strength samples (SenTix[®] HW). Apparent color was determined spectrophotometrically using platinum–cobalt standards (SM 2120 C). Ultrapure water

type 1 was used in blanks and reagents. Precision varied across compounds, and the wide range of concentrations analyzed: 3–20% relative standard deviations. Accuracy was better than 5% in all analyses. Analytical quality assessment was performed using ion balance, ion-calculated vs. measured conductivity, and ion-estimated vs. measured alkalinity (Moiseenko et al. 2013). Samples with marked deviations corresponded to low ionic strength, which showed overestimated calcium (1) or magnesium (4) levels, which were substituted by zero values in the numerical analyses. Chloride was not considered in the factorial analysis because of the high number of values below the quantification limit. For other variables, limits of quantification were used in the numerical analyses (Table 2). During the 2014–2015 laboratory analysis, no aluminum measures were performed. However, for a subset of 10 lakes of the original survey, aluminum data were available from monthly sampling during 2019–2020, which were only used to confirm some mineral equilibrium assumptions.

Geomorphology, lithology, and land cover

Three main drivers important for water chemistry variation were considered: the parent rock, the ultimate primary source of solutes; land cover, which may condition water–rock interactions; and watershed and waterbody morphology that may determine the interaction duration. Climate is relatively similar across the survey area (Padrón et al. 2015); therefore,

altitude was the only variable considered as a surrogate of potential climatic effects.

Lake and watershed geomorphological descriptors (1 : 5000) were available from Mosquera et al. (2017b), whose site coding was maintained. Geological information was extracted from a 1:100,000 geological map (Dunkley and Gaibor 2009), which was used to calculate the area of the main lithostratigraphic classes for each lake watershed. The Cajas bedrock corresponds to a complex imbricate layering of volcanic formations (i.e., eight in the surveyed lakes) of varying age (7–37 Ma), from the late Eocene to Miocene, and some minor areas of intrusive rocks (Supporting Information Table S1; Fig. S1). The geological formations vary in dominant parent rock (rhyolite, andesite, dacite, and diorite) and material (tuffs, breccia, lava, lapilli, and sandstone), but all of them show a large secondary variability within the formation.

Although the páramo landscape appears relatively homogeneous at first glance, lake watersheds may markedly differ in vegetation cover and development (Fig. 2). The identified land cover classes included páramo grassland vegetation (e.g., *Calamagrostis*), *Loricaria* and *Gynoxis* shrubs, *Polylepis* open forest, montane evergreen forest, rocky páramo, bare rock, eroded land, wetlands, rivers, and water bodies (Supporting Information Fig. S2). The land covered by the respective classes was uneven (Supporting Information Table S2), and the montane forest was exclusively present in the Lake Llaviucu watershed. The land cover map was

Table 2. Summary of the water chemistry variation in the study lakes of the Cajas Massif, Southern Ecuadorian Andes.

Variable	Units	Minimum	First quartile	Median	Mean	Third quartile	Maximum
Conductivity	$\mu S_{20} \text{ cm}^{-1}$	4.3	28	48	52	69	191
pH		4.6	6.6	7.0	7.0	7.5	8.5
Calcium	$\mu\text{eq L}^{-1}$	~ 0*	200	400	457	640	1922
Magnesium	$\mu\text{eq L}^{-1}$	~ 0*	71	116	138	194	697
Sodium	$\mu\text{eq L}^{-1}$	5	29	44	47	61	117
Potassium	$\mu\text{eq L}^{-1}$	< 3†	< 3†	3	4	6	37
Alkalinity	$\mu\text{eq L}^{-1}$	47	260	440	525	720	2208
Sulfate	$\mu\text{eq L}^{-1}$	10	55	76	88	104	343
Chloride	$\mu\text{eq L}^{-1}$	< 10†	< 10†	< 10†	—	< 10†	30
Silica	$\mu\text{mol L}^{-1}$	13	67	90	90	108	196
Nitrate	$\mu\text{eq L}^{-1}$	0.01	0.02	0.15	0.26	0.34	2.8
TP	$\mu\text{mol L}^{-1}$	0.02	0.12	0.22	0.26	0.31	1.40
SRP	$\mu\text{mol L}^{-1}$	< 0.02‡	< 0.02‡	< 0.02‡	0.05	0.05	0.61
TOC	mg L^{-1}	0.15	3.6	5.0	5.9	6.6	> 21†
DOC	mg L^{-1}	0.15	2.1	3.0	4.1	5.3	> 21†
Apparent color	CU	7	20	28	37	39	187
Iron	$\mu\text{mol L}^{-1}$	0.18	0.64	1.07	1.71	1.92	15.25
Manganese	$\mu\text{mol L}^{-1}$	0.05	0.11	0.25	0.43	0.48	5.04
Aluminum‡	$\mu\text{mol L}^{-1}$	1.30	1.83	1.97	2.11	2.15	3.20

*Estimated by cation–anion balance because below quantification limits ($20 \mu\text{eq L}^{-1}$ for calcium and magnesium, and $15 \mu\text{eq L}^{-1}$ for chloride).

†Beyond quantification limit values.

‡Data only for 10 lakes. Ammonium was below the quantification limit ($1 \mu\text{eq L}^{-1}$) in all lakes.

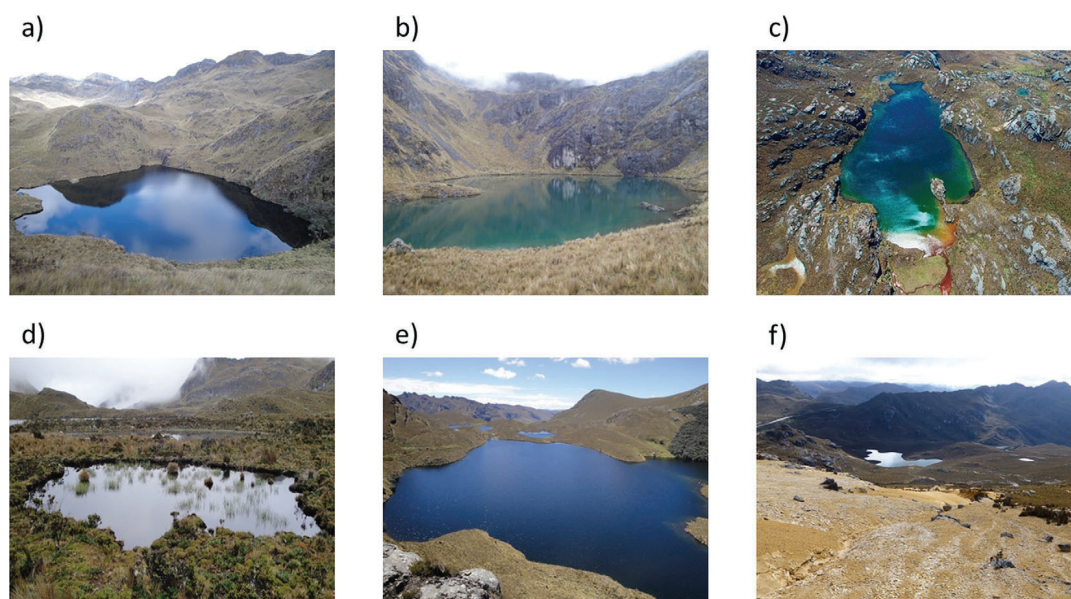


Fig. 2. Some illustrative lakes and landscapes from Cajas Massif in Southern Ecuadorian Andes: **(a)** Laguna de la Cascada, #99; **(b)** Cardenillo, #100; **(c)** Cocha totorilla 1, #149; **(d)** Ingacasa, #36; **(e)** Estrellascocha de Quitahuayco; and **(f)** example of the land cover class “eroded land.”

produced by heads-up digitalization of the aerial photographs of the project SIG-Tierras (2010–2014, www.sigtierras.gob.ec). The images ($30 \times 30 \text{ cm}^2$ resolution) were orthorectified and georeferenced. Only one digitizer performed the manual task for consistency, and several people repeatedly checked for omissions and mistakes. ArcGIS 10.0 (ESRI Inc.) was used with a screen zoom of the photographs consistently below a 1:200 scale. The scale of cartographic digitalization was 1:5000. The area of each land cover class within the lake watershed was calculated from the digitized land cover contour shapefile, and the lake watershed shapefile ($3 \times 3 \text{ m}^2$ resolution) using the ArcGIS 10.0 analysis tools and summarize function.

Numerical analyses

Descriptive statistics, analyses of variance, Tukey's honest significant differences, and other statistical analyses detailed below were performed using R (v. 4.0.4). Except for pH and silica, most water chemistry components had a skewed distribution; hence they were log-transformed in numerical studies. Maximum likelihood factor analysis (*factanal* R-function) was used to investigate the correlation structure among the water chemistry variables. Varimax rotation was applied to facilitate axis interpretation, and the optimal number of factors was determined using the *nFactors* R-package. The influence of potential drivers on the main water chemistry variation was investigated using multivariate linear regression (*lm* R-function) based on altitude, geomorphological, lithological, and landcover descriptors. Fifteen explanatory variables were considered; lake mean depth, watershed/lake area ratio, main rock proportions (rhyolite, dacite, and diorite), geological formation age, land cover proportions (páramo, rocky páramo,

Polylepis forest, shrubs, bare rock, eroded land, water bodies, and wetlands), and altitude. Andesite, the most common substrate across lake basins, determines the typical conditions from which other substrates can cause deviations. Therefore, only the percentages of the other 3 substrates were included as potential deviations from the andesite norm. Drivers with skewed distributions were log-transformed (i.e., mean depth, watershed/lake ratio), and all of them were standardized (z-scores) to obtain coefficients that directly indicate the degree of influence in the regression. We ranked all possible models (2^{15}) using the corrected Akaike's information criterion (AIC_c), which is more appropriate for relatively small datasets, and the *dredge* function from the MuMIn R package (v.1.43.17). Regression coefficients were standardized to allow comparisons of their relative magnitudes between the models. The coefficients of all models with an $AIC_c < 4$ higher than the lowest AIC_c were averaged (*model.avg* function): the coefficient absolute mean deviation from zero indicates the variable explanatory capacity and the coefficient range shows the uncertainty associated with that deviation (Dormann et al. 2018). Speciation and solubility diagrams were determined using Geochemist's Workbench® (Aqueous Solutions LLC), version GWB 2021, SpecE8, and Act2 programs, respectively (Bethke 2008).

Results

Water chemical variation

The Cajas lakes typically showed low ionic content, circumneutral pH, low nutrient, and slightly brownish conditions (Table 2). Although the ionic content was relatively low (conductivity always $< 200 \mu\text{S}_{20} \text{ cm}^{-1}$), most water bodies were

not sensitive to acidification (alkalinity > 200 $\mu\text{eq L}^{-1}$). Acidic water bodies (i.e., $\text{pH} < 6.5$) were uncommon and limited to small ponds. Calcium was commonly the dominant cation, although magnesium also showed high values and was dominant in a subset of lakes (Fig. 3). The potassium concentration was extremely low compared to other cations, including sodium. Bicarbonate and sulfate could be dominant among the anions (Fig. 2), yet the latter was not associated with acidic conditions. Chloride levels were generally below quantification limits (Table 2), which indicated an atmospheric origin consistent with the low chloride content (< 10 $\mu\text{eq L}^{-1}$) in the deposition of Southern Andes (Beiderwieden et al. 2005). High values ($\sim 30 \mu\text{eq L}^{-1}$) were only found in the Quinuas river basin, close to the only mountain road crossing the study area, which connects Cuenca and Guayaquil cities (e.g., lakes 81–83, Fig. 1). Nitrogen components had extremely low concentrations; ammonium was always below the quantification limit, while nitrate concentration seldom exceeded > 1 $\mu\text{eq L}^{-1}$. Phosphorus values were also usually low; therefore, water bodies were oligotrophic, with few exceptions. The lake color ranged from crystal clear to reddish and brown tones. Accordingly, organic matter (TOC and DOC) and iron content revealed a wide variation (Table 2).

The chemical variables showed clear correlation patterns (Supporting Information Fig. S3). The factor analysis indicated that these relationships could be summarized by four main latent factors, which explained 53% of the total variance (Table 3). *F1* could be interpreted as a total ionic strength factor, provided mainly by calcium and magnesium cations (water hardness) that primarily determined alkalinity and conductivity values, with a secondary sodium contribution (Table 3). The higher the *F1* score, the lower the apparent color and TP. Therefore, the higher the alkalinity, the more transparent and less productive the environment becomes. *F2* denoted the organic matter content, which appeared largely independent of the inorganic chemical characteristics, and was only weakly associated with the apparent color.

F3 was primarily related to silica and monovalent cations, indicating a more congruent dissolution of aluminum–silicate

Table 3. Variable loadings on four significant main axes (*F1*–*F4*) of a water chemistry factorial analysis.*

Variable	<i>F1</i>	<i>F2</i>	<i>F3</i>	<i>F4</i>
Log (alkalinity)	0.98		0.17	
Log (conductivity)	0.91		0.29	
Log (calcium)	0.90			
pH	0.70		0.17	
Log (magnesium)	0.50			
Log (TOC)		0.98		0.16
Log (DOC)		0.77		
Log (sodium)	0.41		0.83	
Silica		−0.20	0.74	
Log (potassium)			0.43	0.34
Log (sulfate)			0.26	
Log (SRP)			−0.22	0.14
Log (iron)	−0.18			0.93
Log (manganese)				0.56
Log (apparent color)	−0.34	0.33	−0.22	0.50
Log (TP)	−0.31			0.23
Log (nitrate)				−0.17

*Only loadings > |0.14| are shown. Factors explained 22%, 11%, 10%, and 10% of the total variation, respectively.

minerals than *F1*. The association of sulfate with this factor, although weak, might point to a particular bedrock type. Finally, *F4* was characterized by metals, particularly iron. Interestingly, the iron present was not strongly bonded to organic content. Indeed, the apparent color showed a higher loading on *F4* than *F2*, likely related to the reddish color when the iron level was very high. TP (positively) and nitrate (negatively) were associated with *F4*, indicating that water bodies richer in metals tend to be slightly more productive.

Drivers of water hardness variation

Chemical rock weathering should be connected to both the *F1* and *F3* axes of the factor analysis. They should, however,

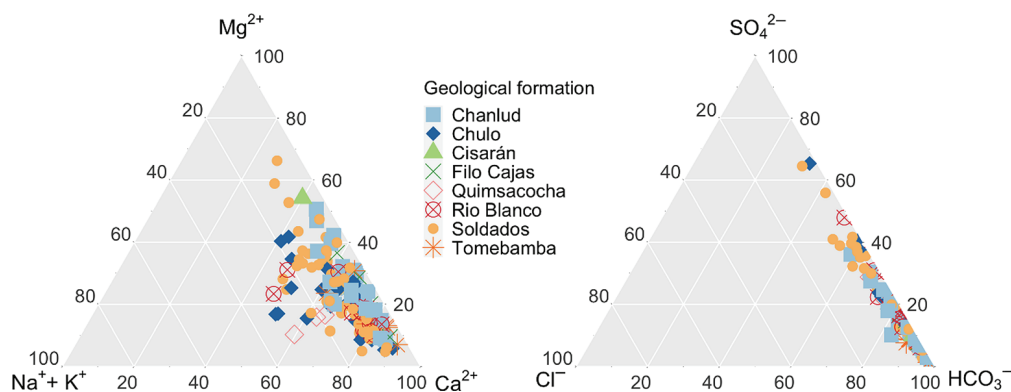


Fig. 3. Ternary diagrams of the relative ionic water composition of the study lakes. Symbols indicate the predominant geological formation in the lake watershed.

be linked to different underlying processes because they emerge in the factor analysis as orthogonal components, indicating independence. Alkalinity and conductivity high loadings on *F1* link the factor to a dominant rock weathering process. High calcium and magnesium (hardness) contributions to *F1*, but not silica, point to a noncongruent mineral dissolution of aluminum–silicates bearing divalent cations and consequently forming secondary minerals that retain silica. Given the wide alkalinity and conductivity range, this primary process should be highly variable across space (Table 2). Indeed, the geological formations showed significant differences in water hardness (Fig. 4a). The high variability within formations was initially unexpected because the lithological composition in most formations comprised andesite and dacite in varying proportions and mixed volcanic materials (Supporting Information Table S1). Rhyolite, which in

principle is less weatherable, only predominated in the Chulo unit, which indeed showed lower than average ionic strength.

Interestingly, the differences in divalent cation levels (and thus ionic strength, alkalinity, and weathering rates) between the geological formations corresponded to their age within the andesite–dacite dominion. The older the volcanic formations, the higher the cation levels (Fig. 4a). Formations of comparable age (i.e., Tomebamba-Filo Cajas, Rio Blanco-Chanlud) showed similar hardness distributions. In contrast, Chulo formation (rhyolite) showed significantly lower hardness levels than the closest andesite-dacite formation by age.

Despite the general rock type and age patterns, *F1*-related variables showed broad variability within some formations (i.e., Soldados, Chanlud, Chulo). Part of this variation could be because some lakes included more than one formation in their watersheds, although this is not a common feature

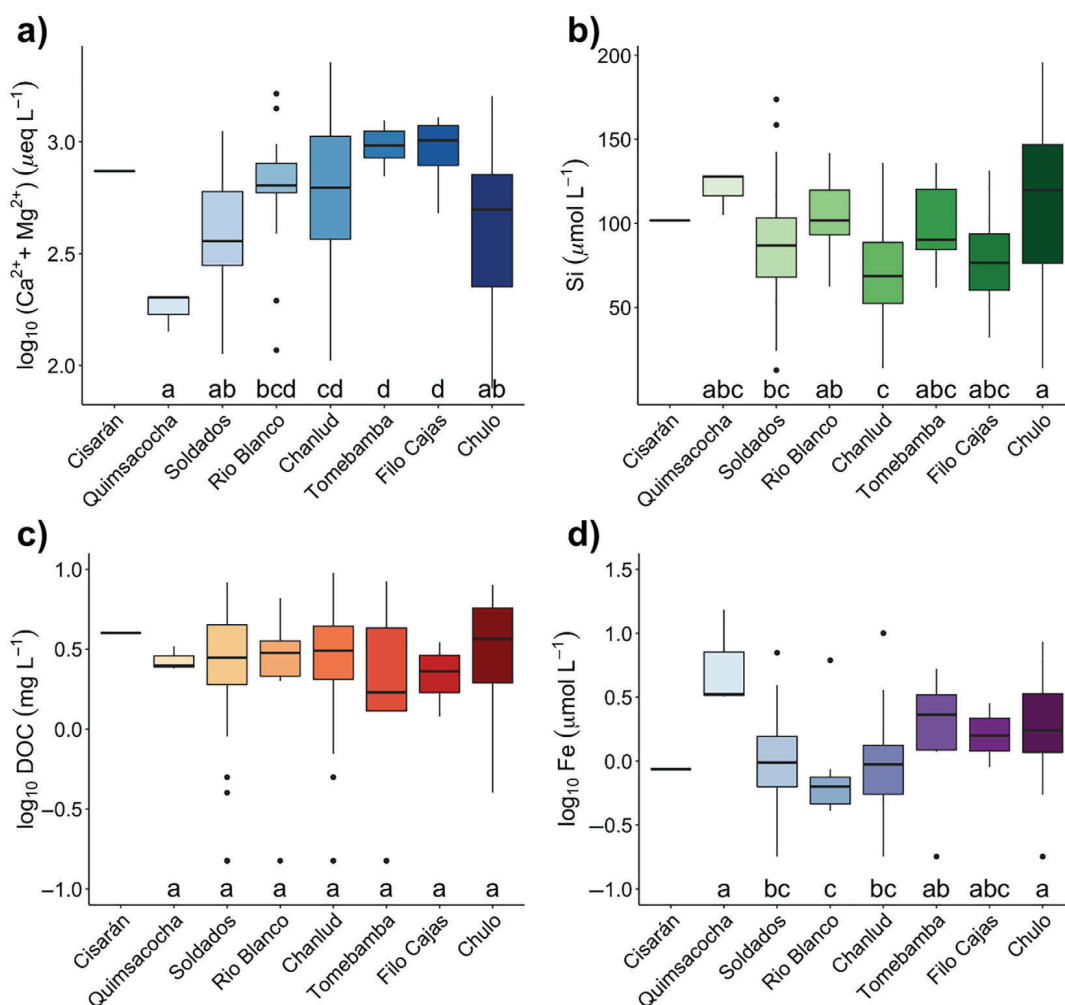


Fig. 4. Chemical variation distribution within the geological formations: (a) water hardness (calcium + magnesium), (b) silica, (c) dissolved organic carbon, and (d) iron. The four chemical components were selected to represent the four axes of the factorial analysis (Table 3). Each lake was assigned to the geological formation with the highest percentage in the watershed. Sharing a lower case letter on the *x*-axis indicates a nonsignificant mean difference between a pair of geological formations (*p*-value, >0.05). The number of lakes, characteristics, and geographical distribution of the geological formations are shown in Supporting Information Table S1 and Fig. S1, respectively.

(Supporting Information Table S2). Therefore, most of the variability should be due to other weathering drivers that may increase the contact between water, carbon dioxide, and minerals. The multivariate regression analysis confirmed, with low uncertainty, that water hardness was favored by rock age and limited by rhyolite (Fig. 5a).

The most significant hardness drivers were geomorphological variables (i.e., mean depth and watershed/lake area ratio). Increasing the hardness with watershed and waterbody size indicated an accumulation process in the drainage basin. In contrast, the influence of land cover features was less conclusive in the models; the coefficients showed considerable variability (Fig. 5a). Wetland, bare rock, and *Polylepis* forest showed positive coefficients in the models. They might enhance the divalent cation content by providing more substrate or moisture and CO_2 at the interface where weathering occurs. Páramo and rocky páramo influence were

highly uncertain; despite some models showing the highest coefficients, they were inconsistently positive or negative, depending on the combination with other variables. To understand the effect of vegetation in weathering, finer resolution in vegetation, soil, and topography details is required. Overall, these models explained approximately 36% of the total hardness variation.

Drivers of silica variation

The contribution of silica to the $F3$ axis in the factorial analysis and the poor loading of divalent cations suggested a secondary weathering process. There were marked average differences between the geological formations (Fig. 4b). However, the differentiating patterns changed from those shown by hardness, which is a clear indication that the causal drivers for $F1$ - and $F3$ -related variables were relatively independent. Indeed, the multivariate regression models showed that

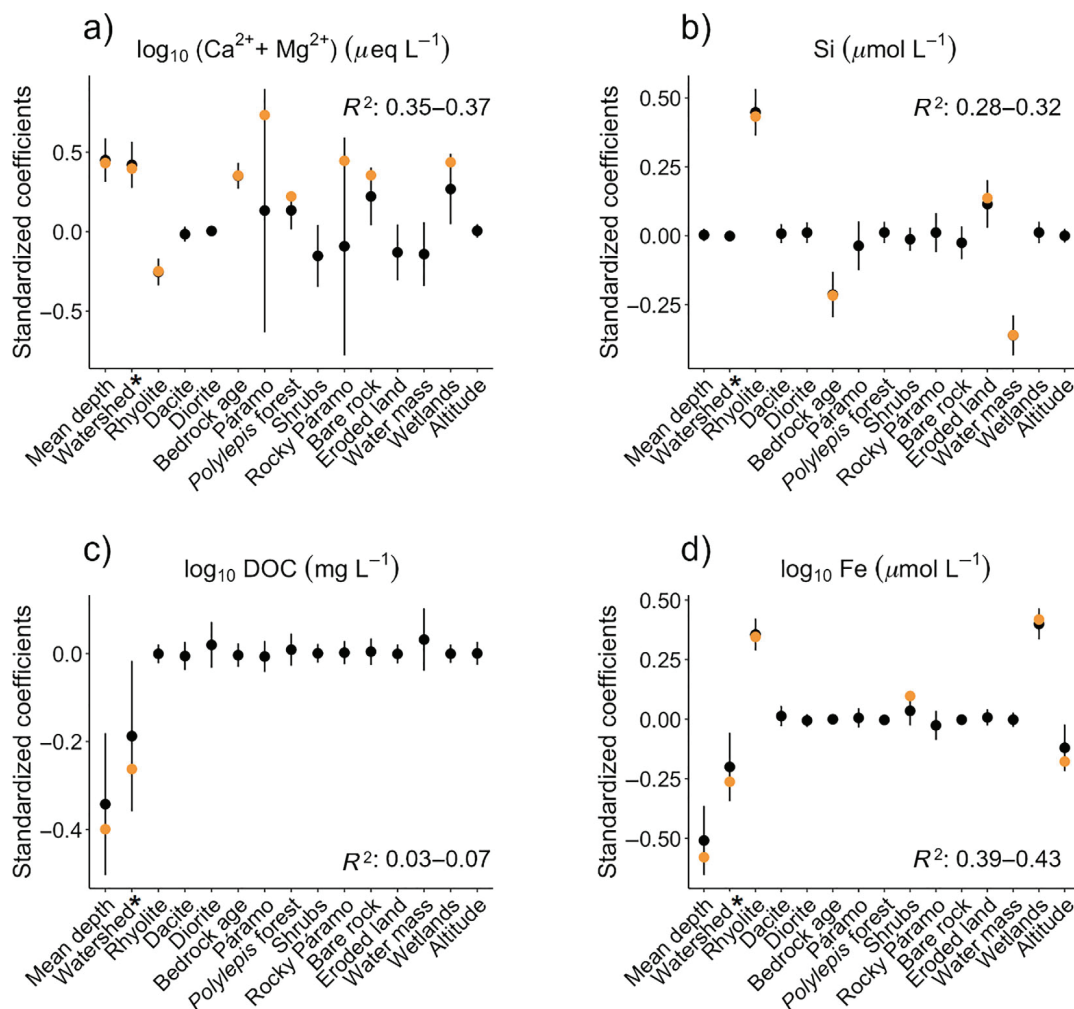


Fig. 5. Driver significance for selected water chemistry components: (a) hardness (calcium + magnesium); (b) silica; (c) dissolved organic carbon; and (d) iron. The plots indicate the mean and range of the standardized regression coefficients of multivariate models with a < 4 AIC_c difference from the best model (indicated by an orange dot). All possible models (2^{15}) were assessed and ranked by the lowest AIC_c . The larger the mean departure from zero and the smaller the range of coefficients, the greater the probability of relevance of the driver. The range of variance explained (R^2) by the selected models is included in the plots. (*) Watershed/lake area ratio.

geomorphological features were not significant for silica levels (Fig. 5b), in contrast to the water hardness case.

Despite the high variation in calcium levels, the relatively constrained silica concentration indicated oversaturation or equilibrium of secondary silicates, such as kaolinite ($\text{Al}_2\text{Si}_2\text{O}_5(\text{OH})_4$) clay (Fig. 6a). Only a few cases were more likely related to aluminum hydroxide minerals (i.e., gibbsite, $\text{Al}(\text{OH})_3$); those with the lowest silica levels.

Rhyolite bedrock contributed positively to silica levels, while rock age contributed negatively, just opposite effects of drivers than on hardness. The presence of eroded land in the watershed had a positive effect. This landscape feature occupies only a small part of the overall territory (Fig. 2e); it may have a marked influence when it is present. The proportion of water mass in the watershed resulted in a pronounced negative effect on silica levels, likely related to biological consumption (e.g., diatoms).

Overall, the regression models explained approximately 30% of silica variation. The patterns found, particularly the decline with rock age and association with eroded land, suggested some relationship with secondary volcanism processes with less extension and more random spatial distribution, which may be exhausted over time. The lack of any relationship with watershed or lake geomorphological features indicates that source areas are relatively small and do not show accumulative effects at the watershed scale.

Drivers of organic matter variation

The organic matter content in lake water ($F2$ in the factor analysis) did not differ between geological formations (Fig. 4c).

Indeed, the regression models only showed some relevance of the geomorphological variables (Fig. 5c). The smaller the lake and its watershed, the higher the DOC levels that could be expected. Although these parameters were significant, their explanation was limited ($\sim 5\%$ of the overall variation), indicating high DOC scattering regardless of lake depth (Supporting Information Fig. S4) or watershed size.

Drivers of metal variation

There were significant differences in the metal levels among the geological formations (Fig. 4d). The concentrations were higher on average in Chulo, Filo Cajas, Tomebamba, and, particularly, Quimsacocha, although only three lakes were sampled in the latter case. The variation was substantial in the other formations, and the higher values overlapped with those in the metal-rich formations.

High iron levels were more likely in small water bodies with smaller watersheds (Fig. 5d), as occurs for DOC, indicating that point sources were not evenly distributed in the landscape. These point sources were markedly more when the rhyolite bedrock was dominant. In addition, the higher the proportion of wetlands in the watershed, the higher the iron levels. These significant drivers accounted for approximately 41% of the variation. Altitude (negatively) and shrubs (positively) contributed appreciably to some models, but the general uncertainty may indicate a spurious contribution.

Water bodies with higher iron concentrations were oversaturated (Fig. 6b). In some lakes, iron precipitation was particularly evident and colorful, associated with inlets connected to wetlands (Fig. 2f). As the metal levels declined and the pH

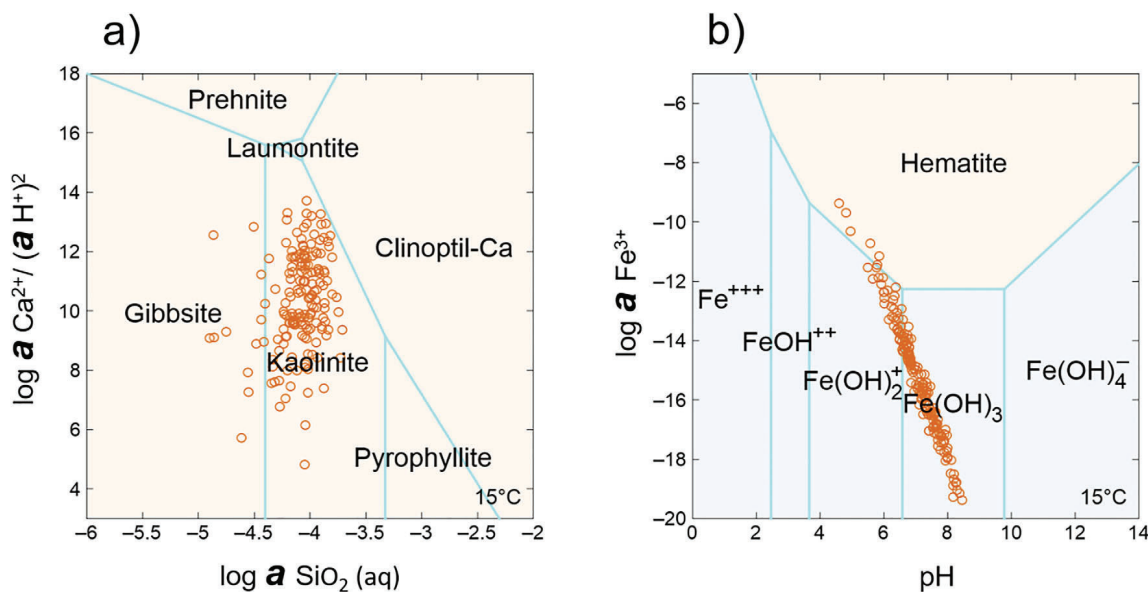


Fig. 6. Water chemistry position of the lakes in theoretical stability diagrams. (a) Mineral stability in a system with varied activities of calcium and silica, and activity = 1 of aluminum (in mineral form) and water. (b) Iron solubility assuming a 0.0002512 oxygen fugacity; an average oxygen value in the surface lake water samples. Temperature was fixed at 15°C in both cases. Reddish background indicates a solid phase, while bluish background represents an aqueous form. Calculations were performed using GWB 2021.

increased, soluble iron hydroxide forms were more likely to occur. Nevertheless, some measured iron could be associated with colloidal and small particles in lakes where hematite (Fe_2O_3) oversaturation is indicated.

Discussion

Water chemical variation and rock weathering

Our results show that high mountain lakes in volcanic basins can present extremely variable water chemistry in relatively small areas. The variation found in Cajas NP was comparable to that in large mountain ranges (Fig. 7; Supporting Information Fig. S5 for pH), where the substrate includes plutonic, metamorphic, and carbonate bedrock changing over large areas (Camarero et al. 2009). Active volcanism produces lava flows that overlap unevenly and heterogeneously distributed tuff, lapilli, and ash. Even more locally, hydrothermal processes reaching the surface create patches of substrate that differ from the dominant rock. Cajas Massif lakes show that this heterogeneity still influences water composition variation in volcanic bedrock dating millions of years. Indeed, the spatial heterogeneity and eventual water chemical variation may be increased by the presence in the watersheds of layers corresponding to several volcanic phases that differ in dominant rock, age, and associated secondary processes.

Lakes on watersheds where rhyolite bedrock dominated had softer water than lake basins where andesite, dacite, or diorite predominated. The latter rock types are richer in plagioclase and pyroxene, which are minerals that are more easily weathered than quartz and orthoclase (White and Branley 1995). Calcium and silica levels indicate that the weathering of these primary minerals is not complete; secondary silicates, most likely kaolinite, are formed. This incongruent

dissolution has been found in other volcanic rock areas (Di Figlia et al. 2007). The high correlation of calcium with alkalinity and conductivity indicates that this partial aluminosilicate dissolution is the primary source of cations. Recent studies of Cajas' andesitic soils indicate that they are depleted in mono- and divalent cations with an accumulation of Al-humus complexes in the soil matrix (Molina et al. 2019) even though these soils are postglacial and therefore relatively young. Consequently, water alkalinity generation primarily occurs in the sub-soil saprolite, which explains why water hardness increases with watershed and lake size. The cation excess increases the longer the water travels through the subsurface before reaching the lake or pond.

In addition to rock type, the surface area available for the reaction influences weathering rates (White and Branley 2003). Older volcanic bedrock presents higher porosity and surface area for hydration and reaction. Our results indicate that the age of the geological formation is a significant driver for divalent cation levels and alkalinity. This finding is consistent with 5-yr field investigations that indicate that older rhyolite rocks with similar initial compositions have faster chemical weathering rates than younger ones (Matsukura et al. 2001). The significance of the bare rock proportion in the watershed also points to the same mechanism, as these outcrops are usually heavily fractured, providing more and fresher surfaces for reaction (Kopáček et al. 2017). Vegetation has been identified as a factor promoting weathering (Burghlea et al. 2015) because it increases the availability of carbon dioxide and protons; however, our results were inconclusive. Páramo and rocky páramo both show positive and negative effects depending on the regression model. Conversely, the role of wetlands appeared robust; it always indicated weathering enhancement when included in the regression models. Nevertheless, there is still a considerable proportion of the hardness variation to be explained. Molina et al. (2019) showed a significant difference in soil chemical weathering related to topographic gradients and vegetation change at spatial scales that cannot be documented in our macroscale landscape study. The uncertainty associated with vegetation variables in the multiple regressions could be related to the lack of resolution at fine spatial scales.

Our factorial analysis suggested a complementary weathering process beyond the predominant cation source. Silica levels, which indicate complete aluminosilicate dissolution, were associated with monovalent cations and sulfate as part of a third main orthogonal factor. The silica drivers identified in the multivariate regression analysis supported the interpretation of an independent complementary weathering process. It was not related to the size of the watershed or the lake; hence, it did not have an extended occurrence that could sustain an accumulative process like that of divalent cations. This process likely occurs in hot spots sparsely distributed in watersheds. The association with eroded land was also noted in this local character. Furthermore, contrary to the hardness

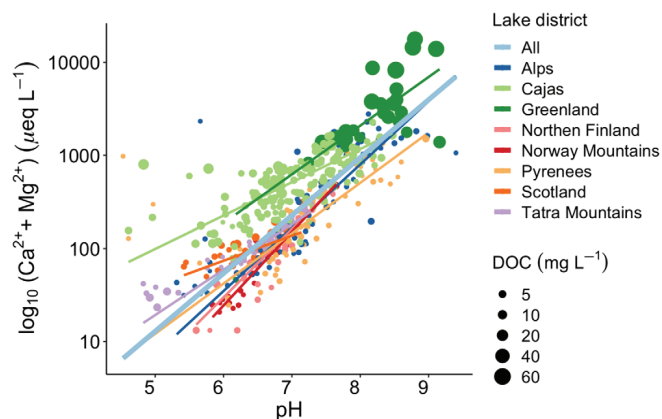


Fig. 7. Relationship between pH and divalent cations in several lake districts in temperate mountain ranges and boreal areas (data from Catalan et al. 2009b) for comparison with Cajas NP (this study data). Theil-Sen linear robust regression (*mblm* R package) was applied to downscale the influence of the outliers, mostly from waters affected by sulfide oxidation. High DOC waters show a higher intercept due to the effect of organic acids on pH.

factors, silica levels were favored in the rhyolite bedrock and declined with rock age. This evidence points to a bedrock affected by former hydrothermal processes, which occur during periods of active volcanism (Pozzo et al. 2002). High water temperatures modify the original aluminosilicates, making secondary ones deficient in cations (Ohba and Kitade 2005) and other processes such as albitization (Engvik et al. 2008). The latter may eventually result in chemical weathering, providing sodium (Cruz et al. 1999). The hydrothermal activity may or may not be associated with sulfur. Both types have been described in the Quimsacocha formation during exhaustive mining prospecting (Morán-Reasco 2017). There is no reason to think that they are not present in other formations, particularly in the Chulo unit, where rhyolite predominates, and thus the likely contingent association with this bedrock in the driver analysis. The decline with the formation age indicates that this original mineral material was not replaced by rock fragmentation, which makes sense if these are spots in the landscape where the initial rock already consists of secondary aluminosilicates, which offer more reaction surfaces (e.g., clays), and thus can provide locally higher silicate values. Sodium-rich volcanic rocks can also be related to tectonic processes (Sun et al. 2020), and faults could be another location for this particular weathering.

Weathering occurring in two distinct environments has been described in other tropical watersheds (White et al. 1998). Plagioclase and hornblende reacted at the heavily fractured bedrock—the saprock interface, as likely occurred in our case. Secondly, biotite and quartz reacted preferentially in the overlying thick saprolitic regolith, providing more K, Mg, and Si to water chemistry. This latter mechanism shows Si delivery in common with our case but differs in the main cations (i.e., Mg). Overall, independent weathering mechanisms seem to be more likely in tropical volcanic watersheds than in temperate watersheds with less intense weathering. Investigating the water systems (streams, subsurface, ponds, and lakes) associated with the eroded land identified in the land cover classification and areas with tectonic faults should shed light on our conjectures.

Silica levels were negatively affected by the water mass proportion in the watershed. This relationship points to aquatic biological consumption without evidence of terrestrial biological pumping effects, as found in other volcanic areas (Benedetti et al. 2002). In contrast, the observed low potassium levels could reflect uptake by terrestrial plants.

No specific atmospheric chemical deposition studies have been conducted in the Cajas NP area. Occasionally, dust deposition arriving at the equatorial Andes as far as the Sahara desert may provide divalent cations (Boy and Wilcke 2008), and biomass burning in the Amazon basin may provide acidifying sulfur and nitrogen compounds, as found in other areas of Southern Ecuador (Fabian et al. 2005). However, it is not possible to evaluate the deposition incidence on the average chemical composition of lakes and its variation without

specific studies. ANC in the Cajas waterbodies is usually high ($> 200 \mu\text{eq L}^{-1}$), but some sensitive sites could be influenced by atmospheric deposition. Low chloride levels indicate that most of the deposition is from westward air masses. However, significant rainfall episodes from the Pacific have been described for nearby areas during the wet season, bringing high salt deposition (Makowski Giannoni et al. 2016). Therefore, atmospheric deposition can provide seasonal and inter-annual variability in Cajas Massif waterbodies. Higher chloride values associated with the only road across the park indicate the system sensitivity.

Brown waters

Average and extreme DOC levels are higher in Cajas Massif lakes than in temperate mountain lake districts (Fig. 7) and similar to some boreal areas (Camarero et al. 2009). In contrast to cations related to rock weathering, DOC is higher in ponds and small lakes with relatively small watersheds. These features indicate a relatively local DOC origin, likely related to the idiosyncratic connections with organic soils proximal to the water body. Land cover features that apparently should be relevant for DOC (Gergel et al. 1999), such as the wetland percentage in the watershed, did not significantly influence our case.

In boreal watersheds, stream DOC originates predominantly from wetland sources during low flow conditions and from forested areas during high flow (Laudon et al. 2011), and detailed hydrology is becoming an essential component of DOC regulation. In the Cajas Massif, extreme values were achieved in small ponds, which are sometimes marginal to other water bodies. As these systems are very shallow, they are not fed with subsoil water but by water draining from immediate surface soils lacking buffering capacity. Consequently, these ponds had lower pH values (~ 5). Comparing across lake districts with significantly different average DOC levels (Fig. 7), Cajas' lakes align with high DOC lake districts (e.g., Greenland) in the relationship between divalent cation levels (or alkalinity) and pH. In these high DOC lake districts, the average pH was lower at the same alkalinity than in low DOC lake districts, showing the relevance of organic acids in providing acidity. Although the direct correlation between pH and DOC is low in Cajas waters, DOC becomes a significant parameter explaining residuals between pH and hardness; therefore, a better fit was obtained with multiple regression ($\text{pH} = 6.37 + 0.0012 \text{ hardness} - 0.026 \text{ DOC}$; $R^2 = 0.46$).

Nevertheless, paludification is not a generalized feature in Cajas lakes and ponds, and a wide range from clear to brownish water was found. Indeed, the apparent color is related to organic matter and metal content, yet there is no strong correlation between the latter two, indicating different sources. The chelation of metals may occur in high DOC systems, but there are lakes with high iron content and low DOC in the Cajas Massif. The organic and metal contents in the Cajas lakes do not share the same main drivers. Compared to iron levels, the drivers' low DOC explanatory capability necessitates an ad

hoc investigation of DOC composition and sources in the páramo lakes.

High iron availability

Iron levels are generally high; however, similar to DOC, the smaller the water body and its watershed, the higher the probability of finding elevated values. The differences between the several geological formations were significant and reflect the idiosyncrasies of the volcanism in each, with rhyolite bedrock resulting in increased iron levels. Nevertheless, the driver with more influence was the proportion of wetlands in the watershed. Water in wetlands may achieve lower pH and redox potential, thus facilitating iron solubility. Lake surface layers are usually well-oxygenated and foster iron precipitation, evident in some colorful lake littoral beds (Fig. 2f). Some iron may remain in colloidal form, as measured concentrations often indicate oversaturation.

Interestingly, TP was associated with iron and manganese in the factorial analyses. Therefore, some iron sources may also provide essential nutrients for primary production. Apatite-bearing iron deposits can be associated with magmatic-hydrothermal events (Allen et al. 1996). Our study considered only lake surface samples. Although dominant cations may change little throughout the water column, this is not the case for metals, whose solubility depends on redox conditions. Because of the persistent stratification, many of these lakes show oxygen depletion in deep layers (Steinitz-Kannan et al. 1983). These layers provide an environment for reduced metal forms and other reduced compounds, such as ammonium, which are undetected in surface waters. The anoxic conditions also facilitate phosphate solubility; therefore, the correlation between iron and phosphorus is possible because of watershed sources or in-lake processes.

Ecological implications

Main ion composition and dissolved organic matter are two primary factors influencing the biota distribution in high-mountain lakes (Kernan et al. 2009). The chemical variation found in Cajas Massif lakes and ponds is comparable to that of all the European mountain ranges (Fig. 7). Therefore, a small area and relatively homogeneous bedrock provide a variety of aquatic chemical niches that is equivalent to large territories of contrasting bedrock. This remarkable feature might foster species richness in relatively small territories of aquatic organisms that are sensitive to cation composition. The Cajas alkalinity range includes the two ecological thresholds (i.e., ~ 200 and $\sim 1000 \mu\text{eq L}^{-1}$) identified in European mountain ranges in terms of community composition (Catalan et al. 2009a). Diatoms and some crustaceans show this nonlinear community response to the alkalinity gradient, which will be interesting to confirm in this far-flung lake district, which shares with European ranges many diatom species (Benito et al. 2019), but not crustaceans (Catalan and Donato-Rondón 2016).

In these volcanic environments, a biologically interesting factor is the Ca : Mg ratio variation (Fig. 3), which is probably related to variations in andesite plagioclase and hornblende proportions. The biological influence of the dominant divalent cation type has been barely explored as a driver of species segregation in aquatic mountain ecosystems, probably because of the lack of a balanced number of sites. Organisms with carbonate shells (e.g., ostracods, mollusks, etc.) are candidates to respond to this factor, as found in other aquatic ecosystems (Dussart 1976; Chivas et al. 1986).

Soils largely depleted in cations enhance the chemical contrast between lakes and ponds. Small and shallow ponds may lack the inflow of water circulating below the soils; consequently, some show the most acidic water or high DOC content, favoring biotic differentiation (Catalan et al. 2009a). We considered many ponds in our study, but many smaller ones exist in the area (Mosquera et al. 2017a); thus, more extreme pH and DOC conditions can be expected in some of them. DOC and TOC levels in the Cajas massif are higher than in temperate high-mountain lakes and comparable to Nordic mountain lakes and tundra lakes (Camarero et al. 2009). However, these high-latitude lakes freeze during winters, a feature non-present in the páramo that may have driven adaptation in other directions. In this regard, tropical high-mountain lakes are unique. Apart from the high average level, DOC has a wide range, making it a possible axis of nonlinear species segregation that might include a wide range of organisms (e.g., rotifers, crustaceans, and chironomids), as has been observed in temperate high-mountain lakes with narrower DOC ranges (Catalan et al. 2009a).

Metals provide a further environmental gradient for biodiversity enhancement, which is not necessarily linked to the organic matter content of water. Vertical redox gradients have been observed in these tropical lakes (Steinitz-Kannan et al. 1983), but specific investigations concerning species adaptations are lacking. Furthermore, horizontal redox gradients from lakes to neighboring wetlands also likely foster species segregation.

The high chemical variability in tropical high-mountain lakes makes them ideal as global change sentinel lakes; some are more susceptible to acidic or dust deposition, while others are better suited to temperature changes impacting redox conditions. In addition, the long, independent chemical gradients offer the possibility of developing local calibration sets for paleoenvironmental reconstructions using indicator organisms, particularly diatoms (Rivera-Rondón and Catalan 2020). Given the high lake heterogeneity, surveillance and reconstructions may require a thoughtful selection of lakes for making meaningful inferences.

Data availability statement

The data supporting this study are available in Zenodo at <https://doi.org/10.5281/zenodo.6506282>.

References

- Allen, R. L., I. Lundstrom, M. Ripa, A. Simeonov, and H. Christofferson. 1996. Facies analysis of a 1.9 Ga, continental margin, back-arc, felsic Caldera province with diverse Zn-Pb-Ag-(Cu-Au) sulfide and Fe oxide deposits, Bergslagen region, Sweden. *Econ. Geol.* **91**: 979–1008. doi:10.2113/gsecongeo.91.6.979
- APHA-AWWA-WEF. 2012. Standard methods for examination of water and wastewater, 22nd ed. American Public Health Association. doi:10.1100/2012/462467
- Armienta, M. A., and others. 2008. Water chemistry of lakes related to active and inactive Mexican volcanoes. *J. Volcanol. Geotherm. Res.* **178**: 249–258. doi:10.1016/j.jvolgeores.2008.06.019
- Beamish, R. J., and H. H. Harvey. 1972. Acidification of La Cloche mountain lakes, Ontario, and resulting fish mortalities. *J. Fish. Res. Board Can.* **29**: 1131–1143. doi:10.1139/f72-169
- Beiderwieden, E., T. Wrzesinsky, and O. Klemm. 2005. Chemical characterization of fog and rain water collected at the eastern Andes cordillera. *Hydrol. Earth Syst. Sci.* **9**: 185–191. doi:10.5194/hess-9-185-2005
- Benedetti, M., and others. 2002. Chemical weathering of basaltic lava flows undergoing extreme climatic conditions: The water geochemistry record. *Chem. Geol.* **201**: 1–17. doi:10.1016/S0009-2541(03)00231-6
- Benito, X., and others. 2019. Identifying temporal and spatial patterns of diatom community change in the tropical Andes over the last c. 150 years. *J. Biogeogr.* **46**: 1889–1900. doi:10.1111/jbi.13561
- Bethke, C. M. 2008. *Geochemical and biogeochemical modeling*, 2nd ed. Cambridge Univ. Press.
- Boy, J., and W. Wilcke. 2008. Tropical Andean forest derives calcium and magnesium from Saharan dust. *Global Biogeochem. Cycl.* **22**: GB1027. doi:10.1029/2007GB002960
- Burghlea, C., D. G. Zaharescu, K. Dontsova, R. Maier, T. Huxman, and J. Chorover. 2015. Mineral nutrient mobilization by plants from rock: influence of rock type and arbuscular mycorrhiza. *Biogeochem.* **124**: 187–203.
- Camarero, L., and others. 2009. Regionalisation of chemical variability in European mountain lakes. *Freshw. Biol.* **54**: 2452–2469. doi:10.1111/j.1365-2427.2009.02296.x
- Carrillo-Rojas, G., B. Silva, M. Córdova, R. Céleri, and J. Bendix. 2016. Dynamic mapping of evapotranspiration using an energy balance-based model over an Andean páramo catchment of Southern Ecuador. *Remote Sens. (Basel)* **8**: 160. doi:10.3390/rs8020160
- Catalan, J., E. Ballesteros, E. Gacia, A. Palau, and L. Camarero. 1993. Chemical composition of disturbed and undisturbed high-mountain lakes in the Pyrenees—A reference for acidified sites. *Water Res.* **27**: 133–141. doi:10.1016/0043-1354(93)90203-T
- Catalan, J., and others. 2009a. Ecological thresholds in European alpine lakes. *Freshw. Biol.* **54**: 2494–2517. doi:10.1111/j.1365-2427.2009.02286.x
- Catalan, J., C. J. Curtis, and M. Kernan. 2009b. Remote European mountain lake ecosystems: Regionalisation and ecological status. *Freshw. Biol.* **54**: 2419–2432. doi:10.1111/j.1365-2427.2009.02326.x
- Catalan, J., and J. C. Donato-Rondón. 2016. Perspectives for an integrated understanding of tropical and temperate high-mountain lakes. *J. Limnol.* **75**: 215–234. doi:10.4081/jlimnol.2016.1372
- Cruz, J. V., R. M. Coutinho, M. R. Carvalho, N. Oskarsson, and S. R. Gislason. 1999. Chemistry of waters from Furnas volcano, Sao Miguel, Azores: Fluxes of volcanic carbon dioxide and leached material. *J. Volcanol. Geotherm. Res.* **92**: 151–167. doi:10.1016/S0377-0273(99)00073-6
- Chivas, A. R., P. de Deckker, and J. M. G. Shelley. 1986. Magnesium content of non-marine ostracod shells: A new palaeosalinometer and palaeothermometer. *Palaeogeogr. Palaeoclimatol. Palaeoecol.* **54**: 43–61. doi:10.1016/0031-0182(86)90117-3
- Di Figlia, M. G., A. Bellanca, R. Neri, and A. Stefansson. 2007. Chemical weathering of volcanic rocks at the Island of Pantelleria, Italy: Information from soil profile and soil solution investigations. *Chem. Geol.* **246**: 1–18. doi:10.1016/j.chemgeo.2007.07.025
- Dormann, C. F., and others. 2018. Model averaging in ecology: A review of Bayesian, information-theoretic, and tactical approaches for predictive inference. *Ecol. Monogr.* **88**: 485–504. doi:10.1002/ecm.1309
- Dunkley, P., and A. Gaibor. 2009. Mapa geológico Cordillera Occidental 2°–3°. Hoja geológica Cuenca-NVF 53. Instituto de Investigación Geológico y Energético—Ecuador, Servicio Geológico Nacional, Ministerio de Minas y Petróleos.
- Dupre, B., and others. 2003. Rivers, chemical weathering and Earth's climate. *C. R. Geosci.* **335**: 1141–1160. doi:10.1016/j.crte.2003.09.015
- Dussart, G. 1976. The ecology of freshwater molluscs in North West England in relation to water chemistry. *J. Moll. Stud.* **42**: 181–198.
- Eggermont, H., J. M. Russell, G. Schettler, K. Van Damme, I. Bessems, and D. Verschuren. 2007. Physical and chemical limnology of alpine lakes and pools in the Rwenzori Mountains (Uganda-DR Congo). *Hydrobiologia* **592**: 151–173. doi:10.1007/s10750-007-0741-3
- Engvik, A. K., A. Putnis, J. D. Fitz Gerald, and H. K. Austrheim. 2008. Albitization of granitic rocks: The mechanism of replacement of oligoclase by albite. *Can. Mineral.* **46**: 1401–1415. doi:10.3749/canmin.46.6.1401
- Fabian, P., M. Kohlpaintner, and R. Rollenbeck. 2005. Biomass burning in the Amazon-fertilizer for the mountaineous rain forest in Ecuador. *Environ. Sci. Pollut. R* **12**: 290–296. doi:10.1065/espr2005.07.272
- Gergel, S. E., M. G. Turner, and T. K. Kratz. 1999. Dissolved organic carbon as an indicator of the scale of watershed influence on lakes and rivers. *Ecol. Appl.* **9**: 1377–1390 doi:10.1890/1051-0761(1999)009[1377:DOCAA]2.0.CO;2.

- Jacobsen, D., and O. Dangles. 2017. Ecology of high altitude waters. Oxford Univ. Press.
- Kamenik, C., R. Schmidt, G. Kum, and R. Psenner. 2001. The influence of catchment characteristics on the water chemistry of mountain lakes. *Arct. Antarct. Alp. Res.* **33**: 404–409. doi:10.2307/1552549
- Kernan, M., and others. 2009. Regionalisation of remote European mountain lake ecosystems according to their biota: Environmental versus geographical patterns. *Freshw. Biol.* **54**: 2470–2493. doi:10.1111/j.1365-2427.2009.02284.x
- Kopáček, J., J. Hejzlar, E. Stuchlik, J. Fott, and J. Vesely. 1998. Reversibility of acidification of mountain lakes after reduction in nitrogen and sulphur emissions in Central Europe. *Limnol. Oceanogr.* **43**: 357–361. doi:10.4319/lo.1998.43.2.0357
- Kopáček, J., and others. 2017. Climate change increasing calcium and magnesium leaching from granitic alpine catchments. *Environ. Sci. Technol.* **51**: 159–166. doi:10.1021/acs.est.6b03575
- Laudon, H., and others. 2011. Patterns and dynamics of dissolved organic carbon (DOC) in boreal streams: The role of processes, connectivity, and scaling. *Ecosystems* **14**: 880–893. doi:10.1007/s10021-011-9452-8
- Makowski Giannoni, S., K. Trachte, R. Rollenbeck, L. Lehnert, J. Fuchs, and J. Bendix. 2016. Atmospheric salt deposition in a tropical mountain rainforest at the eastern Andean slopes of south Ecuador—Pacific or Atlantic origin? *Atmos. Chem. Phys.* **16**: 10241–10261. doi:10.5194/acp-16-10241-2016
- Marchetto, A., and others. 1995. Factors affecting water chemistry of Alpine lakes. *Aquat. Sci.* **57**: 81–89. doi:10.1007/BF00878028
- Massabuau, J. C., B. Fritz, and B. Burtin. 1987. Acidification of fresh-waters (pH-less-than-or-equal-to-5) in the Vosges mountains (Eastern France). *C.R. Acad. Sci. Paris Life Sci.* **305**: 121–124.
- Matsukura, Y., T. Hirose, and C. T. Oguchi. 2001. Rates of chemical weathering of porous rhyolites: 5-year measurements using the weight-loss method. *Catena* **43**: 341–347. doi:10.1016/S0341-8162(00)00129-6
- Michelutti, N., A. P. Wolfe, C. A. Cooke, W. O. Hobbs, M. Vuille, and J. P. Smol. 2015. Climate change forces new ecological states in tropical Andean lakes. *PLoS One* **10**: e0115338. doi:10.1371/journal.pone.0115338
- Moiseenko, T., N. Gashkina, M. Dinu, T. Kremleva, and V. Khoroshavin. 2013. Aquatic geochemistry of small lakes: Effects of environment changes. *Geochem. Int.* **51**: 1031–1148. doi:10.1134/S0016702913130028
- Molina, A., V. Vanacker, M. D. Corre, and E. Veldkamp. 2019. Patterns in soil chemical weathering related to topographic gradients and vegetation structure in a high Andean tropical ecosystem. *Case Rep. Med.* **124**: 666–685. doi:10.1029/2018JF004856
- Morán-Reascos, D. 2017. Analysis of mineralization extension continuity around the Loma Larga high-sulphidation system. Master Thesis. Univ. Central de Ecuador.
- Moser, K. A., and others. 2019. Mountain lakes: Eyes on global environmental change. *Glob Planet Change* **178**: 77–95. doi:10.1016/j.gloplacha.2019.04.001
- Mosquera, P. V., H. Hampel, R. F. Vázquez, M. Alonso, and J. Catalan. 2017a. Abundance and morphometry changes across the high-mountain lake-size gradient in the tropical Andes of Southern Ecuador. *Water Resour. Res.* **53**: 7269–7280. doi:10.1002/2017WR020902
- Mosquera, P. V., H. Hampel, R. F. Vázquez, M. Alonso, and J. Catalan. 2017b. Abundance and morphometry changes across the high mountain lake-size gradient in the tropical Andes of Southern Ecuador. Dryad Dataset. doi:10.5061/dryad.sn058
- Murphy, J., and J. P. Riley. 1962. A modified single solution method for the determination of phosphate in natural waters. *Anal. Chim. Acta* **27**: 31–36. doi:10.1016/S0003-2670(00)88444-5
- Nauwerck, A. 1994. A survey on water chemistry and plankton in high-mountain lakes in Northern Swedish Lapland. *Hydrobiologia* **274**: 91–100. doi:10.1007/BF00014631
- Ohba, T., and Y. Kitade. 2005. Subvolcanic hydrothermal systems: Implications from hydrothermal minerals in hydrovolcanic ash. *J. Volcanol. Geotherm. Res.* **145**: 249–262. doi:10.1016/j.jvolgeores.2005.02.002
- Oñate-Valdivieso, F., and others. 2018. Temporal and spatial analysis of precipitation patterns in an Andean region of southern Ecuador using LAWR weather radar. *Meteorol. Atmos. Phys.* **130**: 473–484. doi:10.1007/s00703-017-0535-8
- Padrón, R. S., B. P. Wilcox, P. Crespo, and R. Céleri. 2015. Rainfall in the Andean páramo: New insights from high-resolution monitoring in Southern Ecuador. *J. Hydrometeorol.* **16**: 985–996. doi:10.1175/JHM-D-14-0135.1
- Pozzo, A., and others. 2002. Influence of volcanic activity on spring water chemistry at Popocatepetl Volcano, Mexico. *Chem. Geol.* **190**: 207–229. doi:10.1016/S0009-2541(02)00117-1
- Psenner, R. 1989. Chemistry of high mountain lakes in siliceous catchments of the Central Eastern Alps. *Aquat. Sci.* **51**: 1015–1621.
- Psenner, R., and J. Catalan. 1994. Chemical composition of lakes in crystalline basins: A combination of atmospheric deposition, geologic background, biological activity and human action, p. 255–314. *In* R. Margalef [ed.], *Limnology now: A paradigm of planetary problems*. Elsevier Science B.V.
- Rivera-Rondón, C. A., and J. Catalan. 2020. Diatoms as indicators of the multivariate environment of mountain lakes. *Sci. Total Environ.* **703**: 135517. doi:10.1016/j.scitotenv.2019.135517



UNIVERSITAT DE
BARCELONA

